Chapter 3

DESIGN AND CHARACTERIZATION OF ORGANIC AND ORGANOMETALLIC MOLECULES FOR SECOND ORDER NONLINEAR OPTICS

Etienne Goovaerts, Wim E. Wenseleers

Department of Physics, Universiteit Antwerpen, Universiteitsplein 1, B-2610 Antwerpen, België

M. Helena Garcia

Faculdade de Ciências da Universidade de Lisboa, R. Ernesto de Vasconcelos, Ed.C1, Campo Grande, 1700 Lisboa, Portugal; Centro de Química Estrutural, Instituto Superior Técnico, Av. Rovisco Pais 1, 1096 Lisboa, Portugal

Graham H. Cross

University of Durham, Department of Physics, Organic Optoelectronics Group, South Road, Durham DH1 3LE, United Kingdom

Contents

1. Introduction 128
   1.1. Brief Overview of Nonlinear Optics 128
   1.2. Second-Order Nonlinear Optics—Scope of This Review 128
   1.3. General Description of Nonlinear Optics 129
   1.4. Hyperpolarizability of Organic Conjugated Molecules 131
   1.5. Theory and Modeling 132
2. Experimental Techniques 135
   2.1. Kurtz Powder Second-Harmonic Generation 135
   2.2. Solvatochromism 135
   2.3. Electric Field Induced Second-Harmonic Generation 136
   2.4. Hyper-Rayleigh Scattering 137
3. Organic Compounds 144
   3.1. Push–Pull Systems 144
   3.2. Octupolar Molecules 152
   3.3. Alternative Approaches 159
4. Organometallic Compounds 159
   4.1. Metallocenyl Derivatives 161
   4.2. η^5-Monocyclopentadienyl/ and Indenyl/Metal Derivatives 163
   4.3. Metal–Carbonyl Complexes 165
   4.4. Metal Complexes Possessing Only Metal–Ligand σ Bonds 170
   4.5. Bimetallic Complexes 171
   4.6. Octupolar Complexes 173
   4.7. Concluding Remarks 174
5. Materials 174
   5.1. Basic Classes of Second-Order Organic Materials 176
   5.2. Polymers for Second-Order Nonlinear Optics 181

Handbook of Advanced Electronic and Photonic Materials and Devices, edited by H.S. Nalwa
Volume 9: Nonlinear Optical Materials
Copyright © 2001 by Academic Press
All rights of reproduction in any form reserved.

ISBN 0-12-513759-1/$35.00

Acknowledgments 182
Appendix: Units and Conventions for NLO Parameters 182
Conversion to SI Units 182
Conventions 182
Unit Conversions 183
References 184

1. INTRODUCTION

1.1. Brief Overview of Nonlinear Optics

With the advent of the laser light source in the beginning of the 1960s [1] and the availability of intense continuous wave and pulsed light beams that resulted, it became possible in practice to explore nonlinear optical effects in materials. In vacuum or at low light intensities in materials, the Maxwell equations of electromagnetism (EM) are linear to a very good approximation, and this leads to the superposition principle of different fields. As a result, there is no interaction between different light beams or between static EM fields and light beams. At light levels now easily attainable with lasers, one enters the field of nonlinear optics (NLO) in which light beams can change frequency, interact with each other, and be influenced by static electrical fields. This new playground for scientists and engineers in the field of optics has proved to be extremely fruitful. A multitude of fascinating effects have been discovered, starting with frequency conversion effects such as second- and third-harmonic generation (SHG and THG) and going on with frequency mixing and white light generation, as well as pulse compression for ultrashort pulse generation, soliton propagation, etc. Also many applications have been found in, e.g., new light sources, high-bandwidth and long-haul optical communication, and optical integrated circuits.

Much of the effort for the development of NLO materials has initially concentrated on inorganic, mostly crystalline, materials. For example, SHG was first discovered in crystalline quartz, and many ionic crystals—generally known by abbreviations such as KDP, KTP, BBO, and LBO—are now available for frequency conversion in the near-ultraviolet (UV), visible, and infrared (IR) regions [2]. Another one of these, lithium niobate ($LiNbO_3$), has also become the material of choice for electro-optic (EO) devices and is often used in the form of thin film waveguides [3]. It turns out that the large EO effects in these systems are mainly due to nuclear motion and therefore show a relatively slow response. Conversely, the electronic response, involved in SHG or THG, is relatively weak in these materials. As an alternative, NLO effects in semiconductor materials have been intensively studied [4]. In this case, the large NLO effects were often related to resonant excitation and buildup of charge-carrier populations. Carrier lifetimes and diffusion are then limiting factors for the speed of the NLO processes. Contrary to the case of ionic crystals, the origin of the large NLO effects in organic materials lies in the high electronic polarizability of their π-electron system [5]. Conjugated organic molecules form very efficient building blocks for NLO materials, with very fast response for nonresonant optical excitation. In this approach one can expect to take advantage of the extreme versatility of organic synthesis and in this way optimize the NLO properties by chemical engineering. Also, these organic materials potentially offer other advantages, such as relative ease of production (maybe at low cost), the low index of refraction useful for some of the applications, and the use of the NLO building blocks in polymeric films suitable for waveguiding or EO integration. Other material aspects apart from the NLO properties have to be considered and are even of paramount importance for technological applications, e.g., processibility and thermal, chemical, and photochemical stability.

1.2. Second-Order Nonlinear Optics—Scope of This Review

Nonlinear optics describes the interaction of strong electric fields, such as those occurring in intense laser beams, with matter. The molecular materials which we will consider are generally nonconducting and nonmagnetic. An applied optical or static electric field, $\boldsymbol{E}$, will rearrange the charge distribution in the molecular unit, and its electric dipole moment μ can be given as a power series in $\boldsymbol{E}$[1]

$$\mu_i = \mu_i^0 + \alpha_{ij}E_j + \beta_{ijk}E_jE_k + \gamma_{ijkl}E_jE_kE_l + \cdots \qquad (1)$$

in which μ^0 is the permanent dipole moment, α is the polarizability, and β and γ are, respectively, the second-order (SO) and third-order (TO) polarizability (or *first* and *second* hyperpolarizability) of the molecule. Symmetry considerations imply that the even-order terms in the applied field (or $\mu^0, \beta, \ldots$) vanish for centrosymmetric molecules, while the odd-order terms ($\alpha, \gamma, \ldots$) are in general nonzero for all molecules. The induced dipole moment contains contributions from displacements of the electrons (electronic polarizabilities), as well as from motion of the atomic nuclei (nuclear or "vibrational" polarizabilities). In a macroscopic description of the optical properties of a medium, an analogous power series is written for the polarization $\boldsymbol{P}$[1]

$$P_i = P_i^0 + \chi_{ij}^{(1)}E_j + \chi_{ijk}^{(2)}E_jE_k + \chi_{ijkl}^{(3)}E_jE_kE_l + \cdots \qquad (2)$$

In this equation $\chi^{(1)}$ is the linear susceptibility and $\chi^{(2)}$ and $\chi^{(3)}$ are the second- and third-order nonlinear susceptibilities of the material. The linear optical properties on the molecular and macroscopic level derive from the polarizability α and the linear susceptibility $\chi^{(1)}$, respectively. For higher field intensities, the higher order terms are at the origin of NLO phenomena, characterized by the hyperpolarizabilities β and γ on the level of the single molecule and on the macroscopic level by the nonlinear susceptibilities. Second- and third-order NLO materials are characterized by a large nonzero $\chi^{(2)}$ and $\chi^{(3)}$, respectively. On symmetry arguments, $\chi^{(2)}$ can be shown to vanish in macroscopically centrosymmetric materials (in general, $\chi^{(3)}$ is nonzero in any medium). Similarly, for individual molecules the first hyperpolarizability is nonzero only for compounds lacking a center of symmetry, and this has been taken as a basic design criterion for SO

[1] Equations are given here for the power series convention in the Gaussian (cgs) unit system. See the Appendix for different conventions and for conversion to SI units.

NLO molecules. High β values are very desirable, but are not sufficient to obtain a good SO NLO material: if the molecular units assemble in a macroscopically centrosymmetric arrangement, the individual contributions to the SO susceptibility $\chi^{(2)}$ sum up to zero. This unfortunately is often the case: most molecules tend to crystallize in centrosymmetric space groups, and also for a random orientational arrangement, as in a polymer, the average symmetry is centrosymmetric and the SO susceptibility vanishes. Therefore, in the development of molecular SO NLO materials, the design of high β molecules is only the first step, and the control of the molecular arrangement is of at least equal importance. A lot of progress has been made in the molecular design, but this being said, one is only now getting closer to the values of the first hyperpolarizability needed for applications, as will be discussed further in this chapter. In this review we will focus our attention on organic and organometallic molecules as the building blocks for SO NLO materials.

Our aim is to cover in this review the ongoing efforts to design, characterize, and optimize the first hyperpolarizability β of organic and organometallic molecules for NLO applications. In the remaining part of this Introduction, we present a more detailed description of NLO effects and of the relation between molecular and macroscopic NLO properties. Also, we briefly survey the theoretical methods which have been employed to calculate these properties. Section 2 is devoted to the description of methods for the experimental determination of molecular SO NLO parameters, with emphasis on the recently widely used hyper-Rayleigh scattering (HRS) technique. The different types of compounds which have been synthesized and characterized for SO NLO are discussed in Sections 3 and 4, for organic and organometallic molecules, respectively, up to the latest developments in this field. Finally, a number of criteria which these compounds have to meet for applications and some materials aspects are considered in Section 5.

1.3. General Description of Nonlinear Optics

In this section we give a summary of the theoretical background needed for the description of NLO properties of organic materials, including the basic definitions and phenomena. This material is covered in more detail in standard textbooks on NLO [5–10]. Although third-order NLO materials will not be treated, the third-order susceptibility of materials is of importance for measuring techniques of SO NLO polarizabilities, in particular for electric field induced second-harmonic generation (EFISHG).

1.3.1. Basic Equations and Effects

Going back to the limit of low electric fields (i.e., linear optics) Eq. (2) can be truncated to $P_i = P_i^0 + \chi_{ij}^{(1)} E_j$ which, combined with Maxwell's equations, is sufficient to give a full phenomenological description of the linear optical properties of a medium. Indeed, the susceptibility is related to the dielectric constant or to the refractive index of the material, in particular for an isotropic material $n^2 = \varepsilon = 1 + 4\pi\chi^{(1)}$. In this relation n, ε, and $\chi^{(1)}$ are functions of the frequency and can assume complex values, the real part of n being responsible for refraction and the imaginary part for absorption.

Several nonlinear optical effects can be readily explained from the basic Eqs. (1) or (2), by considering a system on which a strong, oscillating electric field, $E = E_0 \cos \omega t$, is applied [8]. Indeed, substitution of this sinusoidal field (chosen to be along the z axis) into the second-order term reveals a contribution to the induced polarization

$$P_i^{(2)} = \chi_{izz}^{(2)} E_0^2 (\cos \omega t)^2 = \tfrac{1}{2} \chi_{izz}^{(2)} E_0^2 (1 + \cos 2\omega t) \qquad (3)$$

which contains a direct current (DC) component and a component at twice the applied frequency. The former means that when a strong laser beam is sent through a noncentrosymmetric molecular crystal, a DC voltage may be generated across the crystal. This effect is known as the *optical rectification*. The second term in Eq. (3) shows that the induced dipole will also have a 2ω component. This oscillating macroscopic polarization acts as a source of radiation at 2ω. In a macroscopically noncentrosymmetric medium this leads to the generation of a coherent beam at 2ω. This so-called *frequency doubling* or *second-harmonic generation* (SHG) was first observed in quartz [11]. Analogously, the third-order term will lead to contributions at 3ω, leading to *third-harmonic generation* (THG), and at ω corresponding to various effects including *self-focusing* of the laser beam due to changes of the index of refraction induced by the light intensity. In general, even-order effects (only occurring in asymmetric systems) will result in even-order harmonics ($0, 2\omega, 4\omega, \ldots$) and odd-order responses (occurring in all media) only in odd-order harmonics ($\omega, 3\omega, \ldots$), as is clear from an inspection of the Fourier decomposition of the resulting response [11].

Other NLO effects include changes in the refractive index (and/or absorption coefficient) when a static or optical electric field is applied. These effects can be described more clearly (though completely equivalently) by rewriting (2) as

$$P_i = P_i^0 + \left(\chi_{ij}^{(1)} + \chi_{ijk}^{(2)} E_j + \chi_{ijkl}^{(3)} E_j E_k + \cdots\right) E_j$$

so that the factor within parentheses can be interpreted as a generalization of the linear susceptibility. Consequently, the susceptibility and hence the related refractive index and absorption coefficient now become electric field dependent. When a static electric field is applied to a second-order NLO material, the term in $\chi^{(2)}$ will result in a change in the complex refractive index, proportional to the applied field. This *linear electro-optic effect* is the basis for applications such as EO modulators or switches. The term in $\chi^{(3)}$ leads to a change in refractive index which is quadratic in the applied field. For a static applied field, this is known as the *quadratic electro-optic effect* or DC Kerr effect. More importantly, the quadratic E dependence means that also an oscillating (optical) field induces a change in refractive index with a constant component. With third-order NLO materials it is therefore possible to build "all-optical" or "opto-optical" switches, i.e., light modulators or switches which are controlled by another light beam, rather than by an electrical signal [8, 12, 13].

In the foregoing phenomenological description of some NLO effects, the (hyper)polarizabilities and (nonlinear) susceptibilities are independent of frequency, as a result of the implicit assumption that the NLO response follows the applied field instantaneously. For optical frequencies (in the visible or near-IR range), which are typically comparable to electronic excitation frequencies, dispersion and resonance effects become important. Therefore, all Fourier components of the applied fields and of the resulting dipole moments or polarization fields must be considered separately. The frequency dependence of the corresponding (hyper)polarizability components is then explicitly indicated as fol-

lows:

$$\begin{aligned}
\mu_i^{(\omega)} &= \alpha_{ij}(\omega) E_j^{(\omega)} \\
\mu_i^{(\omega_\sigma)} &= \beta_{ijk}(-\omega_\sigma; \omega_1, \omega_2) \\
&\quad \times E_j^{(\omega_1)} E_k^{(\omega_2)} \qquad (\omega_\sigma = \omega_1 + \omega_2) \\
\mu_i^{(\omega_\sigma)} &= \gamma_{ijkl}(-\omega_\sigma; \omega_1, \omega_2, \omega_3) \\
&\quad \times E_j^{(\omega_1)} E_k^{(\omega_2)} E_l^{(\omega_3)} \qquad (\omega_\sigma = \omega_1 + \omega_2 + \omega_3) \\
&\quad \cdots
\end{aligned} \tag{4}$$

An analogous notation is also used for the susceptibilities. For brevity, the frequency-dependent (hyper)polarizabilities and susceptibilities are introduced here ad hoc, but they can be defined more rigorously via Fourier analysis, starting from corresponding (time-dependent) nonlinear response functions [5]. The first argument of the hyperpolarizabilities is conventionally written with a minus sign, to indicate that it represents a generated photon. Positive frequencies indicate incoming photons. The condition that nonzero hyperpolarizabilities only exist for which the sum of all frequency arguments is zero thus simply corresponds to conservation of energy.

Hyperpolarizabilities and nonlinear susceptibilities are symmetrical under simultaneous permutation of their Cartesian indices and corresponding frequency arguments, e.g.,

$$\gamma_{ijkl}(-\omega_\sigma; \omega_1, \omega_2, \omega_3) = \gamma_{ijlk}(-\omega_\sigma; \omega_1, \omega_3, \omega_2)$$

Consequently, hyperpolarizabilities and susceptibilities associated with frequency doubling are symmetrical under permutation of the second and third index [$\beta_{ijk}(-2\omega; \omega, \omega) = \beta_{ikj}(-2\omega; \omega, \omega)$].[2] Similarly, static hyperpolarizabilities are invariant under any permutation of indices. Finally, when all frequencies and combinations of frequencies involved are far from the resonances of the material, the hyperpolarizabilities and susceptibilities are approximately invariant under any permutation of their indices as well. This approximate symmetry relation is known as Kleinman symmetry [14].

1.3.2. Relation between Microscopic and Macroscopic Nonlinearities

For molecular materials, i.e., materials composed of molecules which largely retain their structure and properties upon condensation, it is most useful to describe the macroscopic susceptibilities via the microscopic (hyper)polarizabilities of the individual molecules [15]. As we will be concerned with organic materials, which are typically molecular materials (as opposed to the traditional inorganic NLO crystals), this microscopic approach will be followed throughout.

1.3.2.1. Number Density and Local Fields

In the simplest possible case of a molecular material consisting of a macroscopic collection of molecules which are all identically oriented, e.g., an organic crystal with only a single molecule per unit cell, the macroscopic NLO susceptibilities are obtained from the microscopic hyperpolarizabilities by a simple scaling [5],

$$\begin{aligned}
&\chi_{ijk}^{(2)}(-\omega_\sigma; \omega_1, \omega_2) \\
&\quad = N f^{\omega_\sigma} f^{\omega_1} f^{\omega_2} \beta_{ijk}(-\omega_\sigma; \omega_1, \omega_2) \\
&\chi_{ijkl}^{(3)}(-\omega_\sigma; \omega_1, \omega_2, \omega_3) \\
&\quad = N f^{\omega_\sigma} f^{\omega_1} f^{\omega_2} f^{\omega_3} \gamma_{ijkl}(-\omega_\sigma; \omega_1, \omega_2, \omega_3)
\end{aligned} \tag{5}$$

where N denotes the number density of molecules and f^ω denotes a local field correction factor, which accounts for the different electric field experienced by a molecule when it is immersed in a dielectric medium. This factor relates the local field $\boldsymbol{e}$ acting on the molecule, to the externally applied field $\boldsymbol{E}$ through $e_i^{(\omega)} = f_i^\omega E_i^{(\omega)}$. For optical fields, Lorentz–Lorenz local field factors [16] are commonly used, given by $f^\omega = (\varepsilon_\omega + 2)/3$, while for static fields, the Onsager local field factor [17], given by $f^0 = \varepsilon_0(\varepsilon_\infty + 2)/(2\varepsilon_0 + \varepsilon_\infty)$ is more appropriate. Here, ε_0 stands for the static dielectric constant of the surrounding medium and ε_∞ for the "internal" dielectric constant of the NLO molecule, at a sufficiently high frequency such that reorientational contributions to the dielectric constant are negligible, but low enough for the electronic and vibrational contributions to ε to be equal to their static limits. Usually, ε_∞ is derived from the refractive index n at optical frequencies, $\varepsilon_\infty \approx n^2$ or $\varepsilon_\infty \approx 1.05 \times n_D^2$, where the empirical factor of 1.05 accounts for the vibrational contribution to ε at lower frequencies. Both the Lorentz and the Onsager local field factors $f^\omega$and $f^0$are based on the assumption that the molecule occupies a spherical cavity in the dielectric medium. Replacing ε_0 in the Onsager local field factor by $\varepsilon_\omega \approx \varepsilon_\infty \approx n^2$ leads to the Lorentz local field factor, valid at optical frequencies, which shows the correspondence between both. Here, the assumption is made that the solute refractive index is equal to that of the solution. Although the latter is not a particularly good approximation for the highly polarizable molecules used in NLO, Lorentz local field factors are practically always applied for optical fields. Also the spherical cavity shape is questionable for the usually very elongated NLO molecules. These approximations are nevertheless made, because the additional parameters needed to improve on the standard Lorentz and Onsager local field factors are very hard to obtain. In the remainder of this chapter we will adopt these simplifications as well, except when the contrary is explicitly mentioned. A more detailed treatment of these issues can be found in Ref. [18].

1.3.2.2. Orientation

Equations (5) are valid only when all NLO molecules in the material have fixed identical orientations. This is rarely true, and the actual orientational distribution is an essential factor determining the macroscopic nonlinearities. This is particularly important for odd-order hyperpolarizabilities, which are antisymmetric under inversion of the molecular geometry. For instance, in a liquid solution or in an isotropic polymer blend, the NLO chromophores are randomly oriented, preventing such materials from possessing a nonzero macroscopic second-order NLO susceptibility $\chi^{(2)}$, even though the constituent molecules may be noncentrosymmetric and have a large β. For a second-order NLO material, it is thus

[2] This has led to contracted notations of $\beta(-2\omega; \omega, \omega)$ as a 3×6 matrix [5, 8].

not sufficient to have asymmetric molecules: a noncentrosymmetric ordering is also required on a macroscopic scale.[3]

For a material in which the NLO molecules have different (but fixed) orientations, the macroscopic susceptibilities should be calculated by summing the hyperpolarizabilities after transformation to a common laboratory coordinate system. Indicating laboratory coordinates by upper case indices and coordinates fixed to the molecule by lower case indices, we have

$$\begin{aligned} &\chi^{(2)}_{IJK}(-\omega_\sigma; \omega_1, \omega_2) \\ &\quad = Nf^{\omega_\sigma} f^{\omega_1} f^{\omega_2} \langle \beta_{IJK}(-\omega_\sigma; \omega_1, \omega_2) \rangle \\ &\chi^{(3)}_{IJKL}(-\omega_\sigma; \omega_1, \omega_2, \omega_3) \\ &\quad = Nf^{\omega_\sigma} f^{\omega_1} f^{\omega_2} f^{\omega_3} \langle \gamma_{IJKL}(-\omega_\sigma; \omega_1, \omega_2, \omega_3) \rangle \end{aligned} \tag{6}$$

where the tensor elements β_{IJK} and γ_{IJKL}, expressed in laboratory coordinates, are obtained from β_{ijk} and γ_{ijkl} in the molecular reference frame by

$$\beta_{IJK} = m_{Ii} m_{Jj} m_{Kk} \beta_{ijk} \qquad \gamma_{IJKL} = m_{Ii} m_{Jj} m_{Kk} m_{Ll} \gamma_{ijkl} \tag{7}$$

The transformation matrix elements m_{Ij} can be expressed in terms of the Euler angles describing the orientation of the molecule with respect to the laboratory frame. The parentheses represent averages over the orientational distribution of the molecules. For a crystal, these reduce to an average over the molecules in one unit cell. In Eq. (6), the spherical cavity local field factors were assumed, so that they can be treated as scalar factors rather than tensors and can be written outside the orientational average. When the material consists of a mixture of several compounds, the averages in (6) simply run over the molecules of all species, each with its own β.

For an isotropic medium, such as a liquid solution, orientational averages can only be nonzero for tensor components in which all indices (X, Y, Z) occur an even number of times. Hence, for an isotropic medium, $\langle\beta\rangle = 0$ and for $\langle\gamma\rangle$ only four different components exist among which only three are independent since they are connected by $\langle\gamma_{ZZZZ}\rangle = \langle\gamma_{XXZZ}\rangle + \langle\gamma_{XZXZ}\rangle + \langle\gamma_{XZZX}\rangle$. When Kleinman symmetry applies, the expressions further simplify and the TO NLO susceptibility of an isotropic medium is determined by only a single independent scalar quantity, often denoted by $\langle\gamma\rangle = \langle\gamma_{ZZZZ}\rangle$ [8, 20].

1.3.2.3. Reorientational Contributions

In Eq. (6) a direct relationship was given between the microscopic and macroscopic NLO parameters of corresponding orders, assuming the NLO molecules have fixed orientations. For a liquid or a gas, however, the constituting molecules can rotate and, depending on their symmetry, can be reorientated by the applied field itself. This leads to additional contributions to the macroscopic nonlinear polarization which are fundamentally different from the molecular electronic (or nuclear) polarizability. Such reorientational contributions have a much slower response time than the purely electronic polarizabilities and therefore can only contribute to certain NLO processes. One example is known in the linear case: the linear susceptibility (or dielectric constant) of a liquid or gas is not only determined by the molecular polarizability α but also (and usually predominantly) by the electric field induced reorientation of permanent dipoles. The latter contribution is proportional to μ^2. Due to its slower response time, it does not contribute to the refractive index at optical frequencies. Similarly, the nonlinear susceptibilities $\chi^{(n)}$ contain reorientational contributions proportional to combinations of lower order polarizabilities and/or the permanent dipole moment. Another general property of these reorientational contributions is their temperature dependence. When the applied fields are not too strong, so that the field induced orientation forms only a small perturbation on the random orientational distribution, the reorientational contributions are inversely proportional to temperature. These contributions are exploited in one of the main characterization techniques for SO NLO molecules based on the EFISHG effect (see Section 2.3). The macroscopic $\chi^{(3)}$ effect can, equivalently, be interpreted as a nonzero $\chi^{(2)}$ induced by the applied DC electric field. In this picture, the orientational alignment of the molecules by the external static electric field acting on the permanent dipoles breaks the centrosymmetry of the liquid or gas, thus allowing it to have a nonzero $\chi^{(2)}$.

1.4. Hyperpolarizability of Organic Conjugated Molecules

To introduce the basic mechanisms by which large hyperpolarizabilities occur in organic molecules, we first consider here an archetypal system, the polyene chain. A conjugated organic system is formed by a series of alternating single and double carbon–carbon bonds (Fig. 1). Such a chain consists of a series of sp^2 hybridized C atoms. Each C atom has three sp^2 orbitals which form σ bonds with three neighboring atoms in a planar triangular coordination. Each C atom then has one electron left in a p orbital, perpendicular to the coordination plane, which can form additional π bonds between carbon atoms. The prototype of a conjugated system is *trans*-polyacetylene (Fig. 1). The highest occupied molecular orbital of such a system consists of linear combinations of p orbitals with the same polarity on pairs of neighbor carbon atoms and opposite polarity between the pairs, corresponding to alternating double and single bonds. This leads, for the infinite chain of *trans*-polyacetylene, to a 2-fold degenerate electronic ground state, by a shift of the double bonds, and hence the π-electronic charge, along the whole chain by one position. It is easy now to induce this charge shift by an external electric field, and therefore such a chain has a very high polarizability. The ground state of a conjugated molecule may be considered as a resonance form of both molecular states. The induced dipole saturates for high electric fields as the electronic structure approaches one of both extreme forms, leading to the desired nonlinear polarizability. The (hyper)polarizabilities may be modeled qualitatively by an electron in a square well potential with an effective width corresponding to the size of the molecule (free-electron model) [21]. However, this model overestimates the increase of the hyperpolarizability with conjugation length ($\gamma \propto N^5$, with N representing the number of repeat units, while ab initio calculations give $\gamma \propto N^{3.2}$ to $N^{3.5}$) [8]. The chain length dependence of γ [22–25], including the saturation behavior at large lengths, is described far more realistically by more refined anharmonic potential models such as

[3] In fact, the reverse is also true: it was shown that strong SHG is possible from centrosymmetric molecules, provided they are packed in a noncentrosymmetric way, for example in a Langmuir–Blodgett film [19]. The effect can be large due to the occurrence of intermolecular charge transfer, but obviously cannot be optimized on the single molecule level.

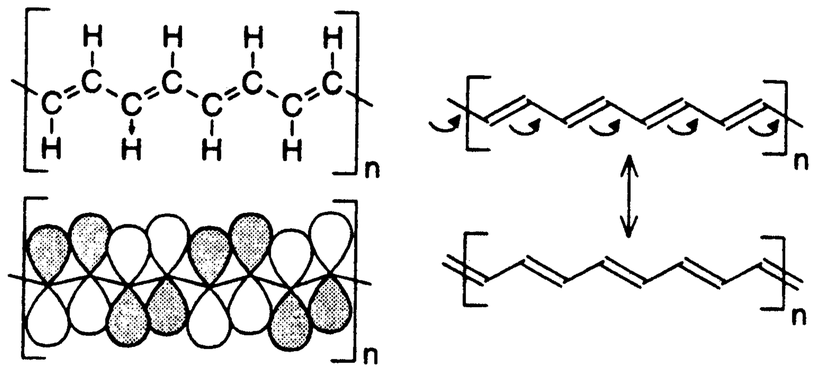

Fig. 1. Basic principle of a conjugated system, exemplified by all-*trans* polyacetylene. Left: Chemical structure and arrangement of the atomic 2p orbitals forming the molecular frontier π orbitals. Right: This conjugated polymer has two degenerate states, related by a shift of the π electronic charge and a reversal of the bond length alternation.

those developed for thiophene, phenylene, and pyrrole oligomers [26–30]. For a finite polyene oligomer or for a conjugated chain with lower symmetry, these two states are no longer exactly degenerate, but the energy difference is still small and typically gives rise to an optical transition in the visible part of the spectrum. Conjugated molecules are therefore often referred to as "organic dyes." When the low-energy optical transition is close to the laser wavelength or certain harmonics thereof, the hyperpolarizabilities can be strongly enhanced (see Sections 1.5.2 and 1.5.3). The optimum transition energy results from a tradeoff between this resonant enhancement and the increasing losses due to absorption [12, 31, 32].

To obtain a linear molecule with a high SO polarizability β the additional requirement of strong asymmetry should be met. This is achieved by asymmetric substitution by an electron donor and an electron acceptor group at both ends of the conjugated chain. The resulting class of systems, often called "push–pull" systems, then yields an asymmetric response. At this time, the highest hyperpolarizabilities known (both second- and third-order) are still those of molecules in which the conjugated backbone is close to an ideal polyene-like chain [33–37]. The longest of these are typically derived from the naturally occurring β-carotene[4] [37]. However, bare polyene chains tend to be extremely susceptible to oxidation. Mainly for this reason other approaches have been used within the framework of push–pull compounds to reach high hyperpolarizabilities. Three such compounds are shown in Figure 2a–c, with different conjugated segments (a modified polyene chain, a phenyl ring, and a phenylene–vinylene unit) and different donor and acceptor moieties, including an organometallic one (Fig. 2c). Among these is *para*-nitroaniline (*p*NA), one of the simplest examples of a push–pull molecule (Fig. 2b), which is often used as a calibration standard for β measurements. The results obtained to date with organic and organometallic push–pull systems will be covered in Sections 3 and 4, respectively.

The proposal by Zyss [41, 42] of high first hyperpolarizabilities in nondipolar molecules has opened a completely new pathway for the design of molecular SO NLO compounds. As he pointed out, besides the vectorial part of the third-order β tensor, which is the only one optimized in push–pull systems, an octupolar contribution is important in general. In fact, it turns out that it can have a comparable magnitude to the vectorial part and that nondipolar molecules with appreciable SO NLO parameters can be designed. An advantage of this approach is that octupolar molecules order more easily into noncentrosymmetric structures than dipolar ones. A lot of work along this track has been going on (see Sections 3 and 4). Several routes to such compounds were proposed and have been implemented both by organic and organometallic synthesis, and a few examples [43–45] are shown in Figure 2. In this case two design rules hold: a high polarizability is obtained from conjugated π-electron systems, and the molecules have to be noncentrosymmetric to make β nonzero. Planar [two-dimensional (2D)] as well as nonplanar octupolar molecules can be envisaged. The multipolar description of SO hyperpolarizability is discussed in Section 3.2, which also gives the state of the art for the design of organic compounds based on this approach. The results reached with organometallic compounds are reviewed in Section 4.6.

Apart from being an interesting new class of systems, the octupolar molecules have the potential to help overcome a number of limitations found for typical push–pull systems. Better opportunities for noncentrosymmetric ordering in crystals or thin films are expected owing to the absence of a permanent dipole moment. This aspect had already been tackled [46] by the design of push–pull molecules with zero, or near-zero, ground-state dipole moment (the POM compound in Table III), but now it is a direct consequence of the molecular symmetry. Also the rodlike shape of most dipolar-optimized molecules is replaced by planar or three-dimensional (3D) shapes which offer different possibilities to overcome the tendency for centrosymmetric alignment using, e.g., sterical effects or preferential hydrogen bonding. As in the case of the traditional systems, chirality may be a useful feature to achieve this goal. Also, a better tradeoff between optical nonlinearity and the transparency region was hoped for to counter the tendency observed in push–pull molecules that improvement in β values usually goes with increasing wavelength of the absorption. Finally, the occurrence of large nondiagonal β tensor elements allows for better solutions of phase-matching problems in SHG and for optimal use of the nonlinearity in EO devices, which are harder to tackle starting from materials with a single optimized tensor element. The so-called Λ-shaped systems (see Section 3.3) were an earlier strategy to solve these problems. It is worth mentioning that octupolar molecules are now also being investigated for possible optimization of the third-order polarizability γ [47, 48].

Today's methods of organic and organometallic synthesis allow for virtually infinite variations in molecular structure. Based on structure–property relations obtained from a combination of experimental and theoretical work, the molecular properties are thus being optimized. This includes the molecular hyperpolarizability, which is the subject of this chapter. Obviously, other optical properties (transparency, etc.), structural features (e.g., noncentrosymmetry in the case of NLO crystals and related to it chirality), and mechanical and chemical properties (solubility, chemical stability including stability against photoinduced decomposition and oxidation, ease of processing, etc.) are of great importance for applications as well and to some extent will be discussed in Section 4.

1.5. Theory and Modeling

1.5.1. Ab Initio and Semiempirical Calculations

It is of great interest to compare experimental results to theoretical results. To make the reader more familiar with this, the terminology regarding theoretical calculations will be briefly summarized here.

Many quantum chemical methods have been developed for the calculation of the electronic structure and other properties

[4] Even much larger polyene-like oligomers (hundreds of double bonds) have been synthesized by Samuel et al. [24] to study the saturation of γ with chain length.

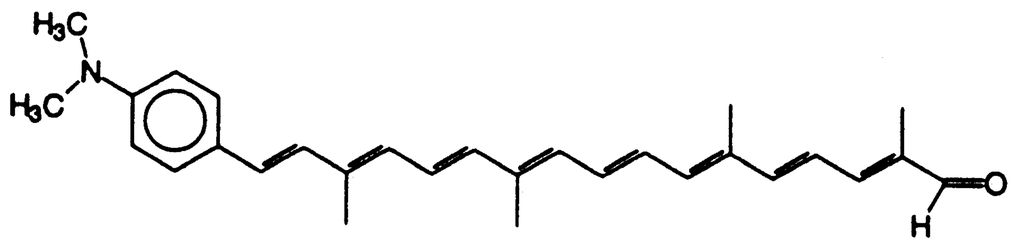

(a)

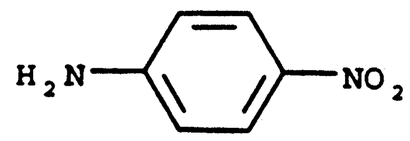

pNA

(b)

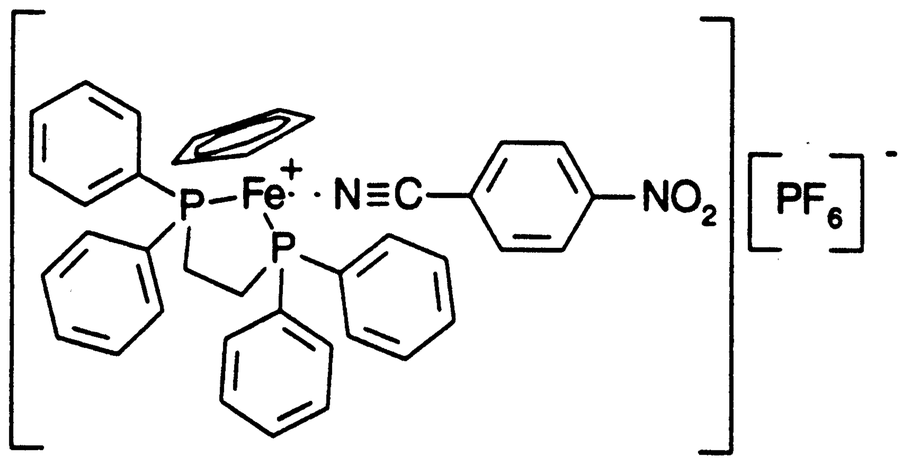

(c)

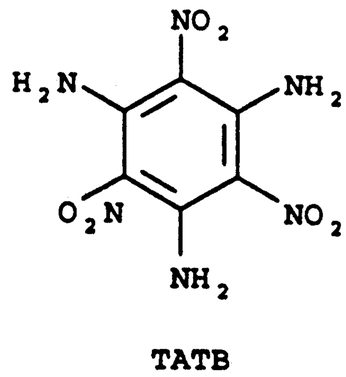

TATB

(d)

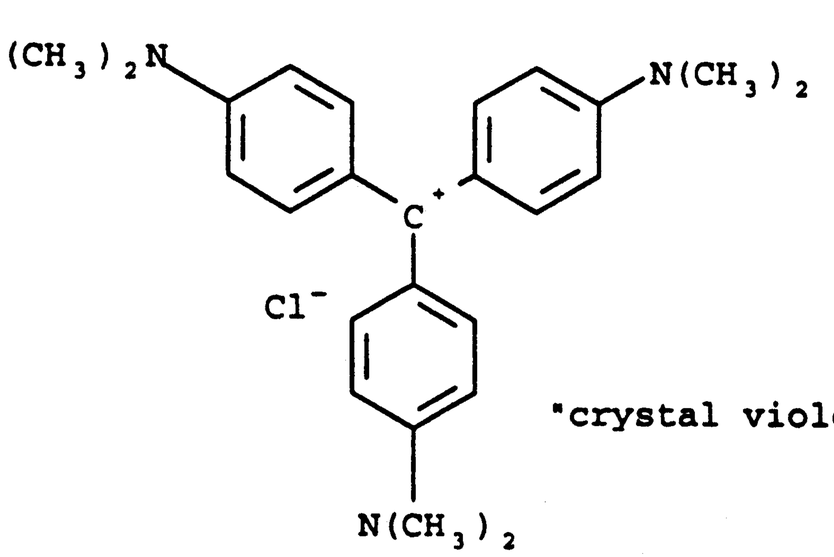

"crystal violet"

(e)

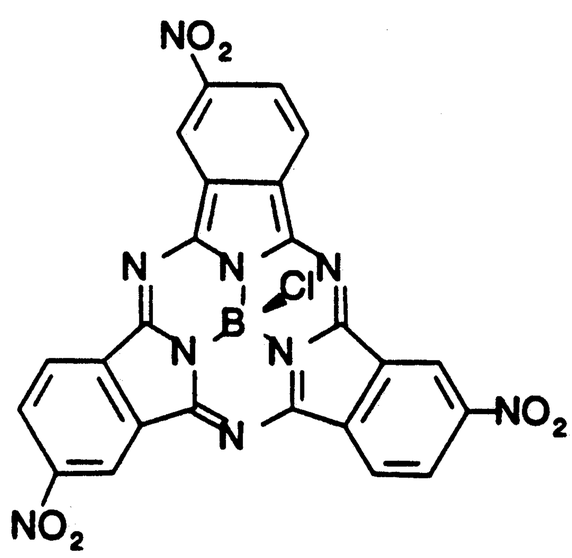

(f)

Fig. 2. Illustrative selection of SO NLO molecules including "push–pull"-type compounds, (a) a long polyene-type compound [38], (b) *para*-nitroaniline (*p*NA) [39], and (c) an efficient organometallic compound [40]; as well as nondipolar (octupolar) compounds, (d) triamino-,trinitrobenzene (TATB) [43] and (e) crystal violet [44]; and a lower-symmetry molecule with predominantly octupolar character, (f) a boron–subphthalocyanine compound [45].

of molecules. These methods can be classified into ab initio and semiempirical methods.[5] Ab initio methods are very demanding on computation time due to the rigorous numerical calculation of all one- and two-electron integrals needed in the calculation, performed at, for instance, the self-consistent field Hartree–Fock level. Computation time increases quickly with increasing number of atoms and with increasing number of basis functions, and such calculations are therefore limited to moderately sized molecules. Basis sets used are, in general, approximations to atomic orbitals (LCAO approach: linear combination of atomic orbitals), with either an exponential (Slater-type orbitals, STO) or Gaussian (Gaussian-type orbitals, GTO) radial part. A minimal basis set, called STO-3G, consists of expansions of the Slater-type atomic orbitals in terms of Gaussian functions. For the accurate calculation of NLO properties, larger basis sets are required than for simply calculating energy and molecular geometry. For instance, in another widely used basis set, 3-21G, each atomic orbital is described by two basis functions (a so-called "split valence" basis set). In addition, p- and d-type basis functions can be included for the hydrogen atoms to provide a better description of the outer regions of the molecule. These additional basis functions are termed "polarization functions" and are indicated by asterisks in the name of the basis set (e.g., 3-21G**).

Semiempirical methods differ from ab initio methods in several approximations. One major simplification is the use of empirical functions for evaluating the integrals rather than actually performance of the numerical integration. Most semiempirical methods only consider the valence electrons explicitly. The inner electrons

[5]The purely empirical "molecular mechanics" models developed for calculating the geometry of molecules are not discussed here because they are of no use in the calculation of NLO properties.

are treated as a fixed core potential. In addition, many integrals are neglected altogether. The functions describing the remaining integrals depend on parameters which are optimized to reproduce experimental (or ab initio) results (e.g., heat of formation and geometry) for a certain test set of molecules. Widely used semiempirical methods include, in order of increasing accuracy, the complete neglect of differential overlap (CNDO), the intermediate neglect of differential overlap (INDO), and the modified neglect of differential overlap (MNDO). A brief overview of these methods and their accuracy in predicting NLO properties can be found, for example, in Ref. [8]. Two improved versions of the MNDO method have been developed, the so-called Austin model 1 (AM1) [49] and parametric method 3 (PM3) [50, 51], which use a better set of empirical parameters than the original MNDO method, and are the most reliable among the semiempirical methods. An important limitation is that they use a minimal basis including only s- and p-type orbitals and thus are not applicable to transition metal compounds.[6]

For completeness, it should be mentioned that for the calculation of NLO parameters, a purely empirical "bond additivity" model has also been used. In this model, the hyperpolarizability of a molecule is considered as the tensorial sum of hyperpolarizabilities associated with individual bonds, in much the same way as the macroscopic susceptibility of a molecular material is obtained as a tensorial sum of hyperpolarizabilities of the constituting molecules. The hyperpolarizabilities of separate bonds are determined empirically. This model has been shown to give satisfactory results for saturated molecules such as alkanes. This can be attributed to the fact that the electrons in such molecules are strongly localized on specific σ bonds. Obviously, such a model cannot be expected to give meaningful results for conjugated molecules, which derive their large hyperpolarizabilities from the delocalization of π electrons over the whole molecule.

1.5.2. *Finite-Field Methods* versus *Sum-over-States Approach*

Regardless of the quantum chemical method used to calculate the electronic structure of a molecule (ab initio or semiempirical), two different approaches can be used to calculate its NLO properties. In the finite-field approach, an applied electric field is included directly in the Hamiltonian itself. The electronic structure (and the dipole moment derived from it) of the ground state of the molecule is then calculated for zero applied electric field and for a number of finite electric fields to determine numerically the derivatives of the dipole moment (or, equivalently, of energy) with respect to electric field, yielding the (hyper)polarizabilities. The finite-field approach is implemented in the widely used semiempirical package MOPAC [53], which uses either MNDO, AM1, or PM3 Hamiltonians [49–51, 54, 55]. Including the electric field in the Hamiltonian is computationally very efficient as only the electronic ground state of the molecule needs to be calculated. However, this approach yields little insight into the factors that determine the calculated hyperpolarizability.

The other approach is derived from perturbation theory, which yields expressions for the (hyper)polarizabilities in terms of excited-state energies and dipole moment matrix elements [56, 57]. For the first hyperpolarizability, expressions have been derived

[6]The extension of the semiempirical MNDO method to include d orbitals (MNDO/d) has been described [52].

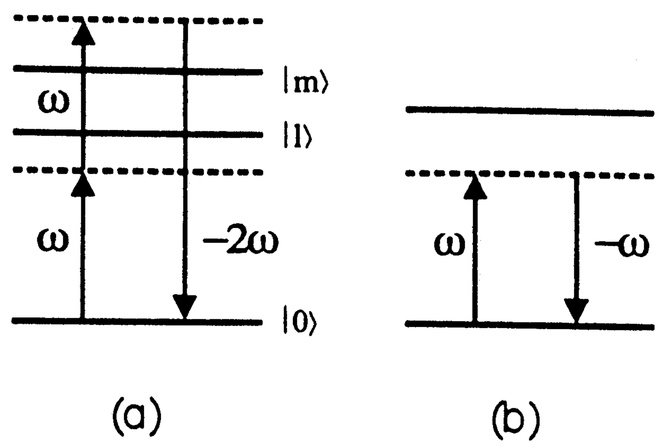

Fig. 3. Energy level diagrams illustrating (a) that one- and two-photon resonances are possible in SHG, in $\beta(-2\omega; \omega, \omega)$, while (b) only a one-photon resonance occurs in the EO effect, in $\beta(-\omega; \omega, 0)$.

[58] of the type (using the Taylor series definition, see Appendix),

$$\beta_{ijk}(-\omega_\sigma; \omega_1, \omega_2) = \frac{1}{\hbar^2} P(i, j, k; -\omega_\sigma, \omega_1, \omega_2) \times \sum_{l\neq 0} \sum_{m\neq 0} \frac{\langle 0|\mu_i|l\rangle \langle l|\bar{\mu}_j|m\rangle \langle m|\mu_k|0\rangle}{(\omega_{0l} - \omega_\sigma)(\omega_{0m} - \omega_2)} \tag{8}$$

where the permutation operator $P(i, j, k; -\omega_\sigma, \omega_1, \omega_2)$ indicates a summation over all six permutations of (i, j, k) with simultaneous permutation of $(-\omega_\sigma, \omega_1, \omega_2)$; $\langle l|\bar{\mu}_j|m\rangle = \langle l|\mu_j|m\rangle - \langle 0|\mu_j|0\rangle\delta_{lm}$, and ω_{0l} is the transition frequency between the ground state and state $|l\rangle$.

Many related expressions, including simplifications for specific NLO processes, can be found in the literature [58–62]. Thus, to calculate the hyperpolarizabilities using these so-called sum-over-states (SOS) expressions, the electronic structure of the ground state as well as of a large number of excited states needs to be calculated. The latter is time consuming as it requires configuration–interaction calculations. However, the SOS approach is a very powerful method in that it automatically yields the frequency dependence of the hyperpolarizabilities. The individual terms of the expressions reflect the contributions from specific transitions, and the effect of near-resonance enhancement is evident from the denominators. The terms in the SOS expressions can be represented schematically in an energy level diagram as illustrated in Figure 3. From these equations it follows that, for example, $\beta(-2\omega; \omega, \omega)$ can be enhanced by a one- or a two-photon resonance and $\beta(-\omega; 0, \omega)$ only by a one-photon resonance. The above expressions are not valid *at* resonance. Phase shifts become important at resonance, which can be phenomenologically incorporated into Eq. (8) by adding imaginary damping factors ($i\Gamma_{j0}$) to the energy differences in the denominators, resulting in a complex hyperpolarizability.

1.5.3. *Two-Level Model*

An important special case of the SOS expression for β is that of the two-level model [39]. Assuming that only a single charge-transfer transition contributes to β and that the dipole moment difference $\Delta\mu$ and the transition dipole μ_{eg} are parallel to each other (chosen to be along the z axis), the first hyperpolarizability only has a zzz component, given by [8, 39] (using the phenomenological convention [58])

$$\beta_{zzz}(-2\omega; \omega, \omega) = \frac{3e^2}{2\hbar m} \frac{\omega_{eg} f_{osc} \Delta\mu}{(\omega_{eg}^2 - \omega^2)[\omega_{eg}^2 - (2\omega)^2]} \tag{9}$$

where f_{osc} is the oscillator strength of the charge-transfer transition and ω_{eg} is its frequency. As this is the simplest model which can account for dispersion of the first hyperpolarizability [39, 63–65], it is often used to compare experimental β values obtained at different wavelengths or with different techniques or to compare experimental hyperpolarizabilities with static values β_0 from theoretical calculations. For this purpose, the transition frequency ω_{eg} is usually taken to be the position (maximum) of the lowest energy strong absorption band.

The two-level model has proven to be particularly fruitful for the understanding of NLO properties in push–pull molecules, which in most cases possess a low-lying well-separated $\pi \rightarrow \pi^*$ transition which accounts for most of the nonlinear polarizability. In many cases, however, contributions from different transitions are expected, and the reduction to β_0 becomes questionable. Moreover, as pointed out by Zyss [42] the two-level model is intimately related to the concept of push–pull molecules and falls short of describing the SO NLO effect in octupolar molecules, where at least two (degenerate) excited states must be involved in the sum of Eq. (8).

2. EXPERIMENTAL TECHNIQUES

In this section an overview is given of the different techniques which are commonly used for the measurement of SO polarizability of molecules. We will be focusing on the differences between the techniques which are important when comparing results in the literature. Among these techniques, solvatochromism measurements, EFISHG, and HRS are aimed at the direct determination of the molecular hyperpolarizability. The more recent, but by now very popular, HRS technique will be more extensively discussed, reflecting new developments and taking into account recent reports on possible problems and caveats. Kurtz powder SHG has been used extensively as a screening method for new compounds. For this reason it will be presented in spite of the fact that it offers information only on the SO NLO susceptibility of the crystals. In a series of papers [66–69], Zerbi and coworkers pointed out a strong relationship between the intensities in vibrational spectra—infrared absorption and Raman scattering—of organic NLO compounds and their first and second hyperpolarizabilities. For a number of cases they showed good correspondence between the parameters derived from such routine spectroscopic techniques and those obtained from the more intricate NLO experiments. Another approach suitable for characterization of the SO NLO properties of compounds in solution, probes SHG in a six-wave mixing configuration [70]. It derives from the investigations which have led to all-optical orientation of chromophores (see also Section 5) and has been applied by the initiating group to several chromophores [71]. Up to now use of both of these methods is not widespread, and we refer to the original articles for more details.

Through different steps of interpretation and modeling (e.g., within the frozen gas model), single molecule NLO properties can in many instances be derived from macroscopic susceptibility measurements of crystals, thin films, or poled polymers, from measurements of SHG, by means of the evanescent wave SHG method, or by EO measurements (see Ref. [72] for a review). It is also worth mentioning here related investigations of charge-transfer processes in molecules by means of electroabsorption measurements, which help to unravel the mechanisms of their SO NLO response [73]. In this chapter we will however restrict ourselves to those methods aiming at a direct determination of the single molecule β values.

2.1. Kurtz Powder Second-Harmonic Generation

In this method, developed by Kurtz and Perry [74], a laser beam is focused onto a crushed crystalline sample, and the intensity of the generated second-harmonic light is detected. In this way, a measure for the macroscopic second-order susceptibility $\chi^{(2)}(-2\omega; \omega, \omega)$ of the crystals is obtained. A good analysis of the results is not trivial and requires a powder with a well-determined grain size. Indeed, the generated second-harmonic intensity depends not only on $\chi^{(2)}$, but also on phase-matching properties, optical absorption, grain size distribution, etc. An accurate determination of the macroscopic $\chi^{(2)}(-2\omega; \omega, \omega)$ of crystalline materials is therefore usually done by SHG measurements on large single crystals (which are generally difficult to grow [75]).

In addition, the relation between macroscopic $\chi^{(2)}$ and molecular β is also dependent on crystal packing. In particular, the Kurtz powder technique is not applicable to compounds which crystallize into a centrosymmetric space group.

Because of the complicated interpretation, the Kurtz powder technique is mainly used only as a first rough screening technique to help select materials which look promising enough for further study with other techniques. If used in this way, i.e., when no accurate $\chi^{(2)}$ values are required, so that knowledge of the grain size distribution is not really needed, the extremely simple sample preparation can be considered as a true advantage of this method.

2.2. Solvatochromism

The solvatochromic method for the determination of molecular first hyperpolarizabilities is not a true NLO measurement, but rather an estimation based on the two-level model [39, 76], in which the necessary parameters are derived from spectroscopic data. Within the two-level model [39] [see Section 1.5.3, Eq. (9)], the first hyperpolarizability depends only on the frequencies of the optical fields, the frequency ω_{eg} and oscillator strength f of the transition between ground and excited state, and the dipole moment difference $\Delta\mu$ between both states. The parameters ω_{eg} and oscillator strength f can be readily obtained from an optical absorption spectrum (position and integrated intensity of the absorption band, respectively). To determine the dipole moment difference between ground and excited state, the spectral shift of the absorption spectrum is measured when the molecule is dissolved in solvents of different polarity. When a dipolar molecule is dissolved, the surrounding solvent molecules are oriented (if dipolar) and polarized by the field of the solute dipole moment. These oriented and polarized solvent molecules in turn exert an electric field on the solute molecule, called the reaction field, which tends to increase the solute dipole moment, lowering the energy of the more dipolar state compared to the less dipolar state of the solute molecule. Thus, for the most common case of a solute molecule which increases its dipole moment upon excitation ($\mu_e > \mu_g$), the transition energy will be lower in more polar solvents. This change in energy is called the solvatochromic shift. Various models have been developed to describe this reaction field and the resulting solvatochromic shift [16, 77]. One of the equations often used to relate the solvatochromic shift to the macroscopic properties of a

solvent is [78]

$$hc\left(\nu_{eg}^{\text{solution}} - \nu_{eg}^{\text{gas}}\right) = \frac{1}{4\pi\varepsilon_0 r^3}\left[2\left(\frac{\varepsilon-1}{\varepsilon+2} - \frac{n^2-1}{n^2+2}\right)\left(\mu_e - \mu_g\right)\mu_g + \frac{n^2-1}{n^2+2}\left(\mu_e^2 - \mu_g^2\right)\right] \tag{10}$$

where ε and n are the solvent dielectric constant (at low frequency) and refractive index (at optical frequencies), and r is the Onsager cavity radius, i.e., the radius of the cavity occupied by the solute molecule. The two terms in this equation correspond to the effects of reorientational and electronic polarization contributions to the solvent dielectric constant ε. Compared to the quasi-instantaneous electronic excitation process, the reorientation of solvent molecules is very slow; hence the orientational distribution of the solvent molecules remains unchanged during the transition and is thus only determined by μ_g. During the excitation, the stabilization energy due to the reorientational component of the reaction field is thus proportional to μ_g^2 and $\mu_e\mu_g$ for the solute ground and excited state, respectively. This explains the first term in (10). Similarly, the second term originates from the electronic polarization contribution to the reaction field, which follows the solute dipole moment quasi-instantaneously, resulting in stabilization energies proportional to μ_g^2 and μ_e^2. Thus, by measuring the absorption spectrum of a compound in two different solvents and measuring the shift of the charge-transfer band, $\Delta\mu = \mu_e - \mu_g$ can be determined from Eq. (10), provided the ground-state dipole moment is known. The latter may, for instance, be determined by solution dielectric constant measurements [16]. The second term in Eq. (10) can often be neglected as the difference in ε between solvents is usually much larger than the difference in n.

As this solvatochromic method is a very indirect way to evaluate β and moreover relies on the two-level model which is only applicable to dipolar molecules and is even then an approximation, this technique generally does not yield accurate β values. However, it is a useful method for predicting general qualitative trends [39]. In particular, the sign of the solvatochromic shift gives valuable information on the sign of $\Delta\mu$ and thus on the sign of β (with respect to the direction of $\vec{\mu}$, that is).

2.3. Electric Field Induced Second-Harmonic Generation

Coherent second-harmonic generation is not allowed in an isotropic medium such as a liquid. By applying a static electric field, dipolar molecules in a liquid can be oriented (or deformed), thus breaking the macroscopic centrosymmetry and enabling coherent frequency doubling of a laser beam incident on the liquid. Macroscopically, this is a third-order process related to $\chi^{(3)}(-2\omega;\ \omega,\ \omega,\ 0)$, which includes contributions from the first hyperpolarizability of molecules oriented by the static field, as well as from the electronic and vibrational second hyperpolarizability [8, 79–81],

$$\chi^{(3)}(-2\omega;\ \omega,\ \omega,\ 0) \propto \left\langle\gamma(-2\omega;\ \omega,\ \omega,\ 0)\right\rangle + \frac{\vec{\mu}^0 \cdot \vec{\beta}(-2\omega;\ \omega,\ \omega)}{5kT} \tag{11}$$

where $\vec{\beta}$ is the vectorial part (or dipolar part, see Section 3.2) of the first hyperpolarizability tensor.[7] This electric field induced second-harmonic generation (EFISHG or EFISH) effect was first observed in calcite crystals by Terhune et al. [82, 83] and others [84]. Later, the effect was also observed and described theoretically for liquids [79, 85–87] and gases [88, 89], including the reorientational contribution. Soon, EFISHG became the most widely used experimental technique for the measurement of molecular first hyperpolarizabilities in liquid solutions [90–94]. Only in recent years has the hyper-Rayleigh scattering technique become comparably or even more widely used.

In EFISHG, a coherent light beam is generated at the second harmonic, usually in non-phase-matching conditions, with a coherence length typically in the tens to hundreds of microns range. In the standard setup, a millimeters wide wedge of the liquid solution is translated through the incident laser beam, resulting in the so-called *Maker fringes* in the EFISHG intensity as a function of displacement of the cell. The static field is generated by a high voltage over electrodes in contact with the solution. To reduce conductivity problems, which can occur even with common solvents, a quasi-static field with constant value over a microsecond time interval is usually employed. A Q-switched Nd:YAG laser with low repetition rate (10–30 Hz) has been the workhorse in many EFISHG instruments, often combined with a H_2 Raman shifter to excite at 1.906 nm, as far as possible from resonance. Recently, EFISHG measurements with a high repetition rate mode-locked laser with tunable frequency have been demonstrated [95]. As in the case of HRS (see next section), it is then possible to apply high-frequency demodulation techniques. In general, the fundamental laser beam may be focused in the liquid for higher efficiency, but the focus should not be too tight to avoid dielectric breakdown of the liquid or other NLO phenomena such as self-(de)focusing. Although referencing to an oriented crystal quartz plate has been a standard in EFISHG, sometimes measurements were calibrated with respect to the solvent [96], which is the so-called internal reference method that later was strongly promoted for HRS experiments (see below).

With the EFISHG technique it is possible to determine the sign of $\chi^{(3)}$, relative to a crystal with a $\chi^{(2)}$ of known sign [92, 94]—in much the same way as relative signs of $\chi^{(2)}$ of second-order NLO crystals are determined [97]—or relative to the sign of the solvent $\chi^{(3)}$, from the concentration dependence of the EFISHG signal. From the measured $\chi^{(3)}$, $\vec{\mu}^0 \cdot \vec{\beta}$ can be derived, provided γ is known from another technique (e.g., γ from THG, after adequate correction for dispersion). For strongly dipolar molecules, γ is most often assumed to be negligible compared to $\vec{\mu}^0 \cdot \vec{\beta}$. Alternatively, the electronic and reorientational terms of Eq. (11) may be discriminated in EFISHG measurements by studying the temperature dependence [79, 86]. Clearly, to deduce β, the dipole moment needs to be determined. Note that even then, only the projection of $\vec{\beta}$ on the direction of $\vec{\mu}^0$ is obtained. In some cases, the angle between $\vec{\mu}^0$ and $\vec{\beta}$ has been found to be surprisingly large (up to nearly 90°, from theoretical calculations) [98].

The fact that, for the nonresonant case, only one independent quantity can be determined is a strong limitation of EFISHG compared to HRS, which even in a linear polarization geometry can be

[7] Numerical prefactors of γ and $\mu^0\beta$ depend on the convention used—the expression given here is valid for any (including B*) except the B (perturbation series) definition, in which the factor $5kT$ should be replaced by $15kT$ (see Ref. [58]).

employed to evaluate the anisotropy and multipolar nature of the β tensor (see Sections 2.4 and 3.2). However, polarized EFISHG measurements can be used to determine deviations from Kleinman symmetry in near-to-resonant conditions for molecules with large off-diagonal β components [99, 100].

2.4. Hyper-Rayleigh Scattering

2.4.1. Background

As mentioned before, coherent frequency doubling can occur only in a macroscopically noncentrosymmetric system. Therefore, the measurement of molecular first hyperpolarizabilities $\beta(-2\omega; \omega, \omega)$ in liquid solutions has long been limited to the EFISHG technique, in which a static electric field is used to break the macroscopic symmetry by orienting the molecules. However, because a liquid is a disordered system and is microscopically noncentrosymmetric, it is possible for a liquid to produce *incoherent* second-harmonic light scattering. This effect was predicted theoretically in 1964 by Yin-Yuan [101], Kielich [102], and Bersohn [103] and was proposed as a new tool for the study of macromolecules in solution [103]. It was first observed in 1965 by Terhune et al. [104], who used it, for instance, to determine the molecular hyperpolarizability β (i.e., β_{xyz}) of the octupolar molecule CCl_4. A thorough theoretical description of this nonlinear scattering and its polarization properties was provided by Bersohn et al. in 1966 [105]. The technique has been used in the study of the nonlinear optical properties and intermolecular interactions of various small molecules (typically organic solvents) in the liquid as well as in the vapor phase [104, 106–109].

Nevertheless, it took until 1991 for this second-harmonic light scattering [110] or hyper-Rayleigh scattering (HRS) [111] to be rediscovered and recognized as a valuable alternative technique for the measurement of $\beta(-2\omega; \omega, \omega)$ of organic NLO molecules in liquid solutions by Clays and Persoons [111, 112]. The effect has been dubbed "hyper-Rayleigh scattering" [111], in analogy with linear elastic scattering from small polarizable particles or molecules [113]. Since then, the technique has become widely used and has been refined by many researchers in the field [18, 40, 43, 110, 114–131]. Unfortunately, upon the reintroduction of HRS for the study of NLO chromophores in solution, a simplification was made [111] to the original setup of Terhune et al. [104], by using only an interference filter to select the second-harmonic wavelength and omitting the monochromator, which was known to be essential to discriminate between HRS and multiphoton fluorescence [107, 108]. It has even been incorrectly assumed that the two-photon fluorescence contribution was to be included in the HRS signal as a genuine β effect [132], while it can in fact be described as a third-order process related to $\mathrm{Im}[\gamma(-\omega; \omega, \omega, -\omega)]$ [8]. The simplified setup was adopted by many others [110, 114, 116, 119, 133–135], even after several articles had been devoted to this problem [115, 124, 136]. This led to many erroneously high β values[8] [110, 133, 137–140], which have later been observed to be much smaller [116–118, 141–143]. Many other reported values (e.g., [144, 145]) should be suspected for the same reason, as most HRS measurements are performed at resonance and without correcting for luminescence by spectral analysis of the scattered light. Other techniques for background reduction which can alleviate this problem will be discussed further on, but it remains advisable to apply these procedures in conjuction with the simple test constituted by the spectral analysis. All said, HRS is a very sensitive and reliable technique for the determination of the molecular hyperpolarizability, provided that the spectral content of the scattered light is systematically recorded by means of a monochromator.

The HRS technique has been shown to possess different advantages compared to EFISHG for the determination of the first hyperpolarizability of molecules. There is no need for the cumbersome kilovolt high-voltage pulses over the liquid, and as a result, conducting liquids (e.g., most polar solvents and solutions of ionic compounds) can also be investigated. Molecules without or with small permanent dipole moments can be easily studied, including the octupolar molecules on which rest hopes for design of new SO NLO materials. Even in the case of dipolar molecules, the β value is measured directly, without need for knowledge of the size and relative direction of the permanent dipole moment, as is the case in EFISHG. Also, due to the incoherent nature of the HRS process, the intensity is linear with concentration (and not quadratic as in EFISHG), allowing for measurements at lower concentration. This can be important when the compound is weakly soluble or has an appreciable absorption at the second-harmonic wavelength. Finally, while EFISHG yields in general only a single independent quantity, HRS yields information about the symmetry of the β tensor through the relative intensities in polarized measurements. The information that can be accessed through the depolarization ratio will be discussed in Sections 2.4.2 and 3.2.1.

In the remaining part of this section a brief description of the theoretical background of the HRS effect and its use as a measurement technique will be given, and an experimental setup used in our own investigations [18, 40, 129] will be described and compared to other ones described in the literature. Also, we will go into further detail concerning the practical application of the technique for the determination of the first hyperpolarizability of molecules.

2.4.2. Basic Description

Consider a macroscopic collection of N molecules subject to an incident light beam polarized along the laboratory Z-axis. The molecules are randomly oriented and also there are no orientational correlations between them. The latter is expected to be a good approximation for gases and for dilute liquid solutions of NLO molecules. The scattered second-harmonic field is obtained by summing the second-harmonic *fields* from the individual molecules.

In a single molecule, subject to the incident beam with angular frequency ω, a dipole moment will be induced with a frequency component $\vec{\mu}^{(2\omega)}$ at 2ω, given by

$$\mu_J^{(2\omega)} = \beta_{JZZ}(-2\omega; \omega, \omega)E_Z^2 \tag{12}$$

where E_Z is the local field associated with the incident beam, and capital indices stand for Cartesian components in the laboratory reference frame. This oscillating dipole will emit electromagnetic radiation at 2ω. The contribution to the second-harmonic field $E_J^{(2\omega)}$ for scattering in the Y direction and polarized along the $J(= X$ or $Z)$ direction is proportional to $\mu_J^{(2\omega)}$. Within the assumptions made, it can be shown [103, 146–148] that the total second-harmonic intensity $\langle I_J^{(2\omega)} \rangle$, which is proportional to

[8] Among other suggested explanations [116, 141], multiphoton fluorescence is the most plausible one in these cases, considering the reported experimental procedures.

$\langle |E_J^{(2\omega)}|^2 \rangle$, is nonzero and identical to the sum of the *intensities* of N individual scatterers,

$$\left\langle I_J^{(2\omega)} \right\rangle = g\left\langle \left| E_J^{(2\omega)} \right|^2 \right\rangle = g\left\langle \left| \sum_{i=1}^{N} E_{J_i}^{(2\omega)} \right|^2 \right\rangle$$
$$= gN\left\langle \left| E_{J_i}^{(2\omega)} \right|^2 \right\rangle = N\left\langle I_{J_i}^{(2\omega)} \right\rangle \tag{13}$$

in which $g = nc\varepsilon_0/2$ (in SI units, conversion to cgs: $g = nc/8\pi$) and $\langle I_{J_i}^{(2\omega)} \rangle$ stands for the second-harmonic intensity scattered by a single molecule, averaged over all possible orientations. Combining Eqs. (12) and (13) leads to

$$\left\langle I_J^{(2\omega)} \right\rangle = GN\left\langle |\beta_{JZZ}|^2 \right\rangle \left(I_Z^{(\omega)} \right)^2 \tag{14}$$

where the proportionality factor G includes the local field correction factors f_ω and $f_{2\omega}$. G is given by [148] (in SI units)

$$G = \frac{32\pi^2}{\varepsilon_0^3 c \lambda_\omega^4 r^2} f_\omega^4 f_{2\omega}^2$$

Note that the scattering intensity is proportional to N (not N^2), as expected for an incoherent process. The orientational averages $\langle |\beta_{JZZ}|^2 \rangle$ of the β components in the laboratory frame can be calculated in terms of the molecular components β_{ijk} (where lower case indices indicate Cartesian components in the reference frame fixed to the molecule), from their transformation properties under rotation. In the case of Kleinman symmetry, this yields the quadratic forms [149]

$$\left\langle \beta_{ZZZ}^2 \right\rangle = \tfrac{1}{7} \sum_i \beta_{iii}^2 + \tfrac{6}{35} \sum_{\substack{i,j \\ i \neq j}} \beta_{iii}\beta_{ijj} + \tfrac{6}{35} \sum_{\substack{i,j,k \\ i \neq j < k \neq i}} \beta_{iij}\beta_{jkk}$$
$$+ \tfrac{9}{35} \sum_{i \neq j} \beta_{iij}^2 + \tfrac{12}{35} \beta_{xyz}^2 \tag{15}$$

$$\left\langle \beta_{XZZ}^2 \right\rangle = \tfrac{1}{35} \sum_i \beta_{iii}^2 - \tfrac{2}{105} \sum_{\substack{i,j \\ i \neq j}} \beta_{iii}\beta_{ijj} - \tfrac{2}{105} \sum_{\substack{i,j,k \\ i \neq j < k \neq i}} \beta_{iij}\beta_{jkk}$$
$$+ \tfrac{11}{105} \sum_{i \neq j} \beta_{iij}^2 + \tfrac{8}{35} \beta_{xyz}^2 \tag{16}$$

Here, the summations are organized in such a way that no identical binary products are included more than once, so the summations over $i \neq j$ include six terms and the summations over $i \neq j < k \neq i$ include three terms ($\beta_{xxy}\beta_{yzz}$, $\beta_{yyx}\beta_{xzz}$, and $\beta_{zzx}\beta_{xyy}$). Analogous expressions for the more general case without the assumption of Kleinman symmetry are given in Ref. [105].

From Eqs. (14), (15), and (16) it is clear that the HRS intensity is a measure of the molecular hyperpolarizability and that measurements of the depolarization ratio $I_X/I_Z = \langle \beta_{XZZ}^2 \rangle / \langle \beta_{ZZZ}^2 \rangle$ gives additional information on the relative magnitudes of the tensor components of β, as different combinations of tensor components contribute to the different polarization components of the scattered light. It is interesting to note from Eqs. (15) and (16) that *all* β tensor components contribute to the HRS intensity, including the component β_{xyz}. The HRS technique therefore also enables first hyperpolarizability measurements of molecules with octupolar symmetry (e.g., with D_{3h} or T symmetry) [43, 104, 110, 118, 150], which is not possible with the EFISHG technique, as both the dipole moment and the vectorial part of β are zero for such molecules. Also the possibility of deriving additional information on the tensor components of β from polarized measurements is unique to the HRS technique, as EFISHG measurements determine only a single scalar quantity $\vec{\mu} \cdot \vec{\beta}$. It has been shown [104, 105, 151] that by using HRS, in principle, a total of six independent combinations of tensor components can be accessed experimentally (or five if β is assumed to be real), which requires the use of both linearly and elliptically polarized incident beams [105]. The number of independent β tensor components is 18 for a real β (and even 36 in general),[9] and reduces to 10 in the case of Kleinman symmetry). The extension to incoherent sum-frequency generation has also been considered [122], but the possibility of determining a larger number of tensor components than with HRS has never been put into practice. In any case the number of unknown independent tensor components is larger than the number of observable quantities, unless additional symmetry considerations reduce this number of independent tensor components.

Obviously, the use of linearly polarized light is not an important limitation in the case of push–pull systems in which only the diagonal component β_{zzz} along the long axis of the conjugated chain is expected to be important. For the limiting case of an ideal linear molecule, exhibiting only a single (diagonal) nonzero β component, Eqs. (15) and (16) reduce to

$$\left\langle \beta_{ZZZ}^2 \right\rangle = \tfrac{1}{7}\beta_{zzz}^2 \quad \text{and} \quad \left\langle \beta_{XZZ}^2 \right\rangle = \tfrac{1}{35}\beta_{zzz}^2 \tag{17}$$

leading to a depolarization ratio of $\frac{1}{5}$. Thus, the unpolarized detection of the scattered second-harmonic intensity allows for the determination of β_{zzz}, and a measurement of the depolarization ratio provides an indication whether the assumption of a single dominant β component is indeed valid.

A more elaborate theoretical description of HRS, including cooperative scattering contributions due to orientational correlations between molecules, has been given by Bersohn et al. [105]. We are mainly concerned with HRS from dilute solutions of NLO chromophores, in which orientational correlations between chromophores can be neglected. It should be realized though, that cooperative effects are important for the HRS signals from the solvents and may therefore significantly affect the calibration of the HRS measurements using the internal reference method based on literature values (e.g., from EFISHG) for a solvent (see Section 2.4.3.3).

2.4.3. *Experimental Determination of Hyperpolarizabilities*

Equation (14) shows that measuring the second-harmonic scattering intensity provides a measure of β. However, the proportionality constant between $N\langle \beta_{IJJ}^2 \rangle$ and the observed intensity $I_I^{(2\omega)}$ depends on many factors, including the absolute collection and detection efficiency, and—through the quadratic intensity dependence—the laser beam quality, pulse width, and coherence properties of the laser beam. Therefore, to determine hyperpolarizabilities of molecules in solution, HRS measurements are always calibrated against a compound with known β.[10] This ref-

[9] Counting the real and imaginary parts as separate independent variables.

[10] This is different from the EFISHG technique, in which calibration is usually against coherent frequency doubling in a crystalline material, with crystalline quartz as most popular standard.

erence standard may be a solution of another NLO chromophore (external reference method) [144] or it may be the pure solvent itself (internal reference method) [111, 124].

2.4.3.1. *Internal Reference*

The most convenient way to determine the hyperpolarizability of a compound dissolved in a solvent with known β is to use the solvent itself as a calibration standard [111]. When a HRS measurement performed in the pure solvent is compared to one in a dilute solution of a compound in the same solvent, the refractive indices of both samples can be assumed to be the same, so that the refraction and reflection on the walls of the sample cell remain unchanged. The power and geometry of the incident beam as well as the geometry and efficiency of the scattered light collection are thus identical for the unknown and reference samples. In addition, if the usual spherical Lorentz local fields are assumed, these will also be the same in both cases and need not be considered. Small effects due to (thermal) self-defocusing are essentially the same for the dilute solution as for the pure solvent, and thus tend to cancel out as well. The signals can thus be regarded as depending only on the molecular hyperpolarizabilities and the number densities of the solvent and solute molecules,

$$\begin{aligned} S_{\text{solvent}}^{(2\omega)} &\propto N_{\text{solvent}}\left\langle\beta_{\text{solvent}}^2\right\rangle\left(P_Z^{(\omega)}\right)^2 \\ S_{\text{solution}}^{(2\omega)} &\propto \left(N_{\text{solvent}}\left\langle\beta_{\text{solvent}}^2\right\rangle\right. \\ &\quad \left. + N_{\text{solute}}\left\langle\beta_{\text{solute}}^2\right\rangle\right)\left(P_Z^{(\omega)}\right)^2 \end{aligned} \tag{18}$$

where $\langle\beta^2\rangle$ stands for the appropriate orientational average of the β tensor: $\langle\beta_{XZZ}^2\rangle$ or $\langle\beta_{ZZZ}^2\rangle$ for polarized measurements, and $\langle\beta_{XZZ}^2\rangle + \langle\beta_{ZZZ}^2\rangle$ for unpolarized measurements. If both measurements are performed under the same experimental conditions, Eqs. (18) lead to

$$\left\langle\beta_{\text{solute}}^2\right\rangle = \frac{N_{\text{solvent}}}{N_{\text{solute}}}\frac{S_{\text{solution}}^{(2\omega)} - S_{\text{solvent}}^{(2\omega)}}{S_{\text{solvent}}^{(2\omega)}}\left\langle\beta_{\text{solvent}}^2\right\rangle \tag{19}$$

When the approximation is made that the β tensors of both solvent and solute are dominated by β_{zzz}, this may also be written as

$$\beta_{\text{solute}}^{zzz} = \sqrt{\frac{N_{\text{solvent}}}{N_{\text{solute}}}\frac{S_{\text{solution}}^{(2\omega)} - S_{\text{solvent}}^{(2\omega)}}{S_{\text{solvent}}^{(2\omega)}}}\,\beta_{\text{solvent}}^{zzz} \tag{20}$$

Although this is expected to be a very good approximation for push–pull NLO chromophores, it is not applicable to systems with a significant octupolar β component nor is it expected to be a particularly good approximation for solvent molecules. In these cases, additional assumptions concerning the ratios between tensor components are needed to improve on this analysis. When the β values of the solvents are calibrated against a common standard (in which β_{zzz} is dominant) using the same approximation, they can be considered as *effective* β_{zzz} values to be used for calibration of other HRS measurements only (e.g., $\beta_{CHCl_3} = 0.49 \times 10^{-30}$ esu [111, 152]). More remarks concerning the choice of this reference standard are given in Section 2.4.3.3. Calibration against the pure solvent is the most convenient reference method as the signal from the pure solvent also needs to be subtracted from the solution signal and therefore has to be measured anyway. Also, because the refraction is not changed, this method is most accurate. Of course, Eqs. (18) may also be used for external reference measurements if the sample and calibration standard are both dilute solutions in the same solvent.

Note that measurements in which the pure solvent is used as the calibration standard are termed "internal reference measurements" here, although the procedure deviates from the internal reference method originally described in Ref. [111]. In the original method, the HRS intensity was measured for a large number of solute concentrations, not necessarily including the pure solvent itself [111, 112, 132]. The slope and intercept of a linear fit to the HRS signal as a function of concentration was then used to determine the β of the solute, relative to the solvent. The unnecessarily high inaccuracy with which the intercept was obtained in this original method [126, 133, 138], often by extrapolation [111, 112, 132] (see, e.g., Fig. 2 in Ref. [138]), has led others to modify the data treatment procedure [124] or to discard the method altogether [118]. A modified procedure, in which the slope is still used but the calibration is based on the pure solvent signal, has also been named "normalized internal reference method" [124]. In our experience, a reliable determination of β can already be obtained from solution measurements for a few[11] concentrations (and the corresponding solvent measurement), rather than from the slope of an extensive series of concentration-dependent (hence time-consuming) measurements.

2.4.3.2. *External Reference*

When the hyperpolarizability of the solvent is not known, a calibration by "external reference," e.g., against another solvent, is required.[12] The same method is also routinely used in less sensitive setups with which the signals from pure solvents cannot be detected [120]. Between different solvents, additional factors need to be taken into account as the refractive indices are different. Therefore, the local field factors do not cancel out anymore, and moreover the different refraction leads to a different focusing of the laser beam and a different collection geometry.

To assess the effect of the different focusing of the laser beam, consider a Gaussian laser beam which is focused in a rectangular sample cell, to a focal region with mutually related [153] beam waist width w_0 and length $z_0 = (n_\omega\pi/\lambda)w_0^2$. As the laser intensity is proportional to $1/w_0^2$, the generated HRS intensity per unit volume in the focal region is proportional to $1/w_0^4$. It will be assumed that the laser is sufficiently tightly focused to make sure that the scattered light originating from the whole focal volume is collected. The total scattering intensity integrated over the focal volume ($V_f \propto z_0 w_0^2 \propto (n_\omega\pi/\lambda)w_0^4$) is then only proportional to the refractive index

$$I_{tot}^{(2\omega)} \propto \frac{1}{w_0^4} \times \frac{n_\omega\pi}{\lambda}w_0^4 = \frac{n_\omega\pi}{\lambda} \tag{21}$$

It is interesting to note from Eq. (21) that the total HRS intensity is independent of the focusing angle due to the exact compensation of the effects of focal length and beam waist. Therefore, the

[11] One solvent is sufficient in principle, but using more than one concentration allows the identification of problems such as aggregation effects.

[12] Alternatively, if β is known for some compound dissolved in this solvent, that solvent may be calibrated against the compound by internal reference [111].

most suitable focal length for focusing the laser is the longest focal length for which the focal region can still be imaged completely onto the detector. If problems still occur due to dielectric breakdown, self-focusing, or higher order effects, an even weaker focusing may be preferable [116, 118, 123]. Till now, only the purely geometrical factors related to the laser beam are taken into account (not the local field factors, etc.). A second geometrical issue to be considered is the collection of the scattered light. The refraction of the scattered light at the cell interfaces leads to changes in collected solid angle ($\sim$factor $1/n_{2\omega}^2$ for a planar interface) and in the reflection losses (transmission factors T_ω and $T_{2\omega}$), which leads for a rectangular cell to [154]

$$S_{\text{solvent}}^{(2\omega)} \propto n_\omega \frac{1}{n_{2\omega}^2} T_\omega^2 T_{2\omega} f_\omega^4 f_{2\omega}^2 N \left\langle \beta_{\text{solvent}}^2 \right\rangle \left(P_Z^{(\omega)} \right)^2 \qquad (22)$$

The changes of the transmission factors T_ω and $T_{2\omega}$ between solvents can often be neglected. They are, of course, more important when solution measurements are compared to gas-phase measurements [154]. Note that Eq. (22) has been derived for a specific experiment with tight focusing and a rectangular sample cell. Other geometrical correction factors are required for some of the setups described in the literature [116, 118, 123], which use high (peak) powers and therefore a weak (or no) focusing to prevent dielectric breakdown. Also, in some cases a cylindrical sample cell is used [116, 125].

2.4.3.3. *Calibration Standards*

Many of the HRS measurements of molecular first hyperpolarizabilities are, directly or indirectly, calibrated against chloroform, for which the literature β value of 0.49×10^{-30} esu (EFISHG, from Ref. [152]) is often adopted, making the assumption that β is dominated by the β_{zzz} component [111]. This choice has the practical advantage that different β values can in principle be mutually compared. The procedure (including the assumption that β is dominated by β_{zzz}) is further justified by the fact that reasonable β_{zzz} values are obtained for relatively well-known NLO chromophores such as *p*NA (see also Table I) [111] and that an alternative analysis [132], based on ratios between the different tensor components of β_{CHCl_3} from a theoretical (gas-phase) calculation, led to only a minute correction (namely to a slightly higher effective β for $CHCl_3$ of 0.52×10^{-30} esu). The latter correction could be included, but has the disadvantage of introducing additional assumptions, while other approximations are involved, such as the neglect of intermolecular interactions which are likely to be far more important.

In fact, a recent study of HRS in deuterated chloroform [155] led its authors to question the use of this solvent as a standard, because of the importance of the deviations from single molecule hyperpolarizabilities and the problems of matching this contribution with the EFISHG values for this molecule. Correcting for the cooperative and collision-induced contributions to HRS, a new value of $\beta_{CHCl_3} = 0.39 \times 10^{-30}$ esu was proposed. Up to now this value is not in general use. Also, reasonable agreement was reached between EFISHG and HRS for different push–pull molecules on the basis of the previous standard values. Again one should wonder about other uncertainties in the determination of the former value $\beta_{CHCl_3} = 0.49 \times 10^{-30}$ esu, which may be as important as the correction proposed by Kaatz and Shelton [155].

By calibrating all solution measurements by internal reference to $CHCl_3$ or whichever solvent is used, and by calibrating all solvents against $CHCl_3$, a consistent set of data is obtained, although the absolute calibration of the β values may not be very accurate. It should be stressed that, in view of the cooperative scattering contributions mentioned, the β values for other solvents, obtained by external reference, should not be interpreted as actual molecular hyperpolarizabilities, but rather as "effective" values for HRS, to be used as intermediate results for calibration purposes only.

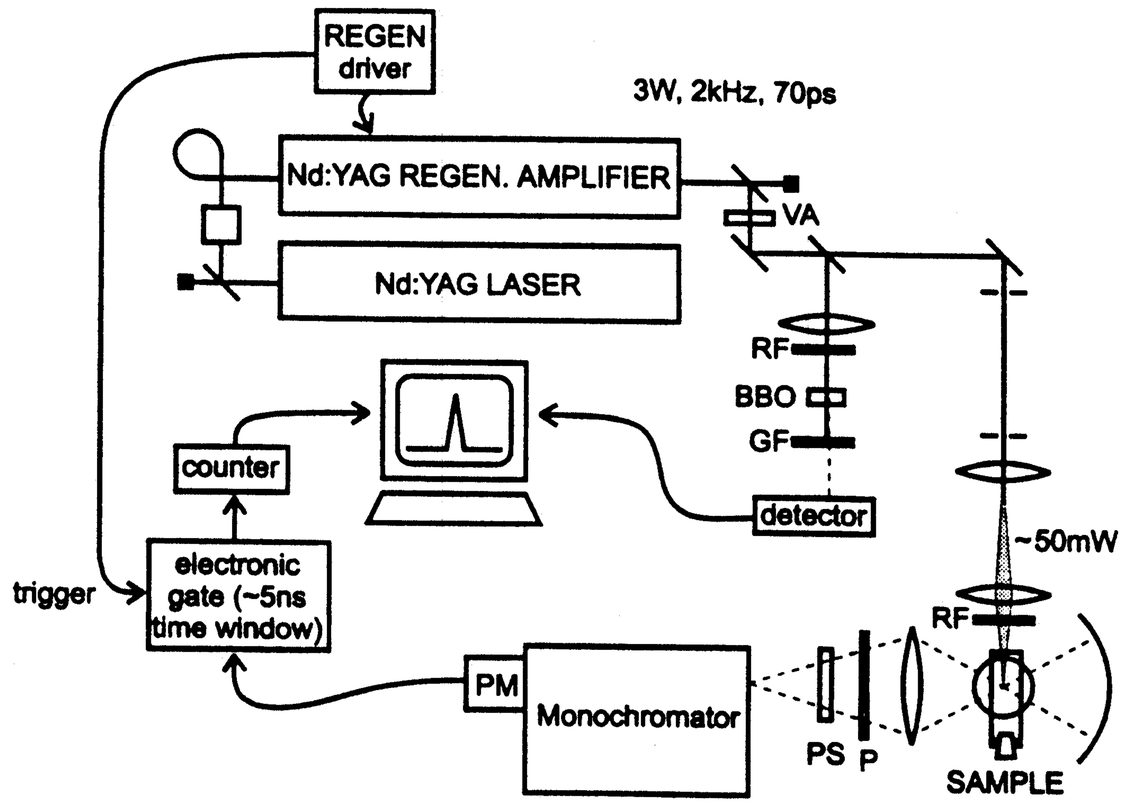

Fig. 4. Experimental setup used for the hyper-Rayleigh scattering measurements. VA, variable attenuator; RF, long wavelength pass filter; BBO, frequency doubling crystal; GF, short wavelength pass filter; P, polarizer (optional); PS, polarization scrambler; PM, photomultiplier.

2.4.4. *Other Experimental Aspects*

In this section we will briefly discuss the experimental setup depicted schematically in Figure 4 that we have employed in our HRS measurements [18, 40, 129, 156], as a starting point to make comparisons with instruments reported elsewhere in the literature.

The laser system used for the HRS measurements consists of a Nd:YAG regenerative amplifier seeded by a mode-locked Nd:YAG laser. The regenerative amplifier produces 70-ps pulses (determined by the seeding laser) at a 2-kHz repetition rate and reaches an average power on the order of 2–3 W. For the HRS measurements, only a small fraction of the available laser power is focused on the sample ($\sim$50 mW) to limit self-(de)focusing and prevent damage to the sample.

The laser beam is led through a variable attenuator and part of the attenuated beam is expanded to a diameter on the order of 20 mm and focused by means of a 100-mm focal length lens onto the sample solution, which is contained in a standard 1-cm-square glass cell. Just after the focusing lens, a 670-nm cutoff filter is placed to eliminate any second-harmonic light which may be generated earlier in the optical setup. The beam expansion serves to avoid two-photon luminescence in the cutoff filter and to obtain tight focusing on the sample, with a focal region only a few millimeters long. The focused beam propagates vertically through the sample cell and is then reflected and focused back into the sample in a slightly shifted position by a confocal spherical mirror. The scattered light is collected at a right angle using a photographic lens and a second confocal mirror (Fig. 4). It is analyzed using a grating monochromator and detected by means of a Peltier cooled

Table I. Representative Selection of Organic SO NLO Molecules for Which Exceptionally Large Nonlinearities Have Been Reported[a]

Compound	λ_{max} (nm)	λ_{exp} (nm)	Parameters[b]	Method; notes; references
*p*NA		1064	$\beta = 34.5$	EFISHG in MeOH [39]
		1064	$\beta = 23 \pm 3$	HRS, int. ref. to $CHCl_3$ [111][c]
		1064	$\beta = 32 \pm 3$	HRS, int. ref. to $CHCl_3$ [114][c]
	347	1064	$\beta = 34$	HRS, int. ref. to $CHCl_3$ [115][c]
		1064	$\beta = 33.5$	HRS, int. ref. to $CHCl_3$ [156][c]
	371	1064	$\beta = 42$	HRS in MeOH [156]
		1900	$\beta = 5.7$	Solvatochromism [8, 175]
		1907	$\beta = 9.2$	EFISHG in acetone [176, 177]
DANS	420	1064	$\beta = 450 \pm 90$	EFISHG in acetone [93]
		1907	$\beta = 73$	EFISHG in $CHCl_3$ [176, 177]
Bacteriorhodopsin	570	1064	$\beta = 2100 \pm 100$	HRS in water [138],[d] later reported to be ~1 order of magnitude lower [116]
All-*trans*-retinal	380	1064	$\beta = 730$	HRS in MeOH [137, 138][d]
		1064	$\beta = 1100$	HRS in $MeNO_2$ [137, 138][d]
	380	1064	$\beta = 136$	HRS in MeOH [116][d]
O1	686	1907	$\mu\beta = 19086$ $\mu\beta_0 = 8019$ $\beta = 2169$ $\beta_0 = 911$	EFISHG [34][e] $\mu = 8.8$ D
O2	680	1907	$\mu\beta = 34770$ $\mu\beta_0 = 14920$	EFISHG [34][e]
O3	744	1907	$\mu\beta = 15000$ $\mu\beta_0 = 5000$	EFISHG [35][e] (exp. error: ±20%)
O4	826	1907	$\mu\beta = 60000$ $\mu\beta_0 = 12200$ $\beta = 7230$ $\beta_0 = 1470$	EFISHG in $CHCl_3$ [36][e] $\mu = 8.3$ D
O5	624	1064	$\beta = 3647 \pm 500$ (in benzene)	HRS [133],[d] erroneous due to fluorescence, β's for **O5** and **O6**, later estimated 12× and 8× lower [117]
O6	656	1064	$\beta = 3296 \pm 500$ (in $CHCl_3$)	
O7	586	1064	$\beta = 1500$	HRS [144][d]
O8	622	1064	$\beta = 1340$	HRS [144][d]

[a] For structures, see Figure 6. More typical compounds *p*NA and DANS are included for comparison.

[b] β values in units of 10^{-30} esu; $\mu\beta$ in 10^{-48} esu; μ in D. Here, β represents the (effective) β_{zzz} component for HRS or β_μ for EFISHG results; $\beta \equiv \beta(-2\omega; \omega, \omega)$ and β_0 is its two-level model-based extrapolation to zero frequency.

[c] HRS in $CHCl_3$, using $\beta_{CHCl_3} = -0.49 \times 10^{-30}$ esu [152] as internal reference standard.

[d] HRS near resonance, using a setup which does not allow correction for fluorescence by spectral analysis of the scattered light.

[e] $\mu\beta$ includes γ contribution (a priori, γ might be large for these long molecules), but arguments have been given to neglect this contribution [36].

photomultiplier. A sheet polarizer is used to analyze the polarization properties of the scattered light, followed by a wedge-type polarization scrambler which equalizes the transmission efficiency for horizontal and vertical polarization. As only low wavelength resolution is required (~1 nm) the monochromator slits are opened much wider (1.25 mm) than the image of the focal region, so the transmitted light intensity does not depend critically upon the precise optical alignment. The glass cell walls are imaged outside the entrance slit to avoid any second-harmonic light generated there. For samples absorbing at 532 nm the focused laser beam is kept at a small well-determined distance from the cell wall closest to the collecting lens to limit reabsorption of the HRS light and eventually correct for it (the collecting confocal mirror is then not used). Also, in external reference measurements, the first confocal mir-

ror, reflecting the laser beam, is not used to limit the effects of different refraction and self-focusing in different solvents.

The sample cell holder allows for precise and reproducible positioning. It also contains a magnetic stirrer head, so a small Teflon-coated stirring rod can be inserted in the sample cell, just next to the laser beam. In this way the solution in the focal region is constantly refreshed for use with samples susceptible to photochemical decomposition. It is advisable to filter the solutions before or during the measurement, since small dust particles or undissolved crystallites can induce dielectric breakdown or other disturbing effects.

In a reference arm, a small fraction of the laser beam is frequency doubled by means of a BBO crystal and detected using a slow photodiode. Care must be taken to prevent any of this second-harmonic light from reaching the monochromator. In recent reports, a well-characterized sample for Kurtz powder SHG has also been employed for this purpose [157]. This reference signal is measured simultaneously with the HRS signal and is used to correct for fluctuations in laser power and pulse width, as in the experiments described by Weinberg [106] and others [107, 108, 134]. The elimination of laser fluctuations is less than perfect, because the coherent phase-matched SHG used in the reference arm has a different dependence on the coherence properties of the laser light than the incoherent HRS scattering [107]. This method is, however, more accurate than correction by the fundamental (average) power squared—a method which is used in more recent work [111] and which does not correct for fluctuations in pulse width.

As HRS photons are only generated during the 70-ps pulses, which arrive only once every 0.5 ms, a huge background suppression is possible by electronically selecting only those photons detected during a 4-ns time window around the arrival of the laser pulse. For signals not correlated to the laser pulse—dark counts, room light, slow two-photon emission—the 4-ns interval every 0.5 ms yields suppression by a factor 10^5, so they become negligible. However, a complete elimination of the (fast) luminescence contributions is only possible by analyzing the spectral content of the scattered light. The gated output pulses are collected in parallel with the digitized signal from the reference arm. The time analyzer also allows monitoring of the time distribution of the pulses detected using a multichannel analyzer which is practical for synchronization.

The single-photon detection technique (unlike, e.g., boxcar integration of the analog signal) yields no information about the *number* of photoelectrons created on the photocathode in a single laser pulse: multiple photons generated by the same laser pulse are observed as a single count, so the count rate cannot exceed the repetition rate (~2 kHz). These pile-up errors are easy to correct for. Corresponding to a given "true" average number of photons per laser pulse, the average detected number is simply obtained from Poisson statistics. The relationship obtained can then be inverted to estimate the true number of photons S_{corr} from the detected number S_{raw} during an integration time T_{int},

$$S_{corr} = -\nu_{rep} T_{int} \ln\left(1 - \frac{S_{raw}}{\nu_{rep} T_{int}}\right)$$

where ν_{rep} is the repetition rate of the laser. When the signal count rate is much lower than this, the probability of having more than one photon during the same pulse is small and the deviation induced by the pile-up effect is negligible.

An example of HRS data is presented in Figure 5, for the case of an organometallic compound dissolved in methanol, showing an appreciable luminescence background resulting from multiphoton absorption. The steps in the procedure for the determination of the HRS intensities are illustrated for the solution and the pure solvent. As luminescence bands of conjugated organic dyes in solution are typically on the order of 100 nm wide, the luminescence signals can be approximated by a straight line within this narrow wavelength range for the purpose of background subtraction. The integration interval cannot be taken to be narrower than about 4 nm, because of the significant intrinsic line width of the HRS spectrum, especially for the solvents (see below). The use of 2.6 to 4-nm bandwidth interference filters instead of a monochromator in HRS measurements, as is often done [43, 111, 112, 114], even while using the internal reference method, is therefore very dubious as the transmission of such a filter varies strongly over the width of the HRS spectrum and does not give reproducible results (and anyway does not suppress the luminescence within the filter bandwidth). But on the contrary, in the present example, the HRS signal would be overestimated by more than a factor of 4 if it were simply measured using a 10-nm bandwidth interference filter [125, 133] without taking the luminescence background into account. Meanwhile, the luminescence was not visible to the naked eye, not even in the focal region inside the sample. While many compounds show a weaker luminescence background (relative to the HRS signal), such a background was almost always detectable. On the other hand, many other conjugated organic dyes are known to show a much stronger two-photon luminescence which can be many orders compared to HRS,[13] as has also been observed by Flipse et al. [115, 136]. In fact, even for crystal violet—which has a very low fluorescence quantum yield and has therefore been used as a "nonfluorescent" reference molecule in HRS (see also Section 3.2)—the fluorescence contribution to HRS is not negligible [158]. The monochromator therefore is an absolutely essential part of the HRS. Nevertheless, in most HRS experiments described to date, the spectral content of the scattered light is not analyzed to correct for luminescence [117, 128, 144, 159–163] (with exceptions [107, 118, 126, 127]).

As mentioned before, the use of very narrow bandwidth interference filters has to be considered carefully. Indeed, the HRS peak, in particular of the small solvent molecules, is not infinitely narrow but is broadened by several mechanisms [106–109, 154, 164] including rotational motion of the single molecules, correlated reorientational motion, and collision-induced broadening. The latter effect yields for, chloroform, e.g., a Lorentzian component of about 50 cm^{-1} wide (i.e., about 1.3 nm at 532 nm), which is on the order of the width of interference filters. Different filter widths will then lead to different transmission of solute and solvent signals which in the internal reference method will bias the final results.

The integrated intensities are now used to calculate β_{solute} from Eq. (20) or (22) for internal or external reference measurements, respectively. Compared to internal reference measurements, even lower laser powers have to be employed for external reference measurements in which different solvents are compared (down to 20 mW average power in our setup) to obtain reliable relative β values, due to the differences in self-(de)focusing. Therefore, in the case of calibrations between two solvents the zero

[13] For example a rhodamine 6G solution yields a luminescence strong enough to easily see the image in front of the monochromator slit, which was used to our advantage in the alignment procedures. In a wavelength scan *only* a broad luminescence signal and no HRS peak is detected.

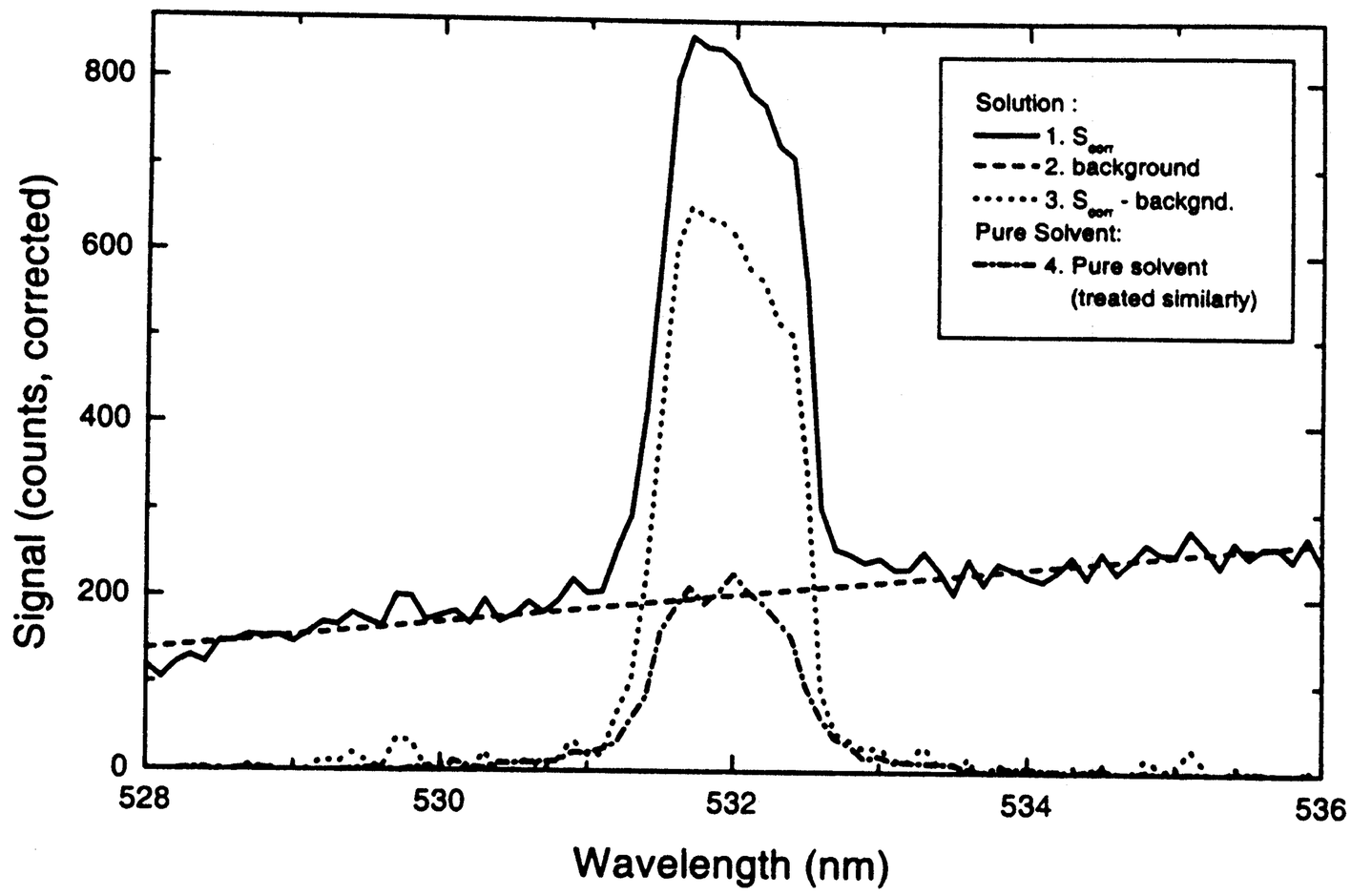

Fig. 5. Example of the treatment of HRS data from a sample of the cobalt complex CoCpDPPE(p-NC−Ph−$N(CH_3)_2$) [40] in MeOH (0.54 g/l; integration time 20 s). (1) The HRS signal already corrected for pile-up (minute effect here) and divided by the reference signal. (2) A linear background is fitted to the outer parts of the scan and (3) subtracted, to eliminate multiphoton fluorescence. (4) The integrated SHG intensity is compared to that from the pure solvent (after analogous treatment) and the hyperpolarizability of the solute is obtained from Eq. (20). The peculiar line shape is determined by the wide monochromator exit slit and imaging effects (e.g., of the second focal region of the beam redirected by a confocal mirror).

power limit of the measured ratio is determined, as in the method of Kaatz and Shelton [154]. Also, optical elements like the confocal mirrors (see Fig. 4) could amplify the effects of different focusing and are not used here. For measurements in a solvent other than $CHCl_3$, first a calibration of the pure solvent against chloroform is performed, after which the internal reference method against this new solvent can be employed for the solutions. This way, the low-power (and hence time-consuming) external reference measurements only need to be performed once for each new solvent.

The laser system described here is quite different from the Q-switched Nd:YAG systems often used for NLO measurements and HRS measurements in particular. Typically, Q-switched Nd:YAG lasers are used with several nanosecond pulses at repetition rates on the order of 10 Hz. The regenerative amplifier system employed by the authors is somewhat more complicated to use and maintain, but produces a far more stable output than the traditional Q-switched systems, which suffer from large pulse-to-pulse variations. These can be strongly reduced by injection seeding. In both types of lasers, diode pumping could yield a major improvement as well. The much higher repetition rate and shorter pulse width of the regenerative amplifier enables us to obtain good sensitivity with only moderate pulse energies, effectively preventing damage to the sample. At the same time, single-photon counting detection can be applied, drastically reducing the background signal compared to the traditional boxcar integration necessarily employed in low repetition rate systems. On the other hand, compared to the extremely high repetition rate mode-locked systems (e.g., 80-MHz Ti:sapphire lasers [121]), the 2-kHz repetition rate has the advantage that an electronic gating can still be employed to almost completely eliminate the dark counts of the photomultiplier.

An alternative method to suppress the luminescence contribution has been developed by Noordman and van Hulst [125]. By analysis of the scattered light with a high time resolution (~80 ps), they discriminate the quasi-instantaneous HRS light from luminescence, which occurs mostly on nanosecond time scales. Variants of this method have been developed [118], including a method based on phase-sensitive detection [128, 135, 165, 166]. The latter especially requires a complicated electronic detection scheme [167], because measurements of the phase (relative to a known nonfluorescent sample [128]) as a function of demodulation frequency are required to discriminate the instantaneous HRS from the slowly decaying fluorescence signal. Even then, the derivation of β involves curve-fitting and extrapolation (to infinite modulation frequency) which critically depend on assumptions such as a single exponential decay in the nanosecond region.[14] Possible effects of molecular reorientation, which typically occurs in the hundreds of picosecond time scale, are also not accounted for. Moreover, as correctly pointed out by Noordman and van Hulst [125], fluorescence signals are likely to exhibit much faster decay components (down to sub-picosecond) which cannot be resolved by electronic means. So even with these electronic methods, only an upper limit to β can be obtained [125]. In conclusion, systematically recording the spectral content of the scattered light remains the only reliable (yet simple) approach to derive β values from HRS. Time-resolved techniques should be considered only as a useful additional method for suppression of the luminescence contributions to improve the signal-to-noise ratio in the wavelength scans for highly fluorescent samples.

[14] See Figure 2 of Ref. [166] and Figures 2 and 4 (the inset) of Ref. [135].

Excitation at longer wavelength, between 1.3 and 1.907 μm, is an alternative route to try to escape multiphoton emission, but even then this possibility has to be considered. As an additional advantage, one can hope to measure β in a nonresonant regime, especially in the case of 1.907 μm excitation. In the last few years several experimental setups have been reported for this purpose, using a nanosecond Nd:YAG laser source combined with either a parametric oscillator [116, 120, 127] or a H_2 or D_2 Raman shifter [117, 130, 143, 168], and alternatively a sub-nanosecond mode-locked Q-switched Nd:YAG laser operating at 1.34 μm [169].

3. ORGANIC COMPOUNDS

During the last two decades a vast amount of research has been devoted to the design of organic molecules for SO (and TO) NLO applications. Excellent reviews of organic SO NLO materials can be found in the literature [8, 170–173] including the effort by Nalwa et al. [174] who systematically compiled these compounds and their properties. In the following we will discuss the different aspects of the design of these molecules and the insight which was gained from the different approaches. In the process we will present a number of exemplary compounds, without striving for completeness. However, for the period since this extensive review, we have attempted to cover in the following subsections most of the literature concerning new compounds which were synthesized and characterized for SO NLO.

Typical SO NLO chromophores [e.g., 4-dimethylamino-4′-nitrostilbene (DANS); Figure 6] have first hyperpolarizabilities on the order of a few hundred $\times 10^{-30}$ esu, which is 2 to 3 orders of magnitude larger than those of small saturated (i.e., having only σ bonds) molecules (solvent molecules, etc.) [8]. In Figure 6 and Table I, only a representative selection of more recently developed SO NLO molecules is listed for which exceptionally high nonlinearities ($\beta = \sim 1000 \times 10^{-30}$ esu or more) have been reported. This selection gives an idea of the kind of molecules being investigated, but at the same time illustrates the many problems associated with the use of reported NLO parameters. Different quantities, $\mu\beta$, $\mu\beta_0$, β, and β_0, are reported, depending on the type of measurement and the preferences of the authors (e.g., the decision whether reduction to the nonresonant values is reliable). Moreover, measurements are made at different wavelengths. Extraction of β from EFISHG results also requires a reliable determination of the dipole moment (and eventually γ) and for a low symmetry molecule the angle between the vectors is needed. As discussed above, calibration issues such as the choice of a reference standard inevitably lead to discrepancies on the order of a factor of 2. In some instances, experimental (and more often theoretical) data are presented in a different convention for the NLO parameters (see Appendix). Finally, the number of erroneous β values is large, especially among the highest values. Apart from calibration issues, the main problems are probably the spurious signals in certain HRS experiments due to fluorescence (see Section 2.4.1), which can lead to dramatically overestimated β values. In spite of all this, a steady increase in magnitude of the NLO parameters is reached by the continuing efforts of design and synthesis, and it is useful now to look at the important trends which are found in series of molecules to learn how to obtain further improvement.

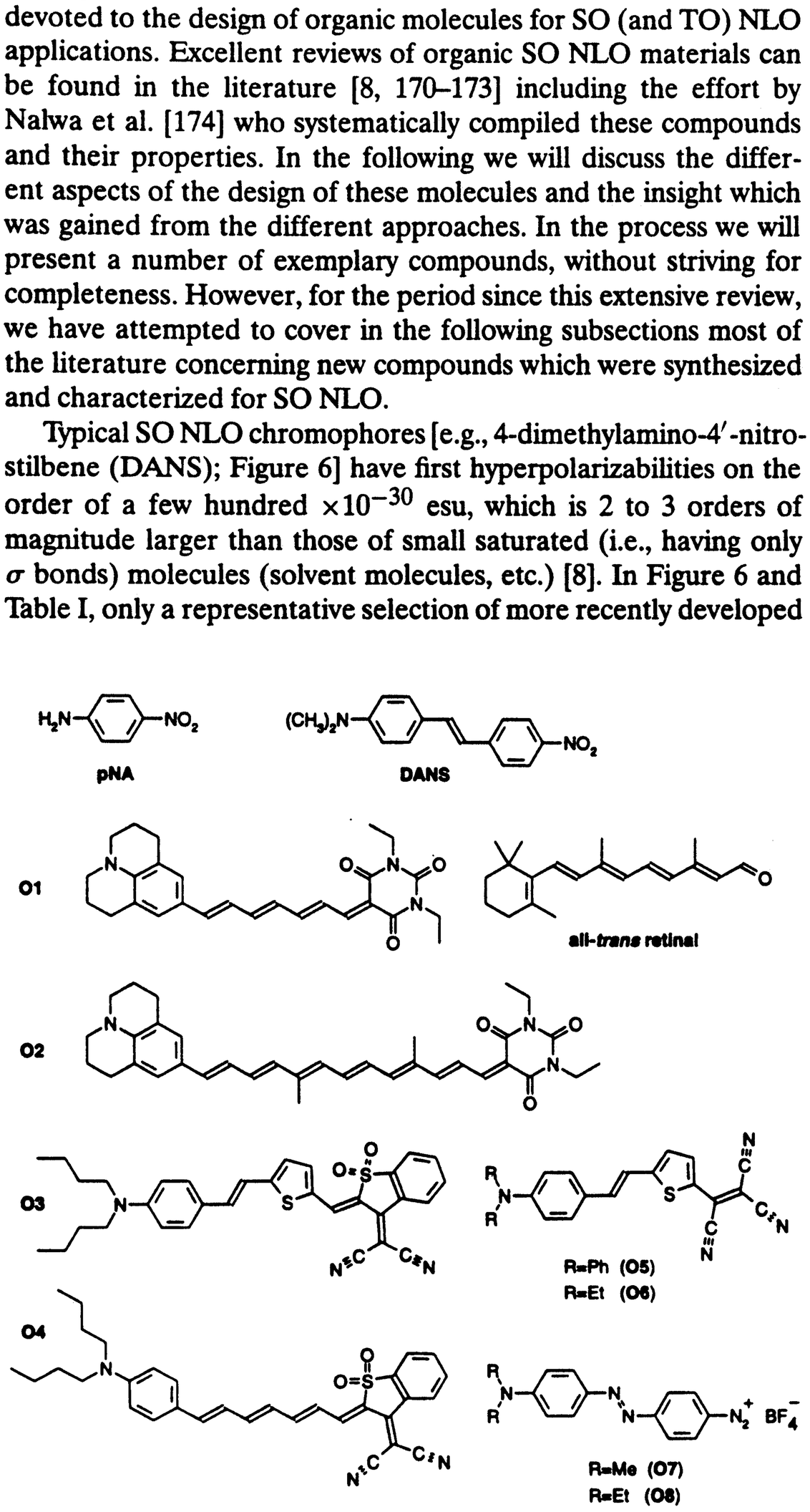

Fig. 6. Chemical structures of the conjugated organic molecules for SO NLO, listed in Table I.

3.1. Push–Pull Systems

3.1.1. Polyene Chains: The Prototype Compounds

In spite of the fact that other conjugated systems, in particular benzene derivatives [39, 90, 91, 93], initiated the quest for organic NLO compounds, the polyene chain as the prototype conjugated system was especially studied as a model system of interest. In the early study of Dulcic [178], one of these compounds was found to possess a high nonlinearity and the importance of the conjugation path and donor/acceptor (D/A) group was realized. About 10 years ago, a series of theoretical and experimental investigations [177, 179–182] were performed (often in comparison with other conjugated segments, see Section 3.1.3) to determine the dependence of the SO nonlinearity on chain length and on the choice of D/A groups. For several such compounds the results of the EFISHG investigation are summarized in Table II. For the polyenes a power law increase $\beta = \sim L^x$ as a function of conjugation length L was found with exponents in the range of $x \cong 1.9$–3.5 depending on the D/A combination (Refs. [177] and [180], and compilation in Ref. [174], p. 115), which easily compensates for the increasing molecular volume. An optimum length of about 20 units was estimated for polyene chains. Also the dependence on D/A combination was studied. As known from charge-transfer studies in molecules, series of donors and acceptors can be chosen with increasing strength. For a series of commonly used substituents [174], one finds:

$$\begin{aligned}\text{Acceptors:}\quad & SO_2CH_3 < CN < CHO < COCF_3 \\ & < NO < NO_2 < CHC(CN)_2 < C_2(CN)_2\end{aligned}$$

$$\begin{aligned}\text{Donors:}\quad & OCH_3 < OH < Br < OC_6H_5 < OCH_3 \\ & < SCH_3 < N_2H_3 < NH_2 < N(CH_3)_2,\end{aligned}$$

but many other groups have been used (see, e.g., compounds in Table II). Correlation was also possible with so-called substituents (Hamett) constants, σ_p and σ_n, used in color chemistry [177] to

Table II. Illustrative Push–Pull Compounds with Polyene Chains as Conjugated Segment. Dependence on Conjugation Length and on Variation of the Donor and Acceptor Substituents

Compound	λ_{max} (nm)		$\mu\beta$ (10^{-48} esu)	μ (D)	β (10^{-30} esu)	Ref.
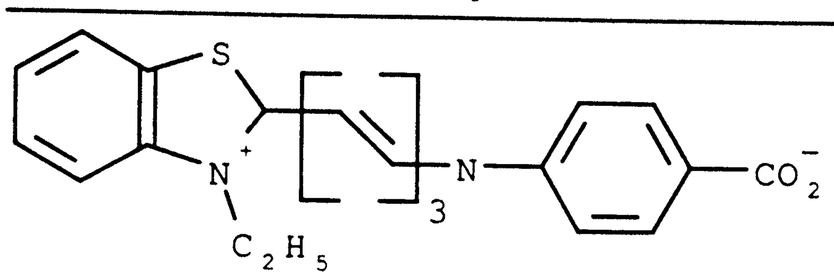	498	EFISHG[a,b]	$\mu\beta$ 1500			[178]
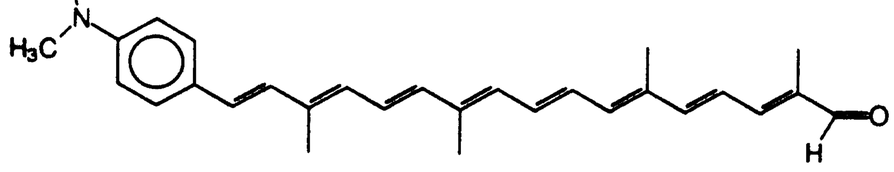	498	EFISHG[c,d]	$\mu\beta$ 8900	 7.0	$\beta(0)$ 490	[38] [181]
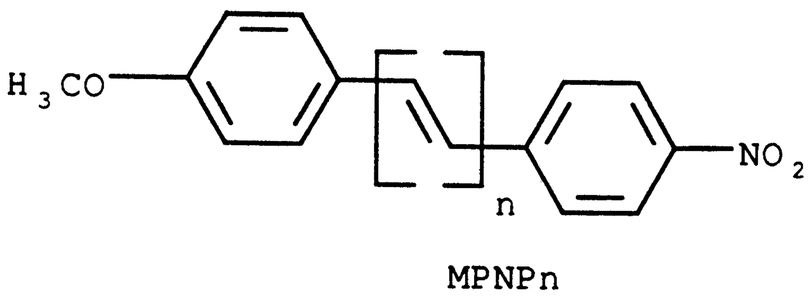 MPNPn	n =		EFISHG[e,f]	$\mu\beta$		$\beta(0)$	[180]
	1			460	5.7	78	
	2			810	6.0	106	
	3			1810	6.6	188	
	4			2460	6.7	211	
	5			4360	7.0	340	
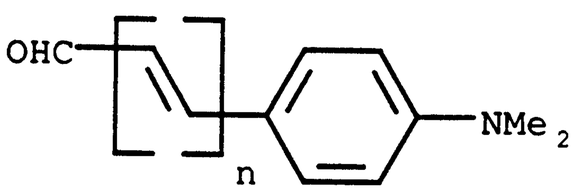	n =		EFISHG[g]	$\mu\beta$		β	[177]
	0	326	*f*		5.1	63	
	1	384	*d*		5.6	30	
	2	412	*d*		6.0	52	
	3	434	*d*		6.3	88	
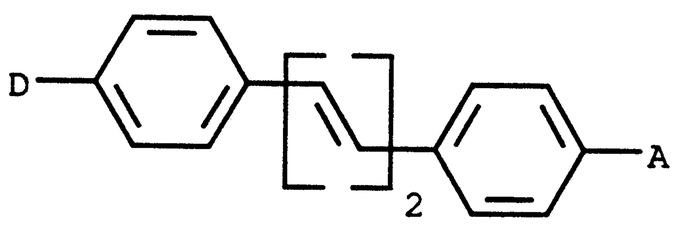	D/A		EFISHG[g,d]	$\mu\beta$		β	[177]
	OMe/CN	360			4.5	27	
	Br/NO_2	378			3.5	21	
	OMe/NO_2	397			4.8	47	
	SMe/NO_2	398			4.5	55	
	NMe_2/NO_2	442			4	107	
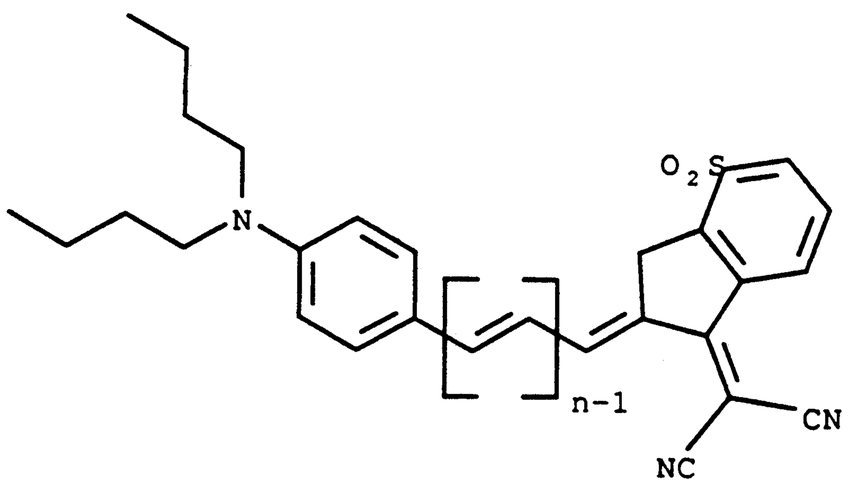	n =		EFISHG[g,d]	$\mu\beta$		$\beta(0)$	[36]
	1	603		950	6.1	85	
	2	695		5200	6.9	310	
	3	773		13500	8.2	470	
	4	826		60000	8.3	1470	

[a] $\lambda = 1.89\ \mu$m.

[b] In dimethyl sulfoxide.

[c] $\lambda = 1.34\ \mu$m.

[d] In $CHCl_3$.

[e] $\lambda = 1.0$.

[f] In *p*-dioxane.

[g] $\lambda = 1.907\ \mu$m.

predict the position of charge-transfer absorption bands. The β values can be increased by about 1 order of magnitude, going from weak to stronger D/A substitution, but at too strong polarization of the conjugated molecule one goes over a maximum value. In later studies [35, 36, 38, 183, 184] it was shown that this maximum value is dependent on the polyene chain length and on D/A combination, which has led to extremely high $\mu\beta$ and β values (see, e.g., Table II), even after reduction to static values using the two-level model. Another series of related compounds are retinal chromophores (including vitamin A acetate) and their derivatives, which have been investigated by HRS (Ref. [138], but corrected values in [116]), which yield static β's in the (7–77) $\times$ 10^{-30} esu range, depending on the strength of the acceptor substituent.

An additional very important observation was the systematic dependence of the NLO properties on solvent polarity [185, 186]. It was realized that, in a reaction field model, the electric field exerted on the dipolar molecule by the solvent had an effect equivalent to that of the D/A substitution, which could be described by an internal field. Combination of this concept with the two-level model and the mixing of the resonance forms of the conjugated molecule led to the bond length alternation model, which is further discussed in the next section.

3.1.2. *The Bond Length Alternation Model—Unified Description of* $\alpha, \beta, \gamma, \ldots$ *of Push–Pull NLO Molecules*

While ab initio and semiempirical calculations can predict trends in hyperpolarizabilities for specific molecules with reasonable precision, they provide little insight in the structure–property relationships that govern the NLO properties of organic conjugated molecules. Therefore, apart from these quantum chemical calculations, simple models are required to understand these relationships. The two-level model is an example of such a model, which has yielded good insight into the resonant enhancement of the hyperpolarizability. However, the major breakthrough in recent years is probably the model largely developed by Marder and coworkers which has led to a unified description of linear and nonlinear polarizabilities [186]. One of the main ideas behind this model is to describe the optical properties of conjugated systems as a function of a geometric parameter called "bond length alternation" (BLA), describing the difference in length of alternating bonds of a polyene-like chain. Therefore, it will be referred to as the "BLA model," although it is meant to include a number of ideas developed by many authors [33, 34, 36, 183, 185–194]. The main aspects of the BLA model will be introduced briefly here, but for a more detailed description we refer the reader to the original articles.

Consider a nonsubstituted, symmetrical, conjugated chain on which an electric field E is applied. The induced dipole moment μ is then expected to evolve with E as depicted qualitatively in Figure 7. For weak electric fields the dipole moment varies linearly with E, while at higher fields, the dipole moment tends to saturate, resulting in a sigmoidal curve. From this qualitative picture, the evolution of the linear and nonlinear hyperpolarizabilities with applied field can be obtained by simply plotting the subsequent derivatives of the $\mu(E)$ curve. Indeed, as $\mu, \alpha, \beta, \gamma, \ldots$ are defined as proportional to the subsequent coefficients in the Taylor series, there exists a derivative relationship between all of them. This leads to the typical picture shown in Figure 7, with the evolution of α, β, and γ showing one, two, and three extrema. This picture has been confirmed by quantum chemical calculations for various polyene-like molecules [33, 34, 183, 185, 186, 192] and in fact, the various positive and negative extrema of the hyperpolarizabilities can be attributed to corresponding positive and negative terms in the quantum mechanical sum-over-states expressions [185, 192]. This very general evolution of the hyperpolarizabilities with a hypothetical applied field becomes extremely interesting when combined with the so-called equivalent internal field model, introduced by Oudar and Chemla [39, 187]. This model states that the effect of asymmetrical substitution on a conjugated molecule may be considered equivalent to the application of an electric field over the conjugated chain. Thus, the rather complicated evolution of the hyperpolarizabilities with E depicted in Figure 7 is also expected to describe the evolution of these quantities with increasing D/A strength, and, for a given push–pull molecule in liquid solution, also the evolution with solvent polarity due to the extra field ("reaction field") exerted by the polar solvent molecules on a dipolar solute molecule. Experimental evidence for this has been gathered for various push–pull polyenes with a wide variety of donor and acceptor groups [33, 34, 36, 183, 186, 190, 195]. These experiments show that for a given conjugated chain, β can be optimized by selecting the appropriate donor and acceptor groups [34, 190, 195]. Similarly, the third-order polarizability γ can also be varied as predicted by tuning the donor and acceptor groups [33]. While the picture of Figure 7 is reproduced for many polyene-like molecules, the horizontal scale in terms of electric field or D/A strength may be different for different conjugated chains. It was therefore an important achievement to realize that a more generally valid model is obtained when the properties are described as a function of the *bond length alternation*, a geometrical parameter defined as the average difference in length between adjacent carbon−carbon bonds in the polyene chain [33, 36]. In terms of this BLA parameter, the extrema and zero crossings of the (hyper)polarizabilities are found to occur at fixed positions. For instance, the maximum in α, the zero crossing of β, and the large, negative peak of γ all occur near BLA = 0, i.e., when all bonds are of equal length as in a cyanine molecule. This situation (BLA = 0) is therefore often referred to as the cyanine limit. Similarly, the extrema in β occur at a value of BLA = ($\pm 0.05 \pm 0.01$) Å [34, 36]. Instead of the BLA, the closely related *bond order alternation* is also often used [186, 192].

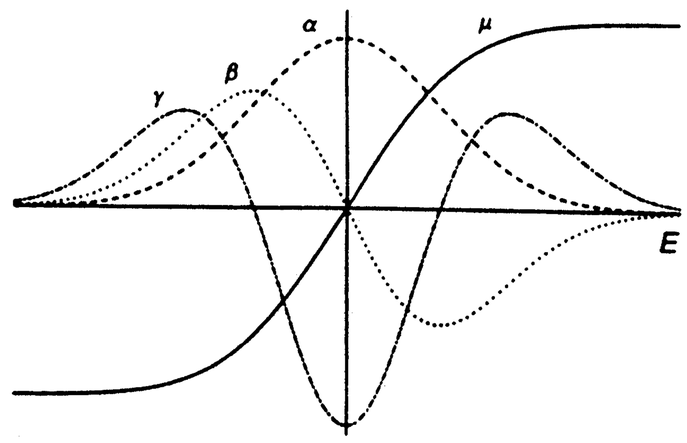

Fig. 7. Schematic plot of μ, α, β, and γ of a conjugated chain as a function of applied field. A plot as a function of BLA of a polyene chain would give essentially the same plot. Hence, it is known as the BLA diagram (After Ref. [186].)

After the relation between BLA and the hyperpolarizabilities was established from quantum chemical calculations and the typical evolution of β and γ supported by experiments, a simple theoretical model has been developed to allow analytical results to be obtained based on these ideas [191]. This consists of a two-state

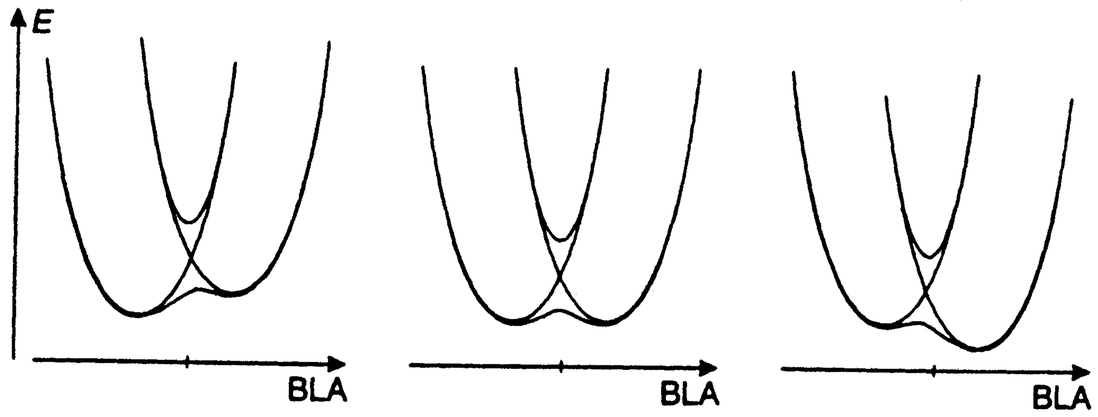

Fig. 8. Configuration coordinate diagrams of push–pull polyenes, according to the two-state model [191] showing the evolution from a neutral polyene-like structure (left), via a partly charge separated cyanine-like structure (middle), to a strongly charge separated polyene-like structure (right). For a cyanine-like molecule, in which all bond lengths are equal, the off-diagonal matrix element of the Hamiltonian is in fact larger than depicted here, resulting in a smoother ground state potential with only a single minimum (at BLA = 0) [186].

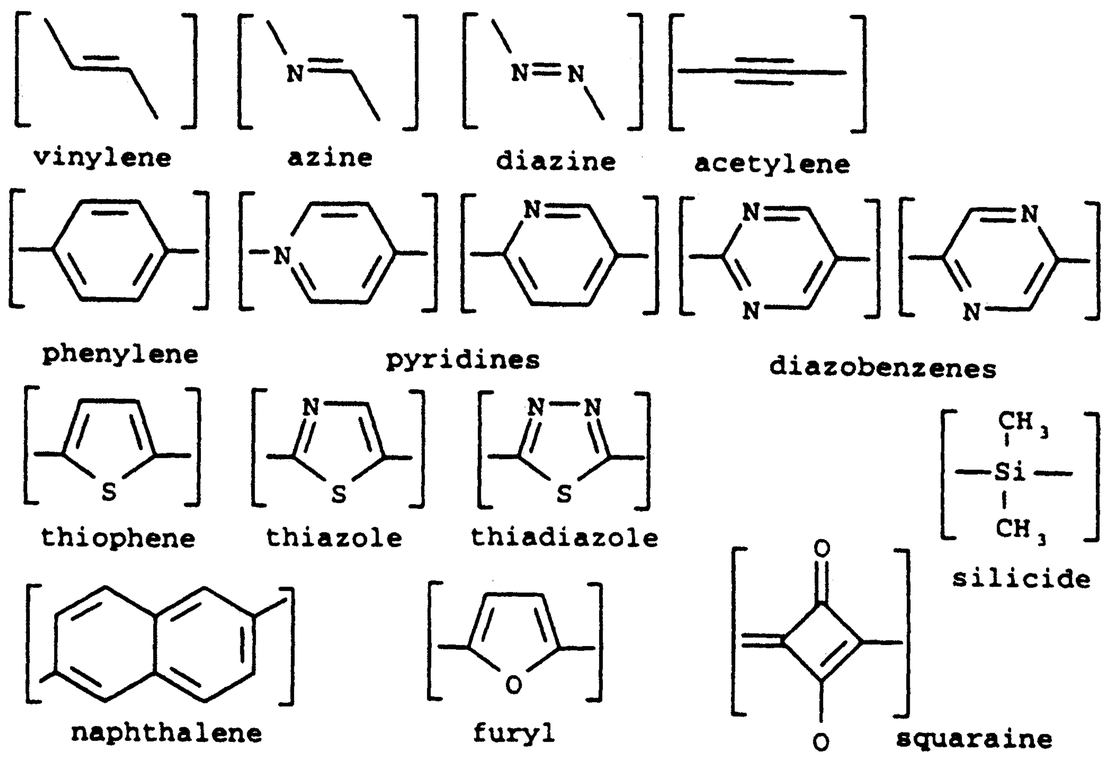

Fig. 9. Illustrative (nonexhaustive) series of conjugated segments used as building blocks for (pseudo)linear push–pull molecules for SO NLO.

model, in which the electronic structure of the ground and excited states of a push–pull molecule are considered as a resonance form of two wave functions. One wave function describes the neutral form of the molecule and the other the completely charge-separated (zwitterionic) electronic structure, with all double and single bonds of the conjugated chain shifted by one bond. Such a system has a strong vibronic coupling: shifting the π electron density forming the double bonds shifts the equilibrium geometry to a geometry with inverted BLA (and vice versa). Thus, the configurational coordinate diagram (configuration coordinate $\equiv$ BLA coordinate) of this system consists of two vibrational potentials, approximated by two identical parabolas, with their minima shifted horizontally representing the different equilibrium geometries associated with both extreme forms of the molecule [BLA = $\pm$0.11 Å, corresponding to alternating single (1.45 Å) and double (1.34 Å) bonds]. Due to the off-diagonal element t of the Hamiltonian, both states mix and the crossing of both parabolas is avoided, as shown schematically in Figure 8. If t is sufficiently large, both potentials are connected smoothly and merge into a ground-state potential with a single minimum. At the cyanine limit, the minima of both parabolas are at the same energy, leading to a resonance structure with equal contributions from the neutral and charge-separated structure and with a minimum of the ground state (as well as excited state) potential at BLA = 0. With changing D/A substituents, or solvent polarity, the energy of the neutral state remains unchanged, while that of the zwitterionic state is lower in higher polarity solvents or with stronger D/A groups, thus shifting the right-hand parabola vertically in Figure 8. Consequently, the ground-state equilibrium position shifts continuously in BLA. This valence bond charge-transfer model leads to analytical formulas for the optical parameters and results are obtained which compare very well to those obtained from quantum chemical methods [191].

This model has been applied mainly to push–pull polyenes and has led to the development of most of the highly nonlinear molecules shown in Figure 6. However, the model can be readily extended to any other push–pull conjugated system as described theoretically by Barzoukas et al. [193, 194].

3.1.3. Other Conjugated Backbones

The ability to determine single molecule hyperpolarizabilities by the EFISHG method was gratefully welcomed as an opportunity to systematically study the structural features which optimize these properties. As discussed before, the mechanisms relevant for push–pull molecules could be efficiently unraveled, and the engineering of this type of molecule was very successful. The Davydov group first made the connection between SO NLO properties and charge transfer over the conjugated segment in substituted benzene derivatives [196]. After the reports on systematic variation of β values in mono- and disubstituted benzene [39, 187, 197–199], a series of different conjugated building blocks have been investigated, in parallel with the studies on polyene chains discussed before (Fig. 9). Stilbene derivatives were soon found to display a much higher β value than the substituted benzenes [93]. One of them is known under the acronym DANS and its structure and measured β values are given in Table III. A detailed comparative study of short conjugated links, such as benzene, biphenyl, stilbene, and styrene, was conducted by Cheng et al. [176, 177], varying the donor and acceptor groups, the relative positions of these groups, and additional substituents (e.g., aza-, azo-, NC-, MeO-, ...) in different positions. The *trans* geometry for donor and acceptor always yielded higher results, and increasing strength of the donor and acceptor could be correlated with increasing hyperpolarizabilities, as in the case of the polyene chains. The longer and planar stilbenes gave the best results, much better than biphenyl. The bad performance of biphenyl was ascribed to the torsion between the phenyl rings due to sterical hindrance, resulting in weaker conjugation. Enhanced planarity by cross-linking the rings in biphenyl or by going to stilbenes leads to better results.

Systematic studies as a function of chain length were performed with oligophenyls [96, 177, 200], oligoynes [177], and oligothiophenes [201]. The poor results for polyphenyls was confirmed, and optimal chain lengths of only two to three are found (correlating well with the maximum red shift of the charge-transfer transition). Also in the polyyne systems the conjugation is weaker and the acetylenic linkage is less favorable than the ethylenic one. In contrast, thiophenes perform very well, as could be expected from their better planarity. In one study [200], phenyl and naphthyl units were employed and anticorrelation was observed between the hyperpolarizabilities and torsion angles. The dithiophenes, however, possess β's comparable to those of the stilbenes with the same D/A combination, and for the oligothiophenes a power law evolution with number of bonds is found, increasing faster than quadratic, which is comparable to the polyene systems. A systematic study for

Table III. Illustrative Push–Pull Compounds with Conjugated (Not Simple Polyene) Chains as Conjugated Segment[a]

Compound	λ_{max} (nm)		μ (D)	β (10^{-30} esu)	Ref.
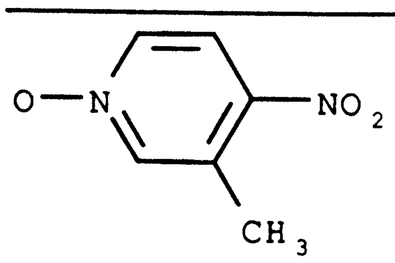 POM	325	HRS[b,c]		7.0	[223]
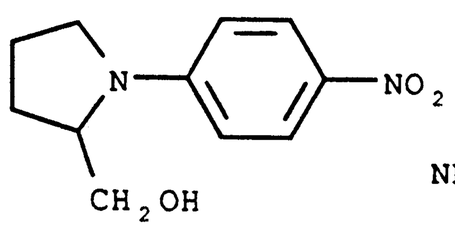 NPP	397	HRS[b,c]		11.1[d]	[223]
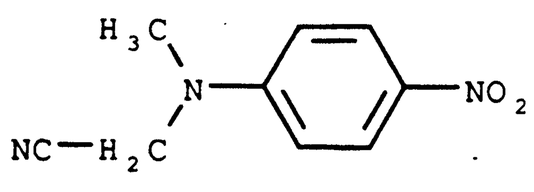 NPAN	360	HRS[b,c]	3.7	15.1	[223]
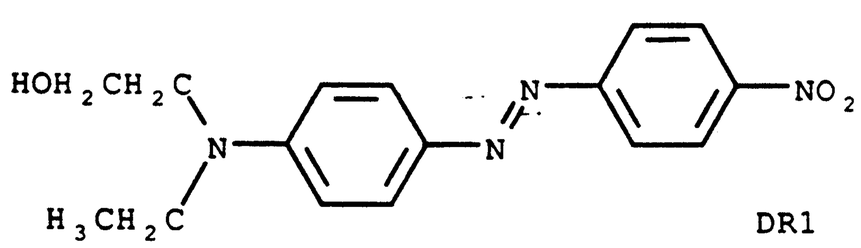 DR1	455	EFISHG[e,f]	7.0 9.0	49 93 (70) $\beta_0 = 65$ ($\beta_0 = 49$)	[176] [208] ([216])
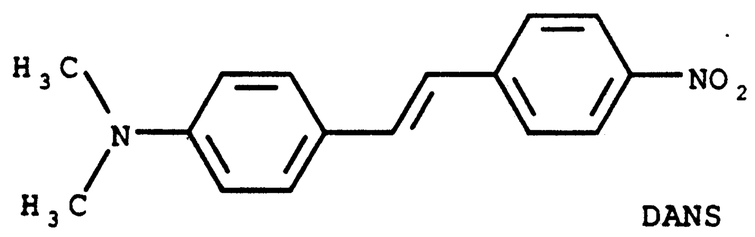 DANS		420 427	EFISHG[b,g] EFISHG[c,e]	6.6	450 ± 90 73 $\beta_0 = 56$	[93] [176]
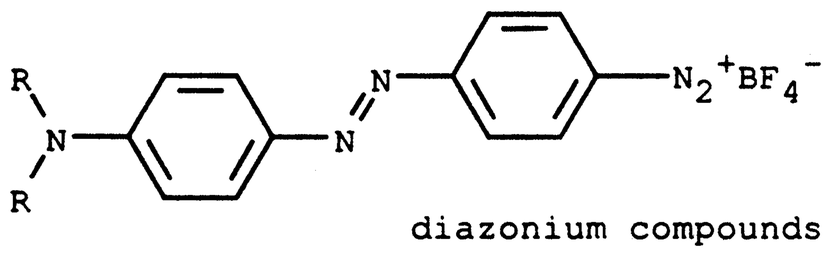 diazonium compounds	R = Me R = Et	586 622	HRS[b,h]		1500 $\beta_0 = 240$ 1340 $\beta_0 = 320$	[144]
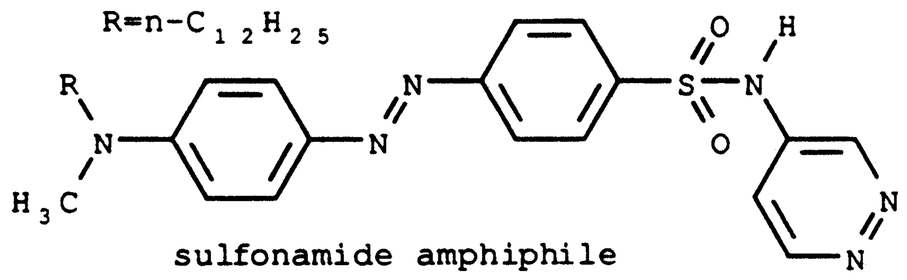 sulfonamide amphiphile		458	HRS[b,j] HRS[j]		411 185 $\beta_0 = 110$	[206]
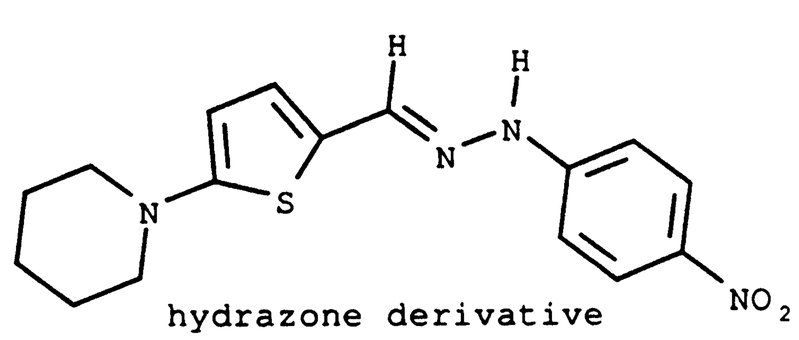 hydrazone derivative		441	EFISHG[e,f]	8.7	53 $\beta_0 = 39$	[207]

continues

Table III. (continued)

Compound		λ_{max} (nm)		μ (D)	β (10^{-30} esu)	Ref.
DEMI ULTRA		DEMI	717	HRS[b,c]	33	780 $\beta_0 = 320$	[18]
		ULTRA	721		19	333 $\beta_0 = 150$	
tricyanovinylthiophene derivatives	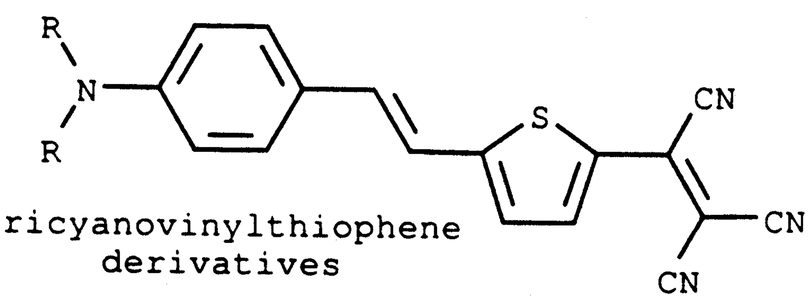	I : $R = CH_3CH_2$	656	EFISHG[e,f] HRS[c,e]	7.0	886 580	[214] [117]
		II : R = phenyl	658	HRS[c,e]	6.6	483	
stilbazolium derivative Z3	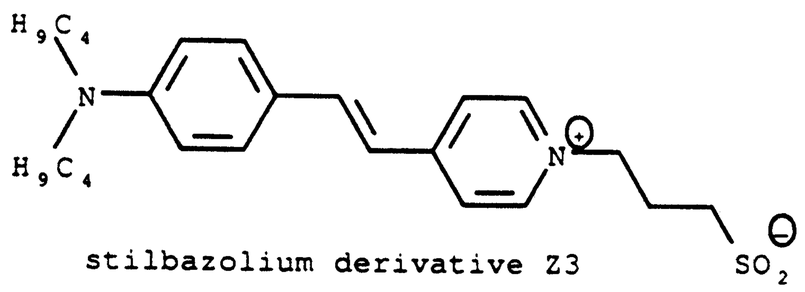		495[h]	HRS[c,e]	39	31 $\beta_0 = 20$	[216]
BOC-protected D-oligopyrrole-A		$n = 1$	376	HRS[b,c]		82	[219]
		2	366			177	
		3	364			277	
pyrrole/thiophene hybrid chain compound	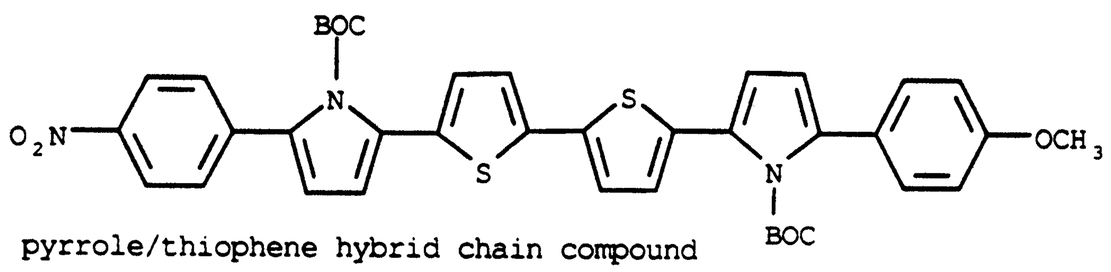		378	HRS[b,c]		440	[219]

continues

oligo-para(phenylene-vinylenes) has not been performed to our knowledge. An important aspect here is that higher β values correlate strongly with decreasing energy (increasing wavelength) of the charge-transfer transition, and for most applications there is a tradeoff between two properties: transparency and NLO efficiency [96, 176].

It should be mentioned that, parallel with this scheme, crystalline organic materials were (and are being) developed for SO NLO applications (mainly SHG and EO devices), for which not only the molecular β has to be optimized, but the crystal structure must be noncentrosymmetric (for a review see Ref. [174]). Combining both conditions is not straightforward, and the compounds for SO NLO crystals are often relatively small, asymmetric, and eventually chiral molecules. The compounds NPAN, NPP, and POM and some data given in Table III are a few examples of this approach, essentially based on the substituted benzene scheme. On the contrary, DR1 and DANS (also in Table III) are essentially rodlike compounds which have been used in host–guest or chromophore-functionalized poled polymers.

There is ample room for choices in organic chemistry, as illustrated in Table III with a selection of the conjugated moieties that have been incorporated in push–pull-type compounds. Occasionally less conventional links were studied, such as silicon-based compounds, in which α electrons are delocalized over the methylsilane segment [202–204]. The variety of D/A pairs, apart from the traditional ones already mentioned, is very large as well (also, the distinction between conjugated chain, and donor or acceptor group is not always clear-cut). In fact, a very large variety of compounds have now been synthesized in the quest for high SO NLO polarizabilities. We will not give a full account of this work here,

Table III. (continued)

Compound		λ_{max} (nm)		μ (D)	β (10^{-30} esu)	Ref.
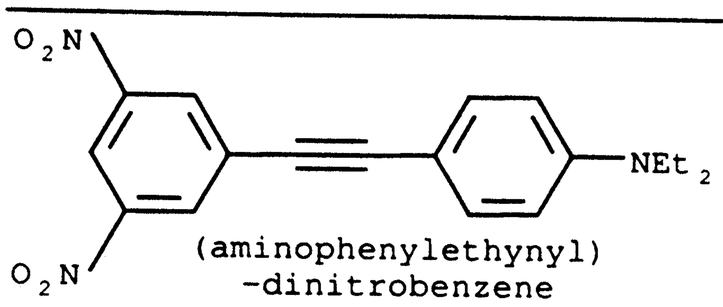 (aminophenylethynyl)-dinitrobenzene		383	EFISHG[b,f]	7.3	87	[99]
phenylethynylisoquinolium derivatives 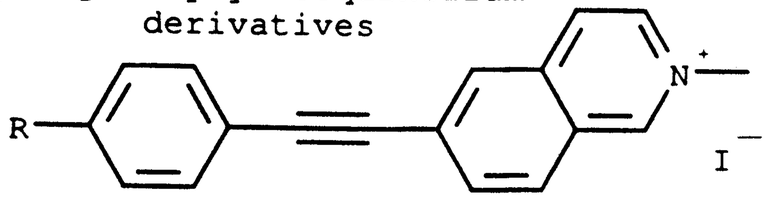	$R = H$	368	HRS[b,f]		51 $\beta_0 = 26$	[221]
	OMe	394	HRS[b,f]		108 $\beta_0 = 42$	
	NMe_2	478	HRS[i,k]		271 $\beta_0 = 108$	

[a] The hyperpolarizabilities are measured EFISHG values or equivalent values derived from HRS (i.e., $\sqrt{(35/6\langle\beta^2\rangle)}$). In some cases static values β_0, extrapolated from the two-level model, are given.

[b] $\lambda = 1.064\ \mu m$.

[c] In $CHCl_3$.

[d] Error in Table 1 of Ref. [223] and thus values were recalculated via β_{xxx} and β_{xyy}.

[e] $\lambda = 1.907\ \mu m$.

[f] In *p*-dioxane.

[g] In aceton.

[h] In methanol.

[i] $\lambda = 1.319\ \mu m$.

[j] In dimethylformamide (DMF).

[k] In MeCN.

but concentrate on the developments not yet included in the review by Nalwa et al. [174]. Also in this respect we do not claim complete coverage of the literature.

As was already shown by Cheng et al. [176] for a series of push–pull molecules, a quite general phenomenological relationship is found between the wavelength of the charge-transfer band, expressing the degree of charge transfer, and the static value of the first hyperpolarizability. As reviewed by Bosshard et al. [205], all the available points for one-ring (benzene) and two-ring (stilbene and dithiophene) compounds are found on straight lines in a semilog plot of β_0 vs λ_{eg}, with the double ring systems on a higher and steeper line than the benzene derivatives. This included a large number of points including different substitutions and heterocyclic rings. Combined with a transparency criterion, this puts an upper limit on the achievable figure with this class of compounds. For example, if transparency is required up to 400 nm, such as in most SHG applications, one ends up with $\beta_0 < 20 \times 10^{-30}$ esu while more than 10 times higher figures are available for EO applications in the near-IR region. This seems to indicate that for a given type of conjugated chain, the efficiency–transparency tradeoff is the only degree of freedom, and variations in design can be used mainly to optimize other aspects, such as chemical, thermal, or optical stability, or symmetry suitable for crystal growth and/or NLO engineering. However, the remaining good news is that this dependence is different for different conjugated systems, and one can hope to find significant improvements with well-chosen conjugated segments. As discussed in the next sections, other approaches also have been initiated to tackle this problem, such as the multipolar design of SO NLO molecules, three-dimensional approaches with electronic interactions between different chromophores, and the new degrees of freedom in the design offered by organometallic compounds. We will now discuss a number of compounds developed over the last 5 years.

A series of ionic aza compounds with the diazonium acceptor group has been characterized by means of HRS (as EFISHG is not suitable for ionic species) [144]. Very high static hyperpolarizabilities are found (Table III) but are correlated with a red shift of the optical band and with values fitting in the double-ring series. The strong electron withdrawal properties of the diazonium group are able to increase the charge transfer in the ground state (or the effective internal field in the BLA-type picture) to further increase β_0 as was demonstrated from comparison with DANS and its diethyl variant. It is of interest to see that for very good conjugated chains as employed here, even the strongest available D/A combination does not push the compound over the maximum in the β vs internal field diagram. This is in line with the conclusion of Blanchard-Desce and Barzoukas [194] that this maximum can be further increased by improved conjugated chain and proper D/A

combinations. The extrapolated β_0 values must be considered with great caution, because HRS measurements are performed on resonance (with moreover possible two-photon fluorescence contributions in the reported β's).

A number of similar aza compounds, with a variety of donor groups and a sulfonamide group as acceptor, have been synthesized [206] and two of them were characterized by HRS. They possess a pendant hydrophobic group which makes them suitable for mono- or multilayer ordered film formation. The structure and data of the sulfonamide amphiphile with highest hyperpolarizability are listed in Table III. The β values are quite high, but this is again correlated with the slightly longer peak absorption wavelength. In the other compound, the pyridine end group is replaced by another heterocyclic group, a thiazole ring, with very similar results for the optical and NLO results. Extensive calculations were performed on these two compounds and the other ones in the series, to get insight into the elements which determine the SO NLO properties.

In Table III a hydrazone derivative, out of a series of 10 that have been investigated [207], is shown as an illustration of a compound with a quite high β value based on an interesting combination of conjugated moieties. It combines this with a relatively good transparency region, although it does not escape from the scheme of the two-ring compounds mentioned before [205]. In this study the compound with two benzene rings was taken as a starting point, varying the structure in different ways: use of different donors, exchange of donor and acceptor positions (which are not equivalent here!), and substitution of either one of the benzene rings by thiophene, with β_0 values in the range of 13–39 $\times$ 10^{-30} esu, i.e., somewhat lower but close to the value of DANS. One compound of this family, 4-(1-azacycloheptyl)-benzaldehyde-4-nitrophenylhydrazone (DANPH) forms crystals with interesting NLO parameters [205, 207]. An extension to more compounds combining one phenyl ring with either a phenyl, a thiophyl, or a furyl ring was recently performed [208]. Furyl usually yields a smaller red shift of the absorption band, compared to thienyl, which according to the authors is not always correlated to decreased hyperpolarizability. They ascribe this to the existence of more than one electronic transition in these asymmetric chains and propose to use this feature as a new instrument to escape from the deterministic picture of β_0 vs λ_{max}.

Adducts of tetracyano-*p*-quinodimethane (TCNQ) have been synthesized and shown to have interesting properties for SHG applications [209]: In spite of the strong absorption band in the red region, they are very transparent in the blue region ("blue-window" chromophores) and were shown to possess high $\mu\beta$ values, appropriate for use in poled polymers. Moreover, for the second harmonic in this blue window, above the charge-transfer transition, anomalous linear dispersion is obtained, which later was shown to permit phase matching in films of well-chosen composition [210]. Two of these zwitterionic chromophores, nicknamed DEMI and ULTRA (Table III), have been further characterized and theoretically investigated for their single molecule NLO properties [18, 156, 211]. A molecular figure of merit, $\mu\beta(0) = 9450 \times 10^{-30}$ esu, was determined for DEMI. A careful study of the solvent induced internal field effects to determine the dipole moments in solution was performed, as well as measurements of the solvatochromism of the charge-transfer transition. The latter goes through a maximum as a function of solvent polarity, indicating the cyanine limit for these compounds.

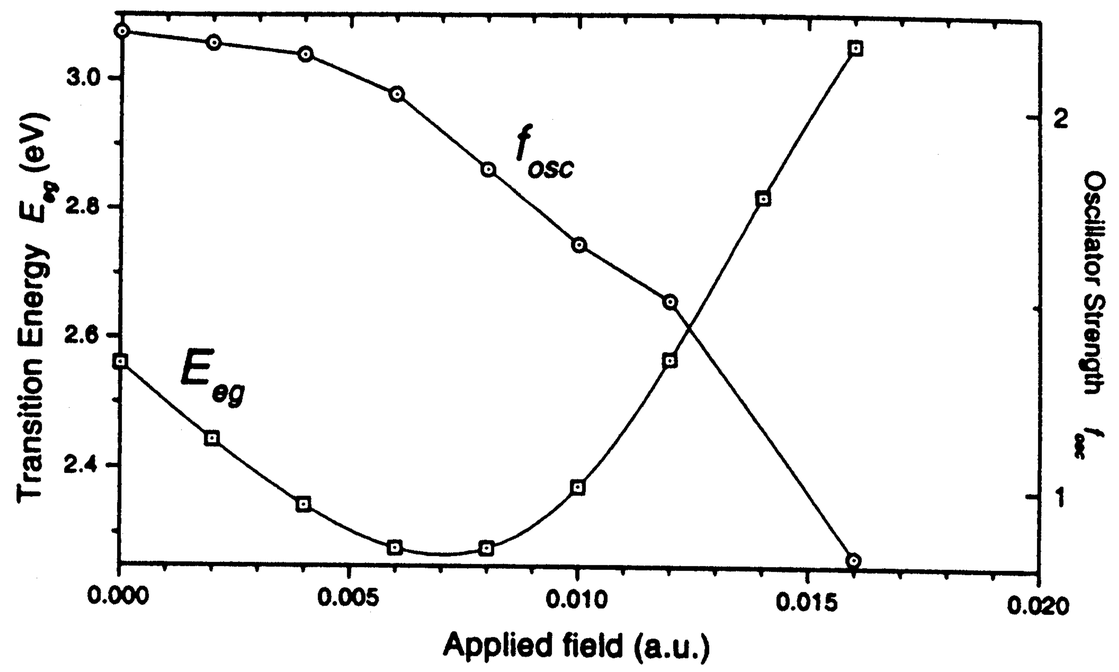

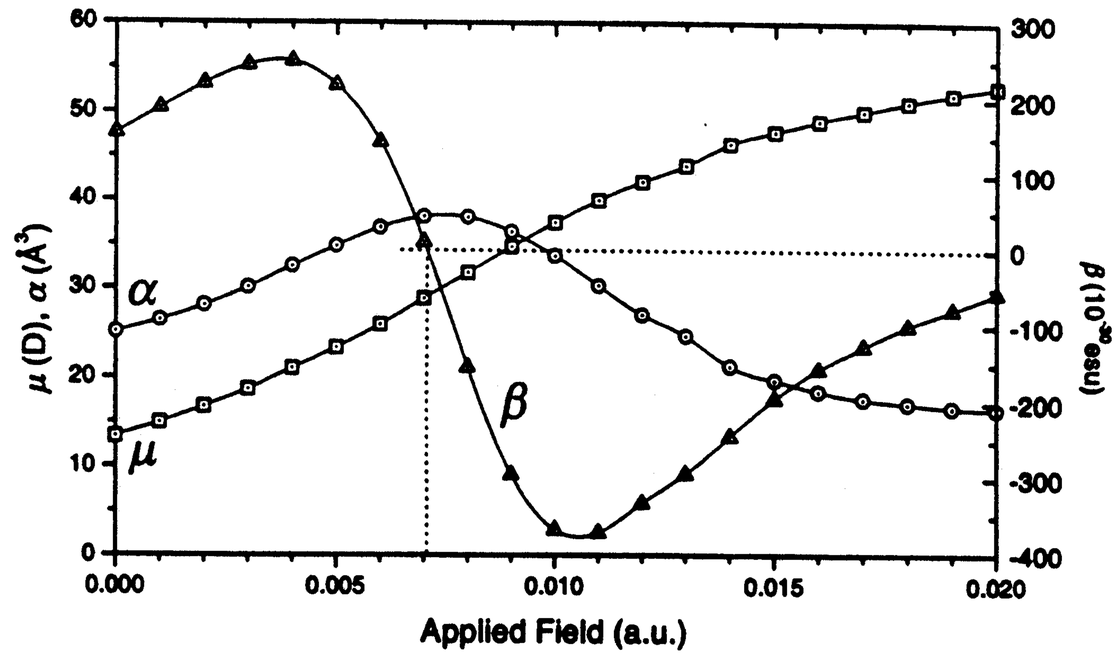

Fig. 10. Theoretical results for DEMI [212]. Evolution of the molecular dipole moment, polarizability, and hyperpolarizability with the reaction field were obtained from single and double configuration interaction calculations (bottom). From less involved self-consistent isodensity calculations, the evolution of the lowest excited state transition energy and transition dipole was also available (middle).

A theoretical investigation of these TCNQ derivatives [18, 209, 213] shows that the ideas of the BLA model can be transposed from polyene chains to these conjugated compounds. In Figure 10 the calculated dipole moments, linear polarizability, and first hyperpolarizability are shown as a function of applied internal field [212]. The derivative relationships between μ, α, and β are obvious, and the maximum of α and the zero crossing point of β correspond to the smallest value of the transition energy E_{eg}, also shown in this figure. This is the point of equal mixing between the two resonant states. The solvatochromism study showed that this point can be reached for DEMI and ULTRA at moderate solvent polarities. This has been confirmed by recent HRS measurements [156, 213] as a function of polarity in toluene/acetonitrile mixtures, shown in Figure 11. The measured β goes through a minimum when the reaction field pushes the molecules to be close to the cyanine limit, corresponding to the point of lowest transition energy observed in the solvatochromism experiment. At this point, one would expect the molecular β to vanish. However, $\beta_{HRS} = \langle\beta^2\rangle^{1/2}$ is an average over all molecules, each having its own microscopic field depending on the solvatation sphere containing varying amounts of both solvent species. It is important to realize that HRS and EFISHG will yield very different results in such circumstances.

The tricyanovinyl ligand has also been investigated for its efficiency as acceptor group using a thiophene–vinylene–phenyl sequence as conjugated bridge and two electron donating groups (Table III). Long wavelength HRS measurements [117] show values for β in the range of 500×10^{-30} esu, which is very interesting even if reduction to a few hundred will follow from extrapolation to the static value β_0. The HRS data could be cross-checked with earlier EFISHG measurements from Wong et al. [214] (also in Table III). These results were also correcting earlier data [133] which probably were overestimated due to multiphoton fluorescence. Further variation on this theme was shown [215] with the comparison between di- and tricyanovinyl as acceptor, and the replacement of the thiophene by a thiazole moiety. The stronger effect of the tricyano group is obvious in the position of the charge-transfer (CT) band (e.g., from 640 to 513 nm upon replacement by dicyanovinyl in ethyl versions of these compounds in Table III) and conversely in the higher NLO response (664 and 150×10^{-30} esu, respectively). No improvement was found from the thiazole compared to thiophene linkage, however.

As mentioned above, zwitterionic compounds offer large dipole moments which can be of interest for application in poled polymers. A stilbazolium-based chromophore (Z3) from a series of these compounds [216] is shown in Table III (its structure is very close to the famous DAST compound [217], in which the anion tosylate group is the end group linked to nitrogen). Compared to the standard compound DR1 it has a worse transparency-to-efficiency tradeoff. This illustrates that it is possible to influence the conjugation path negatively. However, the high dipole moments of nearly 40 D yield interesting $\mu\beta_0$ values around 1000 which leads to interesting macroscopic properties in a poled guest–host polymer. The thermally stable compounds may be suitable for the incorporation in side-chain polymers for EO applications. Other chromophores with quite high $\mu\beta$ were reported by Kubo et al. [218] who characterized three *N*-cyano-*N'*-diethylaminophenyl-1,4-naphthquinonediimines in polymethylmethacrylate (PMMA) by EO measurements in poled films at 1.3 μm, one of the main telecom wavelengths.

A systematic study of a very interesting new alternative for the conjugated backbone, oligopyrroles with butoxycarbonyl (BOC) protection groups, was reported [219]. The donor and acceptor ligands were methoxyphenyl and nitrobenzene, respectively. Comparison could be made with unprotected pyrroles and with thiophene analogs. This synthetic effort was rewarded by very interesting results. For an increasing number (HRS experiments for $n = 1, 2, 3$) of pyrroles with BOC protection, the β value steadily increases (Table III) with only a small shift of the lowest absorption band. It was proposed that not only this CT transition, but also a higher $\pi \rightarrow \pi^*$ transition helps to increase the hyperpolarizability. This idea led to the synthesis of a new compound, also in the table, including a dithiophene between the pyrrole rings to shift the $\pi \rightarrow \pi^*$ band to the same position as the CT band. This was successful and yielded increased β, without loss of transparency. In this case, escaping the two-level model has led to improvement.

Still other conjugated chains are explored, such as the dithienothiophene [220] group, which offers a more rigid structure and shows anomalous solvatochromic behavior. A broad exploration of such alternative backbones was performed, including combinations with acetylene, thienylpyridine, and isoquinone elements [221]. The compounds were systematically characterized for optical and SO NLO properties, and several systems with interesting hyperpolarizabilities combined with a relatively high CT transition (see, e.g., the phenylethynylisoquinolium derivative in Table III). Finally it is worth mentioning a somewhat analogous compound, an (aminophenylethynyl)-dinitrobenzene derivative, which was prepared in an effort to design molecules with large nondiagonal elements of β [99]. In fact, it has interesting NLO properties in its own right (also in the table), such as transparency in the blue combined with an appreciable hyperpolarizability.

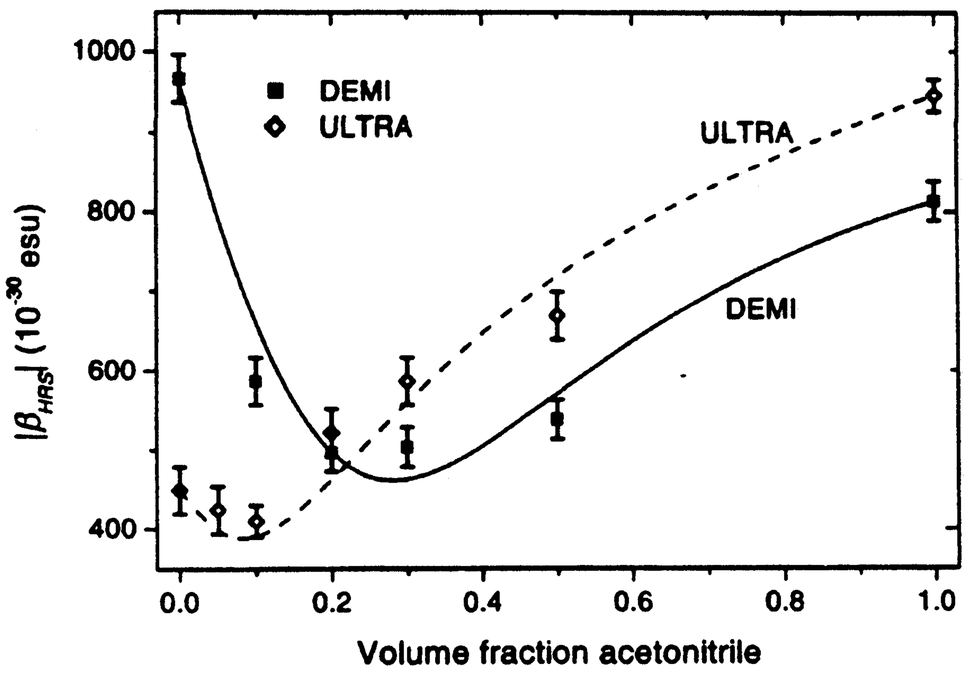

Fig. 11. Experimental HRS results for DEMI and ULTRA in toluene/MeCN solvent mixtures compared to the results of a model in which averaging is considered over different internal fields corresponding to statistically distributed compositions of the solvation shell.

3.2. Octupolar Molecules

3.2.1. *Multipolar Description of Molecular Second-Order NLO*

The near-exclusive attention for linear push–pull systems has long confined the design strategy of new SO NLO compounds to the optimization of a single component of the β tensor, mostly in dipolar molecules. As mentioned before, this was also supported by the most convenient measuring technique at that time, EFISHG, which is only applicable to dipolar species. It was Zyss [41, 42] who first pointed out the importance of the tensorial nature of β for the design of nondipolar molecules, adding a new dimension to molecular engineering in this field. Here we first give a summary of this description of the molecular SO NLO properties based on a multipolar decomposition of the β tensor [42, 222–224].

On the basis of the transformation properties of a third-rank Cartesian tensor [Eq. (7)], the first hyperpolarizability can be decomposed in irreducible tensor components,

$$\beta = \sum_{\substack{J=1,3 \\ -J \le m \le J}} \beta_m^J C_m^J(\theta, \phi) \tag{23}$$

(see, e.g., Ref. [223]) in which $C_m^J(\theta, \phi) = \sqrt{4\pi/(2J+1)} \times Y_m^J(\theta, \phi)$, and $Y_m^J(\theta, \phi)$ are properly normalized tensorial basis functions transforming under rotation like the well-known spherical harmonic functions. In general, the $J = 0$ scalar and $J = 2$ quadrupolar components of β_m^J can be nonzero, but they vanish in the nonresonant (static) case using Kleinman symmetry and overall permutation symmetry of the indices of the Cartesian tensor. The $J = 1$ and $J = 3$ components form the vectorial (or dipolar) and septor (or octupolar) parts of the tensor, corresponding to dipolar and octupolar induced charge distributions,

respectively. The vectorial basis functions transform among each other under rotations, and this is also the case for the octupolar components. The norms of the vectorial and octupolar parts, $\|\beta_J\|^2 = \sum_{-J\le m\le J} |\beta_m^J|^2$, for $J = 1$ and 3, respectively, yield two scalar invariants.

Depending on the symmetry group, tensorial quantities can be shown to vanish up to a certain order of the multipoles, and one can classify symmetry groups as quadrupolar and octupolar, when the first-order of nonvanishing tensor components is $J = 2$ and $J = 3$, respectively. In this sense, e.g., the tetrahedral T_d group and trigonal D_{3h} group are octupolar, and the orthorhombic D_2 group is quadrupolar. These symmetry groups are compatible with a nonzero β tensor, even while the compounds are nonpolar. This yields a classification framework and a systematic approach to study the possibilities for the existence of different NLO effects in molecules. In the static limit considered here, we will talk more loosely about octupolar molecules when the vectorial part $\vec{\beta}$ is zero by symmetry, i.e., no distinction is made with quadrupolar compounds. In this case all other vectorial quantities such as the permanent dipole moment $\vec{\mu}$ vanish as well.

Going back to the general case (but in Kleinman symmetry), the HRS intensity from randomly oriented molecules can be expressed in terms of the two invariants in the case of linear polarization of excitation and analysis (explicit expression in Refs. [223, 224]). In an orthogonal scattering geometry one finds, for instance,

$$\left\langle \beta_{XXX}^2 \right\rangle = \tfrac{1}{35}\left(7\|\beta_{J=1}\|^2 + 2\|\beta_{J=3}\|\|^2\right)$$

and

$$\left\langle \beta_{ZXX}^2 \right\rangle = \tfrac{1}{45}\left(\|\beta_{J=1}\|^2 + \tfrac{12}{7}\|\beta_{J=3}\|^2\right) \tag{24}$$

which are proportional to the HRS intensities measured parallel and perpendicular to the polarization of the incoming laser beam. This demonstrates that the ratio between the norms $\rho = \|\beta_{J=3}\|/\|\beta_{J=1}\|$, which is a scalar invariant as well, is directly related to the experimentally accessible depolarization ratio of the HRS intensities:

$$D = \frac{\beta_{ZXX}^2}{\beta_{XXX}^2} = \frac{1}{9}\frac{7+12\rho^2}{7+2\rho^2} \tag{25}$$

It is straightforward to determine the relative contributions of the dipolar and octupolar components $\|\beta_{J=1}\|^2/\|\beta\|^2$ and $\|\beta_{J=3}\|^2/\|\beta\|^2$ to the Cartesian norm of the whole tensor $\|\beta\|^2 = \sum_{i,j,k} \beta_{ijk}^2 = \|\beta_{J=1}\|^2 + \|\beta_{J=3}\|^2$, from the depolarization ratio.

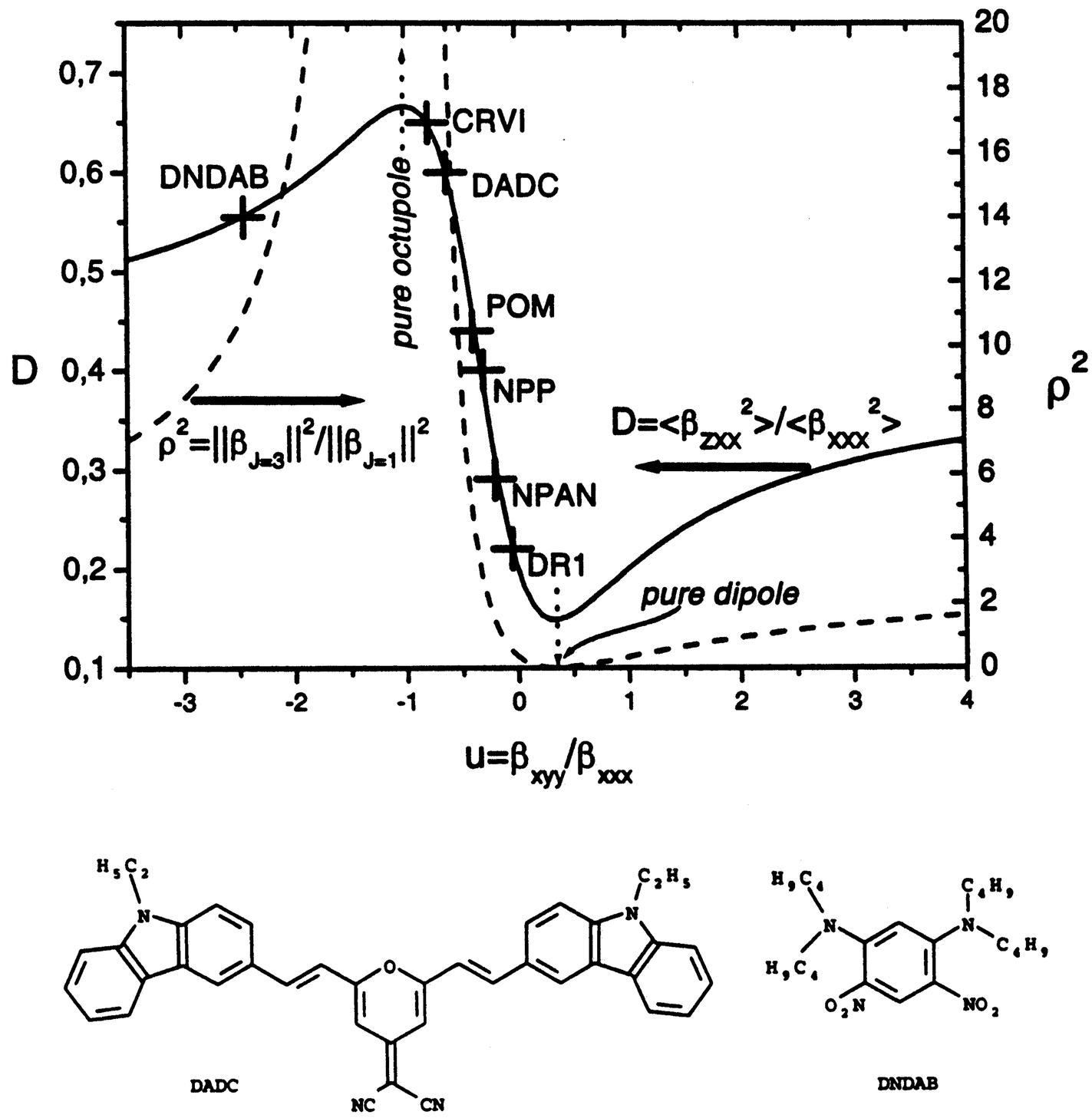

Fig. 12. The in-plane NLO anisotropy of a series of compounds going from push–pull toward octupolar systems, all possessing C_{2v} symmetry (or close to it), linked with the depolarization ratio D and the nonlinear anisotropy ρ (in the approximate 2D description). The push–pull type compounds DR1, NPAN, NPP, and POM are depicted in Table III, the crystal violet (CRVI) molecule in Figure 2, and the structure of the two remaining compounds is shown above the diagram. (From Ref. [223], with permission.)

As a first demonstration of the relevance of this approach, Zyss [42] made a compilation of the information then available from theory and experiment on the tensor components of a series of molecules. Putting this in a 2D diagram (Fig. 4 of Ref. [42]) with $\|\beta_{J=1}\|$ and $\|\beta_{J=3}\|$ as abscissa and ordinate, respectively, clearly shows two facts: (1) The octupolar contribution is significant even for so-called push–pull systems *p*NA, NPAN, or NPP (Table III), and (2) the purely octupolar nonlinearity of several compounds is at least comparable to that of the reference push–pull systems. Unlike the case of multipolar electrostatic fields, there is no general argument for a strong decrease in magnitude of the higher multipole contribution in a tensor describing a given NLO phenomenon.

From the basic Eqs. (19) and (20) given in Section 2.4.2, the polarized HRS intensities are ultimately related to the tensor components. It is not feasible, in general, to determine the individual tensor components. However, for a sufficiently high molecular symmetry only a few independent components are left, and eventually they can be determined. This game was played for a series of molecules with C_{2v} symmetry or higher, ranging from typical push–pull molecules to an octupolar compound (Fig. 12). Considering them as approximatively planar systems, a one-to-one correspondence can be made between the in-plane anisotropy $u = \beta_{xyy}/\beta_{xxx}$ and the ratio of the two remaining independent β components (small Cartesian indices indicate the local coordinate system of the molecule). This is related to the depolarization ratio D, which can be measured, and the nonlinear anisotropy ρ defined above in terms of the multipole contributions. These results also demonstrate that even for so-called push–pull molecules the octupolar part of the tensor is often appreciable.

From the very beginning, the origin of the octupolar hyperpolarizability has been discussed in terms of intramolecular charge-transfer processes [41]. In the push–pull molecules, the single transition considered in the two-level model carries the charge transfer along the chain. The induced moment is directed along the chain and gives rise to a significant dipolar contribution to the hyperpolarizability. In planar molecules (with, e.g., 3- or 4-fold axis) or in three-dimensional octupolar molecules (e.g., T or O symmetry) one also expects that charge-transfer mechanisms would give rise to high induced multipolar charge distributions. In several cases this has been analyzed as a superposition of three or four equivalent coupled charge-transfer processes along different bonds. Let us consider the specific case of the so-called "crystal violet" molecule. In this case, three donor groups can transfer charge to the central ion. Each of these has a dipolar character, but the three vectorial parts along the three bonds sum up to zero. However, the higher multipole contributions are not zero. In fact at least a three-state model is needed to reach an understanding of these phenomena as was further theoretically investigated [225–229]. In two of these studies [226, 228] the influence of the reaction field in polar solvents was also evaluated and found for both the ionic and neutral model molecules to be significant, up to doubling of the octupolar β. In the same spirit, the Onsager reaction field description has been revisited for application to octupolar molecules, with application to TATB [230].

Octupolar molecules are considered to offer a way out of the problem of noncentrosymmetric ordering of SO NLO molecules. While the lack of a permanent dipole moment is considered as an advantage, for instance, for molecular packing in crystals (for a discussion, see Ref. [157]), it certainly precludes orientation of the molecules by a static electric field, as was widely applied in poled polymer systems. Also, the use of quadrupolar or octupolar static electric fields does not seem applicable, because of the decreasing orientational force expected from them. However, a method of dynamical or permanent orientation by an optical multipole field has been proposed and demonstrated [223, 224, 231, 232].

3.2.2. *First Hyperpolarizability of Octupolar Compounds*

The first octupolar molecule for which β (i.e., β_{xyz}) was determined experimentally (by HRS) is CCl_4 [104, 106, 107, 164, 233]. The study of multipolar contributions to the hyperpolarizability and of octupolar *conjugated* molecules started relatively recently, and, contrary to the push–pull family, the number is quite limited. Therefore, we have made an attempt to offer an overview of all the compounds of this family that have been experimentally characterized. In Figure 13 the structure of these compounds is given, and relevant data and literature references are summarized in Table IV. They mostly can be classified according to the different types that were proposed early on [41–44]. The comparison of literature β values is even less straightforward for octupolar molecules than for the push–pull compounds. In the first place different unit systems and conventions can again be encountered. In push–pull systems, the dominant tensor component was often reported, because of the correspondence to the EFISHG results, in the assumptions of only a single nonzero component and $\vec{\beta}//\vec{\mu}$, which was further continued for HRS results, using the EFISHG results for chloroform and *p*NA, e.g., to yield "effective EFISHG" β values. However, for each molecular symmetry the correspondence between this value and relevant tensor components is different, as was realized early on. In fact, different choices have been made to report HRS data of octupolar molecules. A reasonable approach, which seems to be adopted more often now, consists of reporting the basic HRS observable $\beta_{HRS} = \langle\beta^2\rangle^{1/2} = (\langle\beta^2_{ZZZ}\rangle + \langle\beta^2_{XZZ}\rangle)^{1/2}$, which is independent of the assumed local symmetry of the molecule. The further reduction of the data can then start from this quantity. The internal reference method used with the EFISHG calibration led some authors to still report effective values β^{eff}_{EFISHG} which relate to the HRS observable by $\beta^{eff}_{EFISHG} = (\frac{35}{6})^{1/2}\beta_{HRS}$ (for unpolarized light). Finally, for the first reports on planar octupolar molecules with 3-fold symmetry, the in-plane diagonal tensor component was reported, given by $\beta_{xxx} = \sqrt{\frac{21}{8}}\beta_{HRS}$ for this specific case. We have tried to reduce all the available HRS to the value β_{HRS}, with the consequence that one must take the prefactor into account when a comparison is made with the HRS efficiency of tradition push–pull molecules (e.g., the well-known value for *p*NA in MeOH [39] $\beta^{eff}_{EFISHG} = 34.5 \times 10^{-30}$ esu corresponds to $\beta_{HRS} = 14.3 \times 10^{-30}$ esu). For data to be useful, future reports should be accurately documented with respect to the definitions, conventions and units, and reference β which have been employed.

The TATB family has a benzene group in the center and different ligands are asymmetrically positioned on the corners, giving rise to planar or near-planar molecules with 3-fold symmetry. Due to its low solubility this parent compound (structure in Fig. 2) has never been characterized by HRS, and the available data are derived from SHG in the crystalline material [43] and from calculations [225, 228, 230]. HRS results are available for direct analogues of TATB, namely TIATB, THTB, Oct7, and Oct8, using different donor and acceptor groups [234, 235]. The tri-substituted

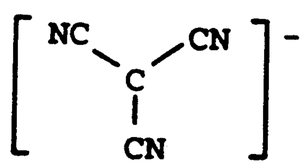

$[C(CN)_3]^-$

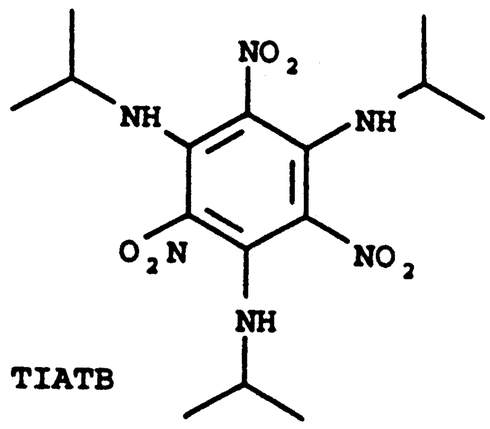

TIATB

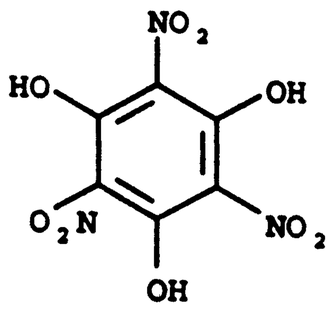

THTB

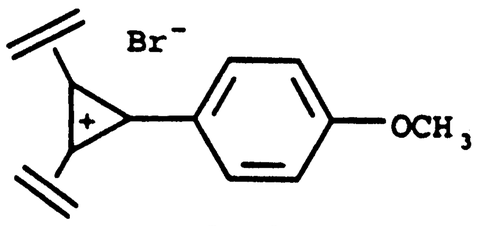

Oct1

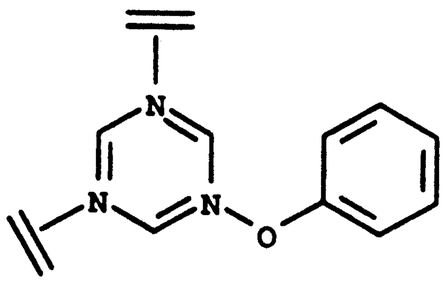

TPOT

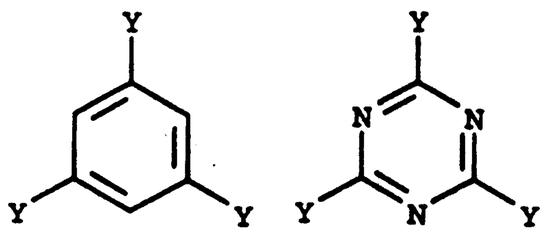

tri-substituted benzene

triazobenzene

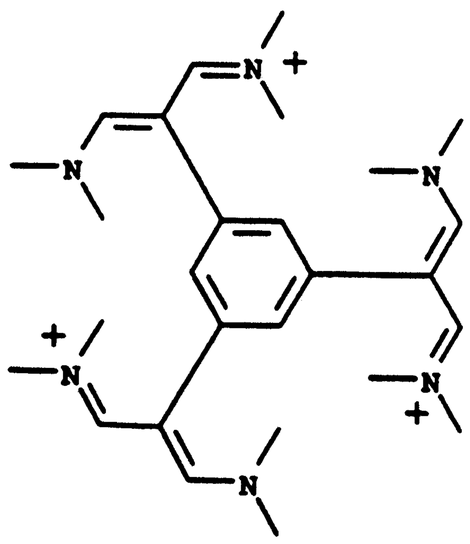

trivinamidinium benzene

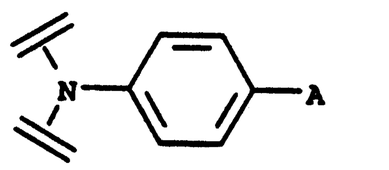

Oct2: A= -CN
Oct3: A= -CHO

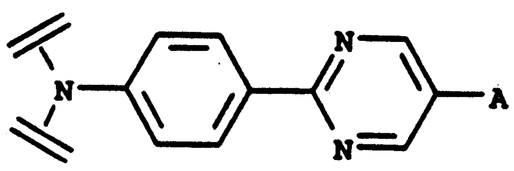

Oct4: A= -CN
Oct5: A= -COOMe

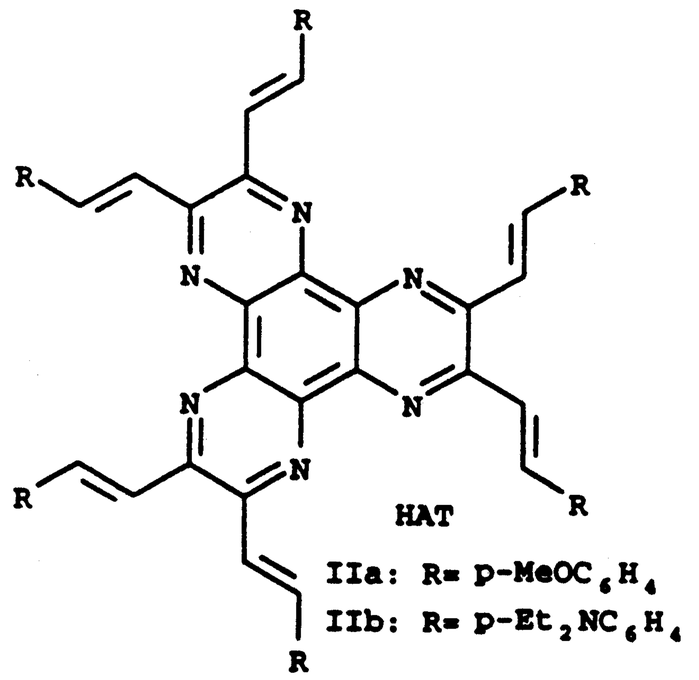

HAT

IIa: R= p-$MeOC_6H_4$
IIb: R= p-$Et_2NC_6H_4$

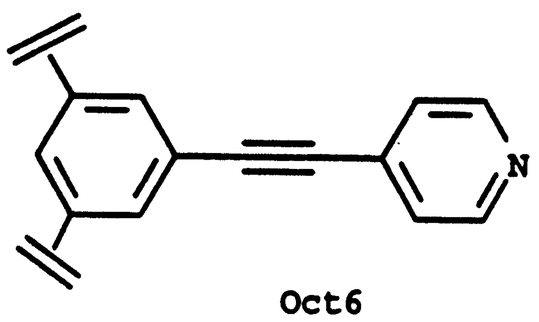

Oct6

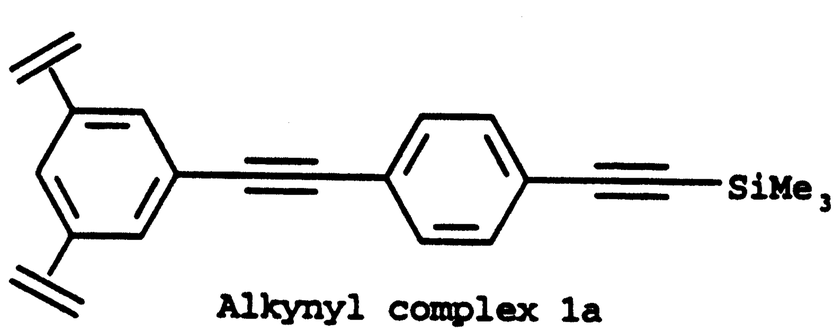

Alkynyl complex 1a

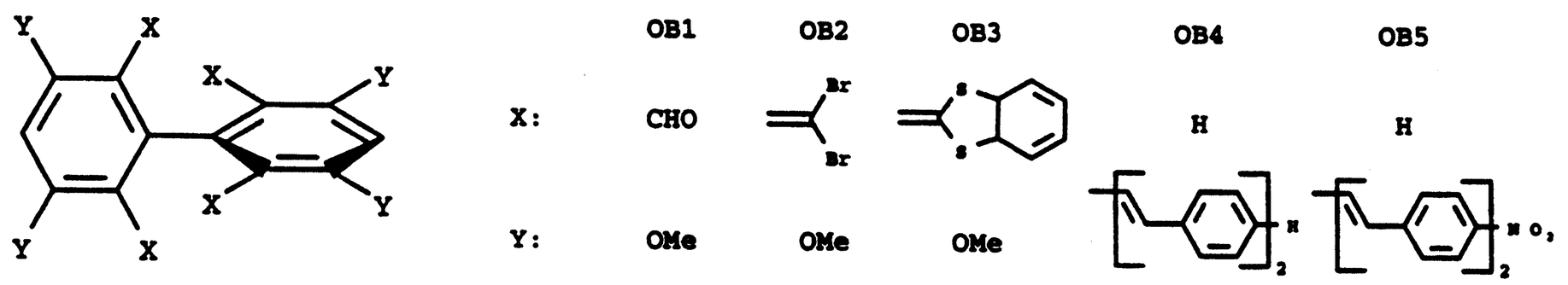

D_{2d} biphenyl derivatives

Fig. 13. Molecular structures of octupolar compounds listed in Table IV. For the star-shaped compounds, only the central part and one ligand are shown (double line signs cutting the two other ligands).

benzenes and triazobenzenes [236], as well as the trivinamidinium-substituted benzene [237], and the compounds TPOT [157], Oct6 [125], the alkynyl complex [48], Oct10, and Oct11 [235] are close family, but they possess only three symmetrically positioned substituents of varying conjugation length and charge-transfer properties. The nitrogen substitution in the trazine ring can be considered as electron-donating toward, e.g., the phenyl groups. Moreover, the triazines, TPOT, Oct10, and Oct11 contain a heterocyclic nitrogen-substituted central ring. Standing out of this series is the TPOT compound with marked chirality, which is deliberately selected to favor noncentrosymmetric crystal growth of this octupolar system. In this context Zyss et al. [157] proposed new design rules for multipolar SO NLO materials both on the level of crystal and optical engineering. Also in a previous design molecule,

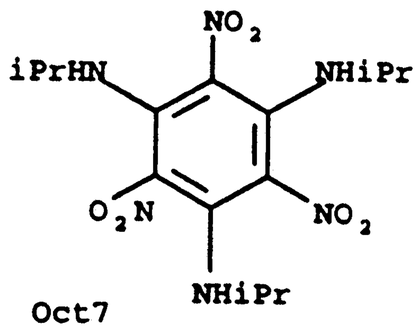

Oct7

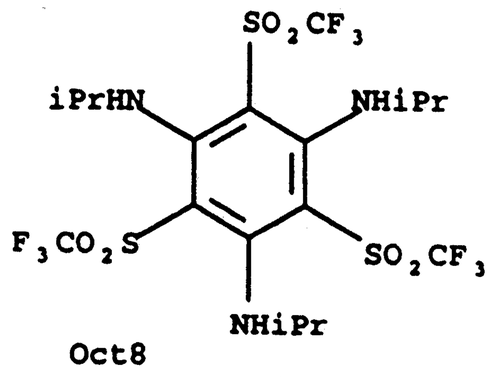

Oct8

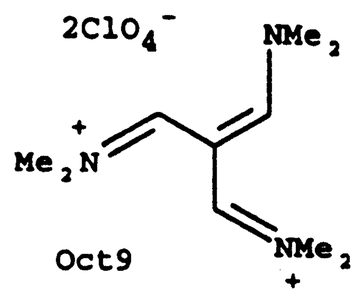

Oct9

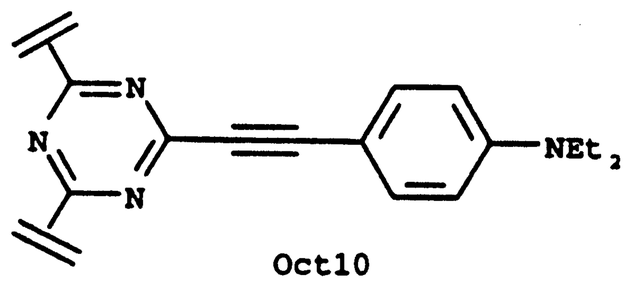

Oct10

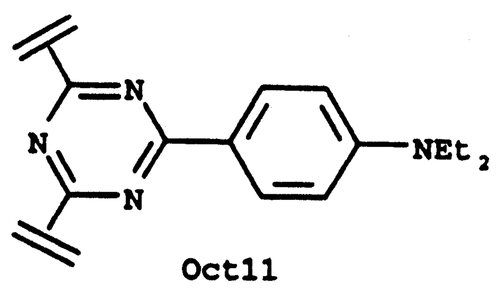

Oct11

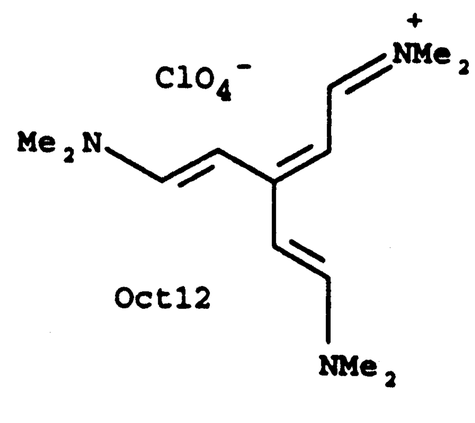

Oct12

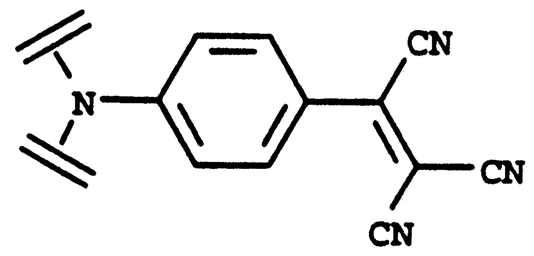

tricyanovinyl-substituted triphenylamine

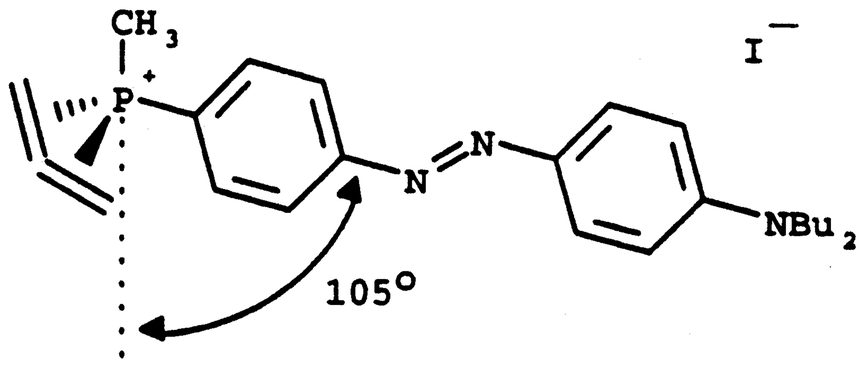

phosphonium chromophore 2 (C_3)

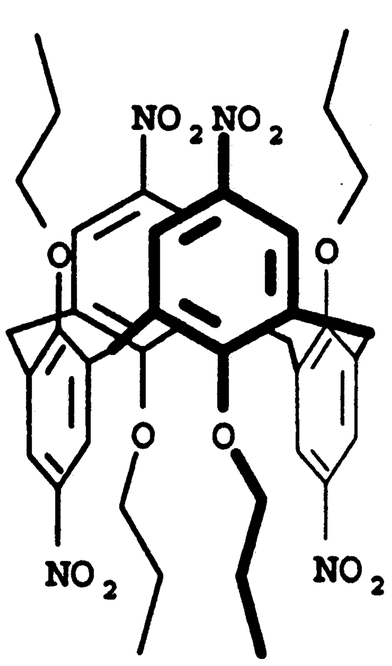

tetracalix[4]arene 1,3-alternate

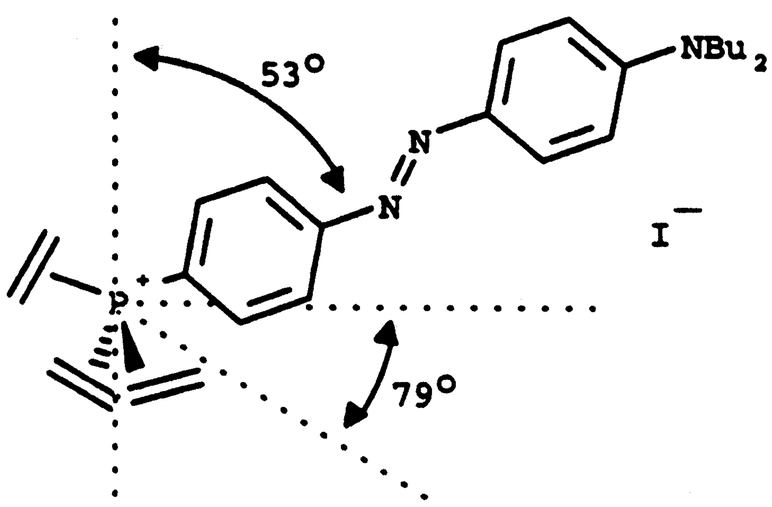

phosphonium chromophore 3 (D_2, near T)

Fig. 13. (Continued).

tribenzyl isocyanure (not listed), a promising result was obtained with a noncanceling crystal stacking, but on the basis of hydrogen bonds between neighboring molecules [238]. In this case, however, the nonlinearity was not very high, due to the poor conjugation between central and peripheral rings.

The hexaazatriphenylene derivatives (HAT) are also centered around an aromatic ring, but in this case the central conjugated segment is enlarged [168]. Other compounds of interest with a large conjugated central region are the subphthalocyanines (a boron–subphthalocynanine is depicted in Fig. 2) and the porphyrines treated in Section 3.3, but in all these cases the mechanisms for higher order polarizability are expected to be more complex than in the TATB analogues.

The star-shaped planar structures, with crystal violet as the parent compound (see Fig. 2) have an atom or ion at the center, 3-fold coordinated with donor or acceptor groups or longer NLO active chromophores. The simple tricyanomethanide molecular ion (Fig. 13) was chosen as a test system for HRS from octupolar molecules, and in spite of the modest β value, this study further supported the multipolar analysis of the SO NLO properties. Crystal violet itself has been extensively investigated and later on was used as a test compound, very much like *p*NA or DANS for

Table IV. Organic Octupolar Molecules for SO NLO[a]

Compound	Symmetry	Solvent	λ_{max} (nm)	λ_0 (nm)	β_{HRS} (10^{-30} esu)	Ref.
$[C(CN)_3]^-$	D_{3h} planar	Methanol	<300	1064	4.3 ± 1.0^b	[150]
Crystal violet	D_3 planar	Acetone	≅585	1064	$358^{b,c}$	[44]
		Methanol			$703^{b,c}$	[158]
					$1890 \pm 460^{b,c}$	[234]
				872	$265 \pm 80^{b,c}$	
				800	$280 \pm 60^{b,c}$	[121]
		Chloroform		900	$207 \pm 40^{c,e}$	[125]
		Chloroform		1500	55^b	[120]
		Acetonitrile		1450	72^b	
		Chloroform		1340	277^c	[223]
TIATB	D_{3h} planar	Chloroform	375	1064	10 ± 3^b	[234]
		Nitromethane	383		12 ± 3^b	
THTB	D_{3h} planar	Acetone	395	1064	17 ± 4^b	[234]
		Methanol	385		15 ± 4^b	
Oct1	D_{3h} planar	Methanol	359	1064	56 ± 12^b	[234]
Tri-substituted benzenes; $Y =$ Cl	D_{3h} planar	Methanol	*d*	1064	5.0	[236]
OH					5.8	
OMe					9.4	
Me					3.6	
Ph					11.5	
Tri-substituted triazobenzenes; $Y =$ Cl	D_{3h} planar	Methanol	*d*	1064	12.6	[236]
OH					14.6	
OMe					21.1	
SH					18.3	
Ph					25.9	
Trivinamidinium benzene	D_{3h} planar	Acetonitrile	365	1064	35	[237]
Oct2	C_3 planar	Chloroform	340	1064	48	[119]
Oct3			369		45	
Oct4			425		97	
Oct5			415		126	
Oct6	D_{3h} planar		302	900	13 ± 2^e	[125]
HAT IIa	C_3 planar	DMSO	460	1560	$7.5^{e,f}$	[168]
HAT IIb	C_3 planar	DMSO	526	1560	$21^{e,f}$	
TPOT	C_3 planar	Chloroform	*d*	1064	18	[157]

continues

the push–pull systems, for a number of investigators performing measurements at different wavelengths with different instruments (Table IV). It owes its very large hyperpolarizability to the resonant or close-to-resonant conditions of the experiments. Proper reduction to zero frequency using a three-level model yields [120] $\beta_{HRS}(0) \cong 19 \times 10^{-30}$ esu ($\beta_{xxx}(0) \cong 30 \times 10^{-30}$ esu) which is comparable in size to *p*NA. There is a large difference between the original result of Zyss et al. [43] and the later measurements, which may be a matter of calibration or another systematic error. Other compounds in this class are Oct2, Oct3, Oct4, and Oct5 [119], Oct9 and Oct12 [235], and the tricyanovinyl-substituted triphenylamines [239], each of which has quite long conjugated ligands instead of the simple CN acceptor groups in tricyanomethanide. In the case of the neutral Oct2–Oct5 compounds and the triphenylamines, which carry acceptor groups (−CN, −OCH, or tricyanovinyl) on the ligands, the central carbon is replaced by a nitrogen atom. In fact, these propeller-shaped compounds are only approximately octupolar and possess a small dipole moment. Stadler et al. [240] reported two more compounds fitting in this series (not listed here), one of which is chiral and should crystallize in a noncentrosymmetric structure, and one has even longer conjugated ligands. However, in both cases the β values are much smaller. The Oct1 molecule is also star-shaped, but the carbon ion is now replaced by a cyclopropylium group. For Oct9 a second experiment

Table IV. (continued)

Compound	Symmetry	Solvent	λ_{max} (nm)	λ_0 (nm)	β_{HRS} (10^{-30} esu)	Ref.
Oct7	D_{3h} planar	Dioxane	375	1064	7.7[b,g]	[235]
Oct8			290		2.7[b,g]	
Oct9	C_{3h} planar	Acetonitrile	320		3.6[b,g]	
		Water	321		11[b]	[237]
Oct10	D_{3h} planar	Acetone	425	1064	168[b,g]	[235]
Oct11			375		67[b,g]	
Oct12	C_{3h} planar	Acetonitrile	430		42[b,g]	
Nitrocalix[4]arenes-1,3-alternate conformer	D_2 3D	Chloroform	291	1064	3.3[e]	[241]
				900	3.7[e]	
Phosphonium chromophore 2	C_3 3D	MeCN	483	1300	123	[242]
Phosphonium chromophore 3	D_2 (near T) 3D		499	1300	162	
Alkynyl complex 1a	D_{3h} planar	THF	342	1064	8	[48]
Tricyanovinal-substituted triphenylamines	D_3 planar	MeCN	522	1500	70[c]	[239]
D_{2d} biphenyl derivatives						
OB1	D_{2d} 3D	Chloroform	248	1064	12	[243]
OB2			251		13	
OB3			320		38	
OB4			361	1340	12	[244]
OB5			401		110	

[a] Molecular structures are shown in Figure 13 except for crystal violet in Figure 2. Near-planar or 3D geometries are indicated with the approximate symmetry. Checks of the expected depolarization ratio $D \cong 2/3$ are reported in all cases, except for the phosphonium chromophores [242], the substituted triazines [236], and the tricyanovinyl substituted triarylamines. THF, tetrahydrofuran.

[b] Converted back to molecular averaged value. $\beta_{HRS} = \langle\beta^2\rangle^{1/2} = (\frac{8}{21})^{1/2}\beta_{xxx}$.

[c] Near-to-resonance conditions.

[d] λ_{max} not reported

[e] Converted using $\beta_{HRS} = (\frac{6}{35})^{1/2}\beta^{eff}_{EFISHG}$.

[f] Wrong reference value for methanol of 0.69 (instead of 0.26) $\times 10^{-30}$ esu [111, 112].

[g] Converted from SI units and for Taylor convention (factor 1/4).

from a different laboratory was reported [237], in water instead of acetonitrile: The difference by more than a factor of 3 between the two values, after proper conversion, is remarkable.

Finally, only a few organic octupolar molecules with 3D structure have been characterized up to now. (Some more examples are found among the organometallic complexes, in Section 4.6.) The nitrocalix[4]arene compound [241] depicted here is a nice example of a 3D structure build up from four units consisting of a simple push–pull molecule, in which the individual dipole moments are oppositely oriented and cancel out. So does the vectorial part of β, as is witnessed by the depolarization ratio. In fact, the octupolar part is also modest, which could be expected from a system with only weak interaction between the four dipolar chromophores that are the subunits of this compound. This example illustrates that it is not sufficient to assemble a molecule with octupolar symmetry from efficient dipolar compounds: The electronic interactions between the different building blocks is essential to obtain a large octupolar component of β. Of the four conformers which were studied [241], a second one, the 1,2-alternate (not shown), also has suitable geometrical properties to yield an octupolar hyperpolarizability. However, in that case the depolarization ratio differs significantly from $\frac{2}{3}$. It turns out that dynamical deviations from the equilibrium geometry yield a distribution of SO NLO properties for the ensemble of molecules which deviates more from the octupolar case for the 1,2-conformer than for the 1,3-conformer. This is an interesting case showing that for nonrigid molecules dynamical deviations from the nominal symmetry can become important. Two more octupolar compounds in Table IV are build by a tetrahedral complexation of the central phosphonium ion [242]. Chromophore 3 is near to tetrahedral, while the trigonal chromophore 2, according to the theoretical analysis of the authors, has a near to octupolar β tensor, in spite of its nonplanar trigonal symmetry. The 3D character of the compounds would allow for interaction between the equivalent conjugated ligands with enhancement of the total SO nonlinearity as measured by the norm $\|\beta\|$ compared to the corresponding ligands, without tradeoff for transparency. Finally, a very different approach was recently followed by Blanchard-Desce et al. [243, 244] to build genuinely organic octupolar molecules with 3D character (D_{2d} symmetry): A biphenyl central moiety is forced to have the phenyl rings in mutually perpendicular planes by the sterical hindrance induced by substituents in *ortho*-positions (X group in the structures OB1–OB5, see Fig. 13). A first group, OB1–OB3, of products was obtained by variation of the electron donating or withdrawing prop-

erties of these substituents [243, 244]. For better transparency in the visible regions, similar or even larger nonlinearities were observed, and this is even more pronounced when the extrapolations to static β values are considered. In a second series, OB4 and OB5, taking X = MeO as an electron-donating sterical hindrance moiety, a vinylene-phenylene conjugated ligand (Y in structure, Fig. 13) was placed in the four adjacent sites [244], which was either neutral (OB4) or electron withdrawing (OB5, with NO_2 end group). While no particular improvement is seen for the former compound, compared to the series without Y ligands, the latter is superior to the benchmark push–pull dye DR1 for a better transparency: $\beta_{HRS} = 110 \times 10^{-30}$ esu ($\beta_{HRS}(0) = 65 \times 10^{-30}$ esu) for the OB5 compound, compared to $\beta_{HRS} = 78 \times 10^{-30}$ esu ($(\beta_{HRS}(0) = 31 \times 10^{-30}$ esu) for DR1, both at 1.34 μm in $CHCl_3$. All the figures become even more favorable when one looks at either the dominant tensor components (β_{zzz} and β_{xzz} for the linear dipolar and the octupolar case, respectively), or at the modulus $||\beta||$ defined for the second nonlinear polarizability. These results give strong experimental support for the claim that octupolar, and particularly 3D, molecules can bring the efficiency/transparancy tradeoff into a more favorable region.

3.3. Alternative Approaches

The previous sections have concentrated on two families of compounds which in fact form limiting cases: The push–pull systems are crudely considered as linear systems with only one diagonal element of the β tensor, while all other elements are zero. The octupolar molecules possess no dipole moment or dipolar part of β due to their symmetry. In fact, as discussed in the previous section, even among the push–pull systems, many have nonnegligible nondiagonal elements, and thus a sizable octupolar part of β. Also in the synthesis efforts directed toward efficient SO NLO crystals different criteria are valid, and this also has often led to compounds which do not fit in the typical (donor–linear conjugated chain–acceptor) design of dipolar molecules. A discussion of nonclassical chromophores for SO NLO by Wong et al. [173] is worth mention here.

An early molecular engineering proposal was that of Λ-shaped molecules [245], which was demonstrated with the example of methanediamines, in which two benzene derivatives are coupled at an angle over the methane carbon. Up to 75% of the Λ-shaped molecules which have been synthesized turn out to crystallize noncentrosymmetrically. Their dipole moment is along the bisectrice of the two axes of charge transfer in the benzene derivatives, and thus large nondiagonal components of the hyperpolarizability are expected, which allows for better phase-matching properties.

The paradigm of fully π-conjugated chains as links between donors and acceptors has also been questioned. Nonconjugatively linked D/A compounds were reported [246] nearly 10 years ago with β values comparable to those of *p*NA. Also, in one of the families of efficient push–pull systems reported earlier [207], the hydrazonium derivatives (see Table III), the molecules contain a nonconjugated bond besides conjugated segments and have partial rotational freedom around this bond. But dipolar or excitonic coupling between chromophores has also been proposed as an alternative scheme [69, 247–250], which would eventually help to circumvent the limits of the efficiency/transparency tradeoff. In a sense the calix[4]arenes [241–251]—among the octupolar conformers discussed in Section 3.2.2, Figure 13, and Table IV—turn out to be an example in which the interaction between the dipolar chromophores is not sufficient to induce considerable enhancement of the hyperpolarizability. However, efficient SHG in thin films has been demonstrated with these compounds, which is related to their structural features [252].

A number of molecules with a more complex network of conjugated bonds are being explored, such as the subphthalocyanines [45, 253] (see Fig. 2 in Section 1.4), porphyrines and their derivatives [145, 254–256]—among which high hyperpolarizabilities have also been observed—and other nonoctupolar compounds for which large off-diagonal elements of β were observed or can be expected [100, 257]. The triptycene derivatives reported earlier by Norvez and Barzoukas [258] could also be considered to belong to the latter group.

As mentioned before, for centrosymmetric molecules β vanishes. However, this statement neglects the dynamical deviations from this symmetry or symmetry breaking due to influence from the surroundings. As mentioned before, Ashwell et al. [19] studied a squaraine compound which as an isolated molecule is centrosymmetric, but in the solid state yields an appreciable SHG efficiency, due to local symmetry breaking. HRS measurements were reported on a related squarilium dye, which also is a priori expected to be a centrosymmetric compound [259]. This could be a case of symmetry breaking in solution, related to the solid-state properties of the squaraine-type compound. It is also useful here to recall the deviations from octupolar symmetry observed [241] for one of the structurally octupolar nitrocalix[4]arene compounds, which were ascribed to dynamical lowering of the symmetry due to the flexibility of the geometrical structure.

Beyond the single-molecule properties, supramolecular effects may prove to be essential to reach highly efficient NLO materials. Also on this level a detailed understanding of mechanisms is needed, and different steps in this direction are being taken. An recent example is the amylose–dye inclusion complex recently studied by HRS [135] in which the guest, a stilbazolium chromophore, yields high hyperpolarizability, while chirality is introduced by the amylose host chosen to form a helical structure. Moreover, the authors report that the static β_0 value is doubled due to guest–host interactions. Finally, the inclusion complex has useful properties for polar orientation and for stability in thin films. Further investigations (e.g., in [159, 260, 261]) are concerned with polymers in which NLO chromophores appear as building blocks. Also in such cases, evidence is reported for interactions between the chromophores which boost the hyperpolarizability compared to the uncorrelated case.

4. ORGANOMETALLIC COMPOUNDS

Organometallic chemistry emerged as a new potential area of research after the pioneering work of Frazier et al. in 1986 [262] that screened SHG efficiencies for more than 60 group VI metal carbonyl derivatives. Although only four of them had shown a conversion efficiency of about the same magnitude as ammonium dihydrogenphosphate (ADP), the ground had been broken. One year later, the first organometallic compound designed to contain the main features thought to be on the basis of SHG, i.e., donor-π-system-acceptor, was reported by Green et al. [263]. This compound, (*Z*)-1-ferrocenyl-2-(4-nitrophenyl)ethylene (**1**), showed an efficiency of 62 times the urea standard. Another ferrocenyl derivative, (*E*)-1-ferrocenyl-2-(1-methyl-4-pyridiniumyl)ethylene iodide (**2**) reported in 1989 by Marder et al. [264], found to be

220 times better than urea on SHG efficiency, showed that the organometallic area could be an interesting field of research for nonlinear optical properties. Some important advantages could be envisaged here relative to inorganic and organic materials. Since NLO response occurs primarily through electronic polarization, organometallic (and also organic) materials constitute a better alternative to inorganic materials, particularly when extremely rapid NLO responses are required, due to the fact that many inorganic materials operate through lattice distortions, which are comparatively slower processes.

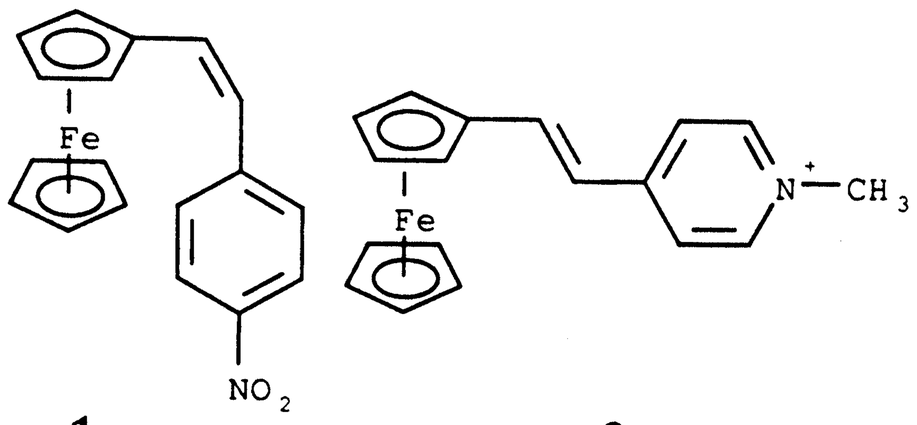

1 2

A likely advantage of organometallics relative to organics may be the possibility of CT involving the metal and one or more coordinated ligands, or metal–metal CT bands in the case of intervalent compounds, and a further enhancement of nonlinearity owing to the new variables introduced by the transition metal, related with its size, nature, and redox ability. These features might lead to large oscillator strengths and provide a substantial contribution to the hyperpolarizability β. On the other hand, new bonding geometries, interacting with nonaromatic and aromatic coligands, can tune molecular hyperpolarizabilities, since they might change the energies of occupied and unoccupied metal d orbitals that interact with the π electron orbitals of the conjugated chromophore.

Besides the molecular structure that can be responsible for high values of the hyperpolarizability β in individual molecules, noncentrosymmetric arrangement is required when attempting to engineer a material with a large $\chi^{(2)}$. Centrosymmetry is responsible for the fact that about 75% of all known nonchiral organic molecules lead to bulk materials with vanishing second-order susceptibilities ($\chi^{(2)}$) [265]. Organic compounds such as *p*NA and DANS, for example, have high values of β at 1.064 μm, 34.5×10^{-30} esu and 450×10^{-30} esu (see Table III), respectively, but both crystalline materials are centrosymmetric and SHG is not observable. The same is found for the organometallic [Fc$-(E)-$CH=CHC$_6$H$_4-4-$NO$_2$] (Fc stands for ferrocenyl), the *trans*-isomer of the well-known compound (1), which also presents a high value of β, 34×10^{-30} esu, about 3 times higher than the *cis*-isomer and a vanishing SHG effect [266–271]. Several approaches have been used to achieve noncentrosymmetry, either artificially as with the cases of Langmuir–Blodgett assembly [272, 273] or electric field poling of polymers [274–277] and self-assembly of molecular layers [278, 279] or at the molecular design level such as the use of chiral functional groups [265], the incorporation of the chromophore in host molecules [280–282], intercalation compounds [283], incorporation of functional groups that promote asymmetric intermolecular hydrogen bonding [284], and creation of coulombic interactions that can overcome dipolar interactions following the explanation of Meredith [285] by variation of counterions [286]. Some of these general procedures to induce acentric crystallization in organic materials have been applied also to organometallic compounds and in particular the variation of counterions has been quite successful. This procedure, applied to organometallic compounds by Marder et al. [264, 267, 287, 288] (to the family [Fc$-(E)-$CH=CH-4-C$_5$H$_4$N-1-Me)][X]), gave efficiencies in a wide range of values—240–125 (X = I), 165–170 (X = Br), 120–75 (X = NO$_3$), 50 (X = BF$_4$), and 13 times urea for both anions X = BPH$_4$ and MeC$_6$H$_4$-4-SO$_3$—measured by the Kurtz powder technique at 1.91 μm. In addition, variations of the counterion in the family of [Ru(N≡CC$_6$H$_4$-4-NO$_2$)((+)-diop)(η^5-C$_5$H$_5$)][X] with X = MeC$_6$H$_4$-4-SO$_3$, Cl, NO$_3$, BF$_4$, PF$_6$, ClO$_4$, or CF$_3$SO$_3$, gave SHG efficiencies, measured at 1.06 μm by the same technique, of 0.4, 0.5, 1.2, 1.9, 2.7, 2.9, and 10 times urea, respectively, clearly showing the influence of the arrangements in the solid state [289]. Therefore, variation of the counterion can be a useful and very straightforward method to engineer materials from molecules with large first hyperpolarizabilities. In the case of neutral dipolar molecules, the other strategies mentioned before for organic molecules are also applicable to organometallic molecules, and in particular the formation of guest–host inclusion complexes has been explored with inclusion of organometallic complexes in chiral β-cyclodextrine, thiourea, tris(*o*-thymotide, and deoxycholic acid [280, 282, 290]. The inclusion compound of [Cr(CO)$_3$(η^6-C$_6$H$_6$)] in thiourea gave a SHG efficiency of 2.3 relative to urea [291].

In addition to all the strategies applicable to organic and organometallic compounds, structures of organometallic compounds can also interact with the architectural flexibility of the ligands to induce acentric crystallization, either by use of chiral chromophores, by chiral coligands, or eventually by creation of chirality at the metal center. A reasonable number of compounds possessing chiral chromophore ligands have been synthesized and their efficiencies have been measured by the Kurtz powder technique. The family [(*S*)-Fe(η^5-C$_5$H$_5$) (η^5-C$_5$H$_3$-2-Me$-(E)-$CH=CHC$_6$H$_4$-4-X)] with X = NO$_2$, CN, or CHO, showed SHG values vs urea, measured at 1.91 μm, in the ranges of 8.0–8.4 for NO$_2$, 1.2–1.6 for CN, and 1.8–2.5 for CHO [292–294].

Two other metallocenyls of ruthenium and osmium, also possessing chiral chromophore ligands namely [(*S*)-Ru(η^5-C$_5$H$_5$)(η^5-C$_5$H$_4$CHMeSC$_6$H$_4$-4-NO$_2$)] and [(*S*)-Ru(η^5-C$_5$H$_5$)(η^5-C$_5$H$_4$CHMe$-$SC$_6$H$_4$-4-NO$_2$)] showed efficiencies of 27 and 21 times urea, measured by the same technique at 1.06 μm [295].

Several chiral ligands were also used for the synthesis of carbonyl chromium derivatives, but the values of SHG obtained were almost negligible with the exception of that for [Cr(CO)$_3$(η^6-nopolbenzyl ether)], which was 4 times the SHG of ADP measured at 1.06 μm by the Kurtz powder technique [262]. Some organometallic compounds derived from Mo and W possessing chiral ligands were also reported, but poor efficiencies were revealed after measurements by the Kurtz powder technique at 1.91 μm, and the best value found was 0.245 times urea, for [MoI(NO)(3-O-1,2:5,6-(CMe$_2$)$_2$-α-D-glucofuranose)(HB(dm pz$_3$)] [296]. The use of a chiral coligand, as a strategy of synthesis to assure acentric crystallization was applied by Garcia et al. to two families of compounds of the general formula [M(N≡CC$_6$H$_4$-4-X)((+)-diop)(η^5-C$_5$H$_5$)][PF$_6$] with M = Fe(II) [297] and Ru(II) and X = NH$_2$, NMe$_2$, Ph, NO$_2$, etc., and it was found [289] that the Fe derivative containing N≡CC$_6$H$_4$-4-NO$_2$ ligand as chromophore was 38 times better than urea, measured at 1.91 μm, and the ruthenium analogue was 2.9 times better than urea, measured at 1.06 μm, both by use of the Kurtz powder technique. It is well known that although chirality ensures noncentrosymmetry it does not ensure the most favorable alignment of the dipoles in

the crystalline lattice, and therefore the optimization of molecular alignment still remains an important step to overcome when bulk SHG efficiencies are required. In addition to all these factors that can contribute to enhancement of the SHG signal, the material should preferably be phase-matchable to minimize the dependence on the powder size. In spite of this, some nonzero SHG efficiencies have been found for centrosymmetric crystals and have been attributed to several origins such as crystal defects, decomposition by the laser beam, noncentrosymmetry of the surface, or fluorescence. Relatively to crystal defects, theoretical calculations by Reinecker et al. [298] suggest that SHG can be induced by CT complexes as impurities in a centrosymmetric host medium. This effect, originated by the static electric fields created in the host by the static dipoles due to the excitation of the CT complexes, can find potential application in composite systems.

Materials. The very large second-order nonlinearity reported for the first organometallic compound designed and synthesized for this purpose, [Fc−(*E*)−CH=CHC$_6$H$_4$-4-NO$_2$] (**1**) [263] opened the field of organometallic chemistry in view of NLO properties. Although its high nonlinearity later was found to be largely due to its asymmetric crystal structure, while it possesed only moderate molecular nonlinearity [268, 270, 287], these results initiated many other NLO studies of organometallic compounds. Several reviews on organometallic materials for NLO have been published during the past decade, compiling and highlighting the emergence of new organometallic materials for SO NLO [299–303].

The first review, authored by Nalwa [299] in 1991 elegantly compiles the work published from the pioneering reports of Frazier et al. in 1986 [262] and Green et al. in 1987 [263] up to 1990. The most SHG efficient organometallic compound mentioned in this review was the ferrocenyl derivative [Fc−(*E*)−CH=CH-4-C$_5$H$_4$N-1-Me)] [I] (**2**) reported in 1989 by Marder et al. [264, 267, 287, 288], as being 220 times more efficient than urea, measured by the Kurtz powder technique, at 1.91 μm. Ten years later this is still the best efficiency value shown by an organometallic compound, though it is significantly smaller than the value for the best organic compound, [*N*−MeC$_5$H$_4$N-4-(*E*)−CH=CHC$_6$H$_4$-4′-NMe$_2$][MeC$_6$H$_4$SO$_3$], with an efficiency value of 1000 times urea; this compound was also reported by Marder et al. in 1989 [286]. The growing interest in organometallics motivated by these earlier promising results and also by the potential technological applications based on NLO properties led to increasing work in the field and consequently many results were reported during the present decade. However, a significant number of the compounds studied—over half a thousand—showed low second-order susceptibilities and very weak efficiencies [262, 264, 267, 287, 288, 292–296, 304–311].

The review published by Whittall et al. [303] in 1998 presents extensively and systematically well-organized tables of results on SO NLO measurements by different techniques and computationally derived second-order hyperpolarizabilities calculated by ZINDO as well.

In this chapter, we will discuss different aspects of the design of organometallic compounds, relating when possible the relationships found between structural features and SO NLO properties. Our bibliography was updated to 1999 and the most relevant results are presented, without striving for completeness.

An attempt to systematize the published results on the basis of the synthesis of organometallic compounds possessing large values for first hyperpolarizability, in view of frequency doubling or the second-harmonic generation effect led us to categorize the following groups of compounds (in Sections 4.1–4.6): (1) metallocenyl derivatives, (2) η^5-monocyclopentadienyl/ and indenyl/metal derivatives, (3) metal–carbonyl complexes, (4) metal complexes possessing only metal−ligand σ bonds, (5) bimetallic complexes, and (6) octupolar complexes.

4.1. Metallocenyl Derivatives

Metallocenyl derivatives (metal = Fe, Ru, or Os) have been the most widely studied of the above mentioned groups. The promising results obtained from the very beginning on large bulk material SHG efficiencies for compounds [Fc−(*E*)−CH=CHC$_6$H$_4$-4-NO$_2$] (**1**) of 62 times urea and [Fc−(*E*)−CH=CHC$_5$H$_4$N-1-Me][I] (**2**) of 220 times urea (the best powder response so far for organometallic compounds) are certainly the main reason for so many SO NLO results for ferrocenyls, compared with other families, either in bulk materials by the Kurtz technique or molecular second-order measurements by EFISHG and HRS techniques. The efficiencies of metallocenyl compounds have been related with high hyperpolarizabilities originated by the donor ability of the organometallic moiety, due to the existence of a metal charge transfer toward an acceptor group placed on the end of an extended π system. Compared with traditional organic D/A systems, the ferrocenyl moiety is equivalent to the methoxyphenyl group in its donor ability. The cases where the acceptor group is another metallic unit are discussed below in Section 4.5 on bimetallic compounds. The donor ability of the ferrocenyl group has been attributed to the low binding energy of the metal electrons [312] and to the low oxidation potential of ferrocenyls combined with the stability of their oxidized form. Use of the ferrocene/ferrocenium redox wave as the internal reference in cyclic voltammetric studies of organometallic compounds is well established, owing to its reversibility and stability. Thus, the effect on the replacement of Fe by Ru in a given structural formula is a reduction of β, in accordance with the easier oxidation of the iron.

Although the UV–visible spectra of many of the ferrocenyl derivatives present both π–π^* and metal–ligand CT transition bands, metal–ligand CT has been considered to be the dominant band in monometallic ferrocenyl derivatives. Therefore, in these cases, the two-level model can be used to calculate the static hyperpolarizability β_0 [313], but the application of this simplified model should be questioned in the cases where π–π^* also contributes significantly to the resonance enhancement [270]. Comparison of the results obtained by EFISHG for the nitro [Fc−(*E*)−CH=CHC$_6$H$_4$-4-NO$_2$] ($\beta = 34 \times 10^{-30}$ esu) and the dinitro [Fc−(*E*)−CH=CHC$_6$H$_4$-2,4-(NO$_2$)$_2$] ($\beta = 20 \times 10^{-30}$ esu) ferrocenyl derivatives indicates that the values of β depend on the best alignment of β_{CT} and the dipole of the molecule, mainly in the plane perpendicular to the axis of the molecule [314]. Increasing the electronic density at the metallocenyl center by methylation of one or two Cp rings increases the metal donor ability and consequently a higher β value is found for [Fc*−(*E*)−CH=CHC$_6$H$_4$-4-NO$_2$] ($\beta = 40 \times 10^{-30}$ esu), which is twice the value for the nonmethylated ferrocenyl [267]. Studies on long-term stability in main-chain, side-chain and guest–host ferrocenyl poled polymers were carried out following their orientation and relaxation by SHG decay [315]. Experiments in poled films of [Fc−(*E*)−(CH=CH)$_n$C$_6$H$_4$-4-NO$_2$] (n = 1, 2) gave electro-optic coefficients in agreement with the expectations based upon the measured values of $\mu\beta$ [316, 317].

Table V. Selection of Metallocenyl Compounds—First Hyperpolarizabilities

Compound		β (10^{-30} esu)	Technique	Ref.
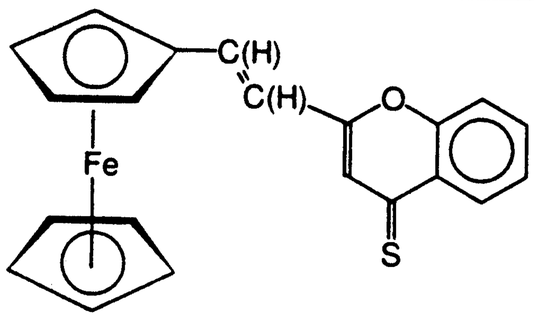		33	EFISHG[a,b]	[319]
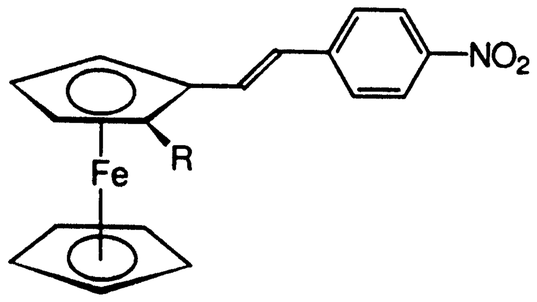	$R = SiMe_3$ $R = Me$	31.5 26.8	EFISHG[a,c]	[320]
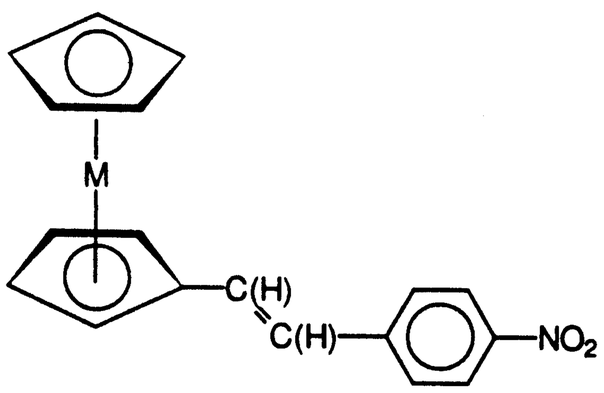	$M = Fe$ $M = Ru$	31 12	EFISHG[d,e]	[268]
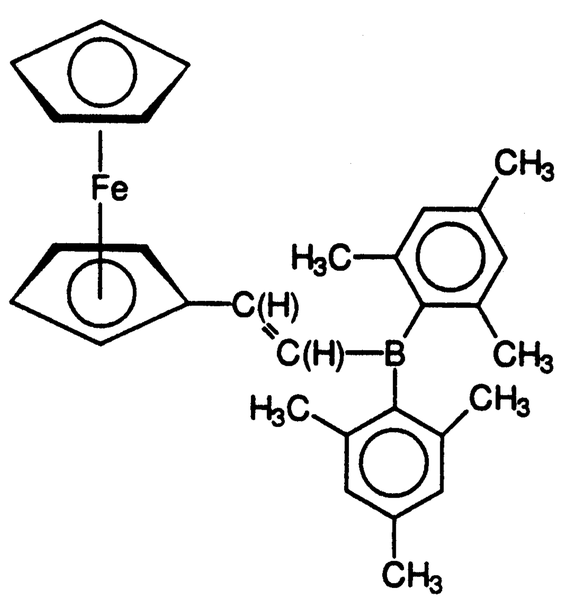		24[f]	EFISHG[a,b]	[321]
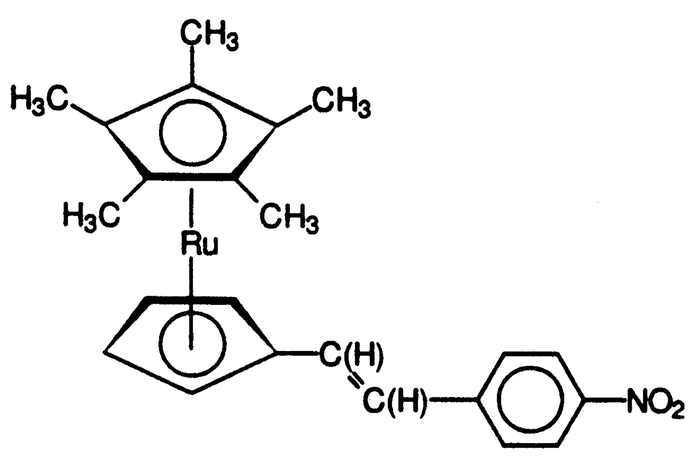		24	EFISHG[d,e]	[268]
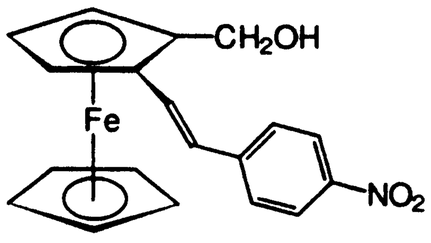		18	EFISHG[a,c]	[320]

continues

Table V. (continued)

Compound	β (10^{-30} esu)	Technique	Ref.
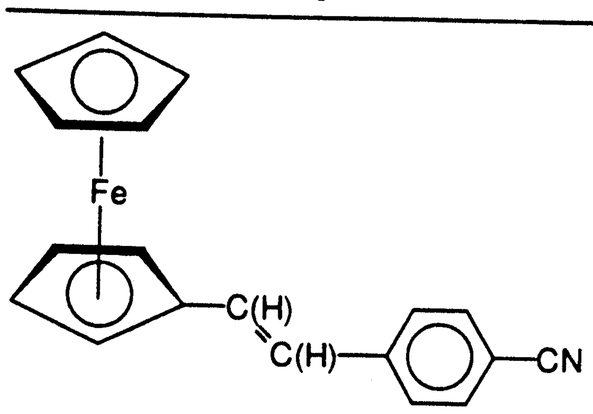	10	EFISHG[d,e]	[268]
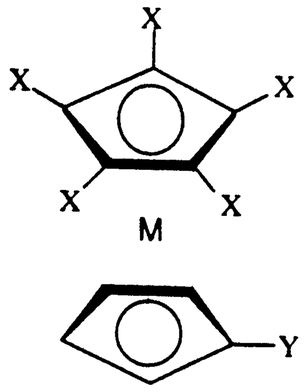 $M = Fe,\ X = H,\ Y = COCH_3$ $M = Ru,\ X = CH_3,\ Y = NO_2$	0.3 0.6	EFISHG[d,e]	[268]

[a] $\lambda = 1907$ nm.

[b] In chloroform.

[c] In dioxane.

[d] $\lambda = 1910$ nm.

[e] In toluene.

[f] Absolute value.

Theoretical studies on second-order hyperpolarizabilities, carried out on ferrocenyl derivatives by use of the computational ZINDO method, revealed good agreement with experimental results both in order of magnitude and sign of the measured values. The calculated values also followed the trend observed for the experimental results across a family of compounds [314, 318]. Experimental data for metallocenyls are presented in Tables V and VI.

4.2. η^5-Monocyclopentadienyl/ and Indenyl/Metal Derivatives

A new family of η^5-monocyclopentadienyliron/ruthenium *p*-nitrobenzonitriles derivatives for NLO emerged in 1993, reported by Garcia et al. [297]. By means of the Kurtz powder technique an efficiency of 38 times urea was found for [Fe(4-N≡$CC_6H_4NO_2$)((+)-diop)(η^5-C_5H_5)][PF_6]. Measurements by HRS also revealed high values of β for some compounds of this family, e.g., [Fe(4-N≡$CC_6H_4NO_2$) (dppe)(η^5-C_5H_5)][PF_6] dissolved in methanol and measured at 1.06 μm gave $\beta = 410 \times 10^{-30}$ esu [40]. Substitution of benzene rings by thiophene conjugating units led to a more efficient electron delocalization and enhancement of the molecular hyperpolarizability revealed by the extremely high value of 910×10^{-30} esu found for the compound [Fe{4-N≡$C(SC_4H_2)_3$}NO_2)(dppe)(η^5-C_5H_5)][PF_6], measured in chloroform by HRS at 1.06 μm [326]. The main structural feature of this family of compounds is the existence of the metal center in the same plane of the chromophore, this allowing metal–ligand π-backdonation via d_{metal}–π^*_{ligand}. The driving force for this donor-π system-acceptor interaction is the existence of the strong acceptor NO_2 group on the end of the π-system. Evidence of π-backdonation was clearly supported by spectroscopic data. Contrary to the case of ferrocenyl-based structures where d orbitals are orthogonal to the axis of the chromophore leading consequently to poor coupling, the localization of the metal and chromophore in the same plane can constitute an advantage by increasing the donor ability of the organometallic subunit.

Accordingly, a family of structurally analogous acetylides was reported in 1996 by Humphrey et al. [327–329], η^5-monocyclopentadienylruthenium-*p*-nitrobenzoacetylides, showing interestingly very large values of β. The compound [Ru(C≡C−C_6H_4-4-(*E*)−CH=CHC_6H_4-4-NO_2)(PPh_3)$_2$(η^5-C_5H_5)] exhibits $\beta = 1455 \times 10^{-30}$ esu, measured by HRS in THF at 1064 nm. A higher value of 1600×10^{-30} esu was reported in 1997 by Wu et al. [330] for another analogous acetylide [Ru(C≡C−C_6H_4-4-(*E*)−CH=CHC_6H_3N-4-Me)(PPh_3)$_2$(η^5-C_5H_5)]. Values of the same magnitude were also reported by Gimeno et al. [328, 331, 332] in 1996 for the indenyl analogues [RuC≡C−(*E*)−CH=CH−(*E*)CH=CHC_6H_4-4-NO_2)(PPh_3)$_2$(η^5-indenyl)] and [RuC≡C−(*E*)CH=CHC_6H_4-4-NO_2)(PPh_3)$_2$(η^5-indenyl)] which present β values of 1320 and 1257×10^{-30} esu, respectively, measured by HRS at 1.06 μm in CH_2Cl_2. Therefore, these results together with the finding that the related "rigid-rod" octahedral ruthenium acetylide compound *trans*-[Ru(*E*)-4,4′-(C≡C−C_6H_4CH=$CHC_6H_4NO_2$)Cl(dppm)$_2$ (see Section 4.4), which revealed the highest β value reported so far for an organometallic, 1964×10^{-30} esu, measured by HRS at 1.06 μm in THF, seem to indicate that acetylide derivatives are the best chromophores for SO NLO.

Table VI. Selection of Ferrocenyl Derivatives—SHG by the Kurtz Powder Technique

Compound		SHG vs Urea[a,b]	Ref.
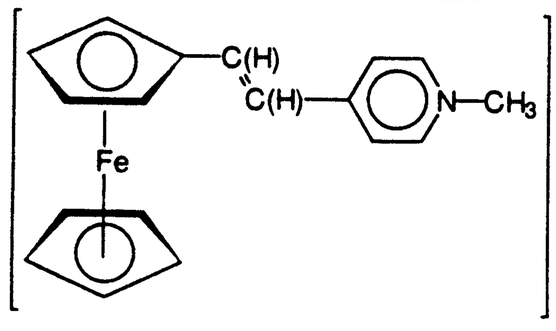	$X = I$	220	[287]
	$X = p\text{-}CH_3C_6H_4SO_3$	13	
	$X = CF_3SO_3$	0	
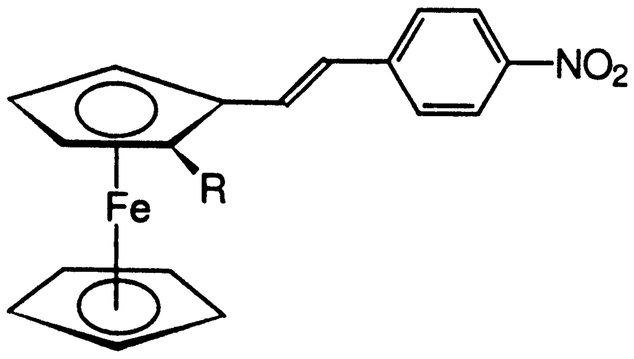	$R = SiMe_3$	100	[320]
	$R = Me$	6	
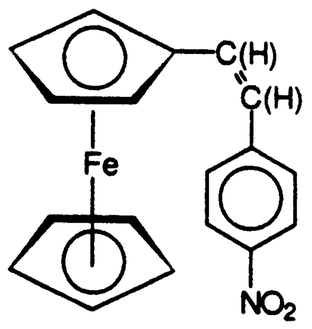		62	[263]
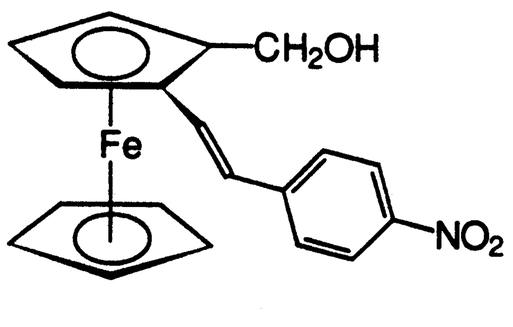		20	[320]
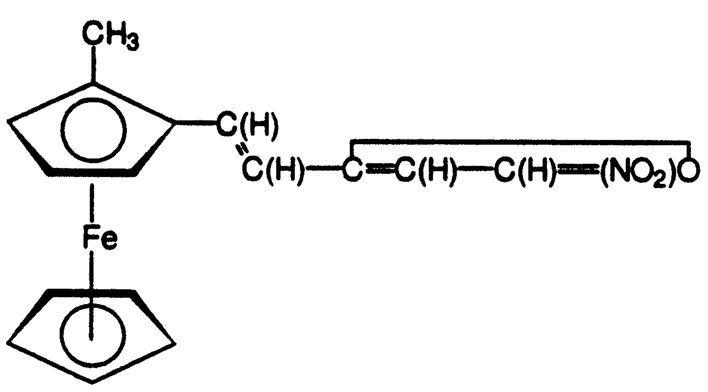		17.5	[292]
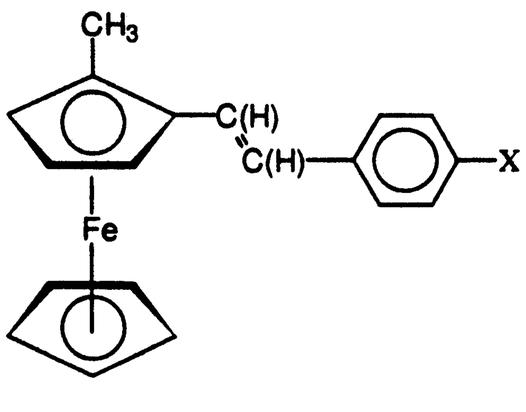	$X = NO_2$	8.4	[292]
	$X = CHO$	1.8	
	$X = CN$	1.6	

continues

In good agreement with the expectation that both extension and planarity of the π-system are crucial for observation of high first hyperpolarizabilities, it was found that the introduction of one double bond between two phenyl rings in the ligand $-C{\equiv}CC_6H_4{-}C_6H_4\text{-}4\text{-}NO_2$ to give $-C{\equiv}CC_6H_4\text{-}4\text{-}(E){-}CH{=}CHC_6H_4\text{-}4\text{-}NO_2$ leads to a significant increase in the β values of the corresponding complexes. The β value of 560×10^{-30} esu [334], determined for compound $[Ru(C{\equiv}C{-}C_6H_4C_6H_4\text{-}4\text{-}NO_2)(PPh_3)_2(\eta^5\text{-}C_5H_5)]$, was raised up to 1455×10^{-30} esu [329] for compound $[Ru(C{\equiv}C{-}C_6H_4\text{-}4\text{-}(E){-}CH{=}CHC_6H_4\text{-}4\text{-}NO_2)(PPh_3)_2(\eta^5\text{-}C_5H_5)]$, both measured by HRS in THF. Despite the importance of the extension on the π-system in donor-

Table VI. (continued)

Compound	SHG vs Urea[a,b]	Ref.
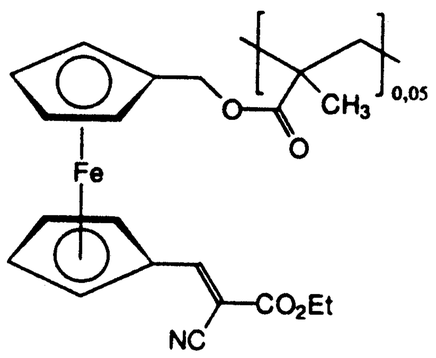 *(conc. 5% in PMMA)*	3.4[c]	[322]
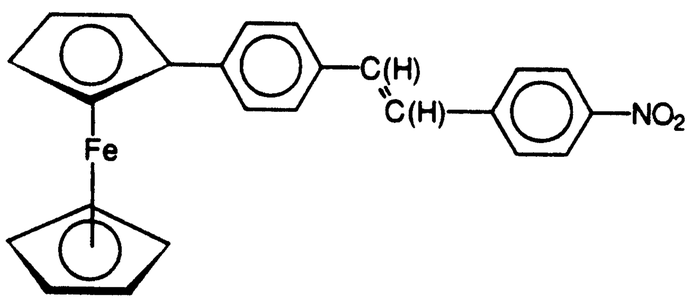	1	[323]

[a] $\lambda = 1907$ nm.

[b] ADP = 0.3 × urea; quartz = 0.1 × urea [40].

[c] SHG = d_{33}(polymer)/d_{11}(quartz). d_{11} (quartz) = 0.50 pm/V or 1.2×10^{-9} esu ($\lambda = 1064$ nm) [324, 325].

π-acceptor structures, it has been found that β hyperpolarizability values saturate easily with chain lengthening [331]. Studies on systematic variation of the metal ion, in the family [M(4-N≡$CC_6H_4NO_2$)(dppe)(η^5-C_5H_5)][PF_6] with M = Fe(II), Ru(II), Ni(II), and Co(III), led to the conclusion that the first hyperpolarizability β increases along the sequence Co, Ni, Ru and Fe, with about a 3-fold increase from Ru to Fe. The better value was found for the iron complex [40].

Both η^5-monocyclopentadienylmetal derivatives of Ni(II) and Co(III) were found to behave as σ acceptor fragments upon coordination of $-N{\equiv}CC_6H_4R$ where R was a donor group (R = NH_2, $N(CH_3)_2$, C_6H_5, OCH_3, H, or F), and presented low values of β measured by HRS, in spite of the planar structure of the coordinated ligand revealed by X-ray diffraction of the compound [Ni(4-$NCC_6H_4NH_2$)(PPh_3)(η^5-C_5H_5)][PF_6]. These poor β values were understood after extended Hückel molecular orbital calculations, which found that the weak delocalization of the frontier π molecular orbitals would be at the origin of a dominant metal–ligand σ bond [129]. Nevertheless, the analogous acetylide [Ni(4-$CCC_6H_4NO_2$)(PPh_3)(η^5-C_5H_5)][PF_6] showed a significant value of β of 221×10^{-30} esu [333] measured in THF, indicating clearly that the acetylide group is more effective on the $d_\pi - \pi^*_{\text{ligand}}$ interaction than the nitrile functional group.

Experimental results for this class of compounds are in Tables VII and VIII. Computationally derived second-order hyperpolarizabilities, carried out on ruthenium and nickel acetylide derivatives by use of ZINDO method, revealed poor agreement with experimental results. Nevertheless, some trends are qualitatively observed across the families of compounds [314, 334].

4.3. Metal–Carbonyl Complexes

In the group of metal–carbonyl compounds, we consider two main families of complexes, based on the structural features responsible for the NLO responses. In the first family, the charge transfer responsible for the hyperpolarizability is perpendicular to the axis of the molecule, as was found in the ferrocenyls (see Section 4.1), due to a coordination of a η^6- or η^5-ligand to the metal carbonyl fragment. The compounds are then the chromium arene carbonyl complexes, [$Cr(CO)_3(\eta^6$-$C_6H_5R)$], the sesquifulvalene manganese complexes [$Mn(CO)_3(\eta^5$-$C_5H_4C_7H_6)$][BF_4] and [$Mn(CO)_2(\eta^5$-$C_5H_4C_7H_6)L$][BF_4] with different ligands L, and the [(η^5-thiophene derivatives) $Mn(CO)_3$][BF_4]. The chromium arene complexes, [$Cr(CO)_3(\eta^6$-$C_6H_5R)$], the first ones to be screened for SHG, showed almost negligible efficiencies [262]. The best values found were 2.3 times urea for the [$Cr(CO)_3(\eta^6$-C_6H_6):thiourea] (1:3) inclusion compound [281, 291, 339, 340], and 3 times ADP (ADP = 0.3 times urea, quartz = 0.1 times urea [341]) for [$Cr(CO)_3(\eta^6$-nopolbenzyl ether)] [262]. The hyperpolarizability of these compounds is attributed to charge transfer along the axis of the molecule, the $Cr(CO)_3$ behaving as an acceptor group in the ground state but as a donor in the excited state in the donor-π-system-acceptor concept. Measurements by EFISHG at 1.91 μm, for compounds $Cr(CO)_3(\eta^6$-$C_6H_5R)$ where R = H, OMe, NH_2, NMe_2, CO_2Me, or $-(E)-CH-CHPh$, gave small β values that were quite insensitive to the electronic influence of the substituents, −0.8, −0.9, −0.6, −0.4, −0.7, and -2.2×10^{-30} esu, respectively, the negative sign indicating a decrease or even change in direction of dipole moment between the ground and the excited state [269, 337, 342]. The sesquifulvalene derivatives have significantly larger hyperpolarizabilities, for example, [$Mn(CO)_3(\eta^5$-$C_5H_4C_7H_6$][BF_4] presents β = 38×10^{-30} esu, measured in MeCN at 1.06 μm by HRS, and [$Mn(CO)_3(\eta^5$-$C_5H_4C{\equiv}CC_7H_6$][BF_4] shows the value of 151×10^{-30} esu measured in the same experimental conditions by the same technique, this being the higher β value reported for this family of compounds [343]. Calculated optical nonlinearities, computationally derived by ZINDO at 1.91 μm for $Cr(CO)_3(\eta^6$-$C_6H_5R)$, show good concordance with the experimental results. The low first hyperpolarizabilities values found for these com-

Table VII. Selection of η^5-Monocyclopentadienyl/ and Indenyl/Metal Derivatives—First Hyperpolarizabilities

Compound		β (10^{-30} esu)	Technique	Ref.
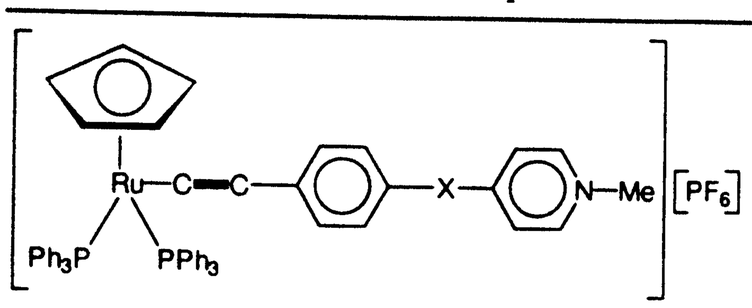	X = C=C	1600	HRS[a,b]	[330]
	X = C≡C	1400		
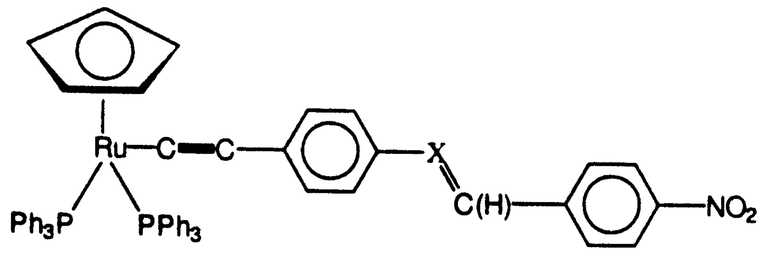	X = CH	1455[c]	HRS[a,d]	[327]
	X = N	840[c]		
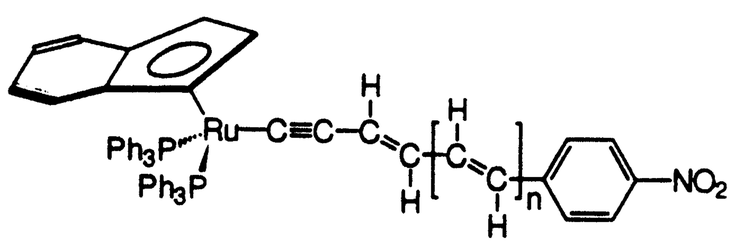	n = 1	1320	HRS[a,b]	[328, 331, 332]
	n = 0	1257		
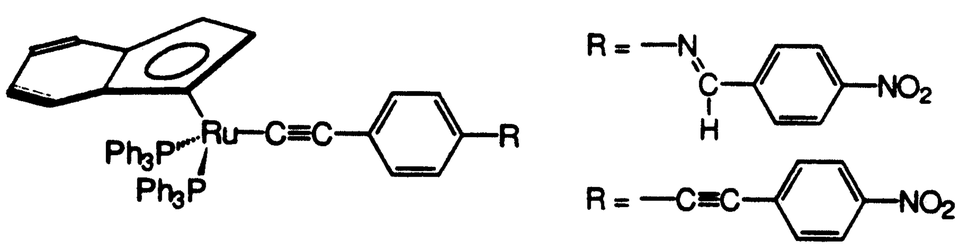		1295	HRS[a,b]	[331]
		1027		
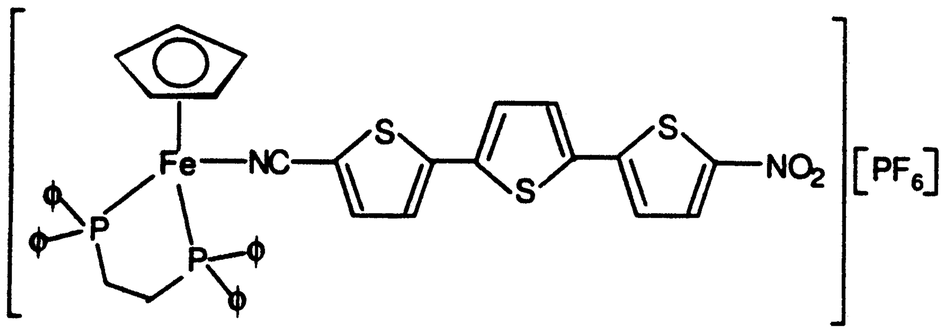		910	HRS[a,e]	[326]
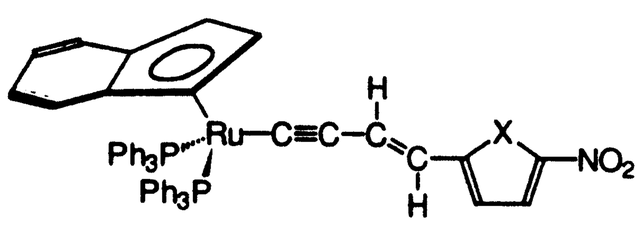	X = O	908	HRS[a,b]	[328, 331, 332]
	X = S	487		
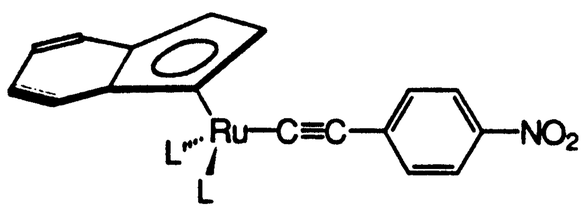	L_2 = 2PPh$_3$	746	HRS[a,b]	[328, 331, 332]
	L_2 = dppm	540		
	L_2 = dppe	516		
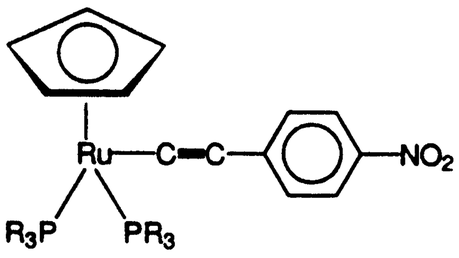	R = Ph$_3$	468	HRS[a,d]	[327]
	R = CH$_3$	248		

continues

Table VII. (continued)

Compound	β (10^{-30} esu)	Technique	Ref.
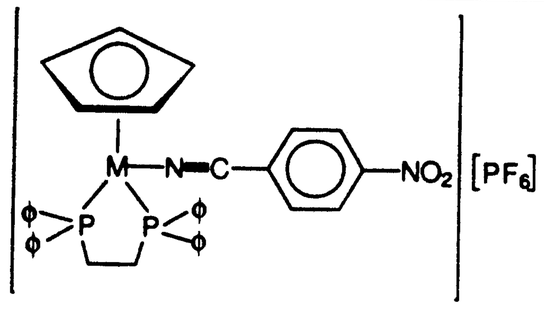	M = Fe M = Ru	410 138	HRS[a,f]	[40]
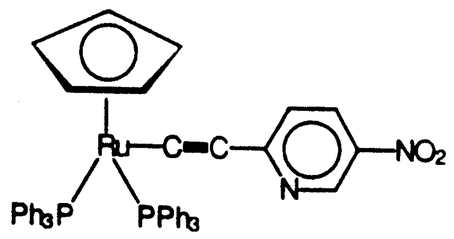	113	HRS[a,d]	[335]
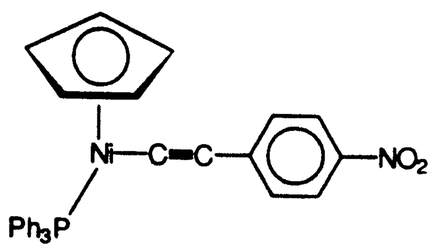	59	HRS[a,d]	[335]
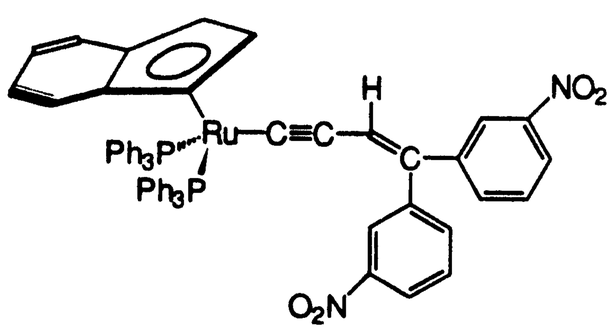	48	HRS[a,b]	[332]
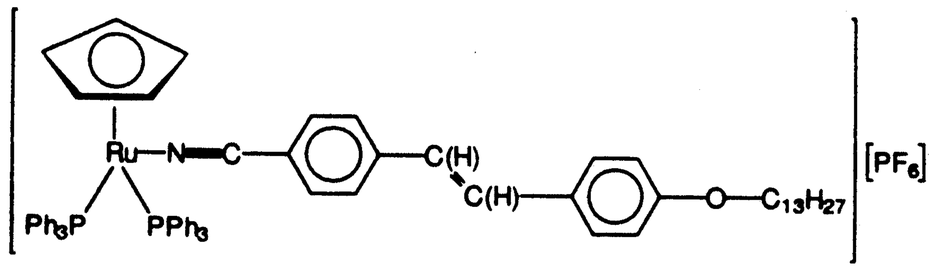	37	EFISHG[g,h]	[336]
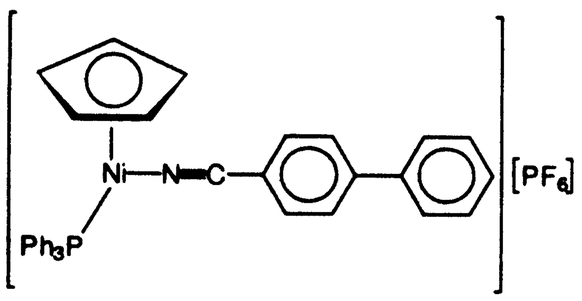	17	HRS[a,f]	[337]
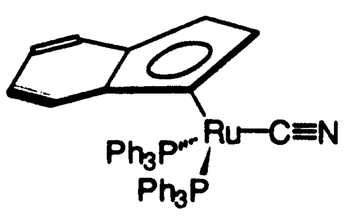	13	HRS[a,b]	[332]

[a] λ = 1064 nm.

[b] In dichloromethane.

[c] In resonance conditions.

[d] In THF.

[e] In chloroform.

[f] In methanol.

[g] λ = 1060 nm.

[h] Langmuir–Blodgett film.

Table VIII. Selection of η^5-Monocyclopentadienyl/ and Indenyl/Metal Derivatives—SHG by the Kurtz Powder Technique

Compound	SHG vs urea[a]	Ref.
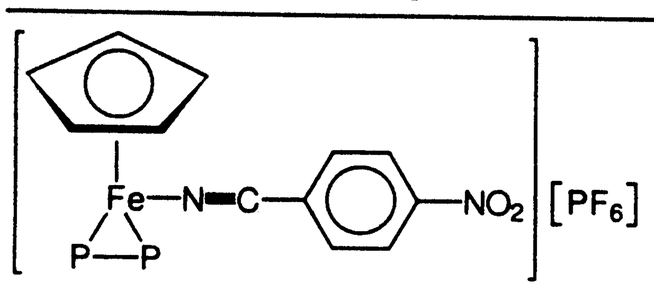 **P—P** = (+)-diop	38[b]	[297]
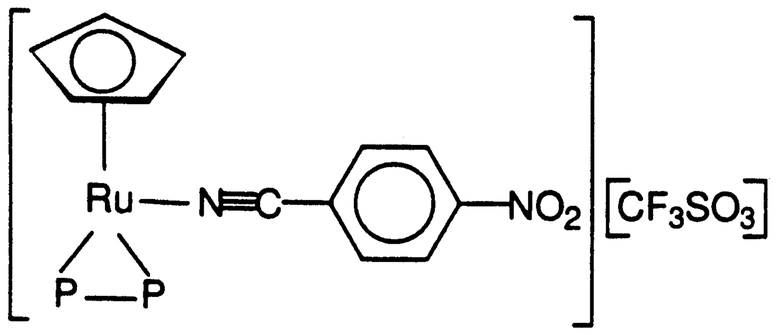 **P—P** = (+)-diop	10[c]	[289]
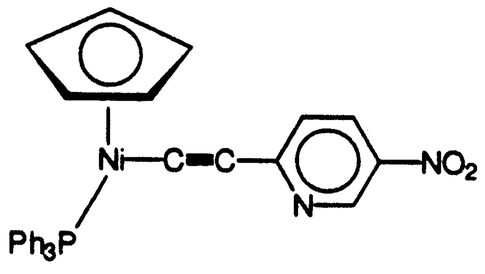	8[c]	[335]
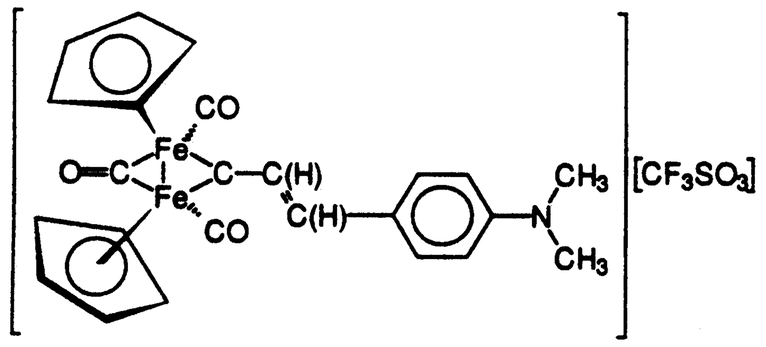	3.6[b]	[305]
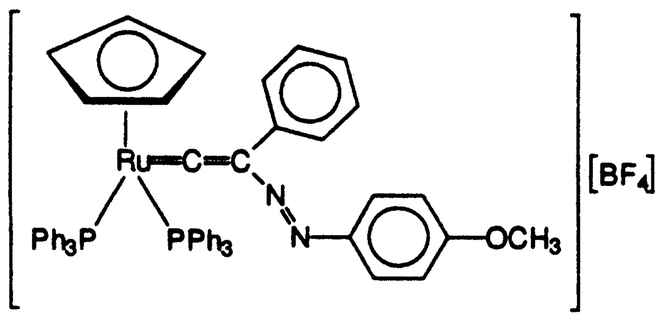	1.05[c]	[306]
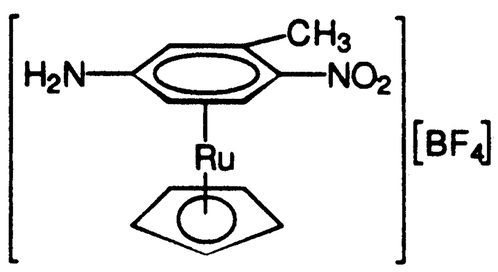	1[c]	[338]

[a] ADP = 0.3 × urea; quartz = 0.1 × urea [341].

[b] λ = 1907 nm.

[c] λ = 1064 nm.

Table IX. Selection of Metal–Carbonyl Complexes for SO NLO—First Hyperpolarizabilities

Compound		β (10^{-30} esu)	Technique	Ref.
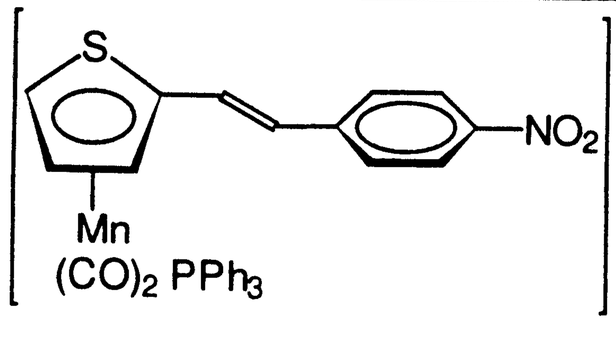		700	HRS[a,b]	[344]
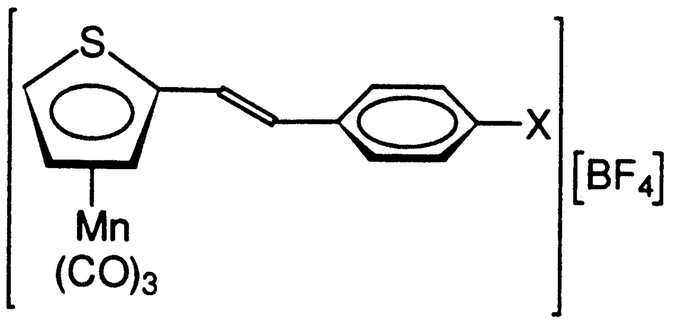	$X = NO_2$	613	HRS[a,b]	[344]
	$X = Br$	534		
	$X = H$	413		
	$X = CH_3$	355		
	$X = CH_3C$	252		
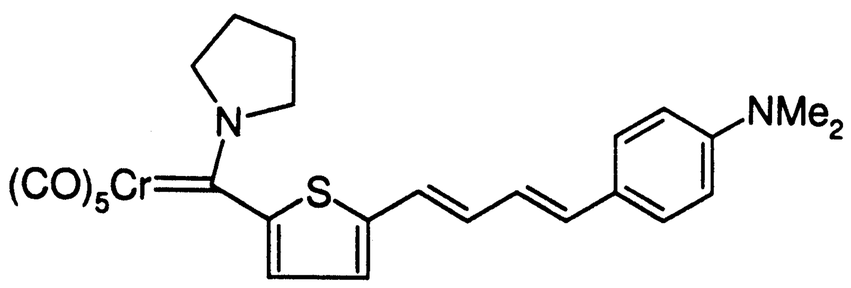		543	HRS[c,d]	[347]
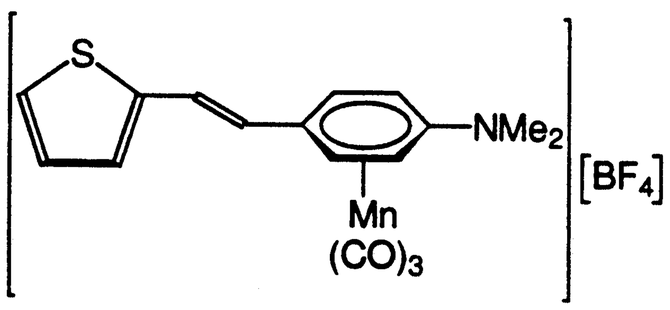		377	HRS[a,b]	[344]
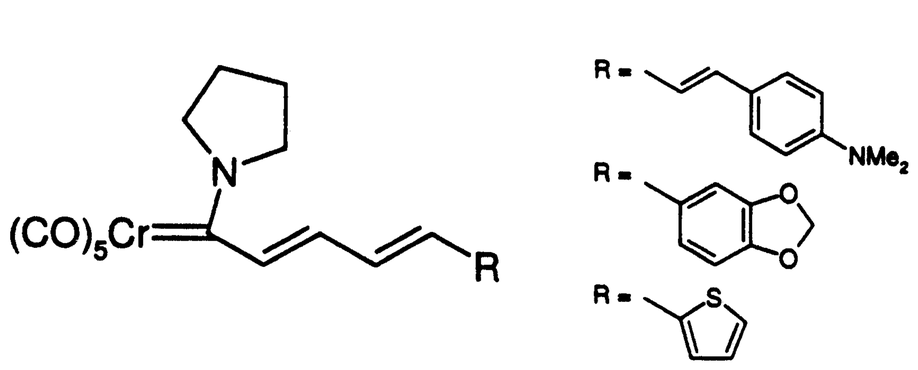		350	HRS[c,d]	[347]
		55		
		50		
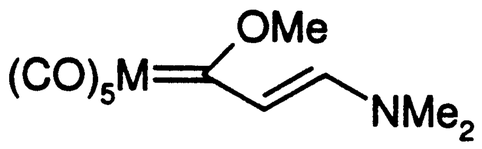	$M = W$	34	HRS[c,d]	[347]
	$M = Cr$	16		
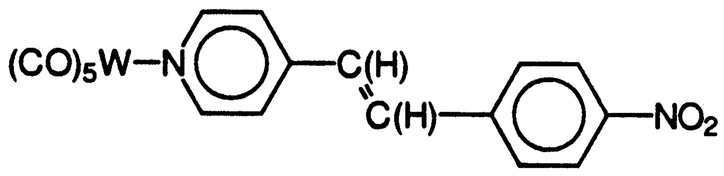		−20[e]	EFISHG[c,f]	[337]
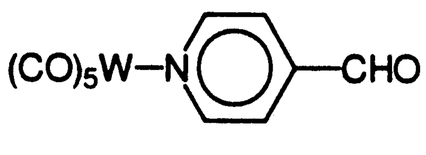		−12[e]	EFISHG[c,f]	[269, 337]

[a] $\lambda = 1064$ nm.

[b] In nitromethane.

[c] $\lambda = 1907$ nm.

[d] In dichloromethane.

[e] Absolute value.

[f] In chloroform.

pounds are explained by the different orientations of the charge-transfer axis and the ground-state dipole direction, leading to a relatively small change of the dipolar moment of the molecule associated with the metal–ligand CT [314, 318]. Calculations on hypothetical molecules with the arene group adequately substituted to increase π conjugation, and consequently to generate better results on first hyperpolarizabilities, gave the best value for $[Cr(CO)_3(\eta^6\text{-}O_2NC_6H_4\text{-}(E)\text{-}CH{=}CH\text{-}(E)\text{-}CH{=}CHC_6H_4\text{-}4\text{-}NH_2)$ with $\beta_{EFISHG} = 27.5 \times 10^{-30}$ esu. Nevertheless, the finding that the hypothetical uncoordinated organic compounds give calculated nonlinearities significantly higher than the corresponding $Cr(CO)_3$ derivatives suggest a low electron-withdrawing ability of carbonyl ligands in these systems. In fact, this hypothesis was corroborated by the calculation of an extremely high value of β of 780×10^{-30} esu for the hypothetical molecule $[Cr(NH_3)_3(\eta^6\text{-}C_6H_5\text{-}(E)\text{-}CH{=}CH\ CHC_6H_4\text{-}4\text{-}NO_2]$ which possesses NH_3 replacing the CO ligands. As a trend it was observed that the calculated values of β for the hypothetical structures were all positive across the family and higher than the ones experimentally observed. Also, the positive values indicate that the localization of the CT axis is now in the plane of the chromophore and not in metal–arene axis as it was for the molecules studied experimentally [314, 318]. Anyway, the first hyperpolarizabilities measured or calculated for this type of structures are very small.

Conversely to low β values found for $(C_6H_5X)Cr(CO)_3$ compounds, the new family of η^5-thiophene derivatives reported by Chung et al. [344] of general formulae $[Mn(\eta^5\text{-}SC_4H_3CH{=}CH\text{-}4\text{-}C_6H_4X)(CO)_3][BF_4]$ where $X = CH_3O$, CH_3, H, Br, or NO_2 revealed significant high values of β of 252, 355, 413, 534, and 613×10^{-30} esu, respectively, measured by HRS in nitromethane at 1064 nm. The explanation found was that (thiophene)$Mn(CO)_3^+$ functions as a ground-state acceptor, but it will behave as a donor in the excited state.

According to the authors, substitution of one carbonyl ligand by the electron-donating group PPh_3 should decrease the electron-withdrawing ability in the ground state and increase the electron-donating ability in the excited state, giving to the compound $[Mn(\eta^5\text{-}SC_4H_3CH{=}CH\text{-}4\text{-}C_6H_4X)(CO)_2(PPh_3)][BF_4]$ even a higher value of first hyperpolarizability, as was experimentally found ($\beta = 700 \times 10^{-30}$ esu). In the second family of metal–carbonyl complexes are placed all the derivatives $M(CO)_5L$, where the charge transfer lying at the origin of the hyperpolarizability is through the axis metal–$L_{chromophore}$, both located in the same plane as was observed for the η^5-monocyclopentadienyl–metal derivatives (see before, Section 4.2). In this situation we find compounds with a metal–nitrogen σ bond and compounds with a metal–carbene bond, which structure satisfies the designed strategy of a planar π-interaction metal–ligand. Compounds with *N*-coordinated ligands such as $W(CO)_5NC_5H_4\text{-}4\text{-}R$, where R = H, NH_2, Ph, Bu^n, COMe, CHO, $(E)\text{-}CH{=}CHPh$, $(E)\text{-}CH{=}CH\ C_6H_4\text{-}4'\text{-}CHO$, $(E)\text{-}CH{=}CH\ C_6H_4\text{-}4'\text{-}NO_2$ or pyrazine, showed low β values of −4.4, −2.1, −4.5, −3.4, −9.3, −12.0, −5.7, −17.0, −20.0, and 6.0×10^{-30} esu, respectively, measured by EFISHG at 1.91 μm [269, 271, 337, 342]. With the exception of pyrazine all the β's were negative, as was observed also for $Cr(CO)_3$ derivatives, presented before. Again negative β's were obtained for compounds $M(CO)_4$(1,10-phen), where M = Cr, Mo, or W. The three compounds presented the same value of $\beta = -13 \times 10^{-30}$ esu, measured in dichloromethane by EFISHG at 1.91 μm. The value of the first hyperpolarizability was -18×10^{-30} esu for $W(CO)_4$(5-NO_2-1,10-phen) also measured in the same experimental conditions. The complexes possessing the metal–carbene bonds showed better values of β, namely $[Cr(CO)_5$(C(N-pyrrole)-5-(2,2′-bithiophene)], $[Cr(CO)_5\ (C(OMe)\text{-}(E)\text{-}CH{=}CHNMe_2]$, and the analogous tungsten complex yielded β = 18, 16, and 34×10^{-30} esu, respectively, measured in chloroform by HRS at 1.06 μm [345]. Computational calculated first hyperpolarizabilities by ZINDO for pentacarbonyl Mo and Cr pyridine derivatives showed concordance with the experimental results [269, 334, 337]. More interesting seem to be the structures with carbene-coordinated ligands attached to $Cr(CO)_5$ and $W(CO)_5$ fragments, particularly some substituted metallocumulenes [346] where a β value of 125×10^{-30} esu was measured by HRS at 1.06 μm for DMF solutions of $(CO)_5Cr{=}C{=}C{=}C{=}CC(NEt_2)C(Me){=}C(NMe_2)_2$. The SHG efficiencies clearly depend on the insertion of C_2 units, but only slight changes are observed when W replaces Cr. The negative solvatochromism observed for these substituted metallocumulenes in highly polar solvents suggests the existence of BLA.

4.4. Metal Complexes Possessing Only Metal–Ligand σ Bonds

This class of compounds includes organometallic and coordination compounds possessing only metal–ligand σ bonds, in several molecular configurations. The recent publication of Qin et al. [348] reviews the influence of octahedral, square pyramidal, tetrahedral, square planar, and linear molecular configurations of coordination compounds on NLO properties. The most prominent compounds of this family of metal–ligand σ bonded complexes, are the rigid-rod octahedral ruthenium σ-acetylides of general formula *trans*-$[Ru(C{\equiv}CC_6H_4R\text{-}4)Cl(dppm)_2]$ (R = NO_2, $C_6H_4NO_2$-4, or CH=CH $C_6H_4NO_2$-4). Humphrey et al. [349] reported the value of 1964×10^{-30} esu measured by HRS at 1.06 μm for solutions of compound *trans*-[Ru(C≡$CC_6H_4CH{=}CH\ C_6H_4NO_2$-4)$Cl(dppm)_2$] in THF. This is the best β value found so far for an organometallic compound. The efficiency of these structures was related to the intense low-energy band in the electronic spectra due to the π donation from the Ru fragment to the acceptor σ-acetylide ligand, as was also observed for the general family of η^5-monocyclopentadienylmetal derivatives (see Section 4.2). Results indicate that the substitution of $PPh_3(\eta^5\text{-}C_5H_5)$ by $Cl(dppm)_2$ do not lead to a dramatic impact on the first hyperpolarizability since β increases from 1455 to 1964×10^{-30} esu, but the authors foresee better results with replacement of the soft donor P-ligands by hard N-ligands. Some gold acetylide derived complexes, $[Au(C{\equiv}CC_6H_4\text{-}4\text{-}R)(PPh_3)]$ with R = H, NO_2, $C_6H_4\text{-}4\text{-}NO_2$, $(E)\text{-}CH{=}CHC_6H_4\text{-}4\text{-}NO_2$, $(Z)\text{-}CH{=}CHC_6H_4\text{-}4\text{-}NO_2$, $C{\equiv}CC_6H_4\text{-}4\text{-}NO_2$, and $N{=}CH\ C_6H_4\text{-}4\text{-}NO_2$, presented β values of 6, 22, 39, 120, 58, 59, and 85×10^{-30} esu measured in THF by HRS at 1.06 μm [328, 333]. As would be expected the lengthening of the π system contributes to the increase of β up to 120×10^{-30} esu. Comparative studies on gold, nickel, and ruthenium derivatives containing σ arylacetylide ligands, showed that the static hyperpolarizability was increased by a factor of 2, 4, and 7, respectively. Also it was found that replacement of phenyl by a heterocyclic ring enlarges the hyperpolarizability in the case of gold and ruthenium compounds [350].

Computational data relative to SO NLO properties of metal acetylide derivatives were also calculated by the ZINDO methodology and show that the general trends are observed, but absolute

values differ significantly from the experimental ones. Discrepancies between calculated and experimental values were also found for the η^5-monocyclopentadienylmetal acetylide derivatives, as was mentioned before, but the application of ZINDO has been successfully used for ferrocenyl derivatives [290].

An extensive family of Zn derivatives of the general formula L-Zn(acac)$_2$ (acac = acetylacetate anion and L is a variety of pyridine, urea, and thiourea derivatives) with square pyramidal configuration was measured by the Kurtz powder technique, and an interesting finding was that the compound with L = (PhNH)C(S)(NH_2) was 10 times more efficient than KDP used as the reference compound. Despite the absence of any intramolecular charge transfer, the NLO effect observed at the macroscopic level can be understood on the basis of the X-ray structural analysis. The compound crystallizes in the space group P_1, and the molecules in the lattice present the dipoles almost parallel along the lattice [351]. Compounds derived from iridium and rhodium, $MCl(CO)_2(NC_5H_4$-4-(E)$-CH=CHC_6H_4$-4-OCH_2 CH(Me)Et, also presented significant values of β, 24.4 and 20.1 $\times 10^{-30}$ esu, measured in chloroform by EFISHG at 1.91 μm [352]. Nevertheless, the square planar complexes *trans*-X-$M(PEt_3)_2$-4-C_6H_5A with M = Pd and Pt, X = Br and I, and A = CHO and NO_2 exhibit lower values of β in the range of 0.5–3.8 $\times 10^{-30}$ esu [269, 290]. Efficiencies of SHG determined by the Kurtz powder technique gave to bromo(2-methyl-4-nitrophenyl)bistriphenylphosphineplatinum/palladium derivatives values of 5–14 times urea [290].

Some new Schiff base mono- and bimetallic complexes of Pd(II) and Pt(II) also revealed interesting values of first hyperpolarizabilities. The best value found in the family [Pd($RC_6H_3CH=N$-C_6H_4R')L] with L = C_5H_5, acac, R, R' = NO_2 and OC_8H_{17} or $N(C_4H_9)_2$ and [Pd($RC_6H_3CH=N$-C_6H_4R')(CNC_6H_4R'')Cl] where R'' = NO_2, OC_nH_{2n+1}, and $N(C_mH_{2m+1})_2$ (n = 4 or 8; m = 1 or 4) was 263 $\times 10^{-30}$ measured by EFISHG at 1.34 μm [353].

Organometallic tetrahedral complexes derived from main group elements such as boranes, silanes, and stannanes, although presenting moderate nonlinearities, are attractive due to their transparency at wavelengths in the visible region after 450 nm. Within the stannanes we find values of β in the range of 13 to 159 $\times 10^{-30}$ esu with the highest value presented by compound [Sn(C_6H_4-4-N=N C_6H_4-4-$NMe_2)_4$] measured by HRS at 1.06 μm in dichloromethane. Modest values of β also were found for silane structures—which are essentially nonpolar—e.g., 38 $\times 10^{-30}$ esu for [C_6H_4(4-NMe_2)($SiMe_2)_6C_6H_4$-4$CH=C(CN)_2$] and 22.5 $\times 10^{-30}$ esu for [Si Me(C_6H_4-4-NMe)$_2$(C_6H_4-4-$CH=C(CN)_2$)] measured by EFISHG at 1.34 μm in solutions of acetone [354–356]. Some other related Si compounds gave values of same magnitude [203, 357]. Studies on polysilyl units as bridging groups revealed less efficiency than that seen for the polyene units, owing to their nonplanar geometry. However, the advantage of polysilyl spacers as an alternative to polyene groups would be the transparency in the visible region, a reversal of the bathochromic effect associated with the lengthening of the polyene chain. Tables X and XI show the main experimental results for these compounds.

4.5. Bimetallic Complexes

Bimetallic compounds for SO NLO are based on the same general structural feature as the monometallic compounds, donor-π-system-acceptor, with the metallic units acting as donor and acceptor groups. Ferrocenyls behave as reasonable donor groups comparable to the methoxyphenyl group as suggested by experiment [268] and theory [318], and some large nonlinearities have been found for bimetallic ferrocenyl (Fc)-containing moieties, both at macroscopic level by means of the Kurtz powder technique and at the microscopic level by EFISHG and HRS. Relatively large values of first hyperpolarizabilities were found for bimetallic sesquifulvalene complexes possessing a (cycloheptatrienyl)tricarbonylchromium unit as acceptor group, namely [FcC≡C(η^7-C_7H_6)Cr(CO)$_3$]. The β value was 570 $\times 10^{-30}$ esu, measured by HRS at 1.06 μm in dichloromethane, and the β value for [Fc$-(E)-$CH=CH(η^7-C_7H_6)Cr(CO)$_3$] was 320 $\times 10^{-30}$ esu, measured in the same experimental conditions [161]. The difference between these results suggests that the triple bond is more effective as a spacer than the double bond. This cannot be considered a rule, and there are some other examples showing the reverse.

Substantial values of β due to resonance enhancement, originated by a charge-transfer excitation close to the second harmonic, were found for compounds possessing the ferrocenyl group attached to the (η^5-thiophene)Mn(CO)$_3^+$ moiety. (*E*,*E*)-2-[{(C_5H_5)FeC_5H_4(CH=CH)$_x$} (C_4H_3S)Mn (CO)$_3$][BF_4] compounds presented in the case of x = 2, a β value of 771 $\times 10^{-30}$ esu and when x = 1 a β value of 670 $\times 10^{-30}$ esu, while the analogous compound without any spacing vinylic group presented the value of 260 $\times 10^{-30}$ esu [344]. Interestingly Fc(η^6-BC_5H_5)Co(η^5-C_5H_5)][PF_6], presenting both D/A groups directly coupled, showed a modest first hyperpolarizability value of β = (90 ± 30) $\times 10^{-30}$ esu, which was is quite unexpected [364]. Some other more complicated structures like [MoX(NO (NHC_6H_3-3-Me-4-N=NC_6H_4-4-(η^5-C_5H_4)Fe(η^5-C_5H_5)) (HB(dmpz)$_3$)] showed efficiencies of 50 and 25 times urea, depending on whether X = Cl or Br, measured by the Kurtz powder technique at 1.91 μm. The corresponding W complex gave lower values of efficiencies in the range of 8 to 53 times urea. The substitution of −N=N− by −CH=CH− in this compound led to the structure (**3**) [MoX(NO)(NHC_6H_3-3-Me-4-CH=CHC_6H_4-4-(η^5-C_5H_4)Fe(η^5-C_5H_5)(HB(dmpz)$_3$)] and to the higher efficiency of 85 times urea, obtained by the same method [296, 365]. Measurements of β for ferrocenyl derivatives of Ni, Pd, and Pt by the EFISHG method at 1.34 μm showed modest values for compounds of the structural type [FcCH=C(S(O)CH_2PhC=NCMe_2CH_2O(N,S-PdCl_2] in the range of 9 to 30.2 $\times 10^{-30}$ esu (Table XII) [361]. The use of the cationic tricarbonyl(cyclohexadienyl)iron complexes as electron acceptor groups bridged by a single alkyne spacer to the ferrocenyl moiety gave a value for β on the order of 140 $\times 10^{-30}$ esu. This value suggests significant acceptor potentiality of the tricarbonyl(cyclohexadienyl)iron complexes [366].

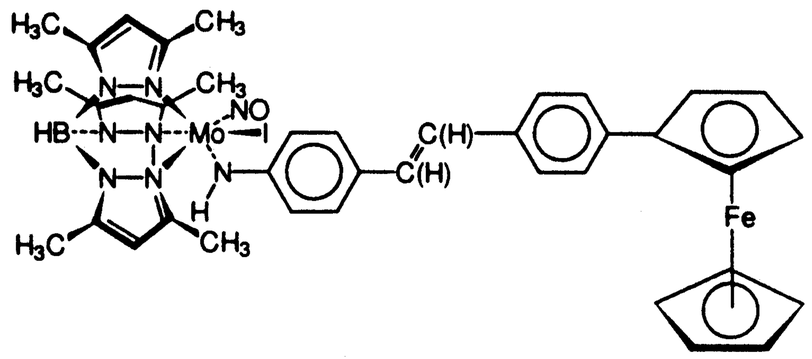

3

Table X. Selection of Complexes Possessing Only Metal−Ligand σ Bonds—First Hyperpolarizabilities

Compound	β (10^{-30} esu)	Technique	Ref.
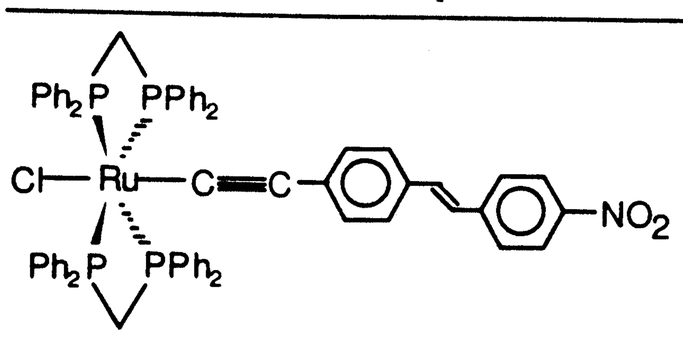	1964	HRS[a,b]	[349]
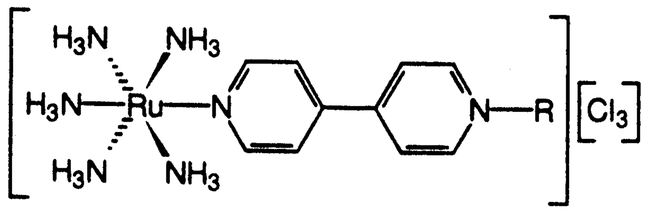	510	HRS[a,c]	[358]
R =	629		
R = 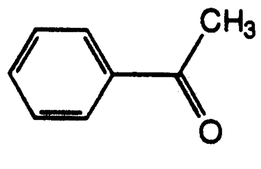	656		
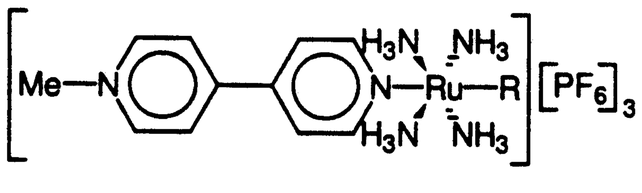			
R = 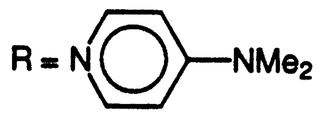	587	HRS[a,b]	[359]
R = 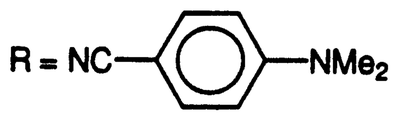	621		
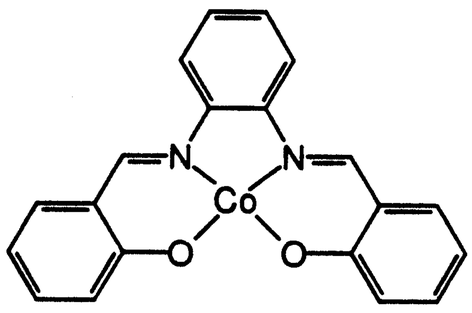	170[d]	EFISHG[e,f]	[268]
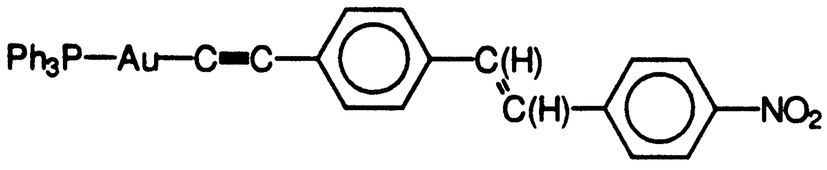	120	HRS[b,g]	[329]
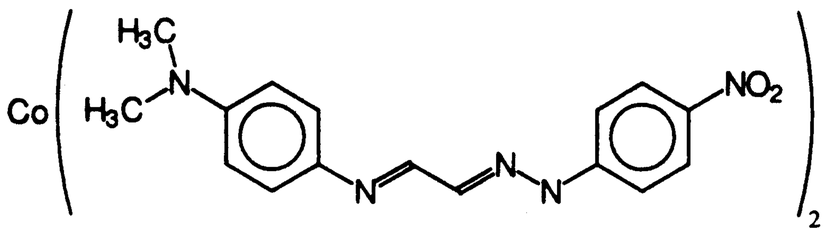	100	EFISHG[e,h]	[360]

continues

Table X. (continued)

Compound	β (10^{-30} esu)	Technique	Ref.
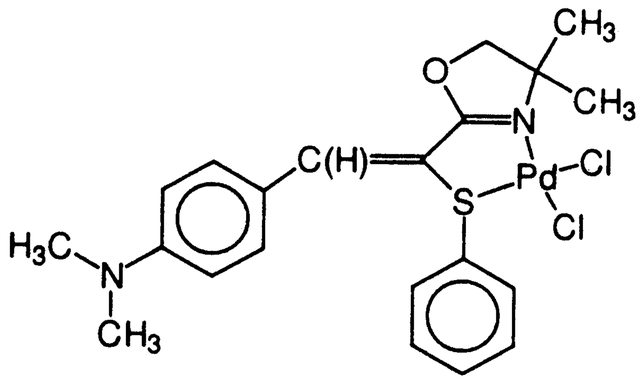	37	EFISHG[e]	[361]
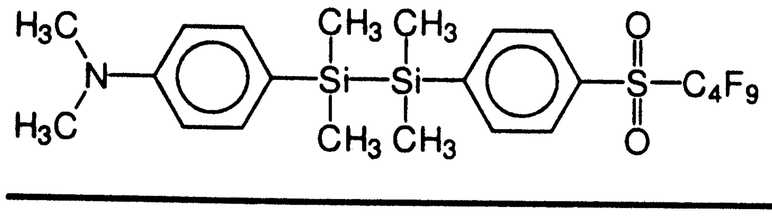	20	HRS[e,f]	[357]

[a] $\lambda = 1064$ nm.

[b] In THF.

[c] In water.

[d] Absolute value.

[e] In chloroform.

[f] $\lambda = 1340$ nm.

[g] $\lambda = 1060$ nm.

[h] $\lambda = 1900$ nm.

Some Ru(indenyl) derivatives were used successfully for bimetallic NLO compounds. The best value found in this set of derivatives was $\beta = 700 \times 10^{-30}$ esu for compound [Ru(C≡C−(*E*)−CH=CHC$_6$H$_4$-4-C≡NW(CO)$_5$)(PPh$_3$)$_2$(indenyl)], measured in dichloromethane at 1.06 μm by HRS. The Cr compound analogous presented $\beta = 465 \times 10^{-30}$ esu in the experimental conditions [328, 331].

Potentially interesting for SO NLO purposes is the family of mixed valence compounds, due to their exhibition of ultrafast electron-transfer behavior. Nevertheless, both mixed valence (Ru(III)–Ru(II)) compounds, Ru(NH$_3$)$_5$-N≡CRu(CN)$_5$ and Ru(NH$_3$)$_5$N≡CRu(PPh$_3$)$_2$(η^5-C$_5$H$_5$), showed quite modest values of $\beta = 209$ and 157×10^{-30} esu, respectively, measured by HRS at 1.064 μm [118, 139, 141]. Recent studies by electroabsorption on compound Ru(NH$_3$)$_5$-N≡CRu(CN)$_5$ indicate that light-induced electron transfer occurs over effective distances that are only ~60% as large as the crystallographic measured separation distance between Ru(III)–Ru(II). As a consequence, small first hyperpolarizabilities are anticipated due to less participation of the intervalence excited state in the process [367].

4.6. Octupolar Complexes

Literature reports on octupolar structures for organometallic compounds are still rather scarce. The approach is the use of nondipolar molecules, which opens a class of systems with potentially better properties in terms of the efficiency/transparency tradeoff and of noncentrosymmetric crystallization. (See Section 3.2 for a discussion and for the purely organic octupolar compounds.)

The first reports on organometallic octupolar molecules came from the group of Zyss [110] on chiral ruthenium complexes with octahedral coordination on the metal ion: Ru-trisbipyridyl (RuTB) and Ru-trisphenanthroline (RuTP). In a later study [140] a RuTB complex with the additional conjugated ligand dibutylaminophenol (Table XIII) was shown to possess a very high hyperpolarizability. In both studies, the β values were overestimated due to multiphoton fluorescence [118, 142], but even the remeasured values $\beta_{HRS} = \langle\beta^2\rangle^{1/2} = 800$–$1000 \times 10^{-30}$ esu and $\beta_{HRS}(0) = 270$–330×10^{-30} esu (see endnote 11 of Ref. [169]) for RuTB with dibutylaminophenol is still the highest result for organometallic octupolars and is among the very high confirmed values for both organic and organometallic compounds.

Lequan et al. [368, 369] showed that tin-tetraorganotines (SnAr$_4$, Ar: aryl ligand) possess interesting hyperpolarizabilities comparable to that of *p*NA (for Ar = C$_6$H$_4$NMe$_2$ or C$_6$H$_4$C$_6$H$_4$NMe$_2$) and even significantly larger when a more conjugated ligand is introduced (Table XIII).

Together with several linear organometallic molecules, Whittall et al. [370] studied the 1,3,5-C$_6$H$_3$(C≡CAu(PPh$_3$))$_3$ compound which has 3-fold symmetry (D_{3h}), but only low hyperpolarizability, $\beta < 6 \times 10^{-30}$ esu, was found.

In addition, interesting complexes with Cu(I) ions incorporated in an octupolar structure (Table XIII) were reported by Cho et al. [168], in particular, hexaazatriphenylene (HAT) and hexaphenyl derivatives thereof, which are planar compounds with three metal coordinating sites and which possess three D/A dipoles arranged with C_3 symmetry. It was found that β increased as the acceptor strength is increased by the complexation of the ligand with Cu(I), in agreement with the theoretical predictions [229, 331]. Values of β_{HRS} were 13 and 82×10^{-30} esu, measured by HRS at 1560 nm in DMSO solutions.

Renouard et al. [169] determined high values of hyperpolarizability for an octupolar Cu complex with tetrahedral coordination of the central Cu ion and conjugated ligands similar to those in the Ru compounds discussed previously (see also Table XIII).

Table XI. Selection of Complexes Possessing Only Metal–Ligand σ Bonds—SHG by the Kurtz Powder Technique

Compound		SHG vs urea[a]	Ref.
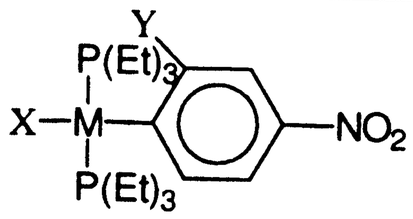	$M = Pt,\ X = Br,\ Y = CH_3$ $M = Pt,\ X = I,\ Y = H$ $M = Pd,\ X = Br,\ Y = H$	14.0–2.0[b,c] 8.0–5.0[b,c] 7.2–2.1[b,c]	[296]
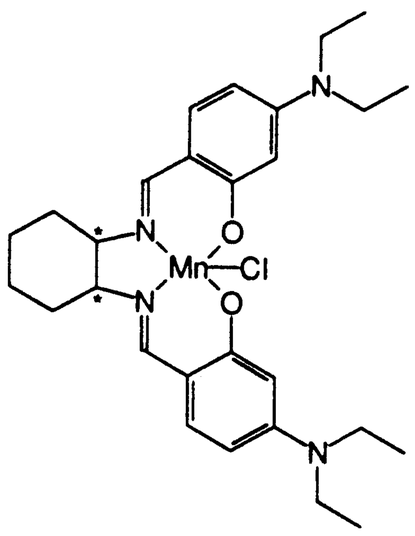		8[b]	[362]
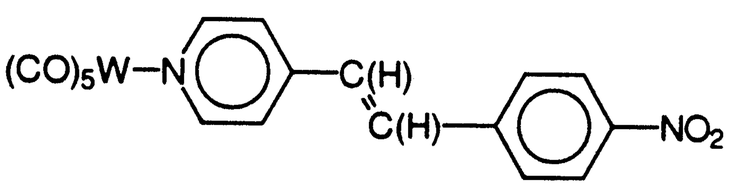		5[b]	[337]
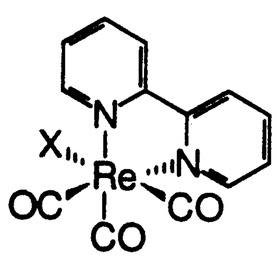	$X = CF_3SO_3$ $X = Cl$	2.0–1.7[b,c] 3.0–1.6[b,c]	[363]
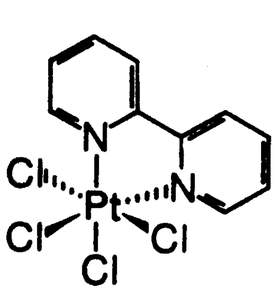		1.2[b]	[161]

[a] ADP = 0.3 × urea; quartz = 0.1 × urea [341].

[b] $\lambda = 1064$ nm.

[c] Values obtained from different experiments with particle size variation.

Finally, the report of Humphrey et al. [48] on ruthenium derivatives of molecules based on the octupolar structure 1,5-triethynylbenzene (Table XIII) showed the encouraging β values of 93 and 94 × 10^{-30} esu measured in THF by HRS at 1064 nm. Studies on the second-generation alkynyl–metal dendrimers are in progress by the same authors [371].

4.7. Concluding Remarks

Until recently it has been a universally held view that an extended π system with considerable molecular dipole moment was the key for the design of organometallics for SO NLO materials and under this concept, significant progress in devising chemical structures based on the two-level model has been made. Nevertheless, so far no organometallic compound suitable for SO NLO technological applications has been found, in spite of the extremely large values of the molecular nonlinearities obtained, which clearly suggest the importance of the exploitation of this field. Some problems of crucial importance for SHG remain to be resolved, namely, the efficiency-transparency tradeoff and the tendency for centrosymmetric packing in the solid state. The focus on alternative concepts for the design of organometallic molecules continues to be the main challenge for the organometallic chemists.

5. MATERIALS

The second-order nonlinear optical response offers a number of optical processing functions. These include the parametric processes of sum and difference frequency generation and the linear electro-optic response. The former functions require strict control over device fabrication and operating conditions since their effi-

Table XII. Selection of Binuclear Organometallics for SO NLO—First Hyperpolarizabilities

Compound		β (10^{-30} esu)	Technique	Ref.
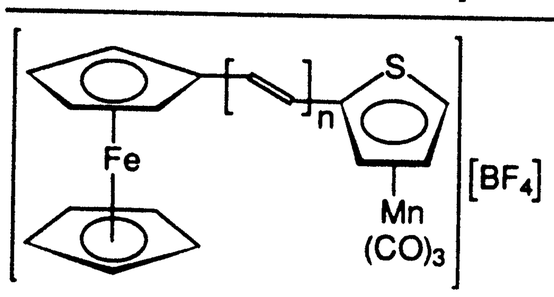	$n = 2$	771	HRS[a,b]	[344]
	$n = 1$	670		
	$n = 0$	260		
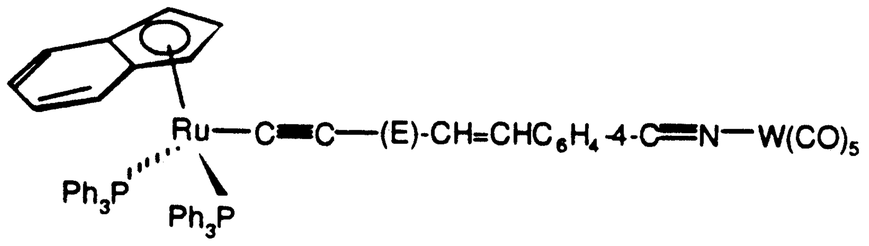		700	HRS[a,c]	[328, 331]
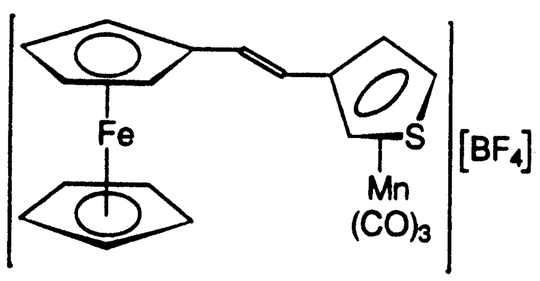		305	HRS[a,b]	[344]
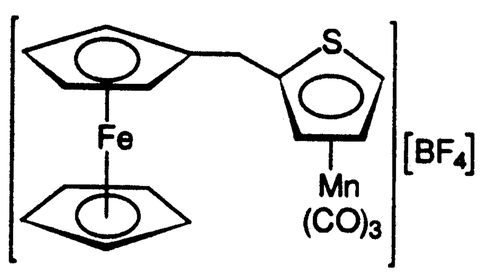		220	HRS[a,b]	[344]
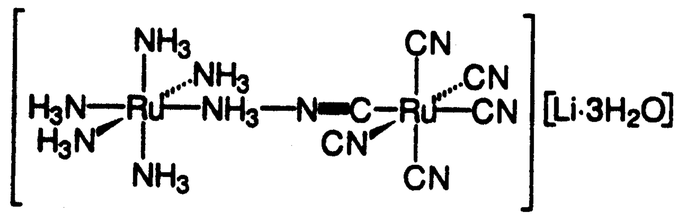		209	HRS[a,d]	[139, 141]
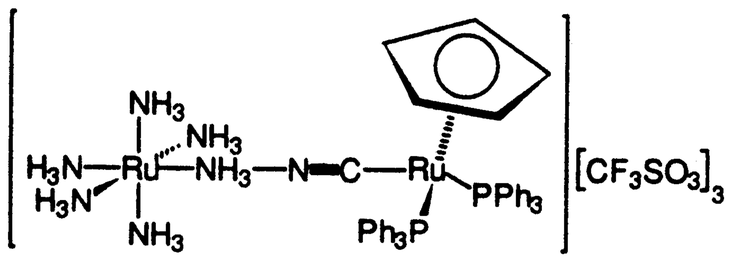		157	HRS[a,b]	[139, 141]
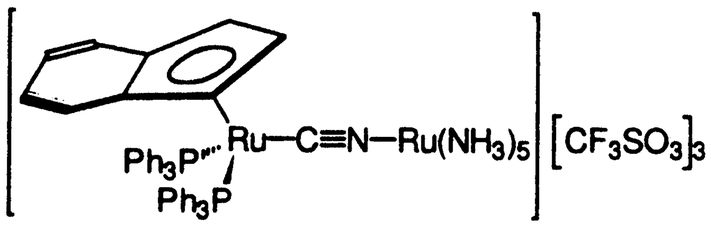		108	HRS[a,e]	[332]
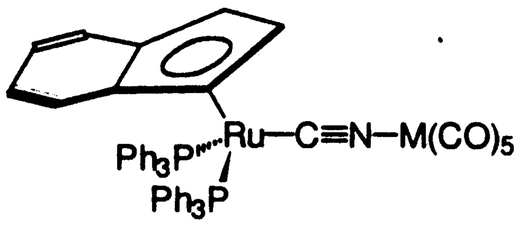	$M = W$	40	HRS[a,c]	[332]
	$M = Cr$	25		

continues

Table XII. (continued)

Compound	β (10^{-30} use)	Technique	Ref.
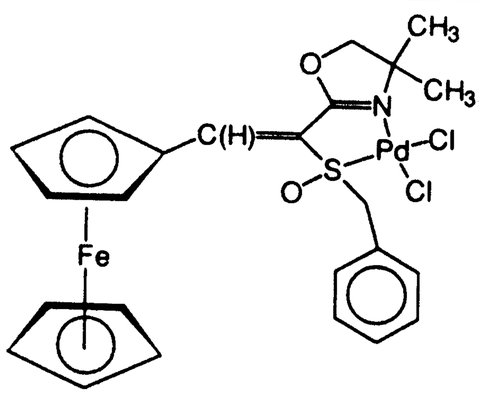	30.2	EFISHG[f,g]	[361]

[a] $\lambda = 1064$ nm.

[b] In nitromethane.

[c] In dichloromethane.

[d] In acetonitrile, no corrected values.

[e] In acetone.

[f] In chloroform.

[g] $\lambda = 1340$ nm.

ciency depends on close phase matching of the propagating fields. Nevertheless, there has been an interest in demonstrating second-harmonic generation, in particular in crystals [196], Langmuir–Blodgett films [372, 373], and polymers [374]. One of the great drivers for this effort in the early part of the 1990s was the prospect of a waveguide frequency doubler for near-IR lasers providing a coherent source of blue light. The main application areas would lie in optical data storage where reducing the wavelength of the reading and writing beams increases the density of the current two-dimensional storage schemes. The limiting factor is an inverse square law dependence on storage density with operating wavelength. The use of organic materials in addressing this area has faced considerable problems, however. Materials with the required optical nonlinearity have proved too unstable or too highly absorbing at the harmonic wavelengths to offer much competition to the two other emerging technologies: frequency doubling using single-crystal KTP [375] or the III-V wide-band gap silicon nitride blue LED and laser diodes [376]. Thus, in light of this disappearing opportunity one must return to the electro-optic response and to parametric effects at longer wavelengths to find strong arguments in favor of use of organic materials in real applications [377].

The linear electro-optic (Pockels) effect was identified early on as one aspect in organics where the advantage of a low dielectric constant was the unique selling point for high-frequency switching devices [378]. Furthermore, the wavelength of operation of high bandwidth telecommunications (around 1.3 and 1.55 μm) places much less of a restriction on the choice of material for devices and means that materials benefiting from low-lying electronic excited states (to enhance the first hyperpolarizability) can be considered. With current developments in wavelength division multiplexing, there is also an interest in frequency-mixing operations at these wavelengths.

The telecommunications industry watchword, however is "reliability." Devices must be placed in the telecommunications system and continue to function within specification for upwards of 5 years and over temperature ranges in the upper limit of between 70 and 80 °C. Over this time optical waveguide devices might be continuously exposed to irradiances exceeding 1 MW cm^{-2} at the infrared wavelengths and have electric fields periodically applied corresponding to typical drive voltages of 5 V. Furthermore, it is almost certain that devices will be required to be hermetically sealed or, if it becomes acceptable to the industry, encapsulated. This, at least, is one aspect in which the organic materials are no different from their inorganic competitors.

Thus, there will be many questions relating to thermal and optical stability and electrical integrity which cannot be answered until a device is actually fabricated and operated. This places a great burden on developers since while it is relatively straightforward to design a new material using rules taken from the chemistry and basic polymer physics in this field, it is almost impossible to predict the performance which will finally characterize it in the device.

5.1. Basic Classes of Second-Order Organic Materials

Once the choice of material has been made at a molecular level there will be the requirement to assemble a noncentrosymmetric medium suitable for device application. Clearly one can hope that a noncentrosymmetric crystal structure will naturally form and provide a suitable material or one can at least engineer the molecular structure to promote the formation of a noncentrosymmetric crystal (as in the case of chiral molecules.) At the next level of molecular engineering, sequential layer assembly of a noncentrosymmetric material such as a Langmuir–Blodgett film or self-assembled multilayer provides an alternative strategy. However, despite considerable effort expended in these areas, it is in the area of oriented polymer films where the most advanced work has taken place and where applications seem more promising.

5.1.1. Crystals

Organic crystals exhibiting second-order optical nonlinearities have been known ever since the invention of the laser and its wider availability [379]. Commonly occurring crystals such as urea have a noncentrosymmetric structure and contain the prerequisite molec-

Table XIII. Organometallic Compounds with Octupolar Symmetry—First Hyperpolarizabilities Measured by HRS

Compound	λ_{max} (nm)	λ_0 (nm)	β_{HRS} (10^{-30} esu)	Ref.
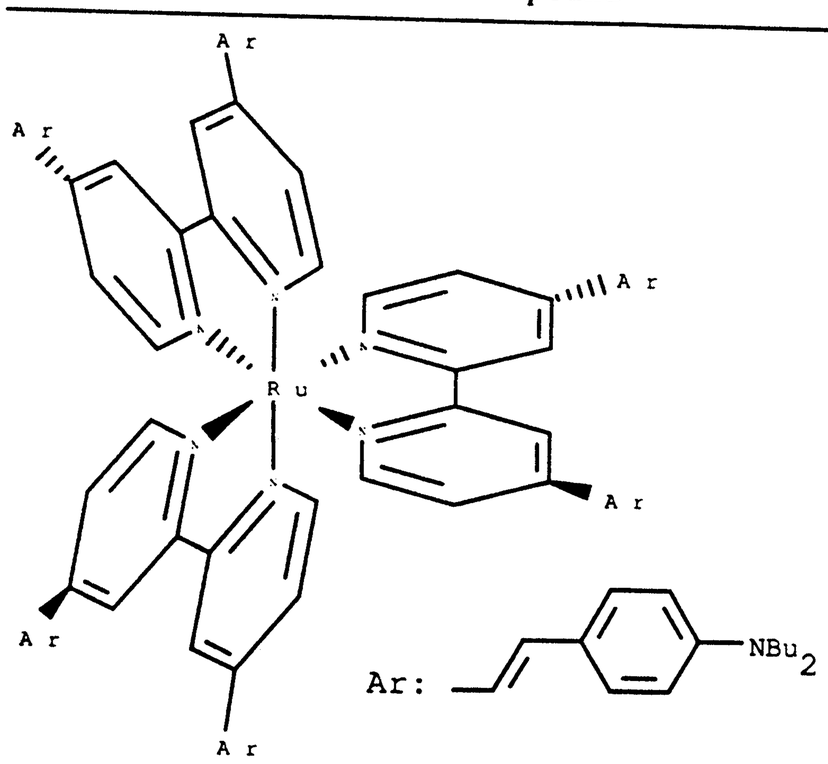	513	1320	800–1000[a,b]	[142]
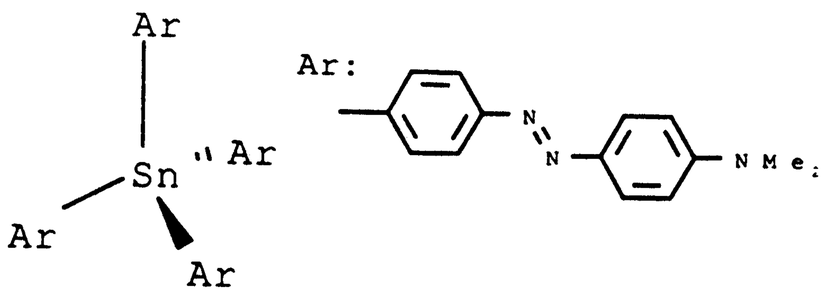	427	1064	120[a,c]	[369]
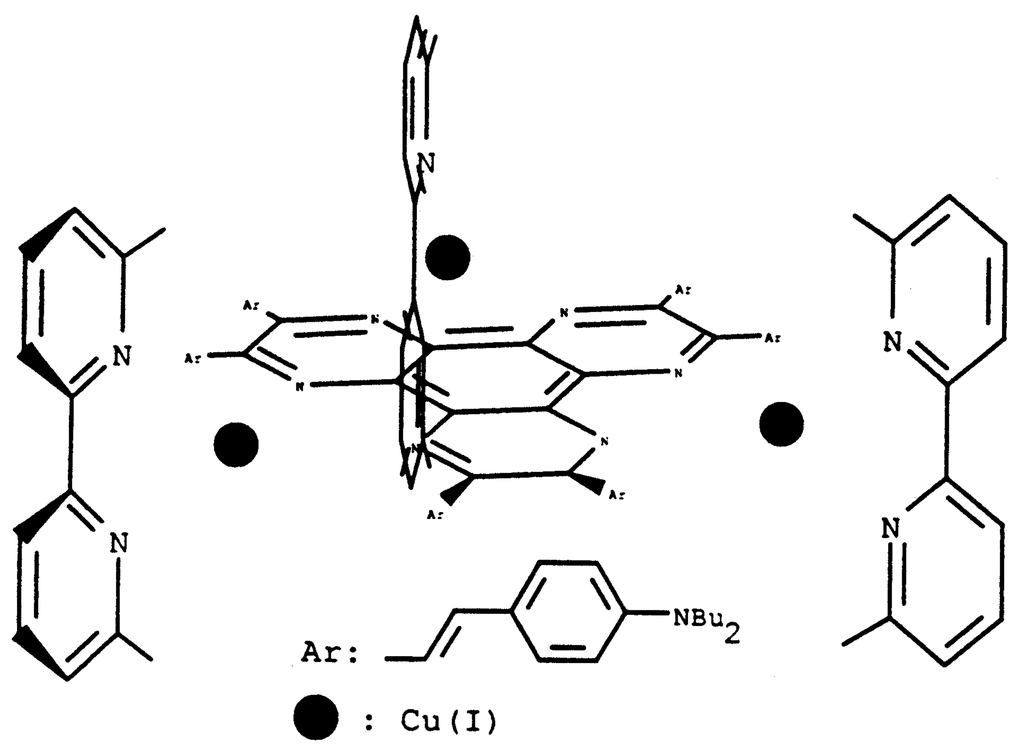	532	1560	82[d,e,f]	[168]
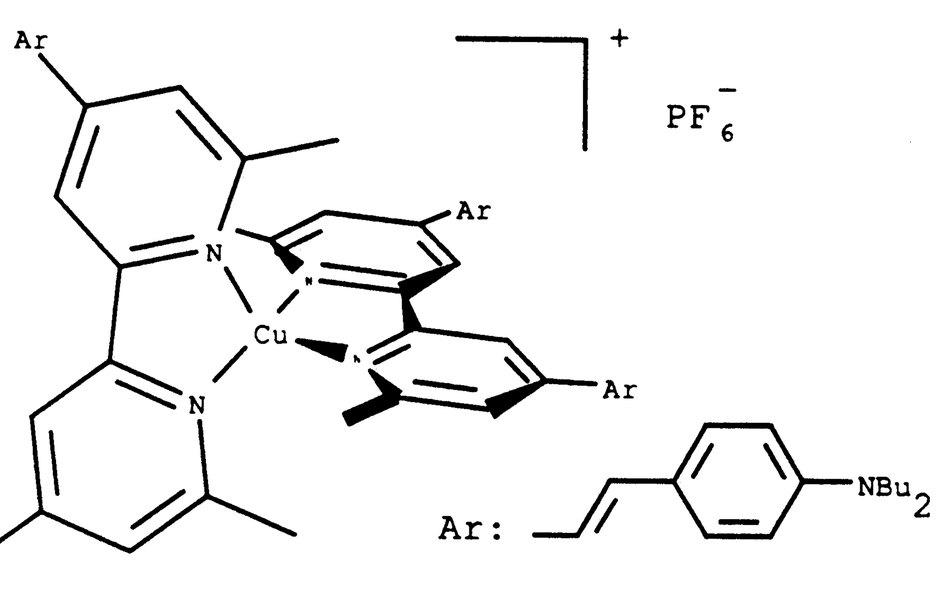	424 (484)[g]	1340	144[h]	[169]

continues

Table XIII. (continued)

Compound		λ_{max} (nm)	λ_0 (nm)	β_{HRS} (10^{-30} esu)	Ref.
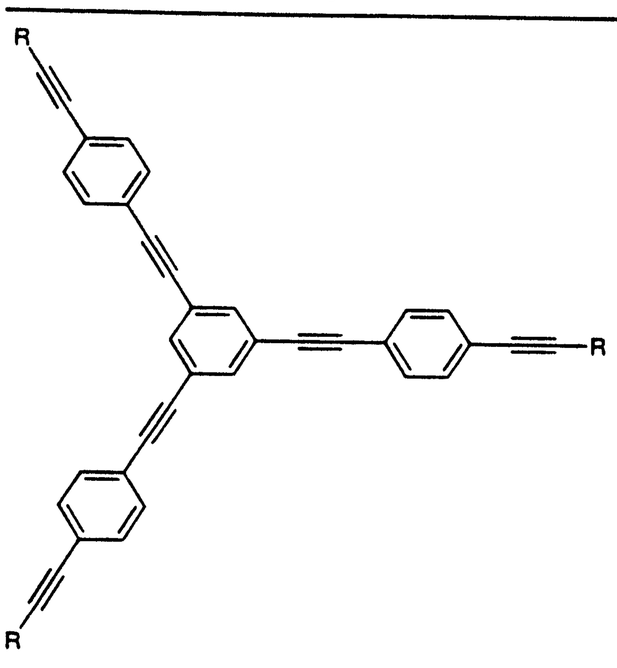	$R = SiMe_3$	342	1064	8^i	[48]
	trans-$RuCl(dppe)_2$	414		94^i	
	trans-$Ru(C{\equiv}CPh)(dppe)_2$	411		93^i	

[a] In dichloromethane.

[b] Too high value in this reference is due to multiphoton fluorescence [118, 142]: value from footnote 11 in Ref. [169].

[c] Reduced using $\beta_{HRS} = \langle\beta^2\rangle^{1/2} = (\frac{4}{7})^{1/2}\beta_{xyz}$.

[d] In DMSO.

[e] Converted using $\beta_{HRS} = (\frac{6}{35})^{1/2}\,\beta^{eff}_{EFISHG}$.

[f] Wrong reference value for methanol of 0.69 (instead of 0.26) $\times 10^{-30}$ use [111, 112].

[g] Shallow band.

[h] In $CHCl_3$.

ular properties so that second-harmonic generation can be seen. Urea is still used as a reference medium for powder screening evaluation of prospective new materials [74]. Measurements of the Pockels response from molecular crystals has been a more recent interest but even so was demonstrated first during the early 1960s [380].

The bulk second-order nonlinear optical coefficients for crystals in principle can be obtained from a knowledge of the crystal structure and the molecular first hyperpolarizability tensor components. We can relate the frequency-dependent second-order susceptibility tensor, $\chi^{(2)}_{IJK}(-\omega_3; \omega_1, \omega_2)$, to the frequency-dependent molecular first hyperpolarizability, $\beta_{ijk}(-\omega_3; \omega_1, \omega_2)$, through a relationship which accounts for the transformation of the molecular nonlinear optical response from the molecular (Cartesian axes, *ijk*) to the macroscopic (Cartesian axes, *IJK*) reference frame [the cosine terms of Eq. (26) below]. Thus each molecule is assumed to provide an independent contribution. With this in mind we can write

$$\chi^{(2)}_{IJK}(-\omega_3; \omega_1, \omega_2) = NF_{IJK}\sum \cos\theta_{Ii}\cos\theta_{Jj}\cos\theta_{Kk}\beta_{ijk}(-\omega_3; \omega_1, \omega_2) \quad (26)$$

in which the sum runs over the molecules in a unit cell as well as over the Cartesian indices i, j, k, and N stands for the number of cells per volume unit.

However, if the first hyperpolarizability used here is the "gas-phase" value, perhaps obtained from measurements in solution or from calculations, a suitable correction for the local effective field is needed since the measured bulk response will be a measurement of the field-modified molecular response. The factor F_{IJK} in Eq. (26) accounts for the local field tensor applicable to molecules in the crystal.

Relationships between the general second-order nonlinear optical susceptibility and the response-specific nonlinear optical coefficients are represented through the following expressions;

$$d_{IM} = \tfrac{1}{2}\chi^{(2)}_{IJK}(-2\omega; \omega, \omega)$$

which refers to the second-harmonic coefficient, d_{IM}, where, due to symmetry in the last two subscripts of the susceptibility tensor (for SHG, degeneracy of the input fields ω_1 and ω_2), the second subscript, M, for d_{IM} contains contractions of the J and K subscripts ($M = 1\ldots6$, $I = 1\ldots3$) and a factor of $\frac{1}{2}$ is introduced and

$$r_{IJK} = -\frac{2\chi^{(2)}_{IJK}(-\omega; \omega, 0)}{n_I^2 n_J^2} = -\frac{4d_{IJK}(-\omega; \omega, 0)}{n_I^2 n_J^2} \quad (27)$$

which refers to the linear electro-optic tensor. Contraction of the first two subscripts in r_{IJK} is performed to reduce the electro-optic tensor to the electro-optic coefficients, r_{NK} ($N = 1\ldots6$, $K = 1\ldots3$).

Within the noncentrosymmetric crystal classes, crystals may be optimized for either the electro-optic effect or for wave mixing effects. If one considers molecules constituting the crystal to have only one dominant β_{ijk} tensor component, it can be shown that these optimizations are mutually exclusive. The electro-optic effect can be optimized by arranging this component to lie parallel to a single macroscopic crystal axis. If the low-frequency driving field can be applied along this direction, there is a large bulk electro-optic effect to be accessed from a diagonal component of

the electro-optic tensor (r_{33}, for example). However, in the case of wave mixing, the bulk effect relies on efficient coupling between the three waves of the interaction. Efficient coupling occurs at "phase matching" when the phase velocities of the waves are equal. For materials exhibiting normal dispersion in the frequency range of interest, this requires a mixture of polarization states for the waves. The wave having the highest frequency (the second harmonic, for example) must be polarized along a direction of lower refractive index so that normal dispersion can be compensated for at some specific angle of propagation in the crystal (the phase-matching angle). Thus it is impossible in such a scheme to achieve phase matching using an (albeit high) diagonal susceptibility component since access to this component is via copolarized fundamental and harmonic fields. In the case of molecules having a single dominant β tensor component, the second harmonic coefficient tensor reduces to two components,

$$d_{31} = \tfrac{1}{2}N\beta_{zzz}F_{IJK}\cos\theta\sin^2\theta \quad \text{and} \quad d_{33} = \tfrac{1}{2}N\beta_{zzz}\cos^3\theta \tag{28}$$

where θ represents the angle between β_{zzz} (z is a principal axis in the molecular coordinate system) and the principal axis in the crystal. The off-diagonal component, d_{31} is optimized when $\theta = 54.74°$. Phase matching may now be achieved, for example, using the type I scheme where fundamental and second-harmonic fields are orthogonally polarized. Such a near optimization is displayed in the crystal NPP where use of hydrogen bonding and chirality ensure both the noncentrosymmetry and optimization of the polar angle needed for efficient phase matching [284]. This crystal has continued to generate interest due to its efficient phase-matching properties. In recent work, NPP has been shown to exhibit efficient cascaded third-harmonic generation [381]. In an example where type II phase matching (orthogonal fundamental field polarization states) has been found, the crystal 2-adamantyl-5-nitropyridine provides a large d_{15} tensor coefficient of 8.6 pm/V at 1550 nm. This value exceeds by at least four times the effective d coefficient of β-barium borate (BBO) [382] which is used currently for optical parametric oscillation. Crystals which optimize the condition for the electro-optic response have also been grown [383, 384] and in particular a cocrystal containing a merocyanine dye has been shown to possess a diagonal electro-optic coefficient tensor component, $r_{11} = 30$ pm/V at 1535 nm [385]. Hydrogen bonding between the merocyanine dye and the partner molecule helps to define the favorable parallel dye alignment. While this value is only just comparable to lithium niobate, for example, which is currently used in electro-optic devices, its origin lies largely in the electronic excitations of the constituent molecules. Similarly, it has been found that organic molecular salt crystals can be found in crystal structures where the nonlinear optical chromophores are practically [286] or even completely [386] parallel. In particular, the crystal 4-*N*, *N*-dimethylamino-4′-*N*′-methylstilbazolium tosylate (DAST) has been used to demonstrate a number of devices of potential commercial interest [387].

Despite such advances, organic crystals have yet to make a great impact in commercial terms. Problems of crystal growth, which in many cases can be overcome for the production of large single crystals, in waveguide formats are more persistent and demanding. Nevertheless, there have been notable successes, in particular where melt growth methods have been replaced by evaporation from seeded solutions in preformed channels [388]. With little other development since this demonstration, however, one would question whether the use of organic crystals for waveguide devices remains a fruitful area for research.

5.1.2. *Langmuir–Blodgett Films and Self-Assembly*

Single molecular layers can be superimposed sequentially and in noncentrosymmetric alignment using Langmuir–Blodgett (LB) deposition [389]. From the earliest observation of SHG from a monolayer LB film [372] and from electro-optic studies [390] most subsequent work has concentrated on growing multiple layer films which retain the noncentrosymmetry and thus the second-order optical nonlinearity. Normal (Y-type) LB deposition would provide layers aligned in opposite polarity, thus cancelling the bulk response. There are a number of ways this problem has been overcome. In the first case, the layers of aligned amphiphilic chromophores are interspersed with inactive LB layers [391] or with layers where the sign of the nonlinearity is opposite in each adjacent layer [392]. In a second approach (Z-type deposition), the ionic interaction between chromophores stabilizes films which are deposited only on each alternate cycle of the LB dipping process. This scheme can provide for exceptional stability in noncentrosymmetric multilayer formation as evidenced in the deposition of highly charge separated styryldicyanomethanide derivatives [393]. Such films, even after many tens of layers, are still relatively thin in terms of optical wavelength. Often the behavior of the second-harmonic power is seen to be roughly quadratic in layer thickness. When the pump beam is undepleted, as will be the case for such thin films, the second-harmonic power, $P_{2\omega}$ as a function of propagation distance, L, through the material can be written as [9]

$$P_{2\omega} = \frac{512\pi^5 d_{eff}^2 P_\omega^2}{\lambda_{2\omega}^2 c n_\omega^2 n_{2\omega}} L^2 \mathrm{sinc}^2\left(\frac{L}{L_c}\right)$$

where n_ω and $n_{2\omega}$ are the refractive indices at the fundamental and second-harmonic frequencies, d_{eff} is the effective second-harmonic coefficient, $\lambda_{2\omega}$ is the second harmonic wavelength, and L_c is the coherence length. Since the coherence length can usually be found to be on the scale of at least a few microns, the sinc^2 function tends toward unity for the usual thicknesses of LB multilayers and the quadratic dependence with length will result. However, the use of LB films for nonlinear optical applications is generally limited by the constraints of deposition. Where they do have some merit is in the control which may be exercised over thickness and over relative orientation of optical nonlinearity. These dual advantages have been exploited to achieve modal dispersion phase matching between the fundamental and second-harmonic waveguide modes while optimizing the overlap integral for SHG between the two modes in a LB waveguide device [394]. The self-assembly of multiple noncentrosymmetric layers has also been studied [279, 395].

5.1.3. *Polymers*

Polymer matrices may contain the NLO active chromophores either as part of the covalent structure of the polymer or as a doped guest bound by noncovalent interactions. The former method is undoubtedly preferred for applications while the latter has allowed much in the way of research and development to be undertaken quickly without new synthesis. After deposition of the polymer film, the chromophores will lie more or less in random relative orientation, but there are two methods to produce noncentrosymmetry.

5.1.3.1. *Electric Field Poling*

In the first method, one uses the dipole moment, μ, of the chromophore to respond to an applied local poling field, E, at a suitable temperature, T_p, where the molecules can rotate on reasonably short time scales. In polymers this can be when the material is in a rubbery or otherwise low-density state, for example, above the glass-to-rubber transition temperature. The single particle energy of interaction, $U(\theta)$ consists predominantly in the scalar product of the molecular dipole moment and poling field to provide the Gibbs distribution function, $G(\theta)$, given by

$$G(\theta) = Z^{-1} \exp\left(\frac{-U(\theta)}{kT_p}\right)$$

where Z is used for normalization. As a first approximation, all dipole–dipole interactions and other specific interactions of the chromophore with its surroundings are neglected. Within this scheme, the energy consists of only a term linear in the applied local poling field and is given by

$$U_1(\theta) = \mu E \cos\theta$$

where θ is the angle between the dipole and poling field unit vectors. In more detailed treatments, account can be taken of the quadratic field dependence of the energy where the anisotropy of the linear polarizability of the molecule, $\Delta\alpha$, is taken into account. A second energy term, $U_2(\theta)$, is included, given by

$$U_2(\theta) = \Delta\alpha E^2 P_2/3$$

where P_2 is the second-order Legendre polynomial of $\cos(\theta)$. Further terms may be added into the single particle interaction energy at higher levels of refinement. An excellent discussion of this topic and of the further consideration of dipole–dipole interactions is available [396]. It is generally agreed, however, that a reasonable description of the interaction for rather dilute NLO polymers (low chromophore content) at most typical achievable poling fields is given solely by $U_1(\theta)$.

After poling, the film is cooled to a temperature where the polar order is expected to be stable over reasonable time scales and in the most common case, the symmetry properties of the second harmonic coefficient provide for only two independent tensor components, d_{33} and d_{31}.

These can be described in terms of statistical mechanics by computing the integral of the Gibbs distribution function over the polar angle, θ, and applying an appropriate projection term relating the microscopic to macroscopic reference frames. Thus, for one-dimensional molecules (i.e., where the microscopic nonlinearity is attributed to a single component parallel to the dipole moment) arranged in azimuthal symmetry (in the substrate plane) we can write the coefficients as

$$d_{31} = \frac{1}{4} N\beta_{zzz} F_{IJK} \frac{\int \cos\theta \sin^2\theta G(\theta)\, d\theta}{\int G(\theta) d\theta}$$

$$d_{33} = \frac{1}{2} N\beta_{zzz} F_{IJK} \frac{\int \cos^3\theta G(\theta)\, d\theta}{\int G(\theta)\, d\theta}$$

The integrals can be evaluated to yield the coefficients in terms of first- and third-order Langevin functions, L_1 and L_3, respectively, as follows,

$$d_{31} = \tfrac{1}{4} N\beta_{zzz} F_{IJK}\left[L_1(p) - L_3(p)\right]$$

$$d_{33} = \tfrac{1}{2} N\beta_{zzz} F_{IJK}\left[L_3(p)\right]$$

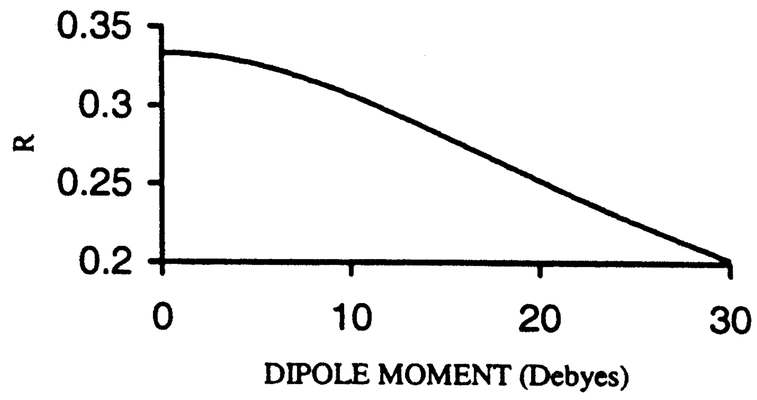

Fig. 14. The second-harmonic coefficient ratio, R, vs dipole moment calculated for an assumed local poling field of 190 MV/m (external poling field ~80 MV/m, Onsager local field factor, $f(0) = 2.4$).

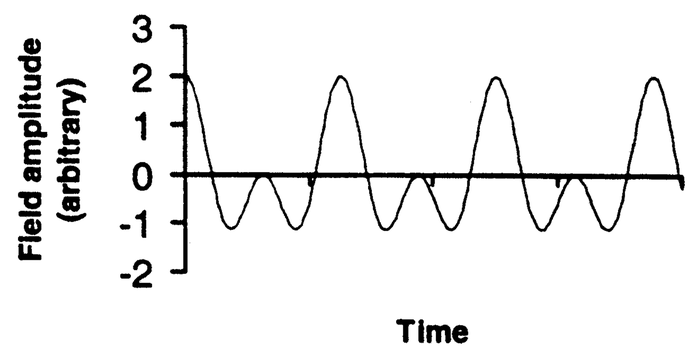

Fig. 15. The amplitude of the resultant field created by the coherent superposition of waves at fundamental and second-harmonic wavelengths.

where $L_1(p) = \coth(p) - (1/p)$, $L_3(p) = [1 + (6/p^2)]L_1(p) - (2/p)$ and $p = \mu E/kT_p$. The functional form of these expressions leads to a ratio, $R = d_{31}/d_{33} = \frac{1}{3}$, over a range where $\mu E/kT_p \ll 1$, and this ratio is commonly observed in the poling of polymers (Fig. 14). However, when the dipole moment of the molecules is exceptionally high, even moderate external poling fields (e.g., 100 MV/m) produce a ratio significantly smaller than this [209].

In principle, Eqs. (27) and (28) show that it should be possible to correlate the measured electro-optic coefficient with the molecular parameter μ and β. However, such a task is notoriously problematic. In the first place, there is no sure way to apply the local field correction factors for molecules other than those that can be approximated by spheres. Since most NLO molecules are elongated, an ellipsoidal description may be more apt [18], but attempts to apply such corrections bring further uncertainties. Perhaps more problematic is the evidence for chromophore aggregation in such polymers. This lowers the effective number density of NLO groups and inevitably produces a disparity between theoretical and experimental data. Efforts to explain aggregation and to overcome it have been pursued in recent studies [397, 398].

5.1.3.2. *Optical Field Poling*

An alternative method to introduce noncentrosymmetry into an isotropic distribution of NLO chromophores is by so-called optopoling or orientational hole burning [399, 400]. Such a process relies on producing an optical field which photobleaches a group of molecules oriented within a narrow range of angles in the overall distribution. This method is particularly useful when poling octupolar molecules [401] (which have no dipole moment) but is a method generally applicable to photo-bleachable molecules of all types [70]. The field is produced by combining coherently a fundamental wave with its second harmonic. The result of the superposition of these fields when in phase is shown in Figure 15. The time average at a point of such a field has a finite value and polarity (note that monochromatic fields have zero time average amplitude

and thus no net polarity). However, the phase relationship of the fields, governing the polarity of the resultant field, is determined by the wave vector mismatch, Δk, between the propagating fundamental and second harmonic fields. In a material with normal dispersion, the polarity will therefore change sign after every coherence length, L_c, given by $L_c = \lambda/4(n_{2\omega} - n_\omega)$ where λ is the wavelength of the fundamental field.

This scheme therefore would provide simultaneously a noncentrosymmetric material coupled with exactly the correct periodicity in $\chi^{(2)}$ for quasi-phase matched frequency doubling [402] from the wavelength of opto-poling.

5.2. Polymers for Second-Order Nonlinear Optics

5.2.1. Basic Properties

Polymers are distinguished by their wide thermotemporal range of physical properties, notably their viscoelastic or viscoplastic behavior [403]. This is due to the chain entanglement in the tertiary structure of the materials which allows relaxations to applied stresses to occur over a spectrum of characteristic times. The engineering benefits of flexibility and the ability to form and reform molded structures at low temperatures arise largely out of these structural properties. Furthermore, most polymers can be dissolved into solution which, for film forming applications, is a benefit for coating of any suitable substrate material. A number of studies are emerging, showing how polymers may be readily integrated with detectors and sources on such substrates [404–407]. Other materials systems which may be integrated as readily are not apparent.

The multiple layer structures necessary for vertical optical waveguide confinement and the two-dimensional patterning needed for lateral confinement are readily achieved in polymeric coatings and thickness control of around ± 0.1 μm or better is routinely available. Developments in the lateral patterning include selective photobleaching [408], photopolymerization [409], field-induced birefringence [410], topographic patterning [411] (e.g., by reactive ion etching), and, more recently, injection molding [412, 413] and other replication techniques [414].

As organic materials, polymers offer extremely wide opportunities for custom synthesis. Control over the refractive index is the prime example of such engineering versatility and the synthesis of copolymers where the refractive index is tuned by controlling the ratio of co-monomer units in the main chain serves to illustrate this. Refractive index differences suitable for the monomode waveguide dimensions compatible with monomode optical fibres are readily achieved by lowering the refractive index of the cladding layer polymer.

Thus, the primary general properties which favor the use of polymers in photonic integration are their ease and versatility of processing and integrability and synthetic versatility. Notice that the common argument for the use of polymers, that of low cost, is not necessarily in the forefront.

5.2.2. NLO Properties

As discussed above the electro-optic effect in polymers is not a naturally occurring property as it is in the crystal materials such as lithium niobate ($LiNbO_3$) but is the product of carefully targeted synthesis and an alignment (poling) procedure. While the magnitude of the electro-optic effect which can be achieved is clearly of importance, and can be as large as in traditional materials, it is the more generic property of the low dielectric constant which continues to make polymeric materials a unique prospect for devices. Compared to that in $LiNbO_3$, the dielectric constant of polymers is 1 order of magnitude lower. Even in lumped element devices this is a clear advantage, giving a lower RC value for the structure, but in traveling wave modulators the benefits are most apparent with operational bandwidths limited only by the speed of the driving electronics or the electrode design (the intrinsic limit to the bandwidth of the electro-optic response is equal to the frequency of the optical resonance dominating it). Flat frequency response in an electro-optic phase shifter out to 60 GHz, for example, has been demonstrated recently [415] and using heterodyne detection, modulation above 110 GHz has also been reported [416].

Consider the device-independent figure of merit, $F_{\text{e-o}}$ for electro-optic materials which takes into account the dielectric constant, ε

$$F_{\text{e-o}} = \frac{n^3 r_{\text{eff}}}{\varepsilon}.$$

Taking typical values for poled polymers, $n = 1.55$, $\varepsilon = 2.5$, and $r_{\text{eff}} = 30$ pm/V we get a figure of merit of 45 pm/V, whereas for $LiNbO_3$ ($n = 2.2$, $\varepsilon = 32$, and $r_{\text{eff}} = 30$ pm/V) we obtain a figure of merit of 10 pm/V. Thus, polymers have now reached a stage where they can in principle exceed the performance of current ferroelectric materials for high-frequency electro-optic devices.

5.2.3. Limitations and Challenges

The diversity of polymer types and chemical composition belies the fact that a certain set of intrinsic properties may be identified as possible limitations to their use in these new areas. For example, it would be difficult to conceive of a polymeric material which showed the same metastable characteristics of fused silica, or a polymer which started from and returned to, an equilibrium state after poling or other thermal excursions during use. These points highlight the fact that polymers have properties, of which some are the product of their thermal and processing histories. Thus, the operational temperature range is the primary consideration and first possible limitation.

Concerning orientational alignment, glassy polymers after thermo-poling are in a nonequilibrium state with respect to their free volume. Annealing of the polymer at some intermediate temperature after poling has been shown to slow the rate of decay of optical nonlinearity which is otherwise observed in many systems and some side chain-type polymers can be quite stable to relaxation [417]. In the case of NLO polymers which are thermally cured resins, the alignment stability can be exceptionally good. Most long-term relaxation behavior in poled glassy polymers can be related to relaxation of free volume. One of the most popular applications of theory to this problem is that of the Kohlrausch–Williams–Watts stretched exponential [418]. This assumes that the polymer contains a spectrum of free volume sites where relaxation takes place and the overall behavior is then seen as a modified exponential decay which fits the following function

$$y(t) = A \exp(-t/\tau)^\beta$$

where $y(t)$ is the measurand, τ is the characteristic relaxation time, and β ($0 < \beta \leq 1$) represents the broadness of the distribution in free volume. However, other empirical fits to the relaxation data

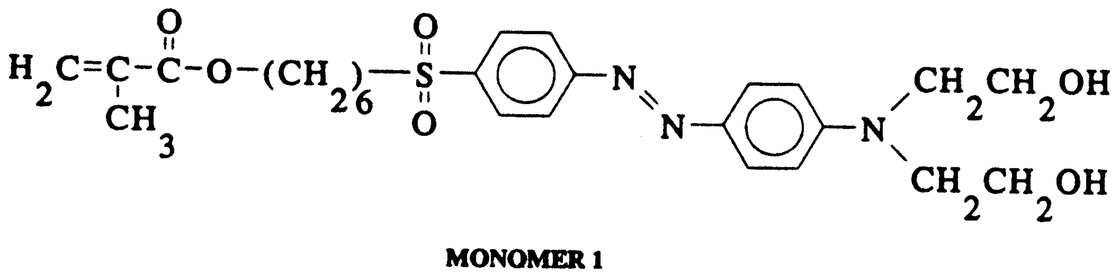

MONOMER 1

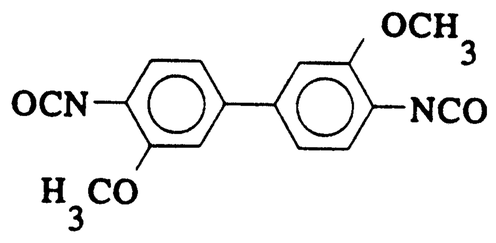

CROSSLINKER

Fig. 16. Structure of the chromophore-containing monomer and the crosslinking agent used in highly stable cross-linked nonlinear optical polymers.

have been applied (e.g., biexponential relaxation [419] and Gaussian distribution of Arrhenius decay [420]) and there is no consensus on the preferred method which seems to depend upon both the material and its precise processing history, as one would expect.

While methods such as annealing at some temperature intermediate between the poling temperature and the temperature of characterization serves to partially stabilize the orientational decay, by far the most dramatic route to stabilizing the decay is through material modifications. Cross-linked polymers in particular are shown to exhibit long-lived optical nonlinearities even at elevated temperatures [421, 422]. One such scheme involves the synthesis of a polyacrylate precursor polymer containing hydroxyl functionalities suitable for condensation cross-linking after poling (Fig. 16).

The copolymer of monomer 1 (Fig. 16) with methyl methacrylate and hydroxyethyl methacrylate is first deposited as a thin film from a solution containing the crosslinker. After drying, electric field poling is conducted at elevated temperature which initiates the cross-linking as poling progresses [423]. The cross-linked polymer film produced through this process shows exceptional stability to thermal relaxation. Films have shown no measurable decay in optical nonlinearity when stored at 100 °C for more than 2000 hours [424] and when measured periodically over a period of 3 years have shown no measurable decay under ambient conditions.

However, there are a few remaining obstacles recognized in this area which need to be overcome. Fundamental amongst these is the tradeoff between device efficiency (low drive voltages, etc.) and thermochemical and photochemical stability of the materials.

There is an inherent sensitivity to oxidation in certain molecular structural features in organic systems [425]. Primarily, oxidative reactions occur at ethylenic bonds such as those forming part of the conjugated bridging group in certain molecules described in Sections 3 and 4. Oxidation often proceeds via reaction with singlet oxygen. There has been some debate over whether this is produced by direct excitation at 1300 nm in waveguides or by an indirect process perhaps involving sensitization from an excited chromophore. However, after extensive studies over the past 10 years it has been established that the ethylenic structural unit is also that which produces molecules with the highest β coefficient. Thus there seems

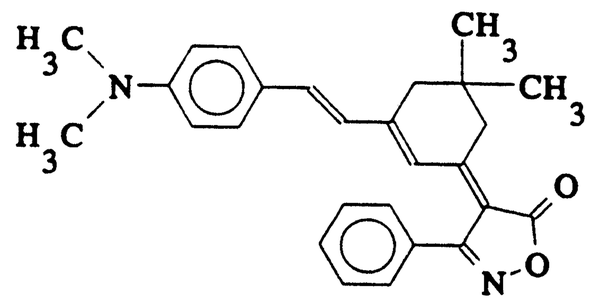

Fig. 17. Chromophore designed for reduced aggregation and high $\mu\beta$ as described in Ref. [426].

currently to be an *impasse* to achieving simultaneously high activity and acceptable photooxidative stability.

Nevertheless, chromophores with these features have been used to demonstrate the full potential of polymers provided these remaining problems can be overcome. The chromophore shown in Figure 17 has an estimated $\mu\beta$ coefficient of 3160×10^{-48} esu and contains structural features designed to prevent aggregation at high guest–host doping levels [426].

A 2-cm active length channel waveguide modulator device fabricated from a 45% (weight/weight) level of this chromophore in PMMA showed a V_π (the voltage needed to produce a net π phase change to the propagating light) of only 1.57 V at 1300 nm. This voltage is below the maximum allowed (currently 3 V) for high-bandwidth modulation using TTL and there is an expectation that in a practical device such as a Mach Zehnder modulator, V_π could be reduced to 1 V. To achieve this low value, a constant high-voltage bias field (300 V) was maintained on the film to hold the polar alignment.

ACKNOWLEDGMENTS

The authors wish to thank M. Paula Robalo and João Rodrigues for their help in the preparation of the bibliography and tables on the organometallic compounds. Financial support from the Flanders Government in its *Action for the Promotion of Participation in EU-research Programs* was provided for the NLO research in the Antwerp laboratory and is gratefully acknowledged. Etienne Goovaerts is a Research Director of the Fund for Scientific Research of Flanders (FWO).

APPENDIX: UNITS AND CONVENTIONS FOR NLO PARAMETERS

Conversion to SI Units

In the SI unit system, the (nonlinear) susceptibilities are defined by the power series

$$P_i = P_i^0 + \varepsilon_0\left(\chi_{ij}^{(1)}E_j + \chi_{ijk}^{(2)}E_jE_k + \chi_{ijkl}^{(3)}E_jE_kE_l + \cdots\right) \quad (29)$$

which differs from the cgs definition (2) by the inclusion of the factor ε_0. The SI units of the jth order susceptibility $\chi^{(j)}$ are $(\mathrm{m}^{j-1}/\mathrm{V}^{j-1})$, as can be derived from their defining Eq. (29) [427]. However, in this work NLO parameters were often quoted in Gaussian units, abbreviated as "esu" (electrostatic units), as these units are more widely used in literature. For the susceptibilities $\chi^{(j)}$ the cgs units are $(\mathrm{cm}^{j-1}/\mathrm{statV}^{j-1})$ [see Eq. (2)]. Conversion factors to SI units are listed below.

For the molecular (hyper)polarizabilities the situation is more confusing, because in the SI system, two different definitions of the

Table XIV. Units and Conversion Factors for NLO

Quantity	Symbol	cgs units	SI units	
Electric field	E	statV/cm	V/m	
Linear susceptibility	$\chi^{(1)}$	dimensionless	dimensionless	
Second-order susceptibility	$\chi^{(2)}$	$\mathrm{cm/statV} = (\mathrm{cm^3/erg})^{1/2} = \mathrm{esu}$	m/V	
Third-order susceptibility	$\chi^{(3)}$	$\mathrm{cm^2/statV^2} = \mathrm{cm^3/erg} = \mathrm{esu}$	$\mathrm{m^2/V^2}$	
			Definition (30)[b]	Definition (31)[c]
Dipole moment	μ	$\mathrm{statC\,cm} = \mathrm{cm^2 statV} = \mathrm{esu}$[a]	C m	C m
Linear polarizability	α	$\mathrm{cm^3}$	$\mathrm{Cm^2/V} = \mathrm{C^2m^2/J}$	$\mathrm{m^3}$
First hyperpolarizability	β	$\mathrm{cm^4/statV} = \mathrm{esu}$	$\mathrm{Cm^3/V^2} = \mathrm{C^3m^3/J^2}$	$\mathrm{m^4/V}$
Second hyperpolarizability	γ	$\mathrm{cm^5/statV^2} = \mathrm{esu}$	$\mathrm{Cm^4/V^3} = \mathrm{C^4m^4/J^3}$	$\mathrm{m^5/V^2}$
1 a.u. of electric field, E		$= 1.71514 \times 10^7$ esu		(cgs)
		$= 5.14192 \times 10^{11}$ V/m		(SI)
1 a.u. of dipole moment, μ		$= 2.54174$ D		
		$= 2.54174 \times 10^{-18}$ esu		(cgs)
		$= 8.47831 \times 10^{-30}$ C m		(SI)
1 a.u. of polarizability, α		$= 1.48176 \times 10^{-25}$ esu		(cgs)
		$= 1.64867 \times 10^{-41}$ $\mathrm{C^2m^2/J}$		[SI, definition (30)]
1 a.u. of second-order polarizability, β		$= 8.63993 \times 10^{-33}$ esu		(cgs)
		$= 3.20662 \times 10^{-53}$ $\mathrm{C^3m^3/J^2}$		[SI, definition (30)]
1 a.u. of third-order polarizability, γ		$= 5.03717 \times 10^{-40}$ esu		(cgs)
		$= 6.23597 \times 10^{-65}$ $\mathrm{C^4m^4/J^3}$		[SI, definition (30)]

[a]The dipole moment is commonly indicated in Debye units: $1\mathrm{D} = 10^{-18}$ esu $= 10^{-18}$ statC cm.

[b]Convention in which ε_0 is absorbed into the (hyper)polarizabilities.

[c]Convention in which ε_0 is written explicitly in the power series for μ.

molecular NLO parameters are used in the literature. One of the SI definitions is identical to the cgs definition (1),[15]

$$\mu_i = \mu_i^0 + \alpha_{ij}E_j + \beta_{ijk}E_jE_k + \gamma_{ijkl}E_jE_kE_l + \cdots \qquad (30)$$

while in the other SI definition, an extra factor ε_0 is included:

$$\mu_i = \mu_i^0 + \varepsilon_0\left(\alpha_{ij}E_j + \beta_{ijk}E_jE_k + \gamma_{ijkl}E_jE_kE_l + \cdots\right) \qquad (31)$$

Obviously, both definitions lead to different SI units for the molecular NLO parameters. Within definition (30), the units of μ, α, β, and γ are (C m), ($\mathrm{C\,m^2/V}$), ($\mathrm{C\,m^3/V^2}$), and ($\mathrm{C\,m^4/V^3}$), respectively. Equivalently, these units are often written (through the relation CV = J) as (C m), ($\mathrm{C^2m^2/J}$), ($\mathrm{C^3m^3/J^2}$), and ($\mathrm{C^4m^4/J^3}$), respectively. When defined by (31), μ, α, β, and γ are expressed in SI units of (C m), ($\mathrm{m^3}$), ($\mathrm{m^4/V}$), and ($\mathrm{m^5/V^2}$), respectively.

In the cgs system, this ambiguity does not occur, and the units of the molecular parameters μ, α, β, and γ, defined by (1), are (statC cm), ($\mathrm{cm^3}$), ($\mathrm{cm^4/statV}$), and ($\mathrm{cm^5/statV^2}$), respectively. These cgs units of α, β, and γ are generally referred to as "esu", and the dipole moment is usually indicated in Debye units ($1\ D = 10^{-18}$ esu $= 10^{-18}$ statC cm). Based on typical sizes and intramolecular fields, a crude but very general argument has been formulated by Chemla and Zyss (see Ref. [5], p. 63) to estimate the order of magnitude of the molecular hyperpolarizabilities of small molecules, yielding $\alpha = 10^{-23}$ $\mathrm{cm^3}$ (cgs), $\beta = \sim 10^{-30}$ esu, and $\gamma = \sim 10^{-37}$ esu. Apart from the SI and Gaussian or cgs units, "atomic units" are also often encountered in the literature, especially in theoretical work. In Table XIV, conversion factors for these units are also listed.

[15]The SI definition whithout the ε_0 factor is usually combined with the Taylor series expression [see Eq. (32)] rather than the power series expression shown here.

Conventions

While it is straightforward to account for different unit systems and the inclusion or otherwise of the ε_0 factor in the polarizabilities in the SI system, several other variations in the definitions of NLO parameters severely complicate the comparison of results reported by different authors.

A well-known ambiguity is that instead of the power series definition (1), the hyperpolarizabilities are often—mainly in theoret-

ical work—defined by a Taylor series,

$$\mu_i = \mu_i^0 + \alpha_{ij}E_j + \frac{1}{2!}\beta_{ijk}E_jE_k + \frac{1}{3!}\gamma_{ijkl}E_jE_kE_l + \cdots \quad (32)$$

which, regardless of the unit system used, results in a factor of 2 and 6 difference in the values of β and γ, respectively.

Not widely appreciated, however, is that many more variations in the definitions of the hyperpolarizabilities occur when specific frequency components are considered, as is the case in any experimental NLO study. This is exemplified by the phenomenological description of SHG given on p. 129, based on (1), which leads to a second-harmonic component of the induced dipole moment of $\frac{1}{2}\beta_{izz}E_0^2\cos 2\omega t$ and therefore is in disagreement with the frequency-dependent definition (4), according to which $\beta(-2\omega;\omega,\omega)$ would produce a twice larger second-harmonic component.[16] This "degeneracy factor," in this case $\frac{1}{2}$, depends on the frequency arguments of β or γ and is thus different for each type of NLO process [90, 428]. The possibility of including these degeneracy factors into the definition (4) of the frequency-dependent hyperpolarizabilities or not [58], combined with the choice between Taylor and power series-based definitions, has led to many different conventions. The various conventions used in the literature are reviewed in Ref. [58]. In this work the so-called B* convention [58] will be used, unless otherwise indicated. This convention is widely used in EFISHG (see Section 2.3) experiments, and hence also in other experimental work which uses calibration standards derived from EFISHG measurements. In particular, the reference value for β of chloroform [152], widely used in HRS literature, and also the frequently used β value of *p*NA in MeOH [39] are both defined in the B* convention. The relation with two other conventions employed in the literature—the Taylor series convention T and the purely phenomenological convention B—is given by $\beta^{\mathrm{T}} = 2\beta^{\mathrm{B}} = 6\beta^{\mathrm{B}^*}$ [58].

Unit Conversions

Conversion factors from cgs to SI units are given by [303, 427]

$$E_{\mathrm{SI}} = 3 \times 10^4 E_{\mathrm{cgs}}$$

$$\chi_{\mathrm{SI}}^{(j)} = \frac{4\pi}{3^{j-1}} \times 10^{-4(j-1)}\chi_{\mathrm{cgs}}^{(j)}$$

$$\mu_{\mathrm{SI}} = \frac{1}{3} \times 10^{-11}\mu_{\mathrm{cgs}}$$

*j*th order polarizability:

$$\mathrm{value}_{\mathrm{SI}} = \frac{1}{3^{j+1}} \times 10^{-(4j+11)}\mathrm{value}_{\mathrm{cgs}} \text{ [for definition (30)]}$$

$$\mathrm{value}_{\mathrm{SI}} = \frac{4\pi}{3^{j-1}} \times 10^{-(4j+2)}\mathrm{value}_{\mathrm{cgs}} \text{ [for definition (31)]}$$

where the boldface **3** stands for 2.99792458, the speed of light in units of 10^8 m/s (see also Table XIV).

In theoretical work, atomic units (a.u.) are also often employed. Conversion factors to SI and cgs units are given by [303, 427].

[16] Closely related to this is yet another source of confusion, namely in the definition of the complex electric field itself, which may [5] or may not [93] include a factor of $\frac{1}{2}$, leading to numerous factors of two in the equations related to NLO [428].

REFERENCES

1. (*a*) T. H. Maiman, *Nature (London)* 187, 493 (1960).
   (*b*) A. Javan, W. R. Bannett, and D. R. Herriott, *Phys. Rev. Lett.* 6, 106 (1961).
   (*c*) R. J. Collins, *Phys. Rev. Lett.* 5, 303 (1960).
2. M. J. Weber, Ed., "Handbook of Laser Science and Technology," Vol. III, Part 1, and Vol. IV, Part 2. CRC Press, Boca Raton, FL, 1986–1987.
3. R. C. Alferness, in "Guided-Wave Opto-Electronics." (T. Tamir, Ed.), Springer-Verlag, Berlin, 1988. S. K. Korotky and R. C. Alferness, in "Integrated Optical Circuits and Components." (L. D. Hutcheson, Ed.), Marcel Dekker, New York, 1987.
4. F. J. Leonberger and J. F. Donnelly, in "Guided-Wave Opto-Electronics." (T. Tamir, Ed.), Springer-Verlag, Berlin, 1988.
5. D. S. Chemla and J. Zyss, Eds., "Nonlinear Optical Properties of Organic Molecules and Crystals." Vol. 1, "Quantum Electronics—Principles and Applications." (Y.-H. Pao, P. F. Liao, and P. Kelley, Eds.). Academic Press, Orlando, FL, 1987.
6. Y. R. Shen, "The Principles of Nonlinear Optics." Wiley, New York, 1984.
7. M. Schubert and B. Wilhelmi, "Nonlinear Optics and Quantum Electronics." Wiley, New York, 1986.
8. P. N. Prasad and D. J. Williams, "Introduction to Nonlinear Optical Effects in Molecules and Polymers." Wiley, New York, 1991.
9. R. W. Boyd, "Nonlinear Optics." Academic Press, New York, 1992.
10. H. S. Nalwa and S. Miyata, Eds. "Nonlinear Optics of Organic Molecules and Polymers." CRC Press, Boca Raton, FL, 1997.
11. P. A. Franken, A. E. Hill, C. W. Peters, and G. Weinreich, *Phys. Rev. Lett.* 7, 118 (1961).
12. G. I. Stegeman, R. Zanoni, and C. T. Seaton, *Mater. Res. Soc. Symp. Proc.* 109, 53 (1988).
13. G. I. Stegeman, in "Organic Materials for Non-Linear Optics II." R. A. Hann and D. Bloor, (Eds.), pp. 311–323. Royal Society of Chemistry, Cambridge, 1991.
14. D. A. Kleinman, *Phys. Rev.* 126, 1977 (1962).
15. R. Silbey, in "Nonlinear Optical Properties of Organic Molecules and Crystals." D. S. Chemla and J. Zyss, (Eds.), Vol. 1, pp. 3–20. Academic Press, Orlando, FL, 1987.
16. C. J. F. Böttcher, "Theory of Electric Polarization." Vol. I, "Dielectrics in Static Fields." Elsevier, Amsterdam, 1973.
17. L. Onsager, *J. Am. Chem. Soc.* 58, 1486 (1936).
18. M. Szablewski, P. R. Thomas, A. Thornton, D. Bloor, G. H. Cross, J. M. Cole, J. A. K. Howard, M. Malagoli, F. Meyers, J.-L. Brédas, W. Wenseleers, and E. Goovaerts, *J. Am. Chem. Soc.* 119, 3144 (1997).
19. (*a*) G. J. Ashwell, G. Jefferies, D. G. Hamilton, D. E. Lynch, M. P. S. Roberts, G. S. Bahra, and C. R. Brown, *Nature* 375, 385 (1995).
    (*b*) J. L. Brédas and F. Meyers, *Nature (London)* 375, 362 (1995).
20. J. P. Bourdin, P. X. Nguyen, G. Rivoire, and J. M. Nunzi, *Mol. Cryst. Liq. Cryst. Sci. Technol. Sect. B Nonlinear Opt.* 7, 1 (1994).
21. K. C. Rustagi and J. Ducuing, *Opt. Commun.* 10, 258 (1974).
22. M.-T. Zhao, B. P. Singh, and P. N. Prasad, *J. Chem. Phys.* 89, 5535 (1988).
23. M.-T. Zhao, M. Samoc, B. P. Singh, and P. N. Prasad, *J. Phys. Chem.* 93, 7916 (1989).
24. I. D. W. Samuel, I. Ledoux, Ch. Dhenaut, J. Zyss, H. H. Fox, R. R. Schrock, and R. J. Silbey, *Science (Washington, DC)* 265, 1070 (1994).
25. I. Ledoux, I. D. W. Samuel, J. Zyss, S. N. Yaliraki, F. J. Schattenmann, R. R. Schrock, and R. J. Silbey, *Chem. Phys.* 245, 1 (1999).
26. P. N. Prasad, E. Perrin, and M. Samoc, *J. Chem. Phys.* 91, 2360 (1989).
27. H. Thienpont, G. L. J. A. Rikken, E. W. Meijer, W. ten Hoeve, and H. Wynberg, Phys. *Rev. Lett.* 65, 2141 (1990).
28. Y. Verbandt, H. Thienpont, I. Veretennicoff, and G. L. J. A. Rikken, *Phys. Rev. B* 48, 8651 (1993).

29. Y. Verbandt, H. Thienpont, I. Veretennicoff, and P. Geerlings, *Chem. Phys. Lett.* 251, 7 (1996).
30. Y. Verbandt, H. Thienpont, I. Veretennicoff, P. Geerlings, and G. L. J. A. Rikken, *Chem. Phys. Lett.* 270, 471 (1997).
31. N. Finlayson, W. C. Banyai, C. T. Seaton, G. I. Stegeman, M. O'Neill, T. J. Cullen, and C. N. Ironside, *J. Opt. Soc. Am. B* 6, 675 (1989).
32. V. Mizrahi, K. W. DeLong, G. I. Stegeman, M. A. Saifi, and M. J. Andrejco, *Opt. Lett.* 14, 1140 (1989).
33. S. R. Marder, J. W. Perry, G. Bourhill, Ch. B. Gorman, B. G. Tiemann, and K. Mansour, *Science (Washington, DC)* 261, 186 (1993).
34. S. R. Marder, L.-T. Cheng, B. G. Tiemann, A. C. Friedli, M. Blanchard-Desce, J. W. Perry, and J. Skindhøj, *Science (Washington, DC)* 263, 511 (1994).
35. M. Ahlheim, M. Barzoukas, P. V. Bedworth, M. Blanchard-Desce, A. Fort, Z.-Y. Hu, S. R. Marder, J. W. Perry, C. Runser, M. Stähelin, and B. Zysset, *Science (Washington, DC)* 271, 335 (1996).
36. M. Blanchard-Desce, V. Alain, P. V. Bedworth, S. R. Marder, A. Fort, C. Runser, M. Barzoukas, S. Lebus, and R. Wortmann, *Chem.—Eur. J.* 3, 1091 (1997).
37. S. R. Marder, W. E. Torruellas, M. Blanchard-Desce, V. Ricci, G. I. Stegeman, S. Gilmour, J.-L. Brédas, J. Li, G. U. Bublitz, and S. G. Boxer, *Science (Washington, DC)* 276, 1233 (1997).
38. M. Blanchard-Desce, J.-M. Lehn, M. Barzoukas, I. Ledoux, and J. Zyss, *Chem. Phys.* 181, 281 (1994).
39. J. L. Oudar and D. S. Chemla, *J. Chem. Phys.* 66, 2664 (1977).
40. W. Wenseleers, A. W. Gerbrandij, E. Goovaerts, M. H. Garcia, M. P. Robalo, P. J. Mendes, J. C. Rodrigues, and A. R. Dias, *J. Mater. Chem.* 8, 925 (1998).
41. J. Zyss, *Nonlinear Opt.* 1, 3 (1991).
42. J. Zyss, *J. Chem. Phys.* 98, 6583 (1993).
43. I. Ledoux, J. Zyss, J. S. Siegel, J. Brienne, and J. M. Lehn, *Chem. Phys. Lett.* 172, 440 (1990).
44. J. Zyss, T. C. Van, Ch. Dhenaut, and I. Ledoux, *Chem. Phys.* 177, 281 (1993).
45. B. del Rey, U. Keller, T. Torres, G. Rojo, F. Agulló-López, S. Nonell, C. Martí, S. Brasselet, I. Ledoux, and J. Zyss, *J. Am. Chem. Soc.* 120, 12808 (1998). Correction of earlier values from A. Sastre, T. Torres, M. A. Díaz-Garcí, F. Agulló-López, C. Dhenaut, S. Brasselet, I. Ledoux, and J. Zyss. *J. Am. Chem. Soc.* 118, 2746 (1996).
46. J. Zyss, D. S. Chemla, and J. F. Nicoud, *J. Chem. Phys.* 74, 4800 (1981).
47. D. R. Greve, S. B. Schougaard, T. Geisler, J. C. Petersen, and T. Bjørnhom, *Adv. Mater.* 9, 1113 (1997). F. Cérioux, H. Maillotte, P. Audebert, and J. Zyss, *Chem. Commun.* 2083 (1999).
48. A. M. McDonagh, M. G. Humphrey, M. Samoc, B. Luther-Davies, S. Houbrechts, T. Wada, H. Sasabe, and A. Persoons, *J. Am. Chem. Soc.* 121, 1405 (1999).
49. M. J. S. Dewar, E. G. Zoebisch, E. F. Healy, and J. J. P. Stewart. *J. Am. Chem. Soc.* 107, 3902 (1985).
50. J. J. P. Stewart, *J. Comput. Chem.* 10, 209 (1989).
51. J. J. P. Stewart, *J. Comput. Chem.* 10, 221 (1989).
52. W. Thiel and A. A. Voityuk, *J. Phys. Chem.* 100, 616 (1996).
53. J. J. P. Stewart, MOPAC, Version 6 (public domain).
54. M. J. S. Dewar and J. J. P. Stewart, *Chem. Phys. Lett.* 111, 416 (1984).
55. H. A. Kurtz, J. J. P. Stewart, and K. M. Dieter, *J. Comput. Chem.* 11, 82 (1990).
56. J. A. Armstrong, N. Bloembergen, J. Ducuing, and P. S. Pershan, *Phys. Rev.* 127, 1918 (1962).
57. B. J. Orr and J. F. Ward, *Mol. Phys.* 20, 513 (1971).
58. A. Willetts, J. E. Rice, D. M. Burland, and D. P. Shelton, *J. Chem. Phys.* 97, 7590 (1992).
59. J.-L. Brédas, C. Adant, P. Tackx, A. Persoons, and B. M. Pierce, *Chem. Rev.* 94, 243 (1994).
60. J. F. Ward and G. H. C. New, *Phys. Rev.* 185, 57 (1969).
61. S. J. Lalama and A. F. Garito, *Phys. Rev. A* 20, 1179 (1979).
62. D. Beljonne, J.-L. Brédas, M. Cha, W. E. Torruellas, G. I. Stegeman, J. W. Hofstraat, W. H. G. Horsthuis, and G. R. Mohlmann, *J. Chem. Phys.* 103, 7834 (1995).
63. C. C. Teng and A. F. Garito, *Phys. Rev. Lett.* 50, 350 (1983).
64. C. C. Teng and A. F. Garito, *Phys. Rev. B* 28, 6766 (1983).
65. Y. Luo, H. Ågren, O. Vahtras, and P. Jørgensen, *Chem. Phys. Lett.* 207, 190 (1993).
66. P. Zuliani, M. Del Zoppo, C. Castiglioni, G. Zerbi, C. Andraud, T. Brotin, and A. Collet, *J. Phys. Chem.* 99, 16242 (1995).
67. C. Castiglioni, M. Del Zoppo, P. Zuliani, and G. Zerbi, *Synth. Met.* 74, 171 (1995).
68. M. Del Zoppo, C. Castiglioni, P. Zuliani, and G. Zerbi, *Adv. Mater.* 8, 345 (1996).
69. A. Gussoni, G. Zerbi, J. J. G. S. van Es, H. A. M. Biemans, and E. W. Meijer. *Synth. Met.* 80, 201 (1996).
70. C. Fiorini, F. Charra, and J.-M. Nunzi, *J. Opt. Soc. Am. B* 11, 2347 (1994).
71. B. Paci, C. Schmidt, C. Fiorini, J.-M. Nunzi, C. Arbez-Gendre, and C. G. Screttas, *J. Chem. Phys.* 111, 7486 (1999).
72. T. Watanabe, H. S. Nalwa, and S. Miyata, in "Nonlinear Optics of Organic Molecules and Polymers." (H. S. Nalwa and S. Miyata, Eds.), pp. 57–88. CRC Press, Boca Raton, FL, 1997.
73. F. W. Vance, R. D. Williams, and J. T. Hupp, *Int. Rev. Phys. Chem.* 17, 307 (1998).
74. S. K. Kurtz and T. T. Perry, *J. Appl. Phys.* 39, 3798 (1968).
75. N. Karl, *Inst. Phys. Conf. Ser.* 103, 107 (1989).
76. M. S. Paley, J. M. Harris, H. Looser, J. C. Baumert, G. C. Borklund, D. Jundt, and R. J. Twieg, *J. Org. Chem.* 54, 3774 (1989).
77. C. J. F. Böttcher and P. Bordewijk, "Theory of Electric Polarization." Vol. II, "Dielectrics in Time-Dependent Fields." Elsevier, Amsterdam, 1978.
78. Ch. Bosshard, G. Knöpfle, P. Prêtre, and P. Günter, *J. Appl. Phys.* 71, 1594 (1992).
79. G. Mayer, *C. R. Acad. Sci. (Paris) Sér. B Sci. Phys.* 267B, 54 (1968).
80. C. K. Miller and J. F. Ward, *Phys. Rev. A* 16, 1179 (1977).
81. J. F. Ward and C. K. Miller, *Phys. Rev. A* 19, 826 (1979).
82. R. W. Terhune, P. D. Maker, and C. M. Savage, *Phys. Rev. Lett.* 8, 404 (1962).
83. P. D. Maker and R. W. Terhune, *Phys. Rev.* 137, 801 (1965).
84. J. E. Bjorkholm and A. E. Siegman, *Phys. Rev.* 154, 851 (1967).
85. S. Kielich, *Chem. Phys. Lett.* 2, 569 (1968).
86. S. Kielich, *IEEE J. Quantum Electron.* QE-5, 562 (1969).
87. G. Hauchecorne, F. Kerhervé, and G. Mayer, *J. Phys. (Paris)* 32, 47 (1971).
88. R. S. Finn and J. F. Ward, *Phys. Rev. Lett.* 26, 285 (1971).
89. R. S. Finn and J. F. Ward, *J. Chem. Phys.* 60, 454 (1974).
90. B. F. Levine and C. G. Bethea, *J. Chem. Phys.* 63, 2666 (1975).
91. B. F. Levine and C. G. Bethea, *Appl. Phys. Lett.* 24, 445 (1974).
92. B. F. Levine and C. G. Bethea, *J. Chem. Phys.* 60, 3856 (1974); 61, 3493 (1974) (erratum).
93. J. L. Oudar, *J. Chem. Phys.* 67, 446 (1977).
94. K. D. Singer and A. F. Garito, *J. Chem. Phys.* 75, 3572 (1981).
95. M. H. Wu, K. Clays, and A. Persoons, *Rev. Sci. Instrum.* 67, 3005 (1996).
96. I. Ledoux, J. Zyss, A. Jutand, and C. Amatore, *Chem. Phys.* 150, 117 (1991).
97. R. C. Miller and W. A. Nordland, *Phys. Rev. B* 2, 4896 (1970).
98. F. Meyers, J.-L. Brédas and J. Zyss, *J. Am. Chem. Soc.* 114, 2914 (1992).
99. R. Wortmann, P. Krämer, C. Glania, S. Lebus, and N. Detzer, *Chem. Phys.* 173, 99 (1993).
100. J. J. Wolff, D. Längle, D. Hillenbrand, R. Wortmann, R. Matschiner, C. Glania, and P. Krämer, *Adv. Mater.* 9, 138 (1997).
101. L. Yin-Yuan, *Acta Phys. Sin.* 20, 164 (1964).
102. S. Kielich, *Bull. Acad. Pol. Sci.* 12, 53 (1964).
103. R. Bersohn, *J. Am. Chem. Soc.* 86, 3505 (1964).
104. R. W. Terhune, P. D. Maker, and C. M. Savage, *Phys. Rev. Lett.* 14, 681 (1965).
105. R. Bersohn, Y.-H. Pao, and H. L. Frisch, *J. Chem. Phys.* 45, 3184 (1966).

106. D. L. Weinberg, *J. Chem. Phys.* 47, 1307 (1967).
107. P. D. Maker, *Phys. Rev. A* 1, 923 (1970).
108. S. Kielich, J. R. Lalanne, and F. B. Martin, *Phys. Rev. Lett.* 26, 1295 (1971).
109. J. P. Neddersen, S. A. Mounter, J. M. Bostick, and C. K. Johnson, *J. Chem. Phys.* 90, 4719 (1989).
110. J. Zyss, Ch. Dhenaut, T. C. Van, and I. Ledoux, *Chem. Phys. Lett.* 206, 409 (1993).
111. K. Clays and A. Persoons, *Phys. Rev. Lett.* 66, 2980 (1991).
112. K. Clays and A. Persoons, *Rev. Sci. Instrum.* 63, 3285 (1992).
113. Rayleigh (John William Strutt) 3rd Baron, *Phil. Mag.* 41, 107, 274 (1871); 41, 447 (1871); 12, 81 (1881).
114. G. J. T. Heesink, A. G. T. Ruiter, N. F. van Hulst, and B. Bölger, *Phys. Rev. Lett.* 71, 999 (1993).
115. M. C. Flipse, R. de Jonge, R. H. Woudenberg, A. W. Marsman, C. A. van Walree, and L. W. Jenneskens, *Chem. Phys. Lett.* 245, 297 (1995).
116. E. Schmälzlin, K. Meerholz, S. Stadler, Ch. Bräuchle, H. Patzelt, and D. Oesterhelt, *Chem. Phys. Lett.* 280, 551 (1997).
117. M. A. Pauley and C. H. Wang, *Chem. Phys. Lett.* 280, 544 (1997).
118. I. D. Morrison, R. G. Denning, W. M. Laidlaw, and M. A. Stammers, *Rev. Sci. Instrum.* 67, 1445 (1996).
119. S. Stadler, F. Feiner, Ch. Bräuchle, S. Brandl, and R. Gompper, *Chem. Phys. Lett.* 245, 292 (1995).
120. S. Stadler, R. Dietrich, G. Bourhill, and Ch. Bräuchle, *Opt. Lett.* 21, 251 (1996).
121. K. Clays and A. Persoons, *Rev. Sci. Instrum.* 65, 2190 (1994).
122. T. Verbiest, M. Kauranen, and A. Persoons, *J. Chem. Phys.* 101, 1745 (1994).
123. S. Stadler, R. Dietrich, G. Bourhill, Ch. Bräuchle, A. Pawlik, and W. Grahn, *Chem. Phys. Lett.* 247, 271 (1995).
124. S. Stadler, G. Bourhill, and Ch. Bräuchle, *J. Phys. Chem.* 100, 6927 (1996).
125. O. F. J. Noordman and N. F. van Hulst, *Chem. Phys. Lett.* 253, 145 (1996).
126. N. W. Song, T.-I. Kang, S. C. Jeoung, S.-J. Jeon, B. R. Cho, and D. Kim, *Chem. Phys. Lett.* 261, 307 (1996).
127. S. F. Hubbard, R. G. Petschek, and K. D. Singer, *Opt. Lett.* 21, 1774 (1996).
128. G. Olbrechts, R. Strobbe, K. Clays, and A. Persoons, *Rev. Sci. Instrum.* 69, 2233 (1998).
129. A. R. Dias, M. H. Garcia, P. Mendes, M. F. M. Piedade, M. T. Duarte, M. J. Calhorda, C. Mealli, W. Wenseleers, A. W. Gerbrandij, and E. Goovaerts, *J. Organomet. Chem.* 553, 115 (1998).
130. M. A. Pauley and C. H. Wang, *Rev. Sci. Instrum.* 70, 1277 (1999).
131. G. Olbrechts, K. Wostyn, K. Clays, and A. Persoons, *Opt. Lett.* 24, 403 (1999).
132. T. Verbiest, E. Hendrickx, A. Persoons, and K. Clays, *Proc. SPIE* 1775, 206 (1992).
133. M. A. Pauley, C. H. Wang, and A. K. Y. Jen, *J. Chem. Phys.* 102, 6400 (1995).
134. G. Liberts and V. Zauls, *Lith. J. Phys.* 35, 591 (1995).
135. K. Clays, G. Olbrechts, T. Munters, A. Persoons, O.-K. Kim, and C. Ling-Siu, *Chem. Phys. Lett.* 293, 337 (1998).
136. M. C. Flipse, R. de Jonge, R. H. Woudenberg, A. W. Marsman, C. van Walree, and L. W. Jenneskens, *OSA Techn. Dig. Ser.* 21, 374 (1995).
137. K. Clays, E. Hendrickx, M. Triest, T. Verbiest, A. Persoons, C. Dehu, and J.-L. Brédas, *Science (Washington, DC)* 262, 1419 (1993).
138. E. Hendrickx, K. Clays, A. Persoons, C. Dehu, and J. L. Brédas, *J. Am. Chem. Soc.* 117, 3547 (1995).
139. W. M. Laidlaw, R. G. Denning, T. Verbiest, E. Chauchard, and A. Persoons, *Nature (London)* 363, 58 (1993).
140. C. Dhenaut, I. Ledoux, I. D. W. Samuel, J. Zyss, M. Bourgault, and H. Le Bozec, *Nature (London)* 374, 339 (1995).
141. W. M. Laidlaw, R. G. Denning, T. Verbiest, E. Chauchard, and A. Persoons, *Proc. SPIE* 2143, 14 (1994).
142. T. Le Bouder, P. Massiot, and H. Le Bozec, *Tetrahedron Lett.* 39, 6869 (1998).
143. C. H. Wang, M. A. Pauley, J. N. Woodford, and A. K. Y. Jen, *Polym. Prepr.* 39, 1132 (1998).
144. S. H. Kang, Y.-M. Jeon, K. Kim, S. Houbrechts, E. Hendrickx, and A. Persoons, *J. Chem. Soc. Chem. Commun.* 635 (1995).
145. S. M. LeCours, H.-W. Guan, S. G. DiMagno, C. H. Wang, and M. J. Therien, *J. Am. Chem. Soc.* 118, 1497 (1996).
146. D. L. Andrews, *Adv. Chem. Phys.* 85, 545 (1993).
147. W. M. McClain, *J. Chem. Phys.* 57, 2264 (1972).
148. K. Clays, A. Persoons, and L. De Mayer, in "Modern Nonlinear Optics, Part 3." M. Evans and S. Kielich, (Eds.), Advances in Chemical Physics Series, Vol. LXXXV. Wiley, New York, 1994.
149. J. J. Cyvin, J. E. Rauch, and J. C. Decius, *J. Chem. Phys.* 43, 4083 (1965).
150. T. Verbiest, K. Clays, A. Persoons, F. Meyers, and J. L. Brédas, *Opt. Lett.* 18, 525 (1993).
151. L. D. Landau and E. M. Lifshitz, "Electrodynamics of Continuous Media." Addison-Wesley, Reading, MA, 1960.
152. F. Kajzar, I. Ledoux, and J. Zyss, *Phys. Rev. A* 36, 2210 (1987).
153. A. Yariv and P. Yeh, "Optical Waves in Crystals." Wiley, New York, 1984.
154. P. Kaatz and D. P. Shelton, *Rev. Sci. Instrum.* 67, 1438 (1996).
155. P. Kaatz and D. P. Shelton, *Opt. Commun.* 157, 177 (1998).
156. W. Wenseleers, Ph.D. Thesis, University of Antwerp (UIA), Antwerp, Belgium, 1999, also *Dissertation Abstracts Internat.* B60, 4038 (2000).
157. J. Zyss, S. Brasselet, V. R. Thalladi, and G. R. Desiraju, *J. Chem. Phys.* 109, 658 (1998).
158. T. W. Chui and K. Y. Wong, *J. Chem. Phys.* 109, 1391 (1998).
159. M. Kauranen, T. Verbiest, C. Boutton, M. N. Teerenstra, K. Clays, A. J. Schouten, R. J. M. Nolte, and A. Persoons, *Science (Washington, DC)* 270, 966 (1995).
160. G. Olbrechts, E. J. H. Put, K. Clays, A. Persoons, and N. Matsuda, *Chem. Phys. Lett.* 253, 135 (1996).
161. U. Behrens, H. Brussaard, U. Hagenau, J. Heck, E. Hendrickx, J. Kornich, J. G. M. van der Linden, A. Persoons, A. L. Spek, N. Veldman, B. Voss, and H. Wong, *Chem.—Eur. J.* 2, 98 (1996).
162. S. Houbrechts, K. Clays, A. Persoons, Z. Pikramenou, and J.-M. Lehn, *Chem. Phys. Lett.* 258, 485 (1996).
163. K. Clays, G. Olbrechts, and A. Persoons, *Chem. Phys. Lett.* 288, 171 (1998).
164. P. Kaatz and D. P. Shelton, *Mol. Phys.* 88, 683 (1996).
165. K. Clays, G. Olbrechts, T. Munters, and A. Persoons, *Polym. Prepr.* 39, 1131 (1998).
166. G. Olbrechts, K. Wostyn, K. Clays, A. Persoons, S. H. Kang, and K. Kim, *Chem. Phys. Lett.* 308, 173 (1999).
167. K. Clays, J. Jannes, Y. Engelborghs, and A. Persoons, *J. Phys. E: Sci. Instr.* 22, 297 (1989).
168. B. R. Cho, S. K. Lee, K. A. Kim, K. N. Son, T. I. Kang, and S.-J. Jeon, *Tetrahedron Lett.* 39, 9205 (1998). Note: In this article the reduction to static β values is performed for octupolar compounds in the standard two-level picture, which is questionable.
169. T. Renouard, H. Le Bozec, S. Brasselet, I. Ledoux, and J. Zyss, *Chem. Commun.* 871 (1999).
170. D. J. Williams, *Angew. Chem. Int. Ed. Engl.* 23, 690 (1984).
171. J. Zyss and J.-F. Nicoud, *Curr. Opin. Solid State Mater. Sci.* 1, 533 (1996).
172. M. G. Hutchings, P. F. Gordon, and J. O. Morley, *Inst. Phys. Conf. Ser.* 103, 97 (1989).
173. M. S. Wong, Ch. Bosshard, F. Pan, and P. Günter, *Adv. Mater.* 8, 677–680 (1996).
174. H. S. Nalwa, T. Watanabe, and S. Miyata, in "Nonlinear Optics of Organic Molecules and Polymers," (H. S. Nalwa, and S. Miyata, Eds.), pp. 89–350. CRC Press, Boca Raton, FL, 1997.
175. R. N. De Martino, E. W. Choe, G. Khanarian, D. Haas, T. Leslie, G. Nelson, J. Stamatoff, D. Stutz, C. C. Teng, and H. Yoon, in

"Nonlinear Optical and Electroactive Polymers." P. N. Prasad and D. R. Ulrich, (Eds.), pp. 169–187. Plenum, New York, 1988.
176. L.-T. Cheng, W. Tam, S. H. Stevenson, G. R. Meredith, G. Rikken, and S. R. Marder, *J. Phys. Chem.* 95, 10631 (1991).
177. L.-T. Cheng, W. Tam, S. R. Marder, A. E. Stiegman, G. Rikken, and C. W. Sprangler, *J. Phys. Chem.* 95, 10643 (1991).
178. A. Dulcic, *Chem. Phys.* 37, 57 (1979).
179. J. O. Morley, V. J. Docherty, and D. Pugh, *J. Chem. Soc. Perkin. Trans. 2* 1351 (1987).
180. R. A. Huijts and G. L. J. Hesselink, *Chem. Phys. Lett.* 156, 209 (1989).
181. M. Barzoukas, M. Blanchard-Desce, D. Josse, and J.-M. Lehn, *Chem. Phys.* 133, 323 (1989).
182. H. Ikeda, Y. Kabawe, T. Sakai, and K. Kawasaki, *Chem. Phys. Lett.* 157, 576 (1989).
183. C. Dehu, F. Meyers, E. Hendrickx, K. Clays, A. Persoons, S. R. Marder, and J.-L. Bredas, *J. Am. Chem. Soc.* 117, 10127 (1995).
184. A. Fort, M. Barzoukas, J. Muller, V. Alain, and M. Blanchard-Desce, *J. Lumin.* 72–74, 494 (1997).
185. F. Meyers, S. R. Marder, B. M. Pierce, and J.-L. Brédas, *Chem. Phys. Lett.* 228, 171 (1994).
186. S. R. Marder, Ch. B. Gorman, F. Meyers, J. W. Perry, G. Bourhill, J.-L. Brédas, and B. M. Pierce, *Science (Washington, DC)* 265, 632 (1994).
187. J. L. Oudar and D. S. Chemla, *Opt. Commun.* 13, 164 (1975).
188. S. R. Marder, D. N. Beratan, and L.-T. Cheng, *Science (Washington, DC)* 252, 103 (1991).
189. J.-L. Brédas, *Science (Washington, DC)* 263, 487 (1994).
190. G. Bourhill, J.-L. Brédas, L.-T. Cheng, S. R. Marder, F. Meyers, J. W. Perry, and B. G. Tiemann, *J. Am. Chem. Soc.* 116, 2619 (1994).
191. D. Lu, G. Chen, J. W. Perry, and W. A. Goddard, III, *J. Am. Chem. Soc.* 116, 10679 (1994).
192. F. Meyers, S. R. Marder, B. M. Pierce, and J.-L. Brédas, *J. Am. Chem. Soc.* 116, 10703 (1994).
193. M. Barzoukas, A. Fort, and M. Blanchard-Desce, *New J. Chem.* 21, 309 (1997).
194. M. Blanchard-Desce and M. Barzoukas, *J. Opt. Soc. Am. B* 15, 302 (1998).
195. K. Mohanalingam, P. Chandra-Ray, and P. K. Das, *Synth. Metals* 82, 47 (1996).
196. B. L. Davydov, L. D. Derkacheva, V. V. Dunina, M. E. Zhabotinskii, V. F. Zolin, L. G. Koreneva, and M. A. Samokhina, *JETP Lett.* 12, 16 (1970).
197. B. F. Levine, *J. Chem. Phys.* 63, 115 (1975).
198. B. F. Levine, *Chem. Phys. Lett.* 37, 516 (1976).
199. A. Dulcic and C. Sauteret, *J. Chem. Phys.* 69, 3453 (1978).
200. G. Pucetti, I. Ledoux, and J. Zyss, *Chem. Phys.* 160, 467 (1992).
201. R. Würtner, F. Effenberger, R. Wortmann, and P. Krämer, *Chem. Phys. Lett.* 173, 305 (1993).
202. A. Krämer, G. Pucetti, I. Ledoux, J. Zyss, and G. Soula, *Organometallics* 10, 3656 (1991); G. Mignani, A. Krämer, G. Pucetti, I. Ledoux, G. Soula, and J. Zyss, *Mol. Eng.* 1, 11 (1991).
203. G. Mignani, M. Barzoukas, J. Zyss, G. Soula, F. Balegroune, D. Grandjean, and D. Josse, *Organometallics* 10, 3660 (1991).
204. D. Hissink, H. J. Bolink, J. W. Eshuis, P. F. van Hutten, G. G. Malliaras, and G. Hadziiannou, *SPIE Proc.* 2025, 37 (1993).
205. Ch. Bosshard, G. Knöpfle, P. Prêtre, S. Follonier, C. Serbutoviez, and P. Günter, *Opt. Eng.* 34, 1951 (1995).
206. S. Kucharski, R. Janik, and P. Kaatz, *J. Mater. Chem.* 9, 395 (1999).
207. C. Serbutoviez, C. Bosshard, G. Knöpfle, P. Wyss, P. Prêtre, P. Günter, K. Schenk, E. Solari, and G. Chapuis, *Chem. Mater.* 7, 1198 (1995).
208. M. S. Wang, U. Meier, F. Pan, V. Gramlich, C. Bosshard, and P. Günter, *Adv. Mater.* 8, 416 (1996).
209. G. H. Cross, D. Healy, M. Szablewski, D. Bloor, M. Malagoli, T. Kogej, D. Beljonne, and J.-L. Brédas, *Chem. Phys. Lett.* 268, 36 (1997).
210. T. C. Kowalcyk, K. D. Singer, and P. A. Cahill, *Opt. Lett.* 20, 2273 (1995).
211. P. R. Thomas, Ph.D. Thesis, University of Durham, United Kingdom, 1998.
212. J. L. Brédas and coworkers, unpublished results. See Refs. [18] and [209] for the results of a previous, less accurate, SOS calculation.
213. W. Wenseleers, E. Goovaerts, P. R. Thomas, M. Szablewski, and G. H. Cross, *Dissertation Abstracts Internat.* B60, 4038 (2000).
214. K. I. Wong, A. K.-Y. Jen, V. P. Rao, K. J. Drost, and R. Mininni, *Mater. Res. Symp. Proc.* 59, 247 (1992).
215. Y.-K. Wang, C.-F. Shu, E. M. Breitung, and R. J. McMahon, *J. Mater. Chem.* 9, 1449 (199).
216. I. Liakatas, M. S. Wong, C. Bosshard, M. Ehrensberger, and P. Günter, *Ferroelectrics* 202, 299 (1997).
217. G. Knöpfle, R. Schlesser, R. Ducret, and P. Günter, *Science (Washington, DC)* 245, 626 (1989).
218. Y. Kubo, T. Takaba, and S. Aramaki, *Chem. Lett.* 3, 255 (1997).
219. L. Groenendaal, M. J. Bruining, E. H. J. Hendrickx, A. Persoons, J. A. J. M. Vekemans, E. E. Havinga, and E. W. Meijer, *Chem. Mater.* 10, 226 (1998).
220. O.-K. Kim and J.-M. Lehn, *Chem. Phys. Lett.* 255, 147 (1996).
221. H. Nerenz, M. Meier, W. Grahn, A. Reisner, E. Schmälzlin, K. Meerholz, C. Bräuchle, and P. G. Jones, *J. Chem. Soc. Perkin Trans. 2* 437 (1998).
222. J. Zyss and I. Ledoux, *Chem. Rev.* 94, 77 (1994)
223. S. Brasselet and J. Zyss, *J. Opt. Soc. Am. B* 15, 257 (1998).
224. J. Zyss and S. Brasselet, *J. Nonlinear Opt. Phys. Mater.* 7, 397 (1998).
225. M. Joffre, D. Yaron, R. J. Silbey, and J. Zyss, *J. Chem. Phys.* 97, 5607 (1992).
226. Y. Luo, A. Cesar, and H. Ågren, *Chem. Phys. Lett.* 252, 389 (1996).
227. Y.-K. Lee, S.-J. Jeon, and M. Cho, *J. Am. Chem. Soc.* 120, 10921 (1998).
228. C. Dehu, V. Geskin, A. Persoons, and J.-L. Brédas, *Eur. J. Org. Chem.* 1267 (1998).
229. M. Cho, H.-S. Kim, and S.-J. Jeon, *J. Chem. Phys.* 108, 7114 (1998); 109, 11131 (1998) (erratum).
230. Y. Luo, P. Norman, and H. Ågren, *J. Am. Chem. Soc.* 120, 11188 (1998).
231. J.-M. Nunzi, F. Charra, C. Fiorini, and J. Zyss, *Chem. Phys. Lett.* 219, 349 (1994).
232. C. Fiorini, J.-M. Nunzi, F. Charra, I. D. W. Samuel, and J. Zyss, *J. Nonlinear Opt. Phys. Mater.* 5, 653 (1996).
233. W. P. Acker, D. H. Leach, and R. K. Chang, *Chem. Phys. Lett.* 155, 491 (1989).
234. T. Verbiest, K. Clays, C. Samyn, J. Wolff, D. Reinhoudt, and A. Persoons, *J. Am. Chem. Soc.* 116, 9320 (1994).
235. R. Wortmann, C. Glania, P. Krämer, R. Matschiner, J. J. Wolff, S. Kraft, B. Treptow, E. Barbu, D. Längle, and G. Görlitz, *Chem.—Eur. J.* 3, 1765 (1997).
236. P. C. Ray and P. K. Das, *Chem. Phys. Lett.* 244, 153 (1995).
237. S. Stadler, C. Bräuchle, S. Brandl, and R. Gompper, *Chem. Mater.* 8, 676 (1996).
238. V. R. Thalladi, S. Brasselet, D. Bläser, R. Boese, J. Zyss, A. Nangia, and G. R. Desiraju, *Chem. Commun.* 1841 (1997).
239. C. Lambert, W. Gaschler, E. Schmälzin, K. Meerholz, and C. Bräuchle, *J. Chem. Soc. Perkin Trans. 2* 577 (1999).
240. S. Stadler, C. Bräuchle, S. Brandl, and R. Gompper, *Chem. Mater.* 8, 414 (1996).
241. P. J. A. Kenis, O. F. J. Noordman, S. Houbrechts, G. J. van Hummel, S. Harkema, F. C. J. M. van Veggel, K. Clays, J. F. J. Engbersen, A. Persoons, N. F. van Hulst, and D. N. Reinhoudt, *J. Am. Chem. Soc.* 120, 7875 (1998).
242. C. Lambert, E. Schmälzin, K. Meerholz, and C. Bräuchle, *Chem.—Eur. J.* 4, 512 (1998).
243. M. Blanchard-Desce, J.-B. Baudin, O. Ruel, L. Jullien, S. Brasselet, and J. Zyss, *Opt. Mater.* 12, 333 (1999).
244. M. Blanchard-Desce, J.-B. Baudin, L. Jullien, R. Lorne, O. Ruel, S. Brasselet, and J. Zyss, *Opt. Mater.* 12, 333 (1999).

245. H. Yamamoto, T. Hosimi, T. Watanabe, and S. Miyata, *J. Chem. Soc. Jpn. Chem. Ind. Chem.* 7, 789 (1990).
246. W. Schuddeboom, B. Krijnen, J. W. Verhoeven, E. G. J. Staring, G. L. J. A. Rikken, and H. Oevering, *Chem. Phys. Lett.* 179, 73 (1991).
247. A. Bahl, W. Grahn, S. Stadler, F. Feiner, G. Bourhill, C. Bräuchle, A. Reisner, and P. G. Jones, *Angew. Chem. Int. Ed. Engl.* 34, 1485 (1995).
248. M. S. Wong, J.-F. Nicoud, C. Runser, A. Fort, M. Barzoukas, and E. Marchal, *Chem. Phys. Lett.* 253, 141 (1996).
249. E. Hendrickx, C. Boutton, K. Claeys A. Persoons, S. Van Es, T. Biemans, and B. Meijer, *Chem. Phys. Lett.* 270, 241 (1997).
250. E. Hendrickx, K. Claeys, and A. Persoons, *Acc. Chem. Res.* 31, 675 (1998).
251. E. Kelderman, L. Derhaeg, G. J. T. Heesink, W. Verboom, J. F. J. Engbersen, N. F. van Hulst, A. Persoons, and D. N. Reinhoudt, *Angew. Chem. Int. Ed. Engl.* 31, 1075 (1992).
252. G. J. T. Heesink, N. F. van Hulst, B. Bölger, E. Kelderman, J. F. J. Engbersen, W. Verboom, and D. N. Reinhoudt, *Appl. Phys. Lett.* 62, 2015 (1993). O. F. J. Noordman, N. F. van Hulst, and B. Bölger, *J. Opt. Soc. Am. B* 12, 2398 (1995).
253. G. de la Torre, P. Vázquez, F. Agulló-López, and T. Torres, *J. Mater. Chem.* 8, 1671 (1998).
254. K. S. Suslick, C.-T. Chen, G. R. Meredith, and L.-T. Cheng, *J. Am. Chem. Soc.* 114, 6928 (1992).
255. M. Yeung, A. C. H. Ng, M. G. B. Drew, E. Vorpagel, E. M. Breitung, R. J. McMahon, and D. K. P. Ng, *J. Org. Chem.* 63, 7143 (1998).
256. S. Priyadarshi, M. J. Therien, and D. N. Beratan, *J. Am. Chem. Soc.* 118, 1504 (1996).
257. M. A. Herranz, N. Martín, L. Sánchez, J. Garín, J. Orduna, R. Alcalá, B. Villacampa, and C. Sánchez, *Tetrahedron* 54, 11651 (1998).
258. S. Norvez and M. Barzoukas, *Chem. Phys. Lett.* 165, 41 (1990).
259. B. He, Q. Zhang, X. Wang, Q. Dai, Z.-H. Lu, C.-W. Yuan, and D. Huang, *Supramol. Sci.* 5, 537 (1998).
260. L. Ma, Q.-S. Hu, D. Vitharana, C. Wu, C. M. S. Kwan, and L. Pu, *Macromolecules* 30, 204 (1997).
261. J. A. Sattigeri, C.-W. Shiau, C. C. Hsu, F.-F. Yeh, S. Liou, B.-Y. Jin, and T.-Y. Luh, *J. Am. Chem. Soc.* 121, 1607 (1999).
262. C. C. Frazier, M. A. Harvey, M. P. Cockerham, H. M. Hand, E. A. Chauchard, and C. H. Lee, *J. Phys. Chem.* 90, 5703 (1986).
263. M. L. H. Green, S. R. Marder, M. E. Thompson, J. A. Bandy, D. Bloor, P. V. Kolinsky, and R. J. Jones, *Nature (London)* 330, 360 (1987).
264. S. R. Marder, J. W. Perry, W. P. Schaefer, B. G. Tiemann, P. C. Groves, and K. J. Perry, *Proc. SPIE-Int. Soc. Opt. Eng.* 1147, 108 (1989).
265. J. F. Nicoud and M. W. Twieg, in " Nonlinear Optical Properties of Organic Molecules and Crystals," (D. S. Chemla and J. Zyss, Eds.), Academic Press, Orlando, FL, 1987.
266. B. G. Tiemann, S. R. Marder, J. W. Perry, and L.-T. Cheng, *Chem. Mater.* 2, 690 (1990).
267. S. R. Marder, B. G. Tiemann, J. W. Perry, L. T. Cheng, W. Tam, W. P. Schaefer, and R. E. Marsh, in "Materials for Nonlinear Optics:Chemical Perspectives," (S. R. Marder, J. E. Sohn, and G. D. Stucky, Eds.), p. 187. American Chemical Society, Washington, DC, 1991.
268. J. C. Calabrese, L.-T. Cheng, J. C. Green, S. R. Marder, and W. Tam, *J. Am. Chem. Soc.* 113, 7227 (1991).
269. L.-T. Cheng, W. Tam, G. R. Meredith, and S. R. Marder, *Mol. Cryst. Liq. Cryst.* 189, 137 (1990).
270. S. R. Marder, D. N. Beratan, B. G. Tiemann, L.-T. Cheng and W. Tam, in "Organic Materials for Nonlinear Optics II," (R. A. Hann and D. Bloor, Eds.), pp. 165–167. Royal Society of Chemistry London, 1991.
271. L.-T. Cheng, in "Organic Molecules for Nonlinear Optics and Photonics," (J. Messier, F. Kajzar, and P. Prasad, Eds.), p. 121. Kluwer, Dordrecht, The Netherlands, 1991.
272. G. G. Roberts, in " Langmuir-Blodget Films," (G. G. Roberts, Ed.), p. 351. Plenum Press, New York, 1990.
273. K. Kajikawa, T. Anzai, H. Takezoe, A. Fukuda, S. Okada, H. Matsuda, H. Nakanishi, T. Abe, and H. Ito, *Chem Phys. Lett.* 192, 113 (1992).
274. K. D. Singer, J. E. Sohn, and S. J. Lalama, *Appl. Phys. Lett.* 49, 248 (1986).
275. M. A. Hubbard, T. J. Marks, J. Yang, and G. K. Wong, *J. Chem Mater.* 1, 167 (1989).
276. G. C. Bjorklund, S. Ducharme, W. Fleming, D. Jungbauer, W. E. Moerner, J. D. Swalen, R. J. Twieg, C. G. Willson, and D. Y. Yoon, in "Materials for Nonlinear Optics: Chemical Perspectives." (S. R. Marder, J. E. Sohn, and G. D. Stucky, Eds.), ACS Symposium Series, Vol. 455, p. 216. American Chemical Society Washington, DC, 1991.
277. K. D. Singer, S. J. Lalama, J. E. Sohn, and R. D. Small, in "Nonlinear Optical Properties of Organic Molecules and Crystals." (D. S. Chemla and J. Zyss, Eds.), Vol. 1, p. 460. Academic Press, San Diego, 1987.
278. D. Li, M. A. Ratner, T. J. Marks, C. Zhang, J. Yang, and G. K. Wong, *J. Am. Chem. Soc.* 112, 7389 (1990).
279. H. E. Katz, G. Scheller, T. M. Putvinski, M. L. Schilling, W. L. Wilson, and C. E. D. Chidsey, *Science (Washington, DC)* 254, 1485 (1991).
280. S. Tomaru, S. Zembutsu, M. Kawachi, and M. Kobayashi, *J. Chem. Soc. Chem. Commun.* 1207 (1984).
281. W. Tam, D. F. Eaton, J. C. Calabrese, T. D. Williams, Y. Wang, and A. G. Anderson, *Chem. Mater.* 1, 128 (1989).
282. S. D. Cox, T. E. Gier, J. D. Bierlein, and G. D. Stucky, *J. Am. Chem. Soc.* 110, 2986 (1988).
283. S. Cooper and P. K. Duta, *J. Phys. Chem.* 94, 114 (1990).
284. J. S. Zyss, J. F. Nicoud, and M. Coquillay, *J. Chem. Phys.* 81, 4160 (1984)
285. G. R. Meredith, in "Nonlinear Optical Properties of Organic and Polymeric Materials." (D. J. Williams, ed.), p. 27, American Chemican Society, Washington, DC, 1983.
286. S. R. Marder, J. W. Perry, and W. P. Schaefer, *Science (Washington, DC)* 248, 626 (1989).
287. S. R. Marder, J. W. Perry, B. G. Tiemann, and W. P. Schaefer, *Organometallics* 10, 1896 (1991).
288. S. R. Marder, J. W. Perry, W. P. Schaefer, E. J. Ginsburg, C. B. Gorman, and R. H. Grubbs, *Mater Res. Soc. Symp. Proc.* 175, 101 (1990).
289. A. R. Dias, M.-H. Garcia, J. C. Rodrigues, M. L. H. Green, and S. M. Kuebler, *J. Organomet. Chem.* 475, 241 (1994).
290. W. Tam and J. C. Calabrese, *Chem. Phys. Lett.* 144, 79 (1988).
291. D. F. Eaton, A. G. Anderson, W. Tam, and Y. Wang, *J. Am. Chem. Soc.* 109, 1886 (1987).
292. H. E. Bunting, M. L. H. Green, S. R. Marder, M. E. Thompson, D. Bloor, P. V. Kolinsky, and R. J. Jones, *Polyhedron* 11, 1489 (1992).
293. J. A. Bandy, H. E. Bunting, M. L. H. Green, S. R. Marder, M. E. Thompson, D. Bloor, P. V. Kolinsky, and R. J. Jones, in "Organic Materials for Nonlinear Optics." (R. A. Hann and D. Bloor, Eds.), p. 219. Royal Society of Chemistry, London, 1989.
294. M. L. H. Green, J. Qin, D, O'Hare, H. E. Bunting, M. E. Thompson, S. R. Marder, and K. Chatakondu, *Pure Appl. Chem.* 61, 817 (1989).
295. Y. Yamazaki, K. Hosono, H. Matsuda, N. Minami, M. Asai, and H. Nakanishi, *Biotechnol. Bioeng.* 38, 1218 (1991).
296. (*a*) B. J. Coe, C. J. Jones, J. A. McCleverty, D. Bloor, P. V. Kolinsky, and R. J. Jones, *J. Chem. Soc. Chem. Commun.* 1485 (1989);
(*b*) B. J. Coe, T. A. Hamor, C. J. Jones, J. A. McCleverty, D. Bloor, G. H. Cross, and T. L. Axon, *J. Chem. Soc. Dalton Trans.* 3427 (1994);
(*c*) B. J. Coe, T. A. Hamor, C. J. Jones, J. A. McCleverty, D. Bloor, G. H. Cross, and T. L. Axon, *J. Chem. Soc. Dalton Trans.* 673 (1995).
297. A. R. Dias, M.-H. Garcia, M.-P. Robalo, M. L. H. Green, K. K. Lai, A. J. Pulham, S. M. Kuebler, and G. Balavoine, *J. Organomet. Chem.* 453, 241 (1993).
298. P. Reinecker, V. M. Agranovitch, and V. I. Yudson, *Chem. Phys. Lett.* 260, 621 (1996).
299. H. S. Nalwa, *Appl. Organomet. Chem.* 5, 349 (1991).
300. S. R. Marder, in "Inorganic Materials." (D. W. Bruce and D. O'Hare, Eds.), p. 116, Wiley, Chichester, UK, 1992.

301. A. R. Dias, M.-H. Garcia, P. J. Mendes, M.-P. Robalo, and J. C. Rodrigues, *Trends Organomet. Chem.* 1, 335 (1994).

302. N. J. Long, *Angew. Chem. Int. Ed. Engl.* 34, 21 (1995).

303. I. R. Whittall, A. M. McDonagh, M. G. Humphrey, and M. Samoc, *Adv. Organomet. Chem.* 42, 291 (1998).

304. J. A. Bandy, H. E. Bunting, M.-H. Garcia, M. L. H. Green, S. R. Marder, M. E. Thompson, D. Bloor, P. V. Kolinsky, R. J. Jones, and J. W. Perry, *Polyhedron* 11, 1429 (1992).

305. J. A. Bandy, H. E. Bunting, M.-H. Garcia, M. L. H. Green, S. R. Marder, M. E. Thompson, D. Bloor, P. V. Kolinsky and R. J. Jones, in "Organic Materials for Nonlinear Optics." (R. A. Hann and D. Bloor, Eds.), p. 225. Royal Society of Chemistry, London, 1989.

306. R. Whittall, M. P. Cifuentes, M. J. Costigan, M. G. Humphrey, S. C. Goh, B. W. Skelton, and A. H. White, *J. Organomet. Chem.* 471, 193 (1994).

307. A. Houlton, J. R. Miller, J. Silver, N. Jassim, M. J. Ahmet, T. L. Axon, D. Bloor, and G. H. Cross, *Inorg. Chim. Acta* 205, 67 (1993).

308. B. J. Coe, C. J. Jones, and J. A. McCleverty, *Polyhedron* 13, 2107 (1994).

309. S. A. O'Reilly, P. A. S. White, and J. L. Templeton, *Chem. Mater.* 8, 93 (1996).

310. X. Wu, J. Qin, D. Liu, B. Wu, and C. Chen, *Nonlinear Opt.* 7, 153 (1994).

311. R. Herrmann, B. Pedersen, G. Wagner, and J.-H. Youn, *J. Organomet. Chem.* 571, 261 (1998).

312. K. Ueno, N. Hamashima, and H. Ogino, *Organometallics* 11, 1435 (1992).

313. R. Loucif-Saïbi, J. A. Delaire, L. Bonazzola, G. Doisneau, G. Balavoine, T. Fillebeen-Khan, I. Ledoux, and G. Pucceti, *Chem. Phys.* 167, 369 (1992).

314. D. R. Kanis, M. A. Ratner, and T. J. Marks, *J. Am. Chem. Soc.* 114, 10338 (1992).

315. (*a*) M. E. Wright, B. B. Cochran, E. G. Toplikar, H. S. Lackritz, and J. T. Kerney, in "Inorganic and Organometallic Polymers II: Advanced Material and Intermediates." (P. Wisian-Neilson, H. R. Allcock, and K. J. Wynne, Eds.), p. 456. American Chemical Society, Washington, DC, 1994.
(*b*) M. E. Wright, E. G. Toplikar, H. S. Lackritz, and J. T. Kerney, *Macromolecules* 27, 3016 (1994).

316. V. Alain, A. Fort, M. Barzoukas, C.-T. Chen, M. Blanchard-Desce, S. R. Marder, and J. W. Perry, *Inorg. Chim. Acta* 242, 43 (1996).

317. V. Alain, M. Blanchard-Desce, C.-T. Chen, S. R. Marder, A. Fort, and M. Barzoukas, *Synth. Metals* 81, 133 (1996).

318. D. R. Kanis, M. A. Ratner, and T. J. Marks, *J. Am. Chem. Soc.* 112, 8203 (1990).

319. B. Illien, P. Jehan, A. Botrel, A. Darchen, I. Ledoux, J. Zyss, P. Le Magueres, and L. Ouahab, *New J. Chem.* 633 (1998).

320. G. G. A. Balavoine, J.-C. Daran, G. Iftime, P. G. Lacroix, E. Manoury, J. A. Delaire, I. Maltey-Fanton, K. Nakatani, and S. Di Bella, *Organometallics* 18, 21 (1999).

321. Z. Yuan, N. J. Taylor, Y. Sun, T. B. Marder, I. D. Williams, and L.-T. Cheng, *J. Organomet. Chem.* 27, 449 (1993).

322. M. E. Wright, E. G. Toplikar, R. F. Kubin, and M. D. Seltzer, *Macromolecules* 25, 1838 (1992).

323. B. J. Coe, C. J. Jones, J. A. McCleverty, D. Bloor, and G. Cross, *J. Organomet. Chem.* 464, 225 (1994).

324. J. L. Oudar and R. Hierle, *J. Appl. Phys.* 48, 2699 (1977).

325. K. Hagimoto and A. Mito, *Appl. Opt.* 34, 8276 (1995).

326. W. Wenseleers, E. Goovaerts, A. Bouwen, M. H. Garcia, M. P. Robalo, P. J. Mendes, and A. R. Dias, *Dissertation Abstracts Internat.* B60, 4038 (2000).

327. I. R. Whittall, M. G. Humphrey, A. Persoons, and S. Houbrechts, *Organometallics* 15, 1935 (1996).

328. S. Houbrechts, K. Clays, A. Persoons, V. Cadierno, M. P. Gamasa, J. Gimeno, I. R. Whittall, and M. G. Humphrey, *Proc. SPIE—Int. Soc. Opt. Eng.* 98, 2852 (1996).

329. I. R. Whittall, M. G. Humphrey, S. Houbrechts, A. Persoons, and D. C. R. Hockless, *Organometallics* 15, 5738 (1996).

330. I.-Y. Wu, J. T. Lin, J. Luo, S.-S. Sun, C.-S. Li, K. J. Lin, C. Tsai, C.-C. Hsu, and J.-L. Lin, *Organometallics* 16, 2038 (1997).

331. S. Houbrechts, K. Clays, A. Persoons, V. Cadierno, M. P. Gamasa, and J. Gimeno, *Organometallics* 15, 5266 (1996).

332. V. Cadierno, S. Conejero, M. Pilar Gamasa, J. Gimeno, I. Asselberghs, S. Houbrechts, K. Clays, A. Persoons, J. Borge, and S. García-Granda, *Organometallics* 18, 582 (1999).

333. I. R. Whittall, M. P. Cifuentes, M. G. Humphrey, B. Luther-Davies, M. Samoc, S. Houbrechts, A. Persoons, G. A. Heath, and D. Begsáni, *Organometallics* 16, 2631 (1997).

334. I. R. Whittall, M. P. Cifuentes, M. G. Humphrey, B. Luther-Davies, M. Samoc, S. Houbrechts, A. Persoons, G. A. Heath, and D. C. R. Hockless, *J. Organomet. Chem.* 549, 127 (1998).

335. R. H. Naulty, M. P. Cifuentes, M. G. Humphrey, S. Houbrechts, C. Boutton, A. Persoons, G. A. Heath, D. C. R. Hockless, B. Luther-Davies, and M. Samoc, *J. Chem. Soc. Dalton Trans.* 4167 (1997).

336. T. Richardson, G. G. Roberts, M. E. C. Polywka, and S. G. Davies, *Thin Solid Films* 179, 405 (1989).

337. L. T. Cheng, W. Tam, and F. Eaton, *Organometallics* 9, 2856 (1990).

338. M. Kimura, H. Abdel-Halim, D. W. Robinson, and D. O. Cowan, *J. Organomet. Chem.* 403, 365 (1991).

339. A. G. Anderson, J. C. Calabrese, W. Tam, and I. D. Williams, *Chem. Phys. Lett.* 134, 392 (1987).

340. D. F. Eaton, A. G. Anderson, W. Tam, and Y. Wang, in "Polymers for High Technology: Electronics and Photonics." (M. J. Bowden and S. R. Turner, Eds.), p. 381, American Chemistry Society, Washington, DC, 1987.

341. T. Kobayash, *IEICE Trans. Electron.* 36, E75 (1992).

342. W. Tam, L. T. Cheng, J. D. Bierlein, L. K. Cheng, Y. Wang, A. E. Feiring, G. R. Meredith, D. F. Eaton, J. C. Calabrese, and G. L. J. A. Rikken, in "Materials for Nonlinear Optics: Chemical perspectives." (S. R. Marder, J. E. Sohn, and G. D. Stucky, Eds.), p. 158, American Chemistry Society, Washington, DC, 1991.

343. M. Tamm, A. Grzegorzeweski, T. Steiner, T. Jentzsch, and W. Werncke, *Organometallics* 15, 4984 (1996).

344. I. S. Lee, H. Seo, and Y. K. Chung, *Organometallics* 18, 1091 (1999).

345. S. Maiorana, A. Papagni, E. Licandro, A. Persoons, K. Clay, S. Houbrechts, and W. Porzio, *Gazz. Chim. Ital.* 125, 377 (1995).

346. G. Roth, H. Fisher, T. Meyer-Friedrichsen, J. Heck, S. Houbrechts, and A. Persoons, *Organometallics* 17, 1511 (1998).

347. E. Licandro, S. Maiorana, A. Papagni, P. Hellier, L. Capella, A. Persoons, and S. Houbrechts, *J. Organomet. Chem.* 583, 111 (1999).

348. J. Qin, D. Liu, C. Dai, C. Chen, B. Wu, C. Yang, and C. Zhan, *Coord. Chem. Rev.* 188, 23 (1999).

349. R. H. Naulty, A. M. McDonagh, I. R. Whittall, M. P. Cifuentes, M. G. Humphrey, S. Houbrechts, J. Maes, A. Persoons, G. A. Heath, and D. C. R. Hockless, *J. Organomet. Chem.* 563, 137 (1998).

350. S. Houbrechts, C. Boutton, K. Clays, A. Persoons, I. R. Whittall, R. H. Naulty, M. P. Cifuentes, and M. G. Humphrey, *J. Nonlinear Opt. Phys. Mater.* 7, 113 (1998).

351. J. Qin, C. Dai, Y. Gou, D. Liu, B. Wu, and C. Chen, *Nonlinear Opt.* 4, 337 (1993).

352. D. W. Bruce and A. Thorthon, *Mol. Cryst. Liq. Cryst.* 231, 253 (1993).

353. J. Buey, S. Coco, L. Díez, P. Espinet, J. M. Martín-Alvarez, J. A. Miguel, S. García-Granda, A. Tesouro, I. Ledoux, and J. Zyss, *Organometallics* 17, 1750 (1998).

354. I. Ledoux, *Synth. Met.* 54, 123 (1993).

355. G. J. Ashwell and D. Bloor, Eds., "Organic Materials Non-linear Optics III." Royal Society of Chemistry, Cambridge, UK, 1993.

356. G. Mignani, A. Kramer, G. Puccetti, I. Ledoux, G. Soula, J. Zyss, and R. Meyrueix, *Organometallics* 9, 2640 (1990).

357. D. Hissink, P. F. van Hutten, G. Hadziioannou, and F. van Bolhuis, *J. Organomet. Chem.* 454, 25 (1993).

358. B. J. Coe, S. Houbrechts, I. Asselberghs, and A. Persoons, *Angew. Chem.* 111, 377 (1999); *Angew. Chem. Int. Engl. Ed.* 38, 366 (1999).
359. B. J. Coe, M. C. Chamberlain, J. P. Essex-Lopresti, S. Gaines, J. C. Jeffery, S. Houbrechts, and A. Persoons, *Inorg. Chem.* 36, 3284 (1997).
360. T. Thami, P. Bassoul, M. A. Petit, J. Simon, A. Fort, M. Barzoukas, and A. Villaeys, *J. Am. Chem. Soc.* 114, 915 (1992).
361. G. Doisneau, G. Balavoine, T. Fillebeen-Khan, J.-C. Clinet, J. Delaire, I. Ledoux, R. Loucif, and G. Puccetti, *J. Organomet. Chem.* 421, 299 (1991).
362. G. Lenoble, P. G. Lacroix, J. C. Daran, S. Di Bella, and K. Nakatani, *Inorg. Chem.* 37, 2158 (1998).
363. J. C. Calabrese and W. Tam, *Chem. Phys. Lett.* 133, 244 (1987).
364. U. Hagenau, J. Heck, E. Hendrickx, A. Persoons, T. Schuld, and H. Wong, *Inorg. Chem.* 35, 7863 (1996).
365. B. J. Coe, S. S. Kurek, N. M. Rowley, J. D. Foulon, T. A. Harmor, M. E. Harman, M. B. Hursthouse, C. J. Jones, J. A. McCleverty, and D. Bloor, *Chemtronics* 5, 23 (1991).
366. E. Hendrickx, A. Persoons, S. Samson, and G. R. Stephenson, *J. Organomet. Chem.* 542, 295 (1997).
367. F. W. Vance, L. Karki, J. K. Reigle, J. T. Hupp, and M. A. Ratner, *J. Phys. Chem. A* 102, 8320 (1998).
368. M. Lequan, C. Branger, J. Simon, T. Thami, E. Chauchard, and A. Persoons, *Chem. Phys. Lett.* 229, 101 (1994).
369. M. Lequan, C. Branger, and A. Persoons, *Adv. Mater.* 6, 851 (1994).
370. I. R. Whittall, M. G. Humphrey, S. Houbrechts, J. Maes, A. Persoons, S. Schmid, and D. C. R. Hockless, *J. Organomet. Chem.* 544, 277 (1997).
371. M. G. Humphrey, A. M. McDonagh, J. P. L. Morrall, M. P. Cifuentes, S. Houbrechts, T. Wada, H. Sasabe, A. Persoons, I. Asselberghs, K. A. Persoons, *Chem. Phys. Lett.* 229, 101 Clays, M. Samoc, and B. Luther-Davies, "XIIIth FECHEM Conference in Organomet. Chemistry," Portugal, 1999, Abstract book, p. 49.
372. O. A. Aktsipetrov, N. N. Akhmediev, E. D. Mishina, and V. Novak, *JETP Lett.* 37, 207 (1983).
373. I. R. Girling, N. A. Cade, P. V. Kolinsky, and C. M. Montgomery, *Electron. Lett.* 21, 169 (1985).
374. G. R. Meredith, J. G. VanDusen, and D. J. Williams, *Macromolecules* 15, 1385 (1982).
375. L. Zhang, P. J. Chandler, P. D. Townsend, Z. T. Alwahabi, S. A. Pityana, and A. J. McCaffery, *J. Appl. Phys.* 73, 2695 (1993).
376. S. Nakamura, *J. Cryst. Growth* 202, 290 (1999).
377. M. J. Canva, M. L. Jager, and G. I. Stegeman, *Polym. News* 23, 78 (1998).
378. P. D. Southgate, and D. S. Hall, *Appl. Phys. Lett.* 18, 456 (1971).
379. P. M. Rentzepis and Y.-H. Pao, *Appl. Phys. Lett.* 5, 156 (1965).
380. (a) R. W. McQuaid, *Appl. Opt.* 2, 320 (1963). (b) G. H. Heilmeier, *Appl. Opt.* 3, 1281 (1964).
381. Z. Wang, D. J. Hagan, E. W. VanStryland, J. Zyss, P. Vidakovik, and W. E. Torruellas, *J. Opt. Soc. Am. B* 14, 76 (1997).
382. Y. X. Fan, R. C. Eckardt, R. L. Byer, C. Chen, and A. D. Jiang, *IEEE J. Quant. Electron.* QE-25, 1196 (1986).
383. G. Knopfle, C. Bosshard, R. Schlesser, and P. Gunter, *IEEE J. Quantum Electron.* 30, 1303 (1994).
384. R. T. Bailey, G. H. Bourhill, F. R. Cruickshank, D. Pugh, J. N. Sherwood, G. S. Simpson, and K. B. R. Varma, *Mol. Cryst. Liq. Cryst.* 216, 363 (1992).
385. M. S. Wong, F. Pan, M. Bosch, R. Spreiter, C. Bosshard, P. Gunter, and V. Gramlich, *J. Opt. Soc. Am. B* 15, 426 (1998).
386. S. R. Marder, J. W. Perry, and W. P. Schaefer, *J. Mater. Chem.* 2, 985 (1992).
387. http://www.moec.com; F. Pan, G. Knopfle, Ch. Bosshard, S. Follonier, R. Spreiter, M. S. Wong, and P. Gunter, *Appl. Phys. Lett.* 69, 13 (1996).
388. T. Kondo, N. Hashizume, S. Miyoshi, R. Morita, N. Ogasawara, S. Umegaki, and R. Ito, *Proc. SPIE* 1337, 53 (1990).
389. I. R. Peterson and I. R. Girling, *Sci. Progr.* 69, 533 (1985).
390. (*a*) G. H. Cross, I. R. Girling, I. R. Peterson, and N. A. Cade, *Electron. Lett.* 22, 1111 (1986).
(*b*) G. H. Cross, I. R. Girling, N. A. Cade, T. D. Earls, and I. R. Peterson, *J. Opt. Soc. Am. B* 4, 962 (1987).
391. I. R. Girling, P. V. Kolinsky, N. A. Cade, J. D. Earls, and I. R. Peterson, *Opt. Commun.* 55, 289 (1985).
392. D. B. Neal, M. C. Petty, G. G. Roberts, M. M. Ahmed, W. J. Feast, I. R. Girling, N. A. Cade, P. V. Kolinsky, and I. R. Peterson, *Electron. Lett.* 22, 460 (1986).
393. G. J. Ashwell, E. J. C. Dawnay, A. P. Kuczynski, M. Szablewski, I. M. Sandy, M. R. Bryce, A. M. Grainger, and M. Hasan, *J. Chem. Soc. Faraday Trans.* 86, 1117 (1990).
394. T. L. Penner, H. R. Motschmann, N. J. Armstrong, M. C. Ezenyilimba, and D. J. Williams, *Nature (London)* 367, 49 (1994).
395. X. G. Wang, S. Balasubramanian, L. Li, X. L. Jiang, D. J. Sandman, M. F. Rubner, J. Kumar, and S. K. Tripathy, *Macromol. Rapid Commun.* 18, 451 (1997).
396. C. P. J. M. van der Vorst and S. J. Picken, in "Polymers as Electrooptical and Photooptical Active Media." (V. P. Shibaev, Ed.), Springer, Berlin, 1997. "Electric field poling of nonlinear optical side chain polymers."
397. A. Chen, V. Chuyanov, H. Zhang, S. Garner, W. H. Steier, J. Chen, J. Zhu, M. He, S. S. H. Mao, and L. R. Dalton, *Opt. Lett.* 23, 478 (1998).
398. A. W. Harper, S. Sun, L. R. Dalton, S. M. Garner, A. Chen, S. Kalluri, W. H. Steier, and B. H. Robinson, *J. Opt. Soc. Am. B* 15, 329 (1998).
399. J.-M. Nunzi, F. Charra, and C. Fiorini, *Condens. Matter News* 2, 6 (1993).
400. F. Charra, F. Devaux, J.-Michel Nunzi, and P. Raimond, *Phys. Rev. Lett.* 68, 2440 (1992).
401. C. Fiorini, F. Charra, J.-M. Nunzi, I. D. W. Samuel, and J. Zyss, *Opt. Lett.* 20, 2469 (1995).
402. M. Houé and P. D. Townsend, *J. Phys. D Appl. Phys.* 28, 1747 (1995).
403. Brandrup and Immergut, Eds., "Polymer Handbook, 3rd ed., Wiley Interscience, New York, 1989.
404. N. Bouadma, J. Liang, R. Levenson, S. Grosmaire, P. Boulet, and S. Sainson, *IEEE Phot. Technol. Lett.* 6, 1188 (1994).
405. I. Faderl, P. Labeye, P. Gidon, and P. Mottier, *J. Lightwave Technol.* 13, 2020 (1995).
406. J. S. Cites, P. R. Ashley, and R. P. Leavitt, *Appl. Phys. Lett.* 68, 1452 (1996).
407. P. de Dobbelaere, F. Vermaerkes, G. Vermeire, P. Demeester, P. van Daele, G. R. Mohlmann, J. L. P. Heidemann, and W. H. G. Horsthuis, *Proc. SPIE* 2285, 352 (1994).
408. W. Feng, S. Lin, B. Hooker, and A. R. Mickelson, *Appl. Opt.* 34, 6885 (1995).
409. T. Kurokawa, N. Takato, and Y. Katayama, *Appl. Opt.* 19, 3124 (1980).
410. J. I. Thackara, G. F. Lipscomb, M. A. Stiller, A. J. Ticknor, and R. Lytel, *Appl. Phys. Lett.* 52, 1031 (1988).
411. G. H. Cross, A. Donaldson, R. W. Gymer, S. Mann, and N. J. Parsons, *Proc. SPIE* 1177, 79 (1989).
412. A. Neyer, T. Knoche, and L. Muller, *Electron. Lett.* 29, 399 (1993).
413. Y. Takezawa, S. Akasaka, S. Ohara, T. Ishibashi, H. Asano, and N. Taketani, *Appl. Opt.* 33, 2307 (1994).
414. X.-M. Zhao, A. Stoddart, S.P. Smith, E. Kim, Y. Xia, M. Prentiss, and G. M. Whitesides, *Adv. Mater.* 8, 420 (1996).
415. W. Wang, D. Chen, H. R. Fetterman, Y. Shi, W. H. Steier, L. R. Dalton, and P.-M. Chow, *Appl. Phys. Lett.* 67, 1806 (1995).
416. D. Chen, H. R. Fetterman, A. Chen, W. H. Steier, L. R. Dalton, W. Wang, and Y. Shi, *Appl. Phys. Lett.* 70, 3335 (1997).
417. H. T. Man and H. N. Yoon, *Appl. Phys. Lett.* 72, 540 (1998).
418. G. Williams and D. C. Watts, *Trans. Farad. Soc.* 66, 80 (1970).
419. H. L. Hampsch, J. Jiang, G. K. Wong, and J. M. Torkelson, *Macromolecules* 23, 3640 (1990).
420. S. Schüssler, R. Richert, and H. Bässler, *Macromlecules* 27, 4318 (1994).

421. C. Xu, B. Wu, O. Todorova, L. R. Dalton, Y. Shi, P. M. Ranon, and W. H. Steier, *Macromolecules* 26, 5303 (1993).
422. L. R. Dalton, A. W. Harper, B. Wu, R. Ghosn, J. Laquindanum, Z. Liang, A. Hubbel, and C. Xu, *Adv. Mater.* 7, 519 (1995).
423. L. Dalton, A. Harper, A. Ren, F. Wang, G. Todorova, J. Chen, C. Zhang, and M. Lee, *Ind. Eng. Chem. Res.* 38, 8 (1999).
424. Y. Shi, W. Wang, W. Lin, D. J. Olson, and J. H. Bechtel, *Appl. Phys. Lett.* 70, 1342 (1997).
425. M. H. Lee, H. J. Lee, S. G. Han, H.-Y. Kim, and Y. H. Won, *Mater. Res. Soc. Symp. Proc.* 413, 287 (1996).
426. A. Chen, V. Chuyanov, S. Garner, H. Zhang, W. H. Steier, J. Chen, J. Zhu, F. Wang, M. He, S. S. H. Mao, and L. R. Dalton, *Opt. Lett.* 23, 478 (1998).
427. I. M. Skinner and S. J. Garth. *Am. J. Phys.* 58, 177 (1990).
428. D. M. Burland, C. A. Walsh, F. Kajzar, and C. Sentein. *J. Opt. Soc. Am. B* 8, 2269 (1991).